Università della Calabria

Facoltà di Farmacia e Scienze della Nutrizione e della Salute

Dipartimento Farmaco-Biologico (MED/05 PATOLOGIA CLINICA)

Dottorato di Ricerca in "Biochimica Cellulare ed Attività dei Farmaci in Oncologia" (XXIV)

PPARγ ligands as novel agents able to inhibit breast tumor growth and progression

Docente Tutor
Prof.ssa Daniela Bonofiglio

Dottoranda
Dott.ssa Donatella Vizza

Coordinatore
Prof. Diego Sisci

Anno Accademico 2010-2011

Index

Scientific publication

1. Guido C., Santoro M., **Vizza D.**, Avena P., Carpino A. and Aquila S. Peroxisome Proliferator-Activated Receptor (PPAR) gamma modulates metabolism in pig sperm. Reproduction, 2011 (In revision).

2. Plastina P., Bonofiglio D., **Vizza D.**, Fazio A., Rovito D., Giordano C., Barone I., Catalano S., Andò S and Bartolo G. Ziziphus jujube fruits as a source of bioactive compounds exerting antiproliferative and apoptotic

effects in human breast cancer cells. Journal of Ethnopharmacology, 2011 (In revision).

3. Catalano S., Mauro L., Bonofiglio D., Pellegrino M., Qi H., Rizza P., **Vizza D.**, Bossi G., Andò S. PPARgamma ligands as antagonists of leptin signaling in breast cancer: in vitro and in vivo effects. American Journal of Pathology 2011; 179:1030-1040.

4. Bonofiglio D., Cione E., **Vizza D.**, Perri M., Pingitore A., Qi H., Catalano S., Rovito D., Genchi G. and Andò S. Bid as a potential target of apoptotic effects exerted by low doses of PPARγ and RXR ligands in breast cancer cells. Cell Cycle 2011; 10: 2344-2354.

5. Giordano C., Catalano S., Panza S., **Vizza D**., Barone I., Bonofiglo D., Gelsomino L., Rizza P., Fuqua S. and Ando` S. Farnesoid X receptor inhibits tamoxifen-resistant MCF-7 breast cancer cell growth through downregulation of HER2 expression. Oncogene 2011; 30: 4129-4140.

6. Bonofiglio D., Cione E., Qi H., Pingitore A., Perri M., Catalano S., **Vizza D.**, Panno M. L., Genchi G., Fuqua S. AW., Andò S. Combined low doses of PPARγ and RXR ligands trigger intrinsic apoptotic pathway in human breast cancer cells. American Journal of Pathology 2009: 175:1270-1280.

Abstracts and oral communications

1. Bonofiglio D., Santoro A., **Vizza D.**, Rovito D., Martello E., Cappello A.R., Barone I., Giordano C., Catalano S., Dolce V., Andò S. Modulatory role of Peroxisome Proliferator-Activated Receptor γ on Citrate Carrier activity and expression. Experimental Biology ASIP, San Diego 21-25 April 2012.

2. Giordano C., **Vizza D.**, Rovito D., Barone I., Bonofiglio D., Panza S., Lanzino M., Fuqua S., Catalano S. and Andò S. Leptin Increases HER2 Stability through HSP90 in Breast Cancer Cells. Experimental Biology ASIP, San Diego 21-25 April 2012.

3. Giordano C., **Vizza D.**, Barone I., Panno ML., Rizza P., Bonofiglio D., Andò S. and Catalano S. Evidences that Leptin Induces HER2 Expression and Enhances Stem Cells Population in Breast Cancer. ENDO Meeting, Boston 4-7 June 2011.

4. **Vizza D.**, Bonofiglio D., Cione E., Perri M., Pingitore A., Qi H., Catalano S., Rovito D., Panno ML., Genchi G., and Andò S. Bid as a potential target of apoptotic effects exerted by low doses of PPARγ and RXR ligands in breast cancer cells. VII Convegno della Fondazione "Lilli Funaro", Cosenza 1-2 Aprile 2011.

5. Rovito D. , Bonofiglio D.,Plastina P., **Vizza D.** and Andò S. Ziziphus jujube fruits as a source of bioactive compounds exerting antiproliferative and apoptotic effects in human breast cancer cells. VII Convegno della Fondazione "Lilli Funaro", Cosenza 1-2 April 2011.

6. Pellegrino M., Catalano S., Bonofiglio D., Qi H., Rizza P., **Vizza D.**, Bossi G., Mauro L. PPARγ Ligand Rosiglitazone Counteracts the Stimulatory Effect of Leptin on Breast Cancer Growth. National Congress of Pathology, Salerno 14-17 October 2010 .

7. **Vizza D.**, Bonofiglio D., Cione E., Perri M., Pingitore A., Qi H., Catalano S., Panno ML., Genchi G.and Andò S. Mitochondrial p53/Bid interaction plays a pro-apoptotic role in response to PPARγ and RXR ligands in breast cancer cells. VI Convegno della Fondazione "Lilli Funaro", Cosenza 21-22 Maggio 2010.

8. Giordano C., **Vizza D.**, Panza S., Barone I, Bonofiglio D, Fuqua SA, Catalano S, Andò S. Activated Farnesoid x Receptor Inhibits Growth of

Tamoxifen-Resistant MCF-7 Breast Cancer Cells, through Down-Regulation of HER2 Expression. Experimental Biology ASIP, Anaheim 24-28 April 2010.

9. Bonofiglio D., Cione E., **Vizza D.**, Perri M., Pingitore A., Qi H., Catalano S., Panno M.L., Genchi G., Andò S. Mitochondrial p53/Bid interaction plays a pro-apoptotic role in response to PPARγ and RXR ligands in breast cancer cells Experimental Biology ASIP, Anaheim 24-28 April 2010.

10. Giordano C., **Vizza D.**, Panza S., Barone I., Bonofiglio D., Fuqua S., Catalano S., Andò S. Farnesoid X Receptor ligand CDCA inibhits growth of tamoxifen-resistant breast cancer cells EMBO Conference on Nuclear Receptors, Catvat/Dubrovnik 25-29 September 2009.

11. Perri A., Bonofiglio D., Qi H., Catalano S., **Vizza D.** and Andò S. Rapid c-Src mediated effects induced by triiodothyronine on proliferative and survival signalling in FB-2 papillary thyroid carcinoma cells. 33° Congresso Nazionale della Società Italiana di Endocrinologia, Sorrento 27-30 May 2009.

12. **Vizza D.**, Bonofiglio D., Cione E., Genchi G., Andò S. Combined low doses of PPARγ and RXR ligands trigger intrinsic apoptotic pathway in human breast cancer cells. XII Workshop on Apoptosis in Biology and Medicine, Porto Pirgos 20-22 May 2009.

13. **Vizza D.**, Bonofiglio D., Cione E., Catalano S., Andò S. Low doses of PPARγ and RXR ligands induce apoptosis in human breast cancer cells. V Convegno della Fondazione “Lilli Funaro”, Cosenza 13-14 Marzo 2009.

Introduction

Breast cancer is the leading cause of death among women in the world. The principal effective endocrine therapy for advanced treatment on this type of cancer is anti-estrogens, but therapeutic choices are limited for estrogen receptor ER-negative tumors, which are often aggressive.

The development of cancer cells that are resistant to chemotherapeutic agents is a major clinical obstacle to the successful treatment of breast cancer, providing a strong stimulus for exploring new approaches in vitro. Using ligands of nuclear hormone receptors to inhibit tumor growth and progression is a novel strategy for cancer therapy.

Peroxisome Proliferator-Activated Receptor gamma (PPARγ), a prototypical member of the nuclear receptor superfamily, plays key roles in energy homeostasis by modulating glucose and lipid metabolism and transport. Moreover, PPARγ can regulate cell proliferation, differentiation and survival (Lemberger T. et al. 1996; Lefebvre P. et al. 2006), immune and inflammatory responses, involved in several diseases including obesity, diabetes, cardiovascular disease and cancer (Lehrke M. and Lazar MA. 2005).

Particularly, heterodimerization of PPARγ with the retinoic acid receptor RXR by their ligands greatly enhances DNA binding to the direct-repeated consensus sequence AGGTCA, which leads to transcriptional activation. (Heyman RA.et al. 1992) (Figure 1).

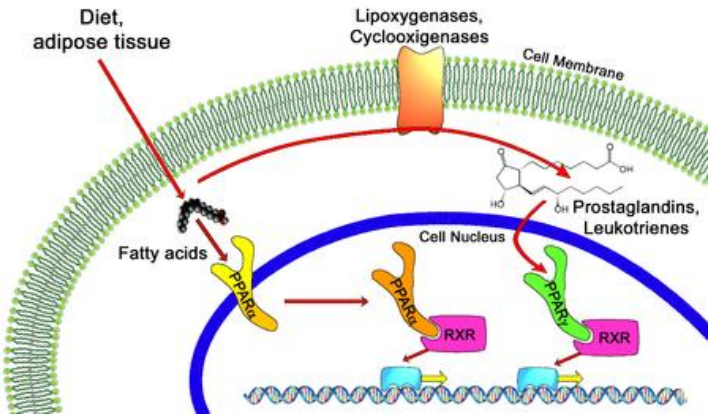

Figure 1. General mechanisms of gene transcription modulation by PPARs

Previous data show that PPARγ, poorly expressed in normal breast epithelial cells (Elstner E.et al. 1998), is present at higher levels in breast cancer cells (Tontonoz P. et al. 1994) and its synthetic ligands, such as thiazolidinediones, induce growth arrest and differentiation in breast carcinoma cells in vitro and in animal models (Mueller E. et al. 1998; Suh N.et al. 1999). Recently, studies in human cultured breast cancer cells show the synthetic PPARγ ligand Rosiglitazone (BRL) promotes antiproliferative effects and activates different molecular pathways leading to distinct apoptotic processes (Bonofiglio D. et al. 2005; Bonofiglio D. et al. 2006; Bonofiglio D. et al. 2009).

Apoptosis, genetically controlled and programmed death leading to cellular self-elimination, can be initiated by two major routes: the intrinsic and extrinsic pathways (Figure 2). The intrinsic pathway is triggered in response to a variety of apoptotic stimuli that produce damage within the cell, including anticancer agents, oxidative damage, UV irradiation, and is mediated through the mitochondria. The extrinsic pathway is activated by extracellular ligands able to induce oligomerization of death receptors, such as Fas, followed by the formation of the death inducing signaling complex, after which the caspases cascade can be activated.

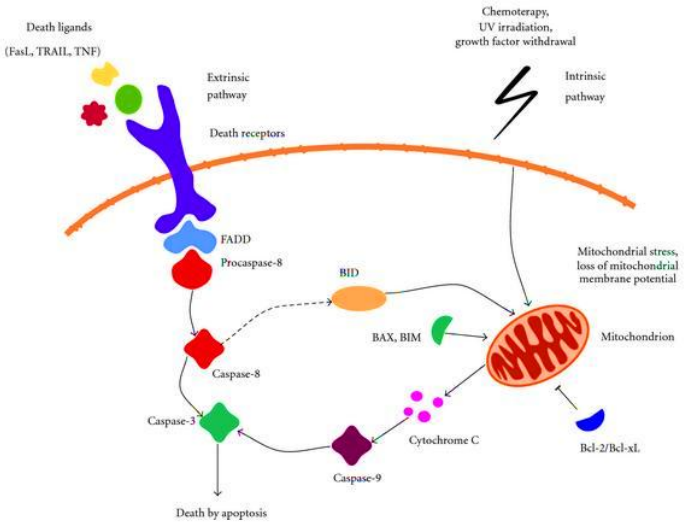

Figure 2. Intrinsic and extrinsic death pathways

Previous data show that the combination of PPARγ ligand Troglitazone with either all-trans retinoic acid or 9-cis-retinoic acid (9RA) can induce apoptosis in

some breast cancer cells (Elstner E. et al. 2002). Furthermore, Elstner et al. demonstrated that the combination of these drugs at micromolar concentrations reduced tumor mass without any toxic effects in mice (Elstner E. et al. 1998).

However, in humans PPARγ agonists at high doses exert many side effects including weight gain due to increased adiposity, edema, hemodilution, and plasma-volume expansion, which preclude their clinical application in patients with heart failure (Arakawa K. et al. 2004; Rangwala SM and Lazar MA. 2004; Staels B. 2005). The undesirable effects of RXR-specific ligands on hypertriglyceridemia and suppression of the thyroid hormone axis have been also reported (Pinaire JA. et al. 2007).

In the first part of my work we have elucidated the molecular mechanism by which combined treatment with BRL and 9RA at nanomolar doses triggers p53-dependent apoptotis in different human breast cancer cells, suggesting potential therapeutic uses for these compounds BRL and 9RA in combination strongly inhibit cell viability in MCF-7, MCF-7TR1, SKBR-3, and T-47D breast cancer cells, whereas MCF-10A normal breast epithelial cells are unaffected.

In MCF-7 cells, combined treatment with BRL and 9RA up-regulated mRNA and protein levels of both the tumor suppressor p53 and its effector p21WAF1/Cip1. Functional experiments indicated that the Nuclear Factor-kB site in the p53 promoter is required for the transcriptional response to BRL plus 9RA. We observed that the intrinsic apoptotic pathway in MCF-7 cells displays an ordinated sequence of events, including disruption of mitochondrial membrane potential, release of cytochrome C, strong caspase 9 activation, and, finally, DNA fragmentation. An expression vector for p53 antisense abrogated the biological effect of both ligands, which implicates involvement of p53 in PPARγ/RXR-dependent activity in all of the human breast malignant cell lines tested.

Taken together, our results suggest that multidrug regimens including a combination of PPARγ and RXR ligands may provide a therapeutic advantage in breast cancer treatment.

Since MCF-7 cells express a wild type p53 protein, while SKBR-3 and T-47D cells harbor endogenous mutant p53, in the second part of our work we elucidated

the mechanism through which PPARγ and RXR ligands triggered apoptotic processes independently of p53 transcriptional activity.

The p53 mutation is found in more than half of all human cancer patients. Cancers with loss of p53 function are often resistant to chemotherapeutic agents mainly because of the absence of p53-dependent apoptosis (Clarke AR. et al 1993; Lowe SW. et al.1993; Lowe SW. et al.1994). The p53-dependent apoptosis largely relies on the capability of p53 to act as a transcription factor, although recent reports show that the transcription-independent function of p53 plays a role in this process as well. For instance, apoptosis can still occur in the presence of inhibitors of protein synthesis, or when p53 mutants unable of acting as transcription factors are ectopically expressed. Part of the transcription-independent mechanism may also involve a direct interaction between p53 and multiple targets in the mitochondria, such as the apoptotic member Bcl-xL, leading to the release of both Bax and Bid from Bcl-xL sequestration. Following a death signal, these pro-apoptotic members undergo a conformational change that enables them to target and integrate into membranes, especially the outer mitochondrial membrane leading to an increased permeabilization (Wei MC. et al. 2000; Wei MC et al. 2001). As noted Bid might serve as a 'death ligand' which translocates as truncated p15Bid (tBid) to mitochondria where it inserts into the outer membrane to activate other resident mitochondrial 'receptor' proteins to release cytochrome C. Alternatively, it is also conceivable that Bid would itself function as a downstream effector participating in an intramembranous pore which releases cytochrome c. To date, Bid is the one molecule absolutely required for the release of cytochrome c in loss-of-function approaches including immunodepletion and gene knockout (Korsmeyer SJ.et al. 2000).

We showed an upregulation of Bid expression enhancing the association between Bid/p53 in both cytosol and mitochondria after the ligands treatment. Particularly, in the mitochondria the complex involves the truncated Bid that plays a key role in the apoptotic process induced by BRL and 9RA since the disruption of mitochondrial membrane potential, the induction of PARP cleavage and the percentage of TUNEL-positive cells were reversed after knocking down Bid. Moreover, PPARγ and RXR ligands were able to reduce mitochondrial GST

activity which was no longer noticeable silencing Bid expression, suggesting the potential of Bid in the regulation of mitochondrial intracellular reactive oxygen species scavenger activity.

Our data, providing new insight into the role of p53/Bid complex at the mitochondria in promoting breast cancer cell apoptosis upon low doses of PPARγ and RXR ligands, address Bid as a potential target in the novel therapeutical strategies for breast cancer. Results showed that BRL and 9RA induce the intrinsic apoptotic pathway through an upregulation of Bid expression and a formation of p53/tBid/Bak multicomplex localized on mitochondria of breast carcinoma cells.

In the last part of my work we have also evaluated the ability of PPARγ ligands to counteract leptin stimulatory effects on breast cancer growth in either in vivo or in vitro models.

Leptin, a peptide hormone mainly secreted by adipocytes, is a pleiotropic molecule that regulates food intake, hematopoiesis, inflammation, immunity, cell differentiation and proliferation (Ahima RS. et al. 2006) (Figure 3).

More recently, leptin has been found to be involved in neoplastic processes, particularly in mammary tumorigenesis (Garofalo C. et al. 2006; Vona-Davis L. et al. 2007) Specifically, in vitro and in vivo studies have shown that leptin stimulates tumor growth, cell survival, and transformation (Catalano S. et al. 2003; Garofalo C. et al. 2006, Mauro L. et al. 2007), and amplifies estrogen signaling, contributing to hormone-dependent breast cancer growth and progression (Catalano S. et al. 2003; Catalano S. et al. 2004).

It has been reported that the antidiabetic thiazolidinediones inhibit leptin gene expression through ligand activation of PPARγ and exert antiproliferative and apoptotic effects on breast carcinoma (De Vos P. et al. 1996; Rieusset J. et al. 1999; Goetze S. et al. 2002; Lee JI. et al. 2007).

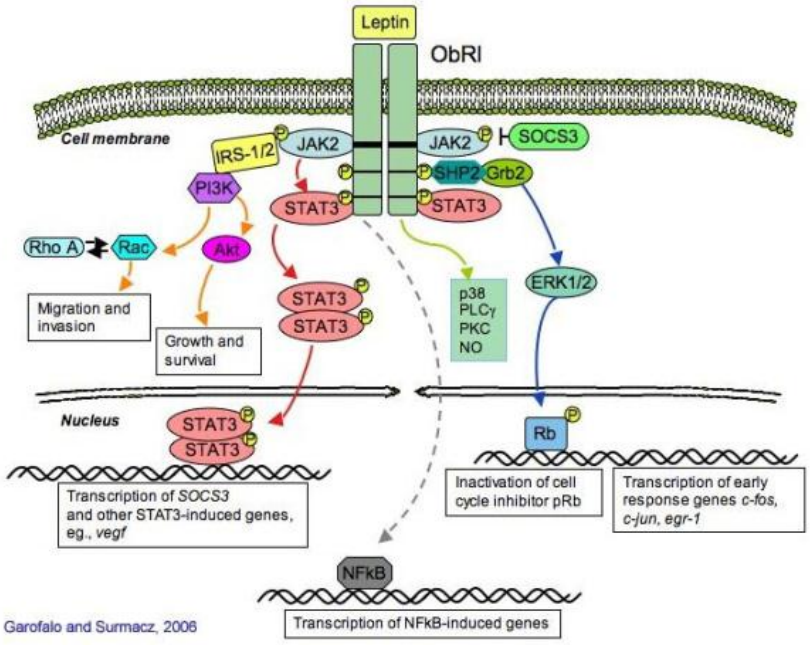

Figure 3. Leptin signaling

Our results have shown that activation of PPARγ prevented the development of leptin-induced MCF-7 tumor xenografts and inhibited the increased cell-cell aggregation and proliferation observed on leptin exposure. PPARγ ligands abrogated the leptin-induced up-regulation of leptin gene expression and its receptors in breast cancer. PPARγ-mediated repression of leptin gene involved the recruitment of nuclear receptor corepressor protein and silencing mediator of retinoid and thyroid hormone receptors corepressors on the glucocorticoid responsive element site in the leptin gene expression regulatory region in the presence of glucocorticoid receptor and PPARγ. In addition, PPARγ ligands inhibited leptin signaling mediated by MAPK/STAT3/Akt phosphorylation and counteracted leptin stimulatory effect on estrogen signaling.

Altogether these findings suggest that PPARγ ligands may have potential therapeutic benefits in the treatment of breast cancer, particulary in obese women.

Materials and Methods

Reagents

BRL 49653 (BRL) was purchased from Alexis (San Diego, CA USA) and solubilised in DMSO.

9-cis retinoic acid (9RA) was obtained from Sigma-Aldrich (Milan, Italy). 9RA was prepared just before use (Sigma-Aldrich) and diluted into medium at the indicated concentration. All experiments involving 9RA were performed under yellow light, and the tubes andculture plates containing 9RA were covered with aluminium foils.

The irreversible PPARγ-antagonist GW9662 (GW) and Cycloheximide (CX) were obtained from Sigma-Aldrich.

Human leptin was obtained from Invitrogen (Milan, Italy).

Plasmids

The p53 promoter-luciferase plasmids, kindly provided by Dr. Stephen H. Safe (Texas A&M University, College Station, TX), were generated from the human p53 gene promoter as follows: p53-1 (containing the - 1800 to + 12 region), p53-6 (containing the - 106 to + 12 region), p53-13 (containing the - 106 to + 40 region), and p53-14 (containing the - 106 to + 49 region) (Qin C. et al. 2002).

The pGL3 vector containing three copies of a peroxisome proliferator response element sequence upstream of the minimal thymidine kinase promoter ligated to a luciferase reporter gene (3XPPRE-TK-pGL3) was a gift from Dr. R. Evans (The Salk Institute, San Diego, CA).

The p53 antisense plasmid (AS/p53) was kindly provided from Dr. Moshe Oren (Weizmann Institute of Science, Rehovot, Israel).

The human wild-type p21WAF1/Cip1 promoter-luciferase (luc) reporter was a kind gift from Dr. T. Sakai (Kyoto Prefectural University of Medicine, Kyoto, Japan).

The pHEGO plasmid, encoding the full length of estrogen receptor α (ERα) cDNA, and the reporter plasmid XETL, a construct containing an estrogen-responsive element, were gifts from Dr. Didier Picard (University of Geneva, Geneva, Switzerland).

The plasmids containing the full-length human leptin promoter or its deletions were gifts from Dr. Marc Reitman (NIH, Bethesda, MD).

As internal transfection control, we cotransfected the plasmid pRLCMV (Promega Corp., Milan, Italy) that expresses Renilla luciferase enzymatically distinguishable from firefly luciferase by the strong cytomegalovirus enhancer promoter.

Cell Cultures

Wild-type human breast cancer MCF-7 cells were grown in Dulbecco's modified Eagle's medium-F12 plus glutamax containing 5% newborn calf serum (Invitrogen) and 1 mg/ml penicillin-streptomycin.

MCF-7 tamoxifen resistant (MCF-7TR1) breast cancer cells were generated in Dr. Fuqua's laboratory similar to that described by Herman maintaining cells in modified Eagle's medium with 10% fetal bovine serum (Invitrogen), 6 ng/ml insulin, penicillin (100 units/ml), streptomycin (100 µg/ml), and adding 4-hydroxytamoxifen in ten-fold increasing concentrations every weeks (from 10^{-9} to 10^{-6} final). Cells were thereafter routinely maintained with 1µmol/L 4-hydroxytamoxifen.

SKBR-3 breast cancer cells were grown in Dulbecco's modified Eagle's medium without red phenol, plus glutamax containing 10% fetal bovine serum and 1 mg/ml penicillin-streptomycin.

T-47D breast cancer cells were grown in RPMI 1640 medium with glutamax containing 10% fetal bovine serum, 1 mmol/L sodium pyruvate, 10 mmol/L HEPES, 2.5g/L glucose, 0.2 U/ml insulin, and 1 mg/ml penicillin-streptomycin.

MCF-10A normal breast epithelial cells were grown in Dulbecco's modified Eagle's medium-F12 plus glutamax containing 5% horse serum (Sigma), 1 mg/ml penicillin/streptomycin, 0.5 µg/ml hydrocortisone and 10 µg/ml insulin.

BT-20 and CHO cells were obtained from the American Type Culture Collection (Manassas, VA), were maintained in Dulbecco's modified Eagle's medium/ Ham's F-12 containing 5% fetal bovine serum (Sigma) supplemented with 1% L-glutamine and 1% penicillin/streptomycin (Sigma).

Cell Viability Assay

Cell viability was determined with the 3-(4,5-dimethylthiazol-2-yl)-2,5-diphenyltetrazolium (MTT) assay (Mosmann T. 1983).

Cells ($2x10^5$ cells/ml) were grown in 6 well plates and exposed to 100 nmol/L BRL, 50 nmol/L 9RA alone or in combination in serum free medium (SFM) and in 5% charcoal treated (CT)-fetal bovine serum; 100 µl of MTT (5 mg/ml) were added to each well, and the plates were incubated for 4 hours at 37°C. Then, 1 ml 0.04 N HCl in isopropanol was added to solubilize the cells. The absorbance was measured with the Ultrospec 2100 Pro-spectrophotometer (Amersham-Biosciences, Milan, Italy) at a test wavelength of 570 nm.

Immunoblotting

Cells were grown in to 70% to 80% confluence and exposed to treatments in SFM or in 1% charcoal treated (CT)-FBS as indicated.

To obtain cytosolic fraction of proteins cells were then harvested in cold PBS and resuspended in lysis buffer containing 20 mmol/L HEPES (pH 8), 0.1 mmol/L EGTA, 5 mmol/L MgCl2, 0.5 M/L NaCl, 20% glycerol, 1% Triton, and inhibitors (0.1 mmol/L sodium orthovanadate, 1% phenylmethylsulfonylfluoride, and 20 mg/ml aprotinin).

For total lysis cells were harvested in cold phosphate-buffered saline (PBS) and resuspended in total RIPA buffer containing 1% NP40, 0.5% Na-deoxycholate, 0.1% SDS plus inhibitors.

To obtain cytosolic and total mitochondrial fraction of proteins, cells were exposed to treatments as for 48 h and harvested by centrifugation at 2,500 rpm for 10 min at 4°C. The pellets were suspended in 250 µl of RIPA buffer plus 10 µg/ml aprotinin, 50 mM PMSF and 50 mM sodium orthovanadate and then 0.1% digitonine (final concentration) was added. Cells were incubated for 15 min at 4°C and centrifuged at 3,000 rpm for 10 min at 4°C, supernatants were collected and further centrifuged at 14,000 rpm for 10 min at 4°C. The supernatant, containing cytosolic fraction of proteins, was collected, while the resulting mitochondrial pellet was resuspended in 3% Triton X-100, 20 mM Na2SO4, 10 mM PIPES and 1 mM EDTA, pH 7.2, incubated for 15 min at 4°C and

centrifuged at 12,000 rpm for 10 min at 4°C. Alternatively, to provide matrix mitochondrial fraction of proteins, mitochondrial pellet was further solubilised in 6% of digitonine in RIPA buffer, for 10 min at 4°C then centrifuged at 14,000 rpm, 4°C, 10 min. The pellets (mitoplasts) were then lysed osmotically and centrifuged at 14,000 rpm 4°C 10 min to discard the membrane residues and recover the soluble matrix content.

Different proteins fractions were determined by Bio-Rad Protein Assay (Bio-Rad Laboratories). Equal amounts of cytosolic, total and mitochondrial proteins (40 μg) were resolved by 11% SDS-PAGE, electrotransferred to nitrocellulose membranes and probed with antibodies directed against p53, p21WAF1/Cip1, PARP, Bid, PPARγ, RXRα, Bad, Bcl-xL, pAKT, total AKT, pSTAT3, total AKT, total STAT, pGR, total GR (Santa Cruz Biotechnology), pERK (Cell Signaling Technology, Milan, Italy), total ERK (Cell Signaling Technology).

As internal control, all membranes were subsequently stripped (0.2 M glycine, pH 2.6, for 30 min at room temperature) of the first antibody and reprobed with anti-GAPDH antibody (Santa Cruz Biotechnology). The antigen-antibody complex was detected by incubation of the membranes for 1 h at room temperature with peroxidase-coupled goat anti-mouse or anti-rabbit IgG and revealed using the enhanced chemiluminescence system (Amersham Pharmacia, Buckinghamshire UK). Blots were then exposed to film (Kodak film, Sigma).

The intensity of bands representing relevant proteins was measured by Scion Image laser densitometry scanning program.

Reverse Transcription-PCR Assay

Cells were grown in 10 cm dishes to 70% to 80% confluence and exposed to treatments in SFM or in 1% CT-FBS as indicated.

Total cellular RNA was extracted using TRIZOL reagent (Invitrogen) as suggested by the manufacturer. The purity and integrity were checked spectroscopically and by gel electrophoresis before carrying out the analytical procedures.

Two micrograms of total RNA were reverse transcribed in a final volume of 20 µl using a RETROscript kit as suggested by the manufacturer (Promega). The cDNAs obtained were amplified by PCR using the following primers:

5'-CCAGTGTGATGATGGTGAGG-3' (p53 forward),

5'-GCTTCATGCCAGCTACTTCC-3' (p53 reverse),

5'-CTGTGCTCACTTCAGGGTCA-3' (p21 forward),

5'-CTCAACATCTCCCCCTTC–3' (p21 reverse),

5'-CGAGAAACGTTTCAGCATCT-3'(ObR Long isoform forward),

5'-CAAAAGCACACCACTCTCTC-3' (ObR Long isoform reverse),

5'- GAAGGAGTCGGAAAACCAAAG-3' (ObR Short isoform forward),

5'-CCACCATATGTTAACTCTCAG-3' (ObR Short isoform reverse),

5'-AGAGCCTTTGGATGACCAGAACAAGGTTCCCT-3' (Ob gene forward),

5'-TTACGAGAGAACTAACTGGAGAGCGACCTTT-3' (Ob gene reverse),

5'-AACAACAGGGTGGGCTTC-3' (cathepsin D forward),

5'-ATGCACGAAACAGATCTGTGCT-3'(cathepsin D reverse),

5'-TTCTATCCTAATACCATCGACG-3' (pS2 forward),

5'-TTTGAGTAGTCAAAGTCAGAGC-3'(pS2 reverse),

5'-TCTAAGATGAAGGAGACCATC-3' (cyclin D1 forward),

5'-GCGGTAGTAGGACAGGAAGTTGTT-3'(cyclin D1 reverse),

5'-CAAGGTTATTTTGATGCATGG-3' (P450arom forward),

5'-TTCTAAGGTTTGCGCATGA-3' (P450arom reverse),

5'-CTCAACATCTCCCCCTTCTC-3' (36B4 forward),

5'- CAAATCCCATATCCTCGTCC-3' (36B4 reverse).

The PCR was performed for 18 cycles for p53, 18 cycles for p21, 30 cycles for cathepsin D and cyclin D1; 35 cycles for ObRL, ObRS, Ob and P450arom; and for 15 cycles to amplify pS2 and 36B4 in the presence of 1 µl of first-strand cDNA, 1 µmol/L each primer, 0.5 mmol/L dNTPs, and TaqDNA polymerase (2 U per tube) (Promega. Corp) in a final volume of 25 µl. To check for the presence of DNA contamination, reverse transcription (RT)-PCR was performed on 2 µg of total RNA without Monoley murine leukemia virus reverse transcriptase (the negative control). The results obtained as optical density arbitrary values were

transformed to percentage of the control taking the samples from untreated cells as 100%.

Analysis of p53 and Bid gene expression was performed using Real-time reverse transcription PCR. cDNA was diluted 1:3 in nuclease-free water and 5 µl were analyzed in triplicates by real-time PCR in an iCycler iQ Detection System (Bio-Rad, USA) using SYBR Green Universal PCR Master Mix with 0.1 mmol/l of each primer in a total volume of 30 µl reaction mixture following the manufacturer's recommendations. Each sample was normalized on its GAPDH mRNA content. Relative gene expression levels were normalized to the basal, untreated sample chosen as calibrator.

Final results are expressed as folds of difference in gene expression relative to GAPDH mRNA and calibrator, calculated following the ΔCt method, as follows:

Relative expression (folds) = 2-(ΔCtsample - ΔCtcalibrator) where ΔCt values of the sample and calibrator were determined by subtracting the average Ct value of the GAPDH mRNA reference gene from the average Ct value of the analyzed gene. For p53, Bid and GAPDH the primers were: 5'-GCTGCTCAGATAGCG ATGGTC-3' (p53 forward) and 5-CTCCCAGGACAGGCACAAACA-3' (p53 reverse), 5'-CCATGGACTGTGAGGTCAAC-3' (Bid forward) and 5'-CTTTGG AGGAAGCCAAACAC-3' (Bid reverse), 5'-CCCACTCCTCCACCTTTGAC-3' (GAPDH forward), 5'-TGTTGCTGTAGCCAAATTCGT-3' (GAPDH reverse).

Negative controls contained water instead of first strand cDNA.

Transfection Assay

MCF-7 cells were transferred into 24-well plates with 500 µl of regular growth medium/well the day before transfection. The medium was replaced with 1% CT-FBS or SFM on the day of transfection, which was performed using Fugene 6 reagent as recommended by the manufacturer (Roche Diagnostics, Mannheim, Germany) with a mixture containing 0.5 µg of p53, p21 and leptin promoter-luc constructs or PPRE, XETL and HEGO reporter-luc plasmid plus 5 ng of pRL-CMV. After transfection for 24 h for promoter-luc plasmids and 6 h for reporter-luc plasmids, treatments were added as indicated. Firefly and Renilla luciferase activities were measured using the Dual Luciferase Kit (Promega). The firefly

luciferase values of each sample were normalized by Renilla luciferase activity and data were reported as relative light units.

MCF-7 cells plated into 10 cm dishes were transfected with 5 µg of AS/p53 using Fugene 6 reagent as recommended by the manufacturer (Roche Diagnostics). The activity of AS/p53 was verified using western blot to detect changes in p53 protein levels. Empty vector was used to ensure that DNA concentrations were constant in each transfection.

Electrophoretic Mobility Shift Assay

Nuclear extracts from MCF-7 cells were prepared as previously described (Andrews NC. et al. 1991). Briefly, MCF-7 cells plated into 10-cm dishes were grown to 70% to 80% confluence, shifted to SFM for 24 h, and then treated as indicated for 6 h. Thereafter, cells were scraped into 1.5 ml of cold PBS, pelleted for 10 sec, and resuspended in 400 µl cold buffer A (10 mmol/L HEPES-KOH [pH 7.9] at 4°C, 1.5 mmol/L MgCl2, 10 mmol/L KCl, 0.5 mmol/L dithiothreitol, 0.2 mmol/L phenylmethylsulfonyl fluoride, and 1 mmol/L leupeptin) by flicking the tube. Cells were allowed to swell on ice for 10 min and were then vortexed for 10 sec. Samples were then centrifuged for 10 sec and the supernatant fraction was discarded. The pellet was resuspended in 50 µl of cold Buffer B (20 mmol/L HEPES-KOH [pH 7.9], 25% glycerol, 1.5 mmol/L MgCl2, 420 mmol/L NaCl, 0.2 mmol/L EDTA, 0.5 mmol/L dithiothreitol, 0.2 mmol/L phenylmethylsulfonyl fluoride, and 1 mmol/L leupeptin) and incubated in ice for 20 min for high-salt extraction. Cellular debris was removed by centrifugation for 2 min at 4°C, and the supernatant fraction (containing DNA-binding proteins) was stored at -80°C.

The probe was generated by annealing single-stranded oligonucleotides and labeled with [32P]ATP (Amersham Pharmacia) and T4 polynucleotide kinase (Promega) and then purified using Sephadex G50 spin columns (Amersham Pharmacia). The DNA sequence of the nuclear factor (NFkB) located within p53 promoter as probe is 5'-AGTTGAGGGGACTTTCCCAGGC-3'.

The DNA sequences, located in leptin promoter, used as probe or as cold competitors were as follows:

GRE: 5'-ATGGTCTGATCTTGGCTCAC- 3' and

5’-GTGAGCCAAGATCAGACCAT-3’;
CRE: 5’-CACCGACGTCATTTGCAGTTCC-3’ and
5’-CACCGACAGCTTTTGCAGTTCC-3’;
Sp1: 5’-GAAAAACTCCGCCCTGGTAAAT-3’ and
5’-ATTTACCAGGCGCGGAGTTTTTC-3’ (Sigma Genosys, Cambridge, UK).
The protein-binding reactions were performed in 20 µl of buffer [20 mmol/L HEPES (pH 8), 1 mmol/L EDTA, 50 mmol/L KCl, 10 mmol/L dithiothreitol, 10% glycerol, 1 mg/ml bovine serum albumin, 50 µg/ml polydeoxyinosinic deoxycytidylic acid] with 50,000 cpm of labeled probe, 20 µg of MCF-7 nuclear protein, and 5 µg of polydeoxyinosinic deoxycytidylic acid. The mixtures were incubated at room temperature for 20 min in the presence or absence of unlabeled competitor oligonucleotides.
The specificity of the binding was tested by adding to the mixture the reaction-specific antibodies anti-PPARγ, anti-RXR, anti-GR, anti Sp1 and anti CREB (Santa Cruz Biotechnology). The reaction mixture was incubated with these antibodies at 4°C for 30 min before addition of labeled probe. The entire reaction mixture was electrophoresed through a 6% polyacrylamide gel in 0.25x Tris borate-EDTA for 3 h at 150 V. Gel was dried and subjected to autoradiography at -80°C.

Chromatin Immunoprecipitation Assay

MCF-7 cells were grown in 10 cm dishes to 50% to 60% confluence, shifted to SFM for 24 h, and then treated for 1 h as indicated. Thereafter, cells were washed twice with PBS and cross-linked with 1% formaldehyde at 37°C for 10 min. Next, cells were washed twice with PBS at 4°C, collected and resuspended in 200 µl of lysis buffer (1% SDS, 10 mmol/L EDTA, 50 mmol/L Tris-HCl, pH 8.1), and left on ice for 10 min. Then, cells were sonicated four times for 10 sec at 30% of maximal power (Vibra Cell 500 W; Sonics and Materials, Inc., Newtown, CT) and collected by centrifugation at 4°C for 10 min at 14,000 rpm. The supernatants were diluted in 1.3 ml of immunoprecipitation buffer (0.01% SDS, 1.1% Triton X-100, 1.2 mmol/L EDTA, 16.7 mmol/L Tris-HCl [pH 8.1], 16.7 mmol/L NaCl) followed by immunoclearing with 60 µl of sonicated salmon sperm DNA/protein

A agarose (DBA Srl, Milan, Italy) for 1 h at 4°C. The precleared choromatin was immunoprecipitated with anti-PPARγ, anti-RXR, anti-GR or anti-RNA Pol II antibodies (Santa Cruz Biotechnology). At this point, 60 µl salmon sperm DNA/protein A agarose was added, and precipitation was further continued for 2 h at 4°C. After pelleting, precipitates were washed sequentially for 5 min with the following buffers: Wash A [0.1% SDS, 1% Triton X-100, 2 mmol/L EDTA, 20 mmol/L Tris-HCl (pH 8.1), 150 mmol/L NaCl]; Wash B [0.1% SDS, 1% Triton X-100, 2 mmol/L EDTA, 20 mmol/L Tris-HCl (pH 8.1), 500 mmol/L NaCl]; and Wash C [0.25 M/L LiCl, 1% NP-40, 1% sodium deoxycholate, 1 mmol/L EDTA, 10 mmol/L Tris-HCl (pH 8.1)], and then twice with 10 mmol/L Tris, 1 mmol/L EDTA. The immunocomplexes were eluted with elution buffer (1% SDS, 0.1 M/L NaHCO3) or with re-chip buffer and were re-immunoprecipitated with anti-PPARγ, anti-NCoR, or anti-SMRT antibodies. Normal mouse serum IgG was used as negative control.

The eluates were reverse cross-linked by heating at 65°C and digested with proteinase K (0.5 mg/ml) at 45°C for 1 h. DNA was obtained by phenolchloroform-isoamyl alcohol extraction. Two microliters of 10 mg/ml yeast tRNA (Sigma) were added to each sample, and DNA was precipitated with 95% ethanol for 24 h at -20°C and then washed with 70% ethanol and resuspended in 20 µl of 10 mmol/L Tris, 1 mmol/L EDTA buffer. A 5 µl volume of each sample was used for PCR with primers flanking a sequence present in the p53 promoter: 5'-CTGAGAGCAAACGCAAAAG-3' (forward) and 5-CAGCCCGAACGCAAAGTGTC- 3 (reverse) containing the NFkB site while the primers flanking GRE sequence present in the leptin promoter region:were 5'-GCCCAGGCTGTAGTGCAAT-3' and 5'-TAGCCAGGTGTGGTGG-3'.

The PCR conditions for the p53 promoter fragments were 45 sec at 94°C, 40 sec at 57°C, and 90 sec at 72°C. The amplification products obtained in 30 cycles were analyzed in a 2% agarose gel and visualized by ethidium bromide staining. The negative control was provided by PCR amplification without a DNA sample. The specificity of reactions was ensured using normal mouse and rabbit IgG (Santa Cruz Biotechnology).

JC-1 Mitochondrial Membrane Potential

The loss of mitochondrial membrane potential was monitored with the dye 5, 5',6 , 6' tetra-chloro-1, 1', 3, 3'- tetraethylbenzimidazolyl-carbocyanine iodide (JC-1) (Biotium, Hayward). In healthy cells, the dye stains the mitochondria bright red. The negative charge established by the intact mitochondrial membrane potential allows the lipophilic dye, bearing a delocalized positive charge, to enter the mitochondrial matrix where it aggregates and gives red fluorescence. In apoptotic cells, the mitochondrial membrane potential collapses, and the JC-1 cannot accumulate within the mitochondria, it remains in the cytoplasm in a green fluorescent monomeric form (Cossarizza A. et al. 1993). MCF-7, SKBR-3 and T-47D cells were grown in 10 cm dishes, transfected with control RNAi or Bid RNAi and then treated with 100 nmol/L BRL and/or 50 nmol/L 9RA as indicated, then cells were washed in ice-cold PBS, and incubated with 10 mmol/L JC-1 at 37°C in a 5% CO2 incubator for 20 minutes in darkness. Subsequently, cells were washed twice with PBS and analyzed by fluorescence microscopy.

The red form has absorption/emission maxima of 585/590 nm. The green monomeric form has absorption/emission maxima of 510/527 nm. Both healthy and apoptotic cells can be visualized by fluorescence microscopy using a wide band-pass filter suitable for detection of fluorescein and rhodamine emission spectra.

Cytochrome C Detection

Cytochrome C was detected by western blotting in mitochondrial and cytoplasmatic fractions. Cells were harvested by centrifugation at 2,500 rpm for 10 minutes at 4°C. The pellets were suspended in 36 µl RIPA buffer plus 10 µg/ml aprotinin, 50 mmol/L PMSF and 50 mmol/L sodium orthovanadate and then 4 µl of 0.1% digitonine were added. Cells were incubated for 15 minutes at 4°C and centrifuged at 12,000 rpm for 30 minutes at 4°C. The resulting mitochondrial pellet was resuspended in 3% Triton X-100, 20 mmol/L Na2SO4, 10 mmol/L PIPES, 1 mmol/L EDTA (pH 7.2) and centrifuged at 12,000 rpm for 10 minutes at 4°C. Proteins of the mitochondrial and cytosolic fractions were determined by Bio-Rad Protein Assay (Bio-Rad Laboratories).

Equal amounts of protein (40 µg) were resolved by 15% SDS-polyacrylamide gel electrophoresis, electrotransferred to nitrocellulose membranes, and probed with an antibody directed against the cytochrome C (Santa Cruz Biotechnology). Then, membranes were subjected to the same procedures described for immunoblotting.

DNA Fragmentation

DNA fragmentation was determined by gel electrophoresis. MCF-7 cells were grown in 10 cm dishes to 70% confluence and exposed to treatments. After 56 h cells were collected, washed with PBS and pelleted at 1,800 rpm for 5 min. The samples were resuspended in 0.5 ml of extraction buffer (50 mmol/L Tris-HCl, pH 8; 10 mmol/L EDTA, 0.5% SDS) for 20 min in rotation at 4°C. DNA was extracted three times with phenol- chloroform and one time with chloroform. The aqueous phase was used to precipitate nucleic acids with 0.1 volumes of 3M sodium acetate and 2.5 volumes cold ethanol overnight at 20°C. The DNA pellet was resuspended in 15 µl of H2O treated with RNase A for 30 min at 37°C. The absorbance of the DNA solution at 260 and 280 nm was determined by spectrophotometry. The extracted DNA (40 µg/lane) was subjected to electrophoresis on 1.5% agarose gels. The gels were stained with ethidium bromide and then photographed.

RNA interference (RNAi).

Cells were plated in 10 cm dishes with regular growth medium the day before transfection to 60–70% confluence. On the second day the medium was changed with 1% CT-FBS or SFM without P/S and cells were transfected with stealth RNAi targeted human Bid mRNA sequence -5'-UGCGGUUGCCAUCAGUCUGCA GCUC-3' (Invitrogen), with a stealth RNAi targeted human PPARγ mRNA sequence 5'-AGAAUAAUAAGGUGGAGAUGCAGGC-3' (Invitrogen), a stealth RNAi targeted human RXRα mRNA sequence 5'-UCGUCCUCUUUAACCCUG ACUCCAA-3' or with a stealth RNAi-negative control (Invitrogen) to a final concentration of 100 nM using Lipofectamine 2000 (Invitrogen) as recommended by the manufacturer. After 5 h the transfection medium was changed with

complete 1% CT-FBS or SFM with P/S in order to avoid Lipofectamine 2000 toxicity, cells were exposed to treatments and subjected to different experiments.

Flow Cytometry Assay

MCF-7 cells (1 x 10^6 cells/well) were grown in 6 well plates and shifted to SFM for 24 h before adding treatments for 48 h. Thereafter, cells were trypsinized, centrifuged at 3,000 rpm for 3 min and washed with PBS. Addition of 0.5 µl of fluorescein isothiocyanate-conjugated antibodies, anti-caspase 9 and anti-caspase 8 (Calbiochem, Milan, Italy), in all samples was performed and then incubated for 45 min in at 37°C. Cells were centrifuged at 3,000 rpm for 5 min, the pellets were washed with 300 µl of wash buffer and centrifuged. The last passage was repeated twice, the supernatant removed, and cells dissolved in 300 µl of wash buffer. Finally, cells were analyzed with the FACScan (Becton Dickinson and Co., Franklin Lakes, NJ).

GST antioxidant enzyme activity and lipid peroxidation.

To measure mitochondrial glutathione S-transferase (GST) activity the mitochondrial suspension was used. Enzyme activity was detected according to the method provided by the manufacturer (Sigma Aldrich). To evaluate lipid peroxidation cells were sonicated in PBS and the crude homogenate was used. The level of lipid peroxidation in control as well as treated cell samples was assayed through the formation of thiobarbituric acid reactive species (TBARS) during an acid-heating reaction as previously described in reference 33. Briefly, the samples were mixed with 1 ml of 10% trichloroacetic acid (TCA) and 1 ml of 0.67% thiobarbituric acid (TBA), then heated in a boiling water bath for 15 min. TBARS were determined by the absorbance at 535 nm and were expressed as malondialdehyde equivalents (MDA) (nmol/mg protein) respect to cellular and mitochondrial.

Site-Directed Mutagenesis

The leptin promoter plasmid-bearing glucocorticoid responsive element–mutated site (p1775 GRE mut) was created by site-directed mutagenesis using a Quik Change kit (Stratagene, La Jolla, CA) and as template the human leptin promoter p1775. The mutagenic primers were 5'-CCAGGCTGTAGTGCAATGGTCT**tgc**CTTGGCTCACTGCAACC-3' and 5'-GGTTGCAGTGAGCCAAG**gca**AGACCATTGCACTACAGCCTGG-3'. Mutations are shown as italic and lower case letters. The constructed reporter vector was confirmed by DNA sequencing.

In Vivo Experiments

Female 45-day-old athymic nude mice (nu/nu Swiss; Charles River Laboratories, Milan, Italy) were maintained in a sterile environment. At day 0, estradiol pellets (1.7 mg per pellet, 90-day release; Innovative Research of America, Sarasota, FL) were subcutaneously implanted into the intrascapular region of the mice. The next day, MCF-7 cells (5.0×10^6 cells per mouse) were inoculated subcutaneously in 0.1 mL of Matrigel (BD Biosciences, Bedford, MA).

Leptin treatment was performed as previously described (Mauro L. et al. 2007). When the tumors reached 0.2 cm^3 (ie, in 4 weeks), the animals received rosiglitazone (10 mg/kg/day) in drinking tap water (Avandia, GlaxoSmith Kline, Middlesex, UK) for 8 weeks. MCF-7 xenograft tumor growth was monitored twice a week by caliper measurements, and tumor volumes (in cubic centimeters) were estimated by the following formula: TV = a (b2)/2, where a and b are tumor length and width, respectively, in centimeters. At week 12, blood samples were collected from the mice, and the animals were sacrificed following standard protocols; the tumors were dissected from the neighboring connective tissue, frozen in nitrogen, and stored at -80°C for further analyses. After blood centrifugation, plasma was collected and kept at -80°C for analyses. Plasma leptin concentration was measured using a commercially available mouse and rat leptin enzyme-linked immunosorbent assay kit (BioVendor, Heidelberg, Germany). All the procedures involving animals and their care were conducted in accordance

with the institutional guidelines and regulations at the Laboratory of Molecular Oncogenesis, Regina Elena Cancer Institute, Rome, Italy.

Histologic Analysis

Tumors, livers, lungs, spleens, and kidneys were fixed in 4% formalin, sectioned at 5 μm, and stained with hematoxylin and eosin Y (Bio-Optica, Milan, Italy). The epithelial nature of the tumors was verified by immunostaining with mouse monoclonal antibody directed against human cytokeratin 18 (Santa Cruz Biotechnology, Milan, Italy), and nuclei were counter stained with hematoxylin. For negative controls, non immune serum replaced the primary antibody.

Three-Dimensional Spheroid Culture and Cell Growth Assays

For three-dimensional cultures, MCF-7 and BT-20 cells plated on 2% agar–coated plates were treated with 1000 ng/mL of leptin (Invitrogen, Carlsbad, CA) and/or 10 μmol/L BRL (Alexis) and 10 μmol/L 15-deoxy-12,14-prostaglandin J2 (PGJ2) (Sigma). After 48 h, three-dimensional cultures were photographed using a phase-contrast microscope (Olympus, Milan, Italy). The extent of aggregation and cell numbers were evaluated as previously reported. (Mauro L. et al. 2007).

[3H]Thymidine Incorporation Assays

MCF-7 and BT-20 cells were treated with leptin (1000 ng/mL) and/or BRL (10 μmol/L) and PGJ2 (10 μmol/L) for 48 h and were pretreated for 2 h with GW9662 (10 μmol/L; Sigma) or transfected with RNA interference (RNAi) for PPARγ where necessary. The assay was performed as previously reported. (Catalano S. et al. 2003).

Statistical Analysis

Statistical analysis was performed using analysis of variance followed by Newman-Keuls testing to determine differences in means. $P < 0.05$ was considered as statistically significant.

Results

Nanomolar concentrations of the combined BRL and 9RA treatment affect cell viability in breast cancer cells

Previous studies demonstrated that micromolar doses of PPARγ ligand BRL and RXR ligand 9RA exert antiproliferative effects on breast cancer cells (Mehta RG. et al. 2000; Elstner E. et al. 2002; Crowe DL. et al. 2004; Bonofiglio D. et al. 2005). First, we tested the effects of increasing concentrations of both ligands on breast cancer cell proliferation at different times in the presence or absence of serum media (data not shown).

Thus, to investigate whether low doses of combined agents are able to inhibit cell growth, we assessed the capability of 100 nmol/L BRL and 50 nmol/L 9RA to affect normal and malignant breast cell lines. We observed that treatment with BRL alone does not elicit any significant effect on cell viability in all breast cell lines tested, while 9RA alone reduces cell vitality only in T47-D cells (Figure 4A). In the presence of both ligands, cell viability is strongly reduced in all breast cancer cells: MCF-7, its variant MCF-7TR1, SKBR-3, and T-47D; while MCF-10A normal breast epithelial cells are completely unaffected (Figure 4A). In MCF-7 cells the effectiveness of both ligands in reducing tumor cell viability still persists in SFM, as well as in 5% CT-FBS (Figure 4B).

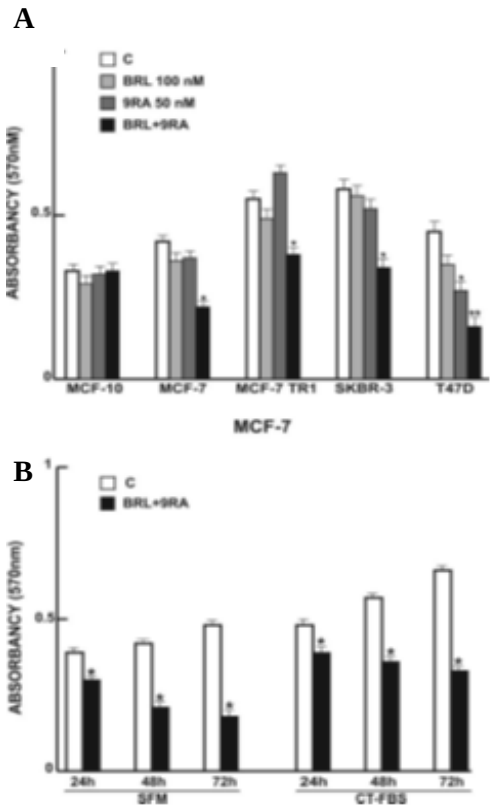

Figure 4. Cell vitality in breast cell lines. (A): Breast cells were treated for 48 h in SFM in the presence of 100 nmol/L BRL or/and 50 nmol/L. 9RA. Cell vitality was measured by MTT assay. Data are presented as mean ± SD of three independent experiments done in triplicate. **(B):** MCF-7 cells were treated for 24, 48, and 72 h with 100 nmol/L BRL and 50 nmol/L 9RA in the presence of SFM and 5% CT-FBS. *P < 0.05 and **P < 0.01 treated versus untreated cells

BRL and 9RA up-regulate p53 and p21WAF1/Cip1 expression in MCF-7 cells

Our recent work demonstrated that micromolar doses of BRL activate PPARγ, which in turn triggers apoptotic events through an up-regulation of p53 expression (Bonofiglio D. et al. 2006). On the basis of these results, we evaluated the ability of nanomolar doses of BRL and 9RA alone or in combination to modulate p53 expression along with its natural target gene p21WAF1/Cip1 in MCF-7 cells. A significant increase in p53 and p21WAF1/Cip1 content was observed by western blot only on combined treatment after 24 and 36 h (Figure 5A). Furthermore, we showed an upregulation of p53 and p21WAF1/Cip1 mRNA levels induced by BRL plus 9RA after 12 and 24 h (Figure 5B).

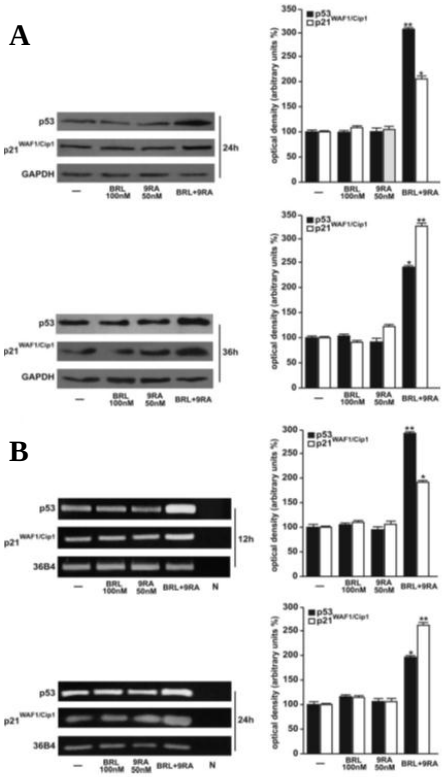

Figure 5. Upregulation of p53 and p21WAF1/Cip1 expression induced by BRL plus 9RA in MCF-7 cells. (A): Immunoblots of p53 and p21WAF1/Cip1 from extracts of MCF-7 cell treated with 100 nmol/L BRL and 50 nmol/L 9RA alone or in combination for 24 and 36 h. GAPDH was used as loading control. The side panels show the quantitative representation of data (mean ± SD) of three independent experiments after densitometry. **(B):** p53 and p21WAF1/Cip1 mRNA expression in MCF-7 cells treated as in A for 12 and 24 h. The side panels show the quantitative representation of data (mean ± SD) of three independent experiments after densitometry and correction for 36B4 expression. *P < 0.05 and **P < 0.01 combined-treated versus untreated cells. N: RNA sample without the addition of reverse transcriptase (negative control).

Low Doses of PPARγ and RXRα ligands transactivate p53 gene promoter

To investigate whether low doses of BRL and 9RA are able to transactivate the p53 promoter gene, we transiently transfected MCF-7 cells with a luciferase reporter construct (named p53-1) containing the upstream region of the p53 gene spanning from -1800 to + 12 (Figure 6A). Treatment for 24 h with 100 nmol/L BRL or 50 nmol/L 9RA did not induce luciferase expression, whereas the presence of both ligands increased in the transactivation of p53-1 promoter (Figure 6B). To identify the region within the p53 promoter responsible for its transactivation, we used constructs with deletions to different binding sites such as CTF-1, nuclear factor-Y, NFkB, and GC sites (Figure 6A). In transfection experiments performed using the mutants p53-6 and p53-13encoding the regions from - 106 to + 12 and from - 106 to + 40, respectively, the responsiveness to BRL plus 9RA was still observed (Figure 6B). In contrast, a construct with a deletion in the NFkB domain (p53-14) encoding the sequence from - 106 to + 49, the transactivation of p53 by both ligands was absent (Figure 6B), suggesting that NFkB site is required for p53 transcriptional activity.

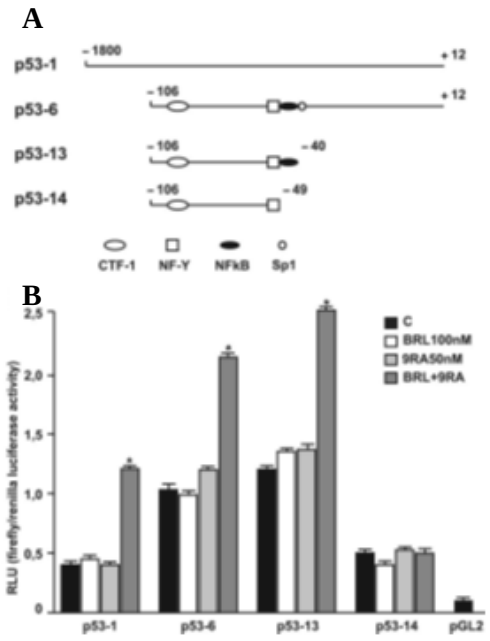

Figure 6. BRL and 9RA transactivate p53 promoter gene in MCF-7 cells. (A): Schematic map of the p53 promoter fragments used in this study. **(B):** MCF-7 cells were transiently transfected with p53 gene promoter-luc reporter constructs (p53-1, p53-6, p53-13, p53-14) and treated for 24 h with 100 nmol/L BRL and 50 nmol/L 9RA alone or in combination. The luciferase activities were normalized to the Renilla luciferase as internal transfection control and data were reported as RLU values. Columns are mean ± SD of three independent experiments performed in triplicate. *P < 0.05 combined-treated versus untreated cells. pGL2: basal activity measured in cells transfected with pGL2 basal vector; RLU, relative light units; CTF-1, CCAAT-binding transcription factor-1; NF-Y, nuclear factor-Y; NFkB, nuclear factor kB.

Heterodimer PPARγ/RXRα binds to NFkB sequence in Electrophoretic Mobility Shift Assay and in Chromatin Immunoprecipitation Assay

To gain further insight into the involvement of NFkB site in the p53 transcriptional response to BRL plus 9RA, we performed electrophoretic mobility shift assay experiments using synthetic oligodeoxyribonucleotides corresponding to the NFkB sequence within p53 promoter. We observed the formation of a specific DNA binding complex in nuclear extracts from MCF-7 cells (Figure 7A, lane 1), where specificity is supported by the abrogation of the complex by 100-fold molar excess of unlabeled probe (Figure 7A, lane 2). BRL treatment induced a slight increase in the specific band (Figure 7A, lane 3), while no changes were observed on 9RA exposure (Figure 7A, lane 4). The combined treatment increased the DNA binding complex (Figure 7A, lane 5), which was

immunodepleted and supershifted using anti-PPARγ (Figure 7A, lane 6) or anti-RXRα (Figure 7A, lane 7) antibodies. These data indicate that heterodimer PPARγ/RXRα binds to NFkB site located in the promoter of p53 in vitro.

The interaction of both nuclear receptors with the p53 promoter was further elucidated by chromatin immunoprecipitation assays. Using anti-PPARγ and anti-RXRα antibodies, protein-chromatin complexes were immunoprecipitated from MCF-7 cells treated with 100 nmol/L BRL and 50 nmol/L 9RA. PCR was used to determine the recruitment of PPARγ and RXRα to the p53 region containing the NFkB site. The results indicated that either PPARγ or RXRα was constitutively bound to the p53 promoter in untreated cells and this recruitment was increased on BRL plus 9RA exposure (Figure 7B). Similarly, an augmented RNA-Pol II recruitment was obtained by immunoprecipitating cells with an anti-RNA-Pol II antibody, indicating that a positive regulation of p53 transcription activity was induced by combined treatment (Figure 7B).

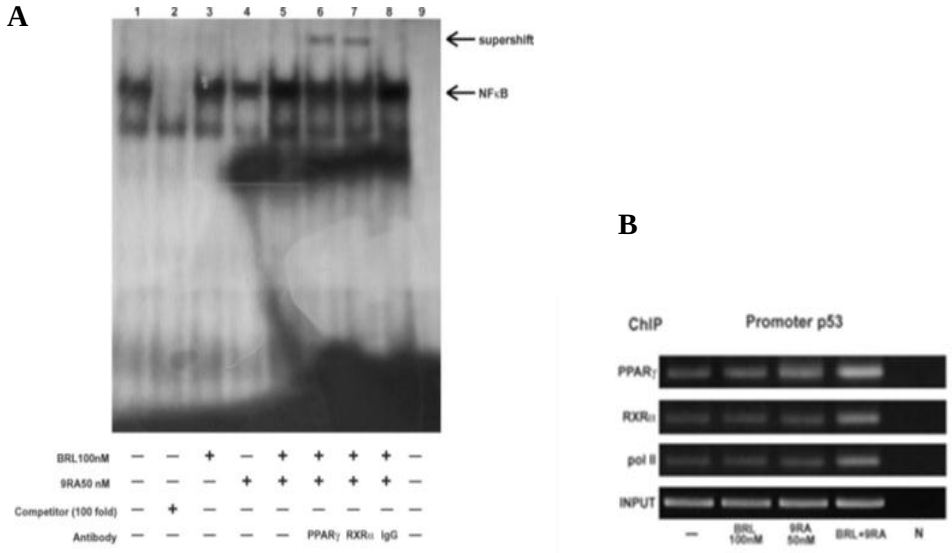

Figure 7. PPARγ/RXRα binds to NFkB sequence in electrophoretic mobility shift assay and in chromatin immunoprecipitation assay. (A): Nuclear extracts from MCF-7 cells (lane 1) were incubated with a double-stranded NFkB consensus sequence probe labeled with [32P] and subjected to electrophoresis in a 6% polyacrylamide gel. Competition experiments were done, adding as competitor a 100-fold molar excess of unlabeled probe (lane 2). Nuclear extracts from MCF-7 were treated with 100 nmol/L BRL (lane 3), 50 nmol/L 9RA (lane 4), and in combination (lane5). Anti-PPARγ (lane 6), anti-RXRα (lane 7), and IgG (lane 8) antibodies were incubated. Lane 9 contains probe alone. **(B):** MCF-7 cells were treated for 1 h with 100 nmol/L BRL and/or 50 nmol/L

9RA as indicated, and then cross-linked with formaldehyde and lysed. The soluble chromatin was immunoprecipitated with anti-PPARγ, anti-RXRα, and anti-RNA Pol II antibodies. The immunocomplexes were reverse cross-linked, and DNA was recovered by phenol/chloroform extraction and ethanol precipitation. The p53 promoter sequence containing NFkB was detected by PCR with specific primers. To control input DNA, p53 promoter was amplified from 3µl of initial preparations of soluble chromatin (before immunoprecipitation). N: negative control provided by PCR amplification without DNA sample.

BRL and 9RA induce mitochondrial membrane potential disruption and release of cytochrome C from mitochondria into the cytosol in MCF-7 cells

The role of p53 signaling in the intrinsic apoptotic cascades involves a mitochondria-dependent process, which results in cytochrome C release and activation of caspase-9. Because disruption of mitochondrial integrity is one of the early events leading to apoptosis, we assessed whether BRL plus 9RA could affect the function of mitochondria by analyzing membrane potential with a mitochondria fluorescent dye JC-1 (Smiley ST. et al. 1991, Crowe DL. et al. 2004). In non-apoptotic cells (control) the intact mitochondrial membrane potential allows the accumulation of lipophilic dye in aggregated form in mitochondria, which display red fluorescence (Figure 8A).

MCF-7 cells treated with 100 nmol/L BRL or 50 nmol/L 9RA exhibit red fluorescence indicating intact mitochondrial membrane potential (data not shown). Cells treated with both ligands exhibit green fluorescence, indicating disrupted mitochondrial membrane potential, where JC-1 cannot accumulate within the mitochondria, but instead remains as a monomer in the cytoplasm (Figure 8A). Concomitantly, cytochrome C release from mitochondria into the cytosol, a critical step in the apoptotic cascade, was demonstrated after combined treatment (Figure 8B).

A

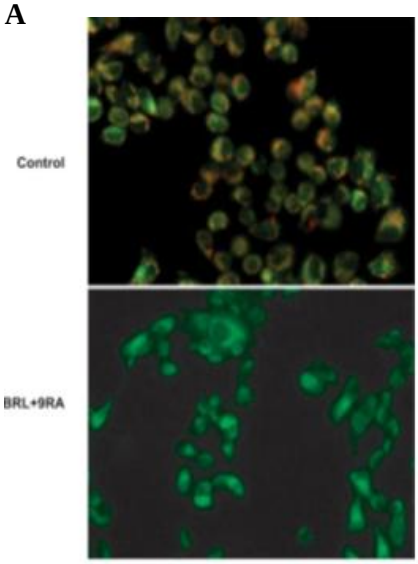

Figure 8. Mitochondrial membrane potential disruption and release of cytochrome C induced by BRL and 9RA in MCF-7 cells. (A): MCF-7 cells were treated with 100 nmol/L BRL plus 50 nmol/L 9RA for 48 h and then used fluorescent microscopy to analyze the results of JC-1 (5,5',6,6'- tetrachloro-1,1',3,3'tetraethylbenzimidazolylcarbocy anine iodide) kit. In control non apoptotic cells, the dye stains the mitochondria red. In treated apoptotic cells, JC-1 remains in the cytoplasm in a green fluorescent form. **(B):** MCF-7 cells were treated for 48 h with 100 nmol/L BRL and/or 50 nmol/L 9RA. GAPDH was used as loading control.

B

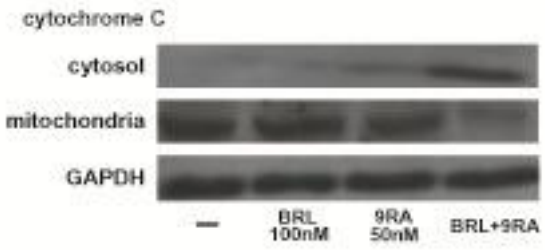

Caspase-9 cleavage and DNA fragmentation induced by BRL plus 9RA in MCF-7 cells

BRL and 9RA at nanomolar concentration did not induce any effects on caspase-9 separately, but activation was observed in the presence of both compounds (Table 1). No effects were elicited by either the combined or the separate treatment on caspase-8 activation, a marker of extrinsic apoptotic pathway (Table 1).

Table 1. Activation of caspase 9 in MCF-7 cells

	% Activation	SD
Caspase 9		
Control	**14,16**	**±5,65**
BRL 100nM	**17,23**	**±1,678**
9RA 50nM	**18,4**	**±0,986**
BRL+9RA	**33,8 ***	**±5,216**
Caspase 8		
Control	**9,20**	**±1,430**
BRL 100nM	**8,12**	**±1,583**
9RA 50nM	**7,90**	**±0,886**
BRL+9RA	**10,56**	**±2,160**

Since internucleosomal DNA degradation is considered a diagnostic hallmark of cells undergoing apoptosis, we studied DNA fragmentation under BRL plus 9RA treatment in MCF-7 cells, observing that the induced apoptosis was prevented by either the PPARγ-specific antagonist GW or by AS/p53, which is able to abolish p53 expression (Figure 9A).

To test the ability of low doses of both BRL and 9RA to induce transcriptional activity of PPARγ, we transiently transfected a peroxisome proliferator response element reporter gene in MCF-7 cells and observed an enhanced luciferase activity, which was reversed by GW treatment (data not shown). These data are in agreement with previous observations demonstrating that PPARγ/RXRα heterodimerization enhances DNA binding and transcriptional activation (Kliewer SA. et al. 1992; Zhang XK. et al. 1992).

Finally, we examined in three additional human breast malignant cell lines: MCF-7TR1, SKBR-3, and T-47D the capability of low doses of a PPARγ and an RXRα ligand to trigger apoptosis. DNA fragmentation assay showed that only in the presence of combined treatment did cells undergo apoptosis in a p53-mediated manner (Figure 9B), implicating a general mechanism in breast carcinoma.

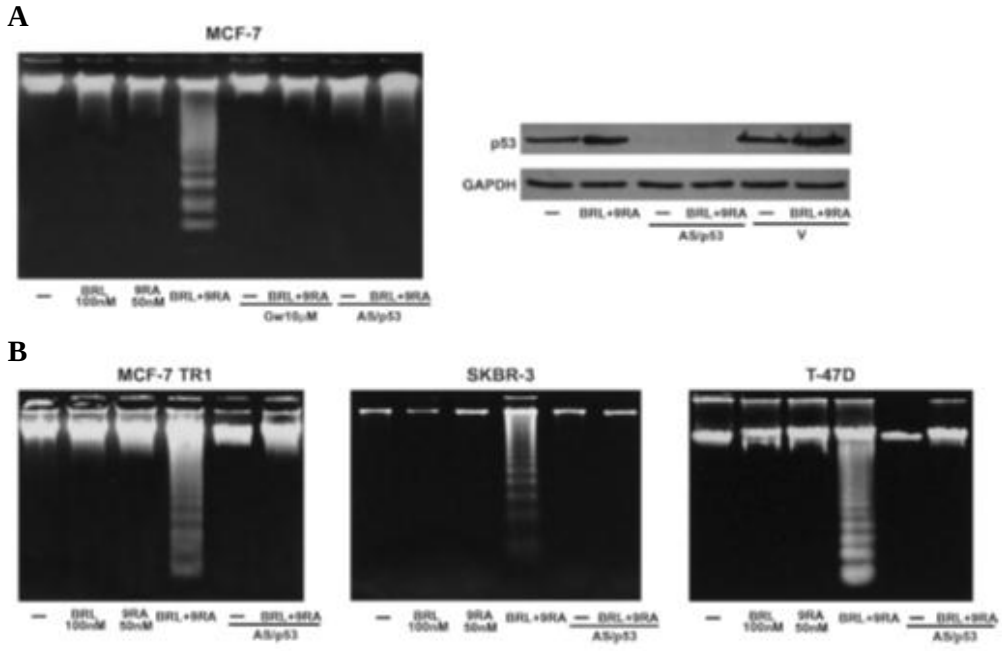

Figure 9. Combined treatment of BRL and 9RA trigger apoptosis in breast cancer cells. (A): DNA laddering was performed in MCF-7 cells transfected and treated as indicated for 56 h. One of three similar experiments is presented. The side panel shows the immunoblot of p53 from MCF-7 cells transfected with an expression plasmid encoding for p53 antisense (AS/p53) or empty vector (v) and treated with 100 nmol/L BRL plus 50 nmol/L 9RA for 56 h. GAPDH was used as loading control. **(B):** DNA laddering was performed in MCF-7TR1, SKBR-3, and T47-D cells transfected with AS/p53 or empty vector (v) and treated as indicated. One of three similar experiments is presented.

p53 and p21 expression upon combined low doses of BRL plus 9RA in breast cancer cells.

On the basis of the above-mentioned results, we aimed to examine the potential ability of nanomolar concentrations of BRL and 9RA to modulate p53 and its natural target gene p21WAF1/Cip1 in MCF-7, SKBR-3 and T-47D breast cancer cells. We revealed that only the combination of both ligands enhanced p53 expression in all breast cancer cells tested in terms of mRNA and protein content, while the increased expression of p21WAF1/Cip1 was highlighted only in MCF-7 cells (Fig. 10A–E), suggesting that p53 mutated form in the other two cell lines tested does not exhibit any transactivation properties. Moreover, as expected we did not observe in SKBR-3 and T-47D cells any modulation of the human wild-

type p21WAF1/Cip1 promoter luciferase activity upon nanomolar concentrations of BRL and 9RA alone or in combination (data not shown), even though PPARγ can mediate the upregulation of p21WAF1/Cip1 independently of p53 (Chung SH. et al. 2002; Hong J. et al. 2004; Bonofiglio D. et al. 2008).

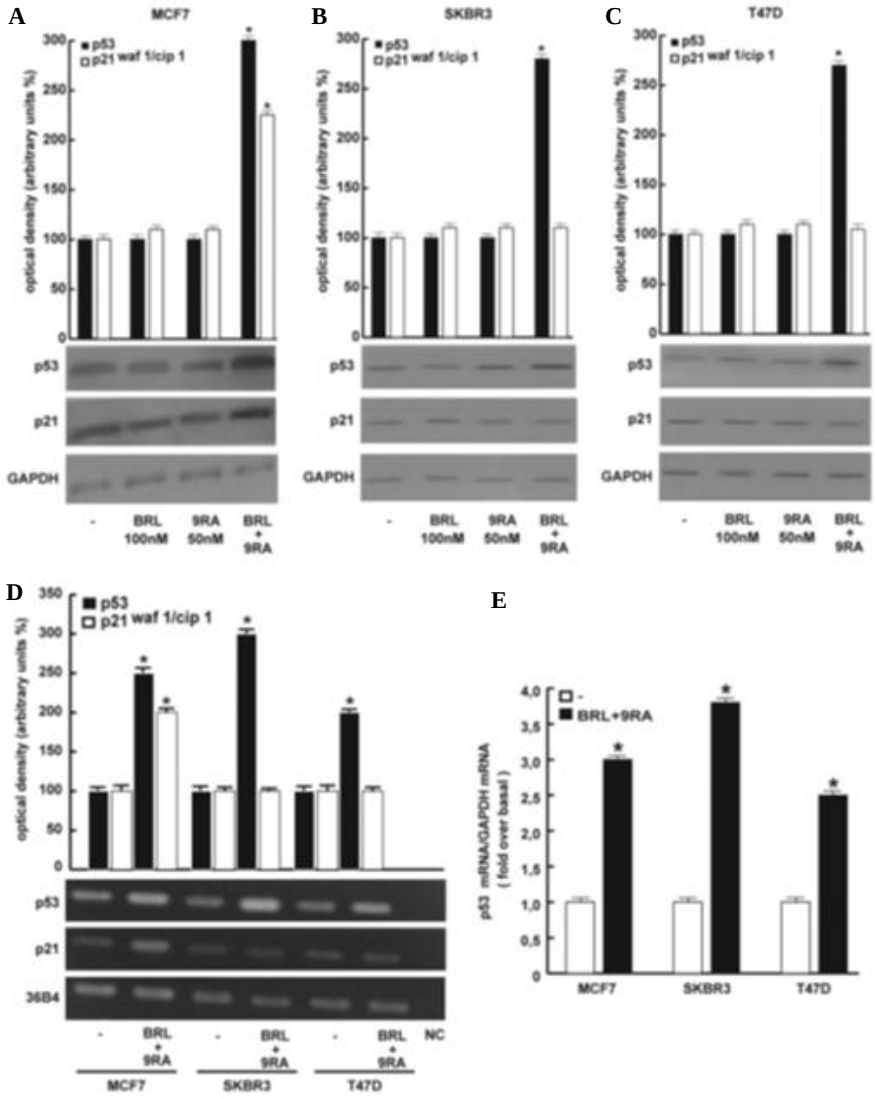

Figure 10. Combined low doses of BRL and 9RA upregulate p53 expression in MCF-7, SKBR-3 and T-47D breast cancer cells.
(A–C) Immunoblots of p53 and p21 from extracts of MCF-7, SKBR-3 and T-47D cells untreated (-) or treated with 100 nM BRL and/or 50 nM 9RA for 24 h. GAPDH was used as loading control. The histograms show the quantitative representation of data (mean ± SD) of three independent experiments in which band intensities were evaluated in terms of optical density arbitrary units and expressed as percentages of the control which was assumed to be 100%. **(D)** p53 and p21 mRNA expression in MCF-7, SKBR-3 and T-47D cells untreated (-) or treated with 100 nM BRL plus 50 nM 9RA for 12 h. The histograms show the quantitative representation of data (mean ± SD) of three independent experiments after densitometry and correction for 36B4 expression and expressed as percentages of the control which was assumed to be 100%. **(E)** Quantitative real-time

PCR analysis of p53 mRNA expression in MCF-7, SKBR-3 and T-47D cells treated as in (D). The histograms show the quantitative representation of data (mean ± SD) of three independent experiments after correction for GAPDH expression. NC: RNA samples without the addition of reverse transcriptase (negative control). *p < 0.05 combined-treated vs. untreated cells.

BRL plus 9RA treatment improves the association between p53 and bid in breast cancer cells.

p53 participates in apoptosis, even by acting directly on multiple mitochondrial targets (Murphy ME. et al. 2004). Therefore, we evaluated the involvement of Bcl-2 proteins family in regulating apoptosis. After 48 h BRL plus 9RA treatment, we determined the protein levels of Bid, Bad, Bcl-xL in both cytosolic and mitochondrial fractions of breast cancer cells. The separate treatment with low doses of either BRL or 9RA did not elicit any noticeable effect on Bid expression (data not shown), in contrast an upregulation of Bid protein content upon the combined treatment was observed in both cytosolic and mitochondrial extracts, while unchanged levels of Bad and Bcl-xL were detected in all the fractions tested (Fig. 11A). The protein synthesis inhibitor cycloheximide (CX) prevented the enhancement of Bid expression, suggesting that Bid is ex novo synthesized (Fig. 11B). The transcriptional activity of Bid was confirmed by using qtPCR, which clearly showed a significant upregulation of Bid mRNA in all breast cancer cells (Fig. 11C). The enhancement of Bid transcript levels upon treatments was reversed after silencing PPARγ, addressing that the effect is PPARγ-mediated (Fig. 11D and E). To examine whether wt and/or mutant p53 protein could associate with Bid in the cytoplasm and colocalize to the mitochondria, we performed co-immunoprecipitation experiments using cytosolic and either whole mitochondria or mitochondrial matrix extracts from breast cancer cells treated for 48 h with BRL plus 9RA. Equal amounts of protein extracts were immunoprecipitated with an anti-p53 antibody and then subjected to immunoblot with anti-Bid antibody. As seen in Figure 9A, in cytosolic immunoprecipitates we detected under physiological conditions the association between p53 and Bid that slightly increased upon BRL plus 9RA treatment, while in whole mitochondria we revealed that p53 was able to interact with the more active truncated Bid, tBid particularly in the presence of the combined treatment (Fig. 12B). In the matrix of

mitochondria no association between the two proteins was observed, suggesting that this physical interaction occurs in mitochondrial membrane likely initiating this organelle dysfunction (Fig. 12C). Since it has been reported the interaction of tBid with other pro-apoptotic proteins resulting in a more global permeabilization of the outer mitochondrial membrane (Korsmeyer SJ. et al. 2000), we also explored the involvement of Bak and Bax. We detected the presence of Bak (Fig. 6A and B), but not of Bax (data not shown) as component of this multiprotein complex. Stemming from our previous findings demonstrating that p53 binds to PPARγ in breast cancer cells (Bonofiglio D. et al. 2006), we investigated in our cellular context a possible association of PPARγ to this protein complex together with its heterodimer RXRα. We observed the presence of both receptors in this complex in cytosol as well as in whole mitochondria, but not in mitochondrial matrix (Fig. 12A–C). The p53/Bid association still occured after knocking down PPARγ and RXRα. To better define the mitochondrial colocalization of p53 and Bid, we used a red-fluorescent dye that passively diffuses across the plasma membrane and accumulates in active mitochondria. In MCF-7 cells the co-expression of both proteins gave rise to a merged image which appears further enhanced in cells treated with BRL plus 9RA (Fig. 12D).

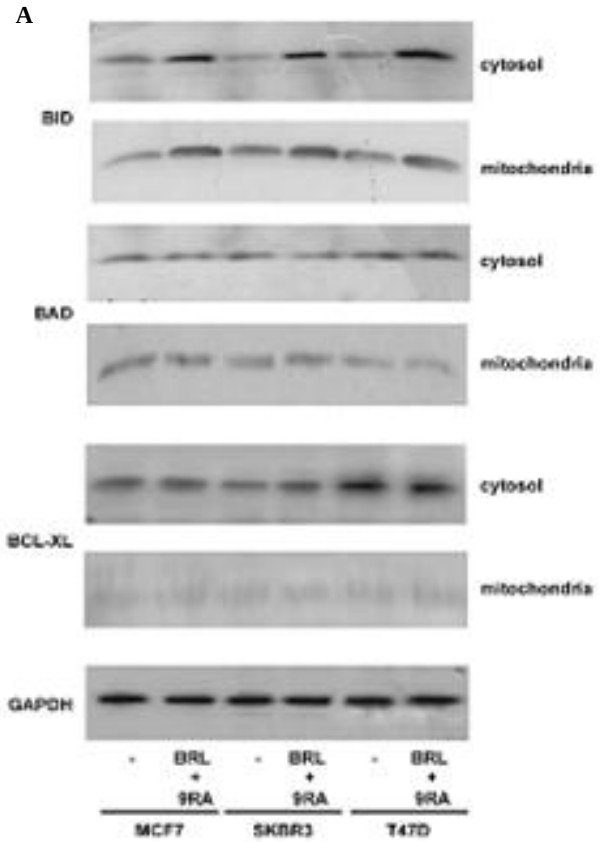
A
cytosol
BID
mitochondria
cytosol
BAD
mitochondria
cytosol
BCL-XL
mitochondria
GAPDH
- BRL + 9RA - BRL + 9RA - BRL + 9RA
MCF7 SKBR3 T47D

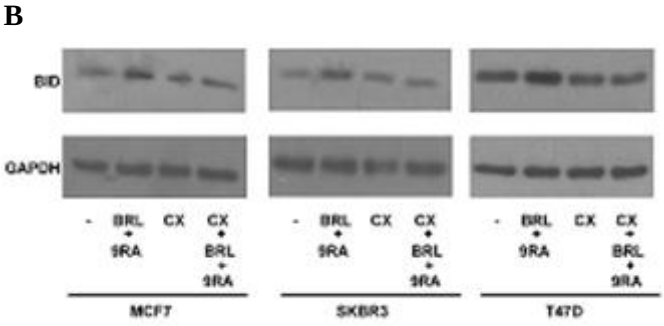
B
BID
GAPDH
- BRL + 9RA CX CX + BRL + 9RA
MCF7 SKBR3 T47D

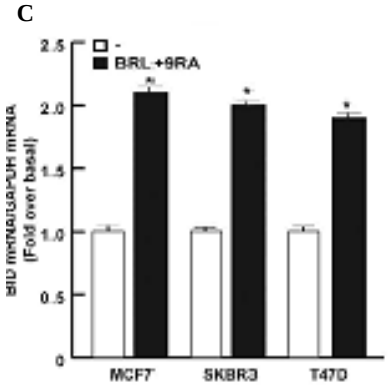
C
-
BRL+9RA
2.5
2.0
1.5
1.0
0.5
0
MCF7 SKBR3 T47D

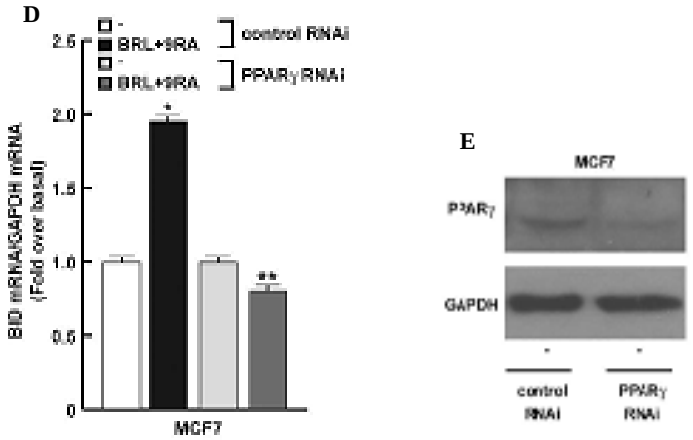

Figure 11. **Upregulation of BID expression by BRL and 9RA in breast cancer cells. (A)** Cytosolic and mitochondrial expression of Bid, Bad and Bcl-xL proteins in MCF-7, SKBR-3 and T-47D breast cancer cells untreated (-) or treated for 48 h with 100 nM BRL plus 50 nM 9RA. GAPDH was used as loading control. One of three similar experiments is presented. **(B)** Immunoblots of BID from total extracts of MCF-7, SKBR-3 and T-47D cells treated as in (A) and/or with 50 μM protein synthesis inhibitor cycloheximide (CX). GAPDH was used as loading control. One of three similar experiments is presented. **(C)** Quantitative real-time PCR analysis of BID mRNA expression in MCF-7, SKBR-3 and T-47D cells treated for 24 h as indicated. **(D)** Quantitative realtime PCR analysis of BID mRNA expression in MCF-7 cells transfected with control RNAi or with PPARγ RNAi and treated for 24 h as indicated. The histograms show the quantitative representation of data (mean ± SD) of three independent experiments after correction for GAPDH expression. **(E)** Immunoblots of PPARγ from extracts of MCF-7 cells transfected with control RNAi or with PPARγ RNAi. GAPDH was used as loading control. *p < 0,05 combined-treated vs. untreated cells. **p < 0,05 combined-treated cells transfected with PPARγ RNAi vs. combined-treated cells transfected with control RNAi.

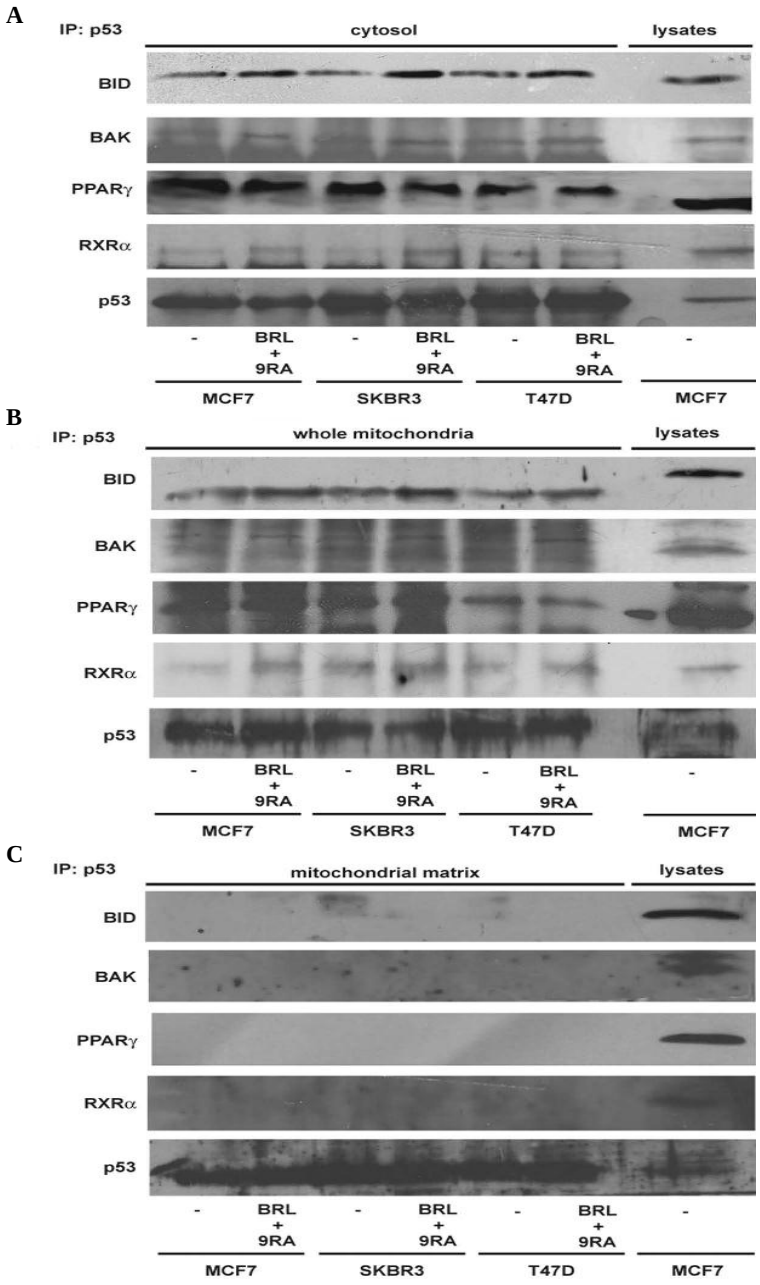
A
IP: p53
cytosol
lysates
BID
BAK
PPARγ
RXRα
p53
-
BRL + 9RA
-
BRL + 9RA
-
BRL + 9RA
-
MCF7
SKBR3
T47D
MCF7
B
IP: p53
whole mitochondria
lysates
BID
BAK
PPARγ
RXRα
p53
-
BRL + 9RA
-
BRL + 9RA
-
BRL + 9RA
-
MCF7
SKBR3
T47D
MCF7
C
IP: p53
mitochondrial matrix
lysates
BID
BAK
PPARγ
RXRα
p53
-
BRL + 9RA
-
BRL + 9RA
-
BRL + 9RA
-
MCF7
SKBR3
T47D
MCF7

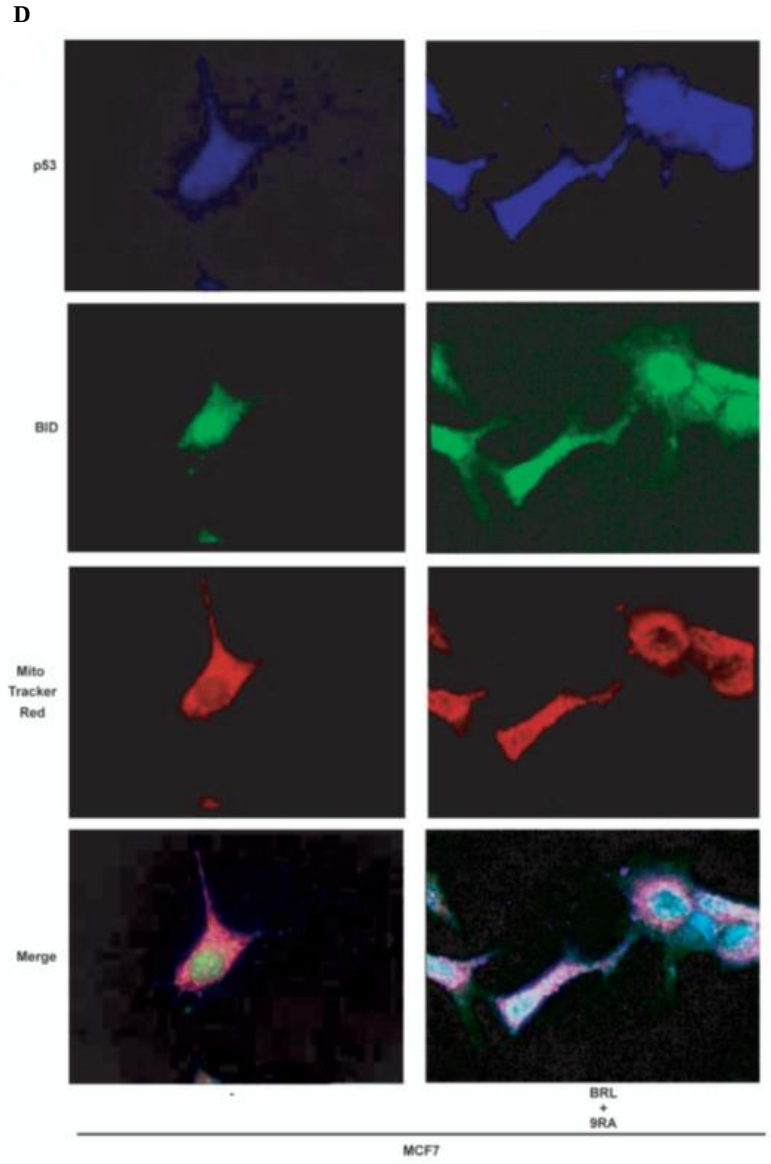

Figure 12. (A–C) Physical association between p53 and BID in breast cancer cells. MCF-7, SKBR-3 and T-47D cells were untreated (-) or treated for 48 h with BRL plus 9RA. Cytosolic **(A)**, whole mitochondrial **(B)** and mitochondrial matrix **(C)** extracts were immunoprecipitated with an anti-serum against p53 (IP:p53) and then the immunocomplexes were resolved in SDS-PAGE. The membrane was probed with anti-BID, anti-BAK, anti-PPARγ and anti-RXRα antibodies. To verify equal loading, the membrane was probed with an antibody against p53. One of three similar experiments is presented. MCF-7 lysates were used as positive control. **(D)** MCF-7 cells untreated (-) or treated with BRL plus 9RA for 48 hours were incubated in MitoTracker Red dye. Cells were immunostained with p53 and BID and then examined by fluorescent microscopy. Blue, p53; green, BID; red, MitoTracker; merge of blue, green and red as expression of colocalization in mitochondria.

Bid is involved in apoptotic events triggered by BRL plus 9RA treatment in breast cancer cells.

In order to validate the key role of Bid in the apoptotic process we used different experimental approaches after silencing Bid expression. We analyzed mitochondrial membrane potential using a fluorescent dye JC-1 in all cell lines tested after BRL plus 9RA treatment. Cells transfected with control RNAi allowed the accumulation of lipophilic dye in aggregated form in mitochondria, displaying red fluorescence as shown in Figure 13A, demonstrating the integrity of the mitochondrial membrane potential. Cells treated with both ligands exhibited green fluorescence, indicating the disruption of mitochondrial integrity, because JC-1 cannot accumulate within the mitochondria, but instead remained as a monomer in the cytoplasm. After silencing Bid expression, red fluorescence was evident in treated cells (Fig. 13A), suggesting that the integrity of the mitochondrial membrane potential is maintained in MCF-7, SKBR-3 and T-47D cells. This result well fits with a significant decrease of PARP cleavage in cells transfected with Bid RNAi and treated with ligands respect to treated cells transfected with control RNAi (Fig. 13B). Indeed in transfected cells with Bid-RNAi TUNEL assay showed after 72 h treatment a strong reduction of the percentage of apoptotic cells respect to treated cells trasfected with control RNAi (Fig. 13C). All these data indicate that Bid plays an important role in the death pathway induced by low doses of PPARγ and RXR ligands in breast cancer cells.

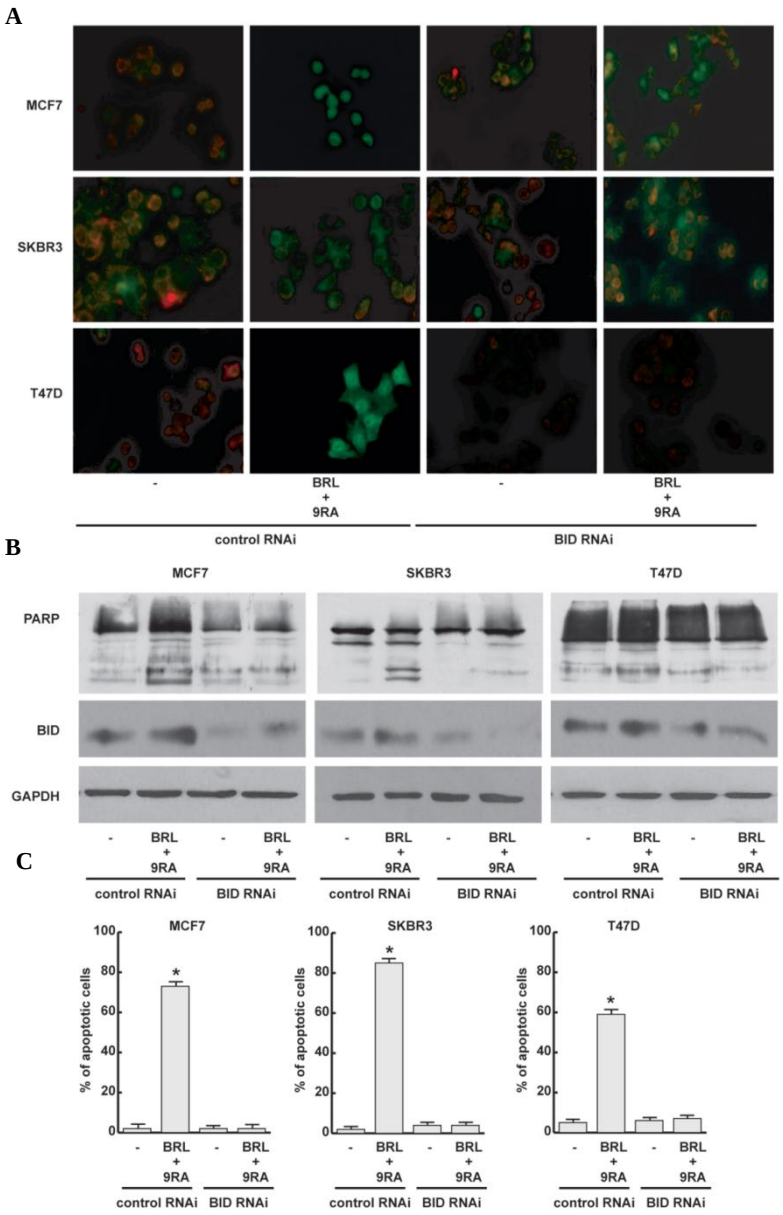

Figure 13. Knocking down BID abrogates apoptotic events in breast cancer cells. (A) MCF-7, SKBR-3 and T-47D cells were transfected with control RNAi or with BID RNAi and treated for 48 h as indicated. The results of JC-1 kit were examined by fluorescent microscopy. **(B)** Immunoblots of PARP and BID from total extracts of MCF-7, SKBR-3 and T47-D cells transfected and treated as in (A). GAPDH was used as loading control. One of three similar experiments is presented. **(C)** Cells were transfected as in (A) and treated for 72 h as indicated. The histograms show the quantitative representation of data (mean ± SD) of three independent experiments performed in triplicates. *$p < 0.05$ combined-treated vs. untreated cells.

BRL plus 9RA reduce glutathione S-transferase antioxidative enzyme activity and induce lipid peroxidation in breast cancer cells.

Since, an isoform of the antioxidant defense glutathione S-transferase (GST) is located at mitochondrial membranes, we measured its enzimatic activity in mitochondrial extracts of MCF-7, SKBR-3 and T-47D cells after BRL plus 9RA treatment. Interestingly, GST activity was reduced respect to untreated cells, while in the presence of Bid RNAi this effect was no longer noticeable (Fig. 14A), addressing that BRL plus 9RA treatment negatively regulate mitochondrial scavenger activity via Bid. Moreover, we estimated the presence of malondialdehyde (MDA), a common end products of lipid peroxidation, as index of oxidative stress induced by both ligands. As shown in Figure 14B, the lipid peroxidation was considerably increased by the treatment in both total cellular and mitochondrial extracts of all breast cancer cells.

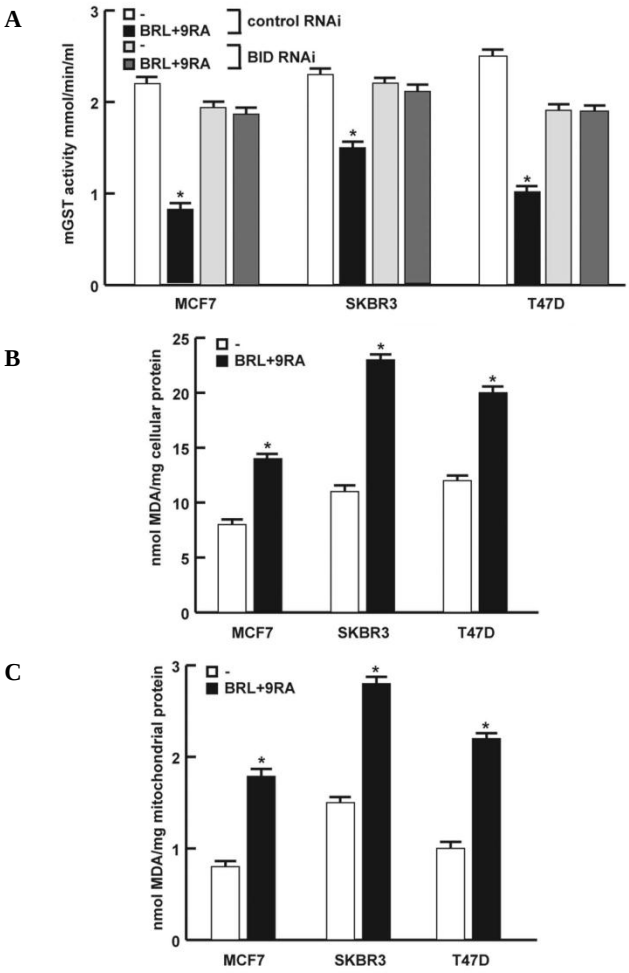

Figure 14. BRL and 9RA reduce glutathione S-transferase (GST) antioxidative enzyme activity and induce lipid peroxidation in breast cancer cells. (A) Glutathione S-transferase activity from mitochondrial extracts (mGST) of MCF-7, SKBR-3 and T-47D cells transfected with control RNAi or with BID RNAi and treated for 24 hours as indicated. **(B)** Lipid peroxidation from total and **(C)** mitochondrial cell extracts of all breast cancer cells treated for 48 h as indicated. *$p < 0.05$ combined-treated vs. untreated cells. MDA: Malondialdehyde.

PPARγ ligands reverse leptin-induced tumor cell growth in vivo and in vitro

In the last part of the present work we aimed to investigate the ability of PPARγ ligands to conteract the stimulatory effect exerted by leptin on tumor cell growth. First we explored the ability of PPARγ ligand BRL to inhibit leptin-induced breast tumor growth in vivo. To this aim, female nude mice, bearing into the intrascapular region of MCF-7 cell tumor xenografts, were treated with leptin and/or BRL. This administration was well tolerated because no change in body weight or in food and water consumption was observed together with no evidence of reduced motor function. In addition, no significant difference in the mean weights or histologic features of the major organs (liver, lung, spleen, and kidney) after sacrifice was observed between vehicle-treated mice and those that received treatment, indicating a lack of toxic effects at the dose given. Histologic examination of MCF-7 xenografts revealed that tumors were primarily composed of tumor epithelial cells. Our results showed that leptin treatment induced tumor growth in mice, as we previously demonstrated (Mauro L. et al. 2007), whereas a significant reduction in tumor volume was observed in the animal group receiving leptin plus BRL (Figure 15A). At week 12, tumor sizes were markedly smaller in animals treated with leptin plus BRL than with leptin alone (Figure 15B). Mean SE plasma leptin levels measured at week 12 were significantly higher in leptin-treated mice (2.050.087 ng/mL, P0.01) than in vehicle-treated mice (1.50 ± 0.05 ng/mL); in contrast, in BRL (1.13 ± 0.06 ng/mL, $P < 0.01$) and BRL + leptin (1.36 ± 0.078 ng/mL, $P < 0.01$) treated mice, leptin concentrations were decreased compared with those in the control and leptin groups. We then performed three-dimensional MCF-7 cell cultures, which closely mimic some in vivo biologic features of tumors (Mauro L. et al. 2004). We showed that BRL treatment (10 µmol/L) inhibited the enhanced cell-cell adhesion induced by leptin (1000 ng/mL) exposure as evidenced by the extent of aggregation scored by measuring the spheroid diameters (Figure 15C). In three-dimensional cultures, BRL decreased cell growth compared with untreated cells and reversed the enhanced leptin cell numbers. Moreover, the effects of leptin and/or BRL on cell proliferation were assessed by [3H]-thymidine DNA incorporation assay. Leptin stimulated the growth of MCF-7 cells; this effect was completely inhibited by BRL treatment

(Figure 15D). Similar results were also obtained using the natural PPARγ ligand PGJ2. The inhibitory effects exerted by PPARγ ligands were no longer noticeable in the presence of the specific PPARγ antagonist GW9662 as well as PPARγ RNAi, demonstrating direct involvement of this nuclear receptor in antagonizing leptin-induced tumor growth (Figure 15D). In ERα-negative breast cancer cells BT-20, BRL also reversed leptin-induced cell aggregation and cell proliferation (data not shown), suggesting that BRL effects are estrogen independent.

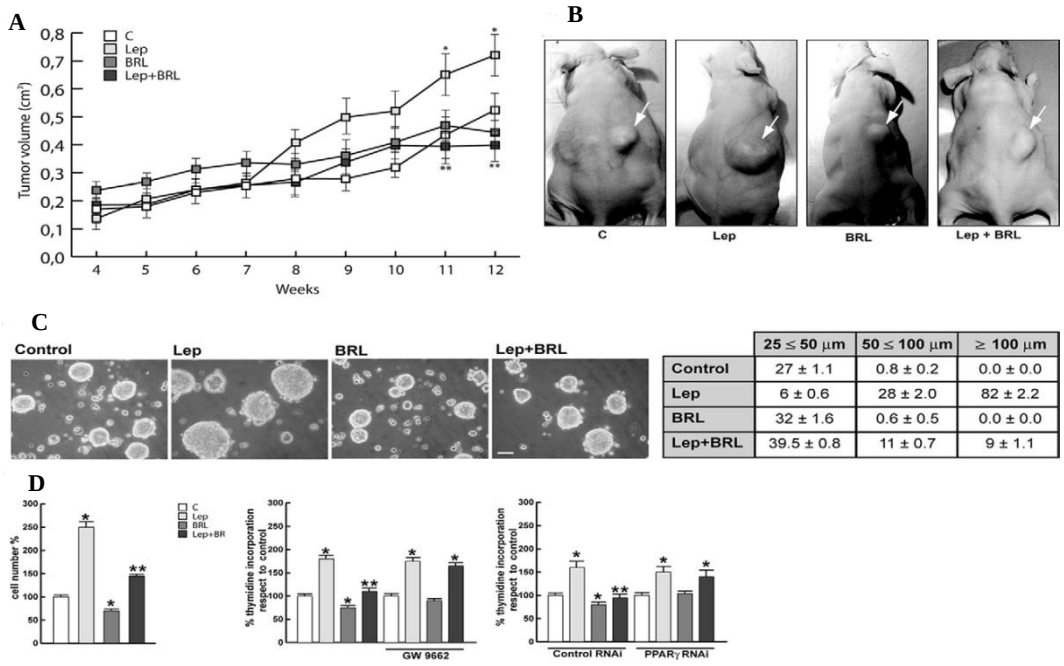

	25 ≤ 50 μm	50 ≤ 100 μm	≥ 100 μm
Control	27 ± 1.1	0.8 ± 0.2	0.0 ± 0.0
Lep	6 ± 0.6	28 ± 2.0	82 ± 2.2
BRL	32 ± 1.6	0.6 ± 0.5	0.0 ± 0.0
Lep+BRL	39.5 ± 0.8	11 ± 0.7	9 ± 1.1

Figure 15. BRL reverses leptin-induced tumor cell growth. (A): Tumor volume from MCF-7 xenografts implanted with estradiol pellets in female nude mice at weeks 4 and 12. The animals were treated with 230 μg/kg/day leptin (Lep) (n = 8), 10 mg/kg/day BRL (n = 8), Lep and BRL (n = 8), or vehicle as control (n = 8). *P < 0.05, leptin-treated group versus control group; **P < 0.05, leptin plus BRL–treated group versus leptin-treated group. **(B):** Representative images of experimental tumors at week 12 (arrows). **(C):** MCF-7 three-dimensional cultures were untreated or treated as indicated for 48 h (top). Scale bar 50 μm. The extent of aggregation was scored by measuring the spheroid diameters. The values represent the sum of spheroids in 10 optical fields under 10 magnification (bottom). **(D):** Cell numbers obtained from three-dimensional spheroids and proliferation determined by [3H]thymidine incorporation in MCF-7 cells transfected and treated as indicated for 48 h. The results are mean ± SE of three experiments. *P < 0.05 versus untreated cells; **P < 0.05 versus leptin.

BRL represses activation of leptin signal transduction pathways in MCF-7 cells

Leptin exerts its biologic function through binding to its receptors, which mediate a downstream signal by activating multiple signaling pathways (Sweeney G. 2002; Ahima RS. et al. 2004). We examined the effects of BRL on ObRs and its transduction pathways. Stimulation of MCF-7 cells with leptin resulted in an increase in ObRL and ObRS, which was reversed by treatment with BRL (Figure 16A). Similar results were also obtained in MCF-7 xenografts (Figure 16B). In addition, as expected, leptin significantly induced phosphorylation of MAPK/STAT3/Akt in in vivo and in vitro models, whereas treatment with BRL completely abrogated the leptin activation of these signaling pathways (Figure 16, C and D).

All these data suggest that the inhibitory action of BRL on leptin-induced tumor growth, cell adhesion, and proliferation involves, at least in part, the ability of PPARγ ligand to modulate ObR expression and antagonize its signaling pathways.

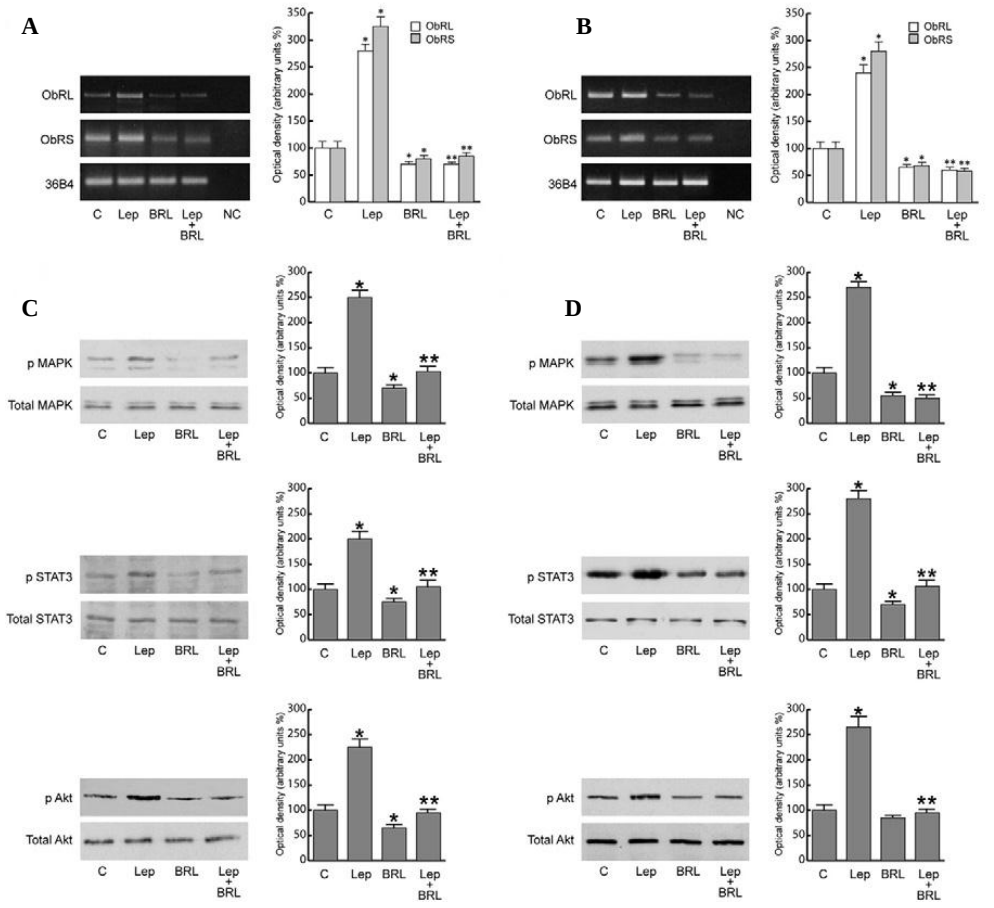

Figure 16. BRL represses leptin (Lep) signaling in MCF-7 cells and xenografts. RT-PCR of ObRL and ObRS mRNA from MCF-7 cells stimulated for 48 h **(A)** and from xenografts **(B).** 36B4 mRNA levels were determined as control. NC indicates RNA sample without the addition of reverse transcriptase (negative control). Representative western blot analysis on protein extracts from MCF-7 cells stimulated for 15 min **(C)** and xenografts excised from control and treated mice **(D)** showing MAPK/STAT3/Akt activation. The immunoblots were stripped and reprobed with total MAPK/STAT3/Akt as loading control. The results are mean ± SE of three separate experiments in which the band intensities were evaluated in terms of optical density arbitrary units and expressed as the percentage of the control assumed to be 100%. *P < 0.05 versus untreated cells; **P < 0.05 versus leptin.

Modulation of Ob expression and its transcriptional activity by BRL

To assess whether BRL can also affect Ob, we performed RT-PCR in MCF-7 cells. We showed in vitro and in vivo models that leptin increased Ob mRNA, whereas BRL reversed this effect (Figure 17A). This latter result led us to ascertain whether PPARγ activation can modulate leptin transcriptional activity. To this aim, we transiently transfected MCF-7 cells with a plasmid containing leptin regulatory sequences p1774 (- 2922 / + 30) and found that leptin induced luciferase activity, which was inhibited by treatment with BRL (Figure 17B). The Ob promoter contains multiple transcription factor binding motifs, including CRE and Sp1 sites and one GRE site (Figure 17B). To determine which cis-acting elements in the Ob promoter can mediate the previously mentioned effects, Ob promoter–deleted constructs – 1975 / + 30 (p1775), - 1546 / + 30 (p1776), and – 805 / +30 (p1778) were tested. In transfection experiments performed using p1775 and p1776 constructs, the responsiveness to leptin was still observed, and BRL still inhibited the increase induced by leptin. In contrast, in the presence of the construct p1778, no up-regulatory effects were noticeable on leptin exposure (Figure 17B). Thus, we performed site-directed mutagenesis assays to evaluate which site was responsible for leptin-induced Ob promoter activation.

We found that only the mutation of the GRE site was involved in mediating the stimulatory effect of leptin (Figure 17C), addressing that the up-regulatory effect of leptin requires the GRE motif. To explore whether leptin affects the activity of GR, we tested its nuclear translocation and phosphorylation at S211. Leptin induced GR nuclear localization with a concomitant increase in S211 phosphorylated GR levels, which were significantly reduced by pre-treatment

with the MAPK inhibitor PD98059 and the JAK/STAT inhibitor AG490. In contrast, the PI3K inhibitor LY294002 did not affect GR phosphorylation status (Figure 18).

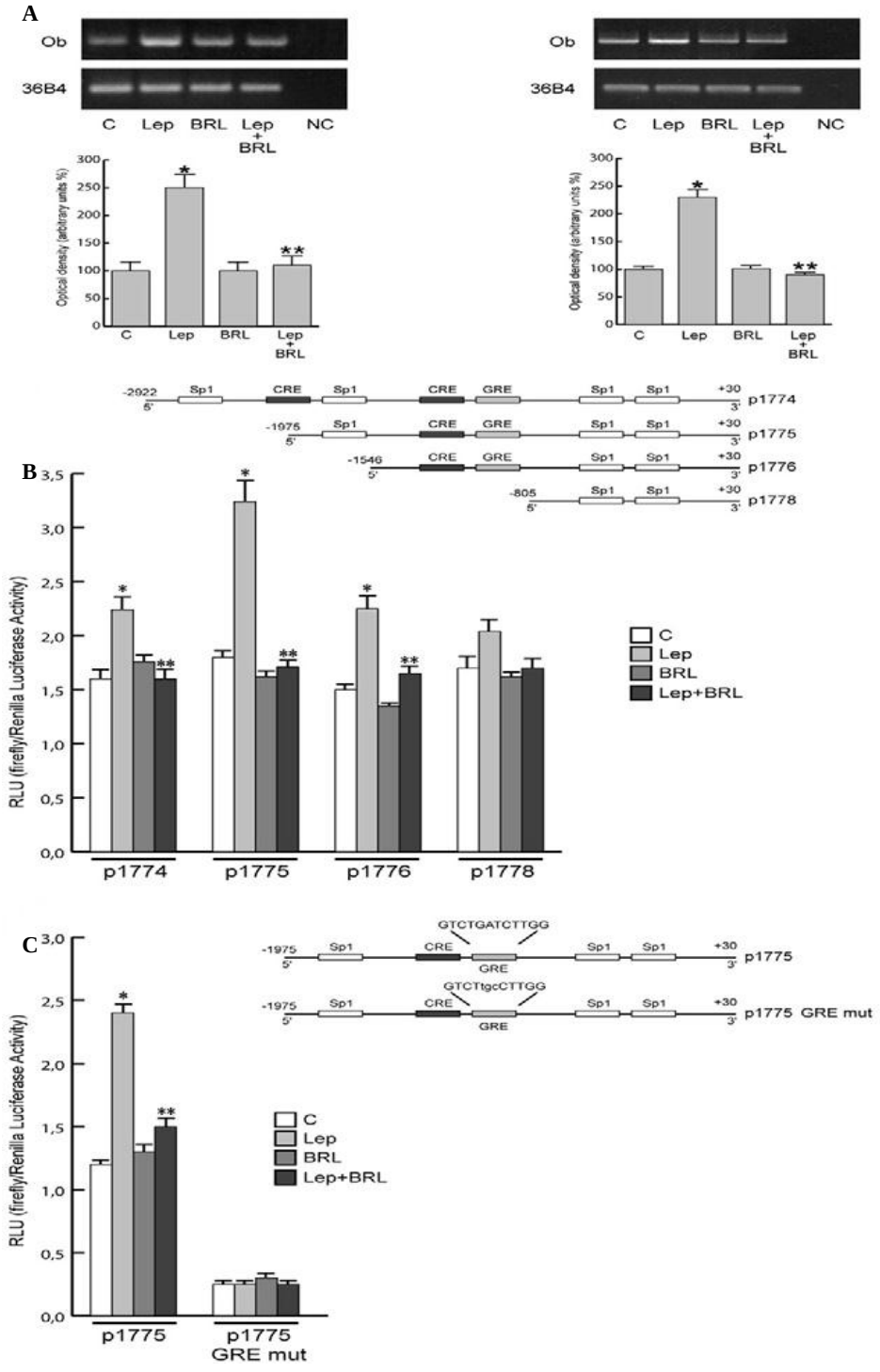

Figure 17. BRL negatively regulates leptin (Lep)-induced Ob expression and its transcriptional activity. (A): RT-PCR of Ob was performed in MCF-7 cells stimulated for 48 h (left panel) and in xenografts (right panel). 36B4 mRNA levels were determined as control. NC, negative control. MCF-7 cells were transiently transfected with luciferase plasmids containing the human leptin promoter (p1774) or its deletions (p1775, p1776, and p1778) **(B)** or p1775 mutated in the GRE site (p1775 GRE mut) **(C).** Schematic maps of the human leptin promoter constructs are included. Cells were untreated or treated with leptin (1000 ng/mL) and/or 10 µmol/L BRL for 24 h. RLU indicates relative light units. The results are mean ± SE of three separate experiments. *P < 0.05 versus untreated cells; **P < 0.05 versus leptin.

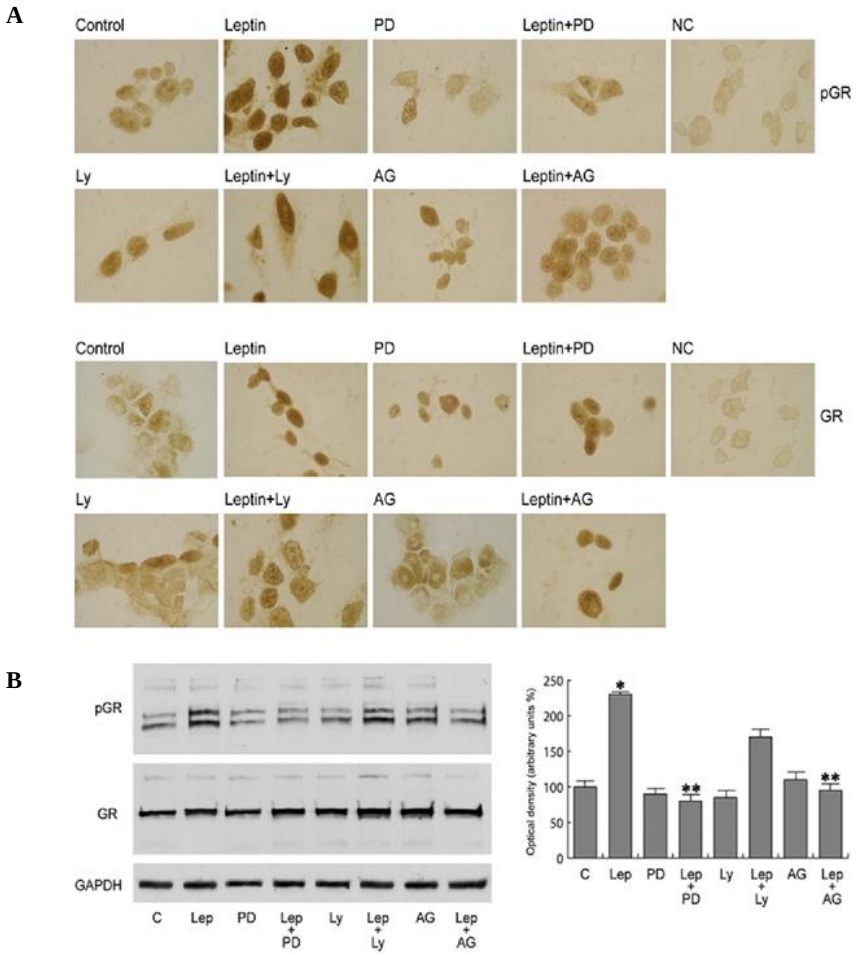

Figure 18. Leptin (Lep) induces nuclear translocation of GR and its phosphorylation (pGR). MCF-7 cells were untreated or treated with 1000 ng/mL of leptin for 15 min or pre-treated with 10 µmol/L PD98059 (PD), AG490 (AG), or LY294002 (LY). **(A):** Immunostaining of pGR and GR. No immunodetection was observed replacing the antibodies with horse serum [negative control (NC)]. **(B):** Representative western blotting for pGR on S211 and GR. Glyceraldehyde-3-phosphate dehydrogenase (GAPDH) was used as loading control. The results are mean ± SE of three separate experiments for pGR

in which the band intensities were evaluated in terms of optical density arbitrary units and expressed as the percentage of the control assumed to be 100%. *P < 0.05 versus untreated cells; **P < 0.05 versus leptin.

PPARγ reverses leptin-induced effects on Ob promoter at the GRE site through corepressor recruitment

To provide insight into the molecular mechanism by which the GRE motif modulates Ob promoter activity, we performed electrophoretic mobility shift assay experiments using as probe the GRE sequence present in the Ob regulatory region. We observed the formation of a complex in nuclear extracts from MCF-7 cells (Figure 19A, lane 1), which was abrogated by 100-fold molar excess of unlabeled probe (Figure 19A, lane 2), demonstrating the specificity of the DNA binding complex. This inhibition was no longer observed using a mutated oligodeoxyribonucleotide as competitor (Figure 19A, lane 3). Leptin and BRL induced a slight increase in the specific band (Figure 19A, lanes 4 and 5), whereas an enhanced DNA binding complex was observed on combined treatments (Figure 19A, lane 6). The inclusion of anti-GR and anti-PPARγ antibodies in the reactions attenuated the specific bands, suggesting the presence of both proteins in the complex (Figure 19A, lanes 7 and 8). Note that the leptin-induced increase in the DNA binding complex was no longer noticeable when a synthetic oligodeoxyribonucleotide corresponding to the CRE or Sp1 motif was used as probe (data not shown). The interaction of GR and PPARγ receptors with the Ob promoter was further elucidated by chromatin immunoprecipitation (ChIP) assays. Using anti-GR or anti-PPARγ antibodies, protein-chromatin complexes were immunoprecipitated from MCF-7 cells treated for 1 h with leptin and/or BRL. Real-time PCR was used to determine the recruitment of GR and PPARγ to the Ob region containing the GRE site. The results indicate that GR was constitutively bound to the Ob promoter in untreated cells and that this recruitment was increased on leptin or BRL exposure and to a higher extent after combined treatments. Immunoprecipitation with anti-PPARγ antibody showed enhanced recruitment of this nuclear receptor to the Ob promoter in the presence of BRL and BRL plus leptin treatments. Similar results were also obtained by

GR/PPARγ Re-ChIP assay. We revealed after leptin treatment an enhanced association of RNA Pol II that was drastically reduced by leptin plus BRL exposure (Figure 19B). To assess whether the decrease in Ob promoter transcriptional activity might be caused by the cooperative interaction between GR/PPARγ and negative transcriptional regulators, we investigated the involvement of NCoR and SMRT, which interact with and function as negative coregulators of GR and PPARγ (Cohen RN. et al. 2006; Ricote M. et al. 2007; van der Laan S. et al. 2008; Ronacher K. et al. 2009) A co-immunoprecipitation assay was performed on nuclear protein fractions from MCF-7 cells treated with leptin and/or BRL. The formation of GR and PPARγ complex was clearly detected in all the conditions tested. Moreover, GR/NCoR and GR/SMRT complexes were slightly revealed in untreated cells, but this association was enhanced by combined treatments. No interaction of the orphan nuclear receptor DAX-1, a corepressor for GR, was observed under the same experimental conditions (Figure 19D). Similar results were obtained in MCF-7 cells immmunoprecipitated with anti-PPARγ antibody (Figure 19D). Re-ChIP assays demonstrated increased NCoR and SMRT occupancy of the GRE-containing region of the Ob promoter after BRL exposure and particularly on combined treatments (Figure 19C). In the presence of a MAPK inhibitor able to interfere with GR phosphorylation, the recruitment of corepressors to the Ob promoter was markedly reduced (data not shown).

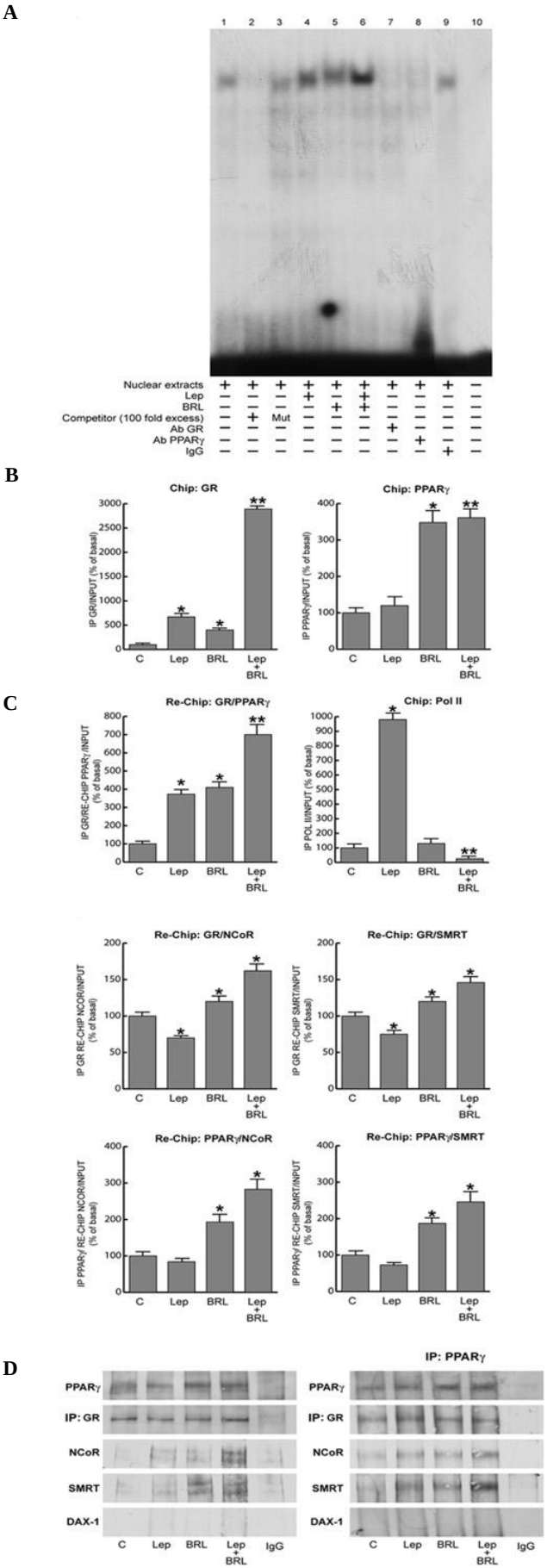
A
1 2 3 4 5 6 7 8 9 10
Nuclear extracts
Lep
BRL
Competitor (100 fold excess)
Mut
Ab GR
Ab PPARγ
IgG
B
Chip: GR
IP GR/INPUT (% of basal)
Chip: PPARγ
IP PPARγ/INPUT (% of basal)
C
Re-Chip: GR/PPARγ
IP GR/RE-CHIP PPARγ/INPUT (% of basal)
Chip: Pol II
IP POL II/INPUT (% of basal)
Re-Chip: GR/NCoR
IP GR RE-CHIP NCOR/INPUT (% of basal)
Re-Chip: GR/SMRT
IP GR RE-CHIP SMRT/INPUT (% of basal)
Re-Chip: PPARγ/NCoR
IP PPARγ RE-CHIP NCOR/INPUT (% of basal)
Re-Chip: PPARγ/SMRT
IP PPARγ RE-CHIP SMRT/INPUT (% of basal)
C
Lep
BRL
Lep + BRL
D
IP: PPARγ
PPARγ
IP: GR
NCoR
SMRT
DAX-1
C
Lep
BRL
Lep + BRL
IgG

Figure 19. PPARγ binds and recruits corepressors to the GRE site in the Ob promoter. **(A):** Nuclear extracts from MCF-7 cells were incubated with GRE probe (lane 1),100-fold molar excess of unlabeled (lane 2) and mutated (Mut) (lane 3) probe was added. MCF-7 nuclear extracts treated with 1000 ng/mL of leptin and/or 10 μmol/L BRL for 6 h (lanes 4, 5, and 6). Anti-GR (lane 7), anti-PPARγ (lane 8) antibodies (Abs) or IgG (lane 9) were added to the mixture. Lane 10 shows probe alone. **(B):** ChIP with the anti-GR, anti-PPARγ, and anti-Pol II antibodies. ChIP with the anti-GR antibody was re-ChIP with anti-PPARγ antibody. **(C):** ChIP with the anti-GR or anti-PPARγ antibodies was re-ChIP with either anti-NCoR or anti-SMRT antibodies. The leptin (Lep) promoter sequence including the GRE site was detected by real-time-PCR with specific primers (see Materials and Methods). The results are mean ± SE of three separate experiments expressed as the percentage of control. *$P < 0.05$ versus untreated cells; **$P < 0.05$ versus leptin. **(D):** MCF-7 cells were treated with 1000 ng/mL of leptin and/or 10 μmol/L BRL for 48 h. Immunoprecipitation was performed using anti-GR (left panel) or anti-PPARγ (right panel) antibodies and then blotted with anti-PPAR, GR, NCoR, SMRT, or DAX-1 antibodies.

BRL abrogates leptin-activated estrogen signaling in MCF-7 cells

We previously demonstrated that leptin can transactivate ERα and enhance aromatase gene expression in breast cancer cells (Catalano S. et al. 2003; Catalano S. et al. 2004). Thus, because PPARγ ligands interfere with leptin signaling, we investigated the ability of BRL to reverse the leptin effects on estrogen signaling.

In MCF-7 cells transiently transfected with XETL construct, we observed that BRL significantly inhibited ERE-dependent transactivation induced by leptin (Figure 20A), and this effect was reversed by pre-treatment with GW9662 (data not shown). Similar results were reproduced in ER-negative CHO cells in which ERα was ectopically expressed (Figure 20A). These data correlated well with the ability of BRL to abrogate in vivo and in vitro models the up-regulatory effects of leptin on mRNA expression levels of the classic estrogen genes cathepsin, pS2, and cyclin D1 (Figure 20B). Besides, in MCF-7 cell cultures and in xenografts, BRL reversed the increase in aromatase expression induced by leptin (Figure 20C). These results indicate that treatment with BRL counteracting leptin action on estrogen signaling may contribute to reduce breast cancer cell growth and progression.

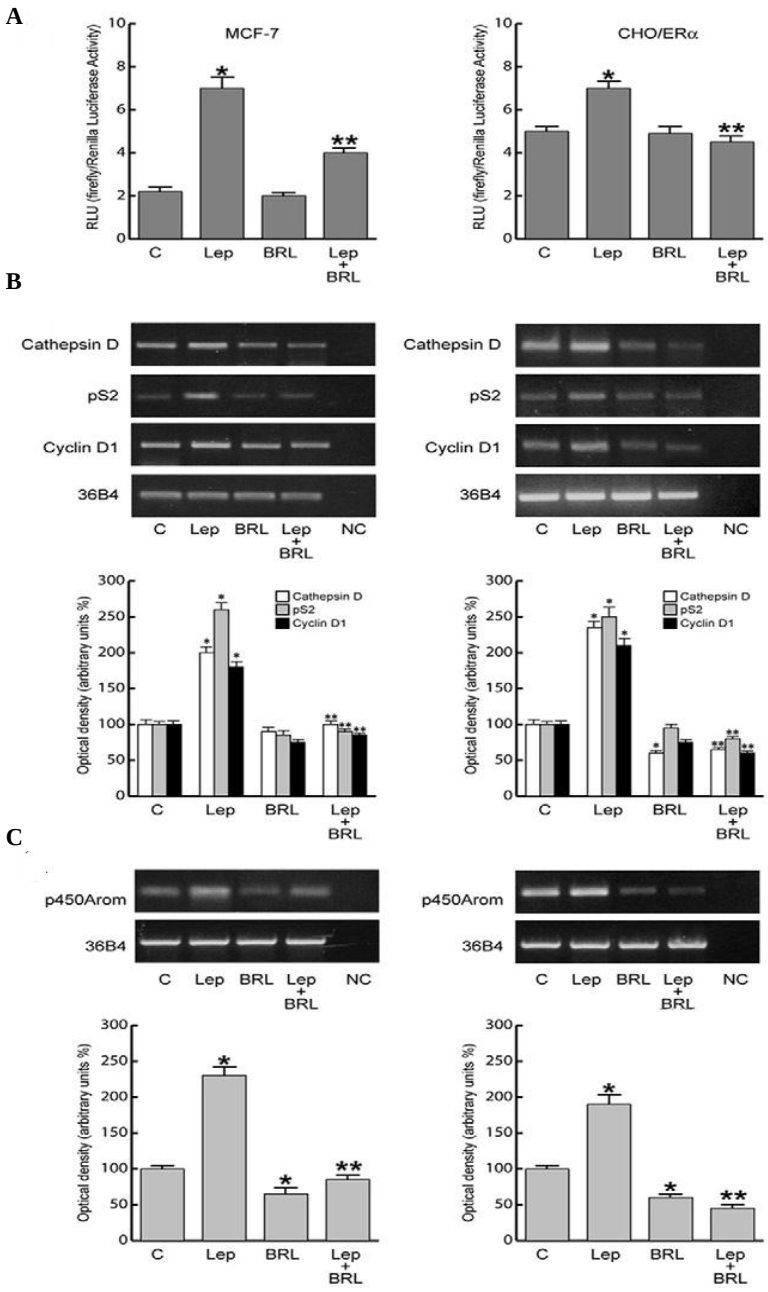

Figure 20. BRL antagonizes estrogen signaling induced by leptin (Lep). (A): MCF-7 cells were transfected with XETL plasmid. CHO cells were cotransfected with XETL and HEGO plasmids (CHO/ER). RLU, relative light unit. The results are mean SE of three independent experiments performed in triplicate. *P < 0.05 versus untreated cells; **P < 0.05 versus leptin. Cathepsin D, pS2, and cyclin D1 **(B)** and aromatase **(C)** mRNA expression in MCF-7 cells treated for 48 h as indicated (left panel) and in xenografts (right panel). 36B4 mRNA levels were determined as control. NC indicates negative control. The results are mean ± SE of three separate experiments in which the band intensities were evaluated in terms of optical density arbitrary units and expressed as the percentage of the control assumed to be 100%. *P < 0.05 versus untreated cells; **P < 0.05 versus leptin.

Molecular mechanism through which PPARγ counteracts leptin expression and function in breast cancer

An hypothetical model of the possible mechanism through which PPARγ activation may modulate leptin expression and function in reducing breast cancer growth is shown in Figure 21. Leptin, through JAK/STAT/MAPK activation, may phosphorylate GR and induce its transactivation, resulting in an increase in leptin promoter activity. This up-regulatory effect on Ob is counteracted by PPARγ through the recruitment of corepressors NCoR and SMRT on the GRE site of the Ob regulatory region in the presence of GR and PPARγ.

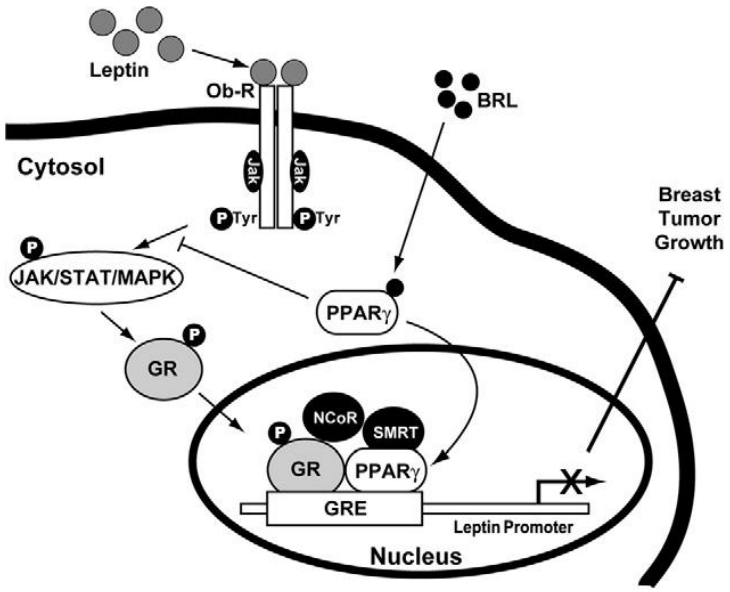

Figure 21. Hypothetical model through which PPARγ counteracts leptin expression and function in breast cancer. Leptin, through JAK/STAT/MAPK activation, increases GR phosphorylation (pGR) and its nuclear translocation. pGR transactivates leptin promoter by binding to GRE motif. In the presence of BRL, PPARγ binds to GRE and, through the formation of GR/PPARγ complex, allows the recruitment of NCoR and SMRT corepressors, thus inhibiting Ob transcription and reducing breast tumor growth.

Discussion

In the present study we have showed the molecular mechanisms by which low doses of PPARγ-ligand BRL and RXR-ligand 9RA trigger apoptotic effects in different breast cancer cell lines and by which BRL reverses leptin-induced tumor cell growth in *vitro* and in *vivo*.

The nuclear receptor PPARγ forms heterodimers with retinoid X receptors alpha (RXRα), which regulate the transcription of various genes implicated in the control of lipid metabolism, insulin synthesis, carcinogenesis, and inflammation (Rangwala SM. et al.2004; Staels B. 2005). The ability of PPARγ ligands to induce differentiation and apoptosis in a variety of cancer cell types, such as human lung (Tsubouchi Y. et al. 2000), colon (Kitamura S. et al. 1999), and breast (Mueller E. et al. 1998), has been exploited in experimental cancer therapies (Roberts-Thomson SJ. 2000), PPARγ agonist administration in liposarcoma patients resulted in histological and biochemical differentiation markers in vivo (Demetri GD. et al. 1999). However, a pilot study of short-term therapy with the PPARγ ligand BRL in early-stage breast cancer patients did not elicit significant effects on tumor cell proliferation, although the changes observed in PPARγ expression may be relevant to breast cancer progression (Yee LD. et al. 2007). On the other hand, the natural ligand for RXR, 9RA has been effective in vitro against many types of cancer, including breast tumor (Wan H. et al 2001; Simeone AM. et al. 2004; Gee MF. et al. 2005, Mizuguchi Y. et al. 2006; Wu K. et al. 2006;). Recently, RXR-selective ligands were discovered to inhibit proliferation of breast cancer cells in vitro and caused regression of the disease in animal models (Bischoff ED. et al. 1998). The additive antitumoral effects of PPARγ and RXRα agonists, both at elevated doses, have been shown in human breast cancer cells (Elstner E. et al.2002; Grommes C. et al. 2004;).

However, high doses of both ligands have remarkable side effects in humans, such as weight gain and plasma volume expansion for PPARγ ligands (Arakawa K. et al. 2004; Rangwala SM and Lazar MA. 2004; Staels B. et al. 2005), hypertriglyceridemia and suppression of the thyroid hormone axis for RXRα ligands (Pinaire JA. et al. 2007). In the present study, we demonstrated that

nanomolar concentrations of BRL and 9RA in combination exert significant antiproliferative effects on breast cancer cells, whereas they do not induce noticeable influences on normal breast epithelial MCF-10A cells. However, the induced overexpression of PPARγ in MCF-10A cells makes these cells responsive to the low combined concentration of BRL and 9RA (data not shown). Although PPARγ is known to mediate differentiation in most tissues, its role in either tumor progression or suppression is not yet clearly elucidated. It has been demonstrated in animals studies that an overexpression of PPARγ increases the risk of breast cancer already in mice susceptible to the disease (Saez E. et al. 2004). However, it remains still questionable if the enhanced PPARγ expression does correspond to an enhanced content of functional protein, which according to previous suggestion should be carefully controlled in a dose-response study (Sporn MB. et al. 2001). For instance, the expression of PPARγ is under complex regulatory mechanisms, sustained by cell-specific distinct promoters mediating the changes in expression of PPARγ (Wang X. et al. 2004). Here we demonstrated for the first time the molecular mechanism underlying antitumoral effects induced by combined low doses of both ligands in MCF-7 cells, where an up-regulation of tumor suppressor gene p53 was concomitantly observed. Functional assays with deletion constructs of the p53 promoter showed that the NFkB site is required for the transcriptional response to BRL plus 9RA treatment. NFkB was shown to physically interact with PPARγ (Chung SW. et al. 2000), which in some circumstances binds to DNA cooperatively with NFkB (Couturier C. et al. 1999; Ikawa H. et al. 2001; Sun YX. et al. 2002). It has been previously reported that micromolar doses of both PPARγ and RXR agonists synergize to generate an increased level of NFkB-DNA binding able to trigger apoptosis in Pre-B cells (Schlezinger JJ. et al. 2002). Our electrophoretic mobility shift assay and chromatin immunoprecipitation assay demonstrated that PPARγ/RXRα complex is present on p53 promoter in the absence of exogenous ligand. Only BRL and 9RA in combination increased the binding and the recruitment of either PPARγ or RXR on the NFkB site located in the p53 promoter sequence. BRL plus 9RA at the doses tested also increased the recruitment of RNA-Pol II to p53 promoter gene illustrating a positive transcriptional regulation able to produce a consecutive series of events in the

apoptotic pathway. Changes in mitochondrial membrane permeability, an important step in the induction of cellular apoptosis, is concomitant with collapse of the electrochemical gradient across the mitochondrial membrane, through the formation of pores in the mitochondria leading to the release of cytochrome C into the cytoplasm, and subsequently with cleavage of procaspase-9. This cascade of events, featuring the mitochondria-mediated death pathway, was detected in BRL plus 9RA-treated MCF-7 cells. The activation of caspase 9, in the presence of no changes in the biological activity of caspase 8, support that in our experimental model only the intrinsic apoptotic pathway is the effector of the combined treatment with the two ligands.

The crucial role of p53 gene in mediating apoptosis is raised by the evidence that the effects on the apoptotic cascade were abrogated in the presence of AS/p53 in all breast cancer cell lines tested, including tamoxifen resistant breast cancer cells. In tamoxifen-resistant breast cancer cells, other authors have observed that epidermal growth factor receptor, insulin-like growth factor-1R, and c-Src signaling are constitutively activated and responsible for a more aggressive phenotype consistent with an increased motility and invasiveness (Knowlden JM. et al. 2003; Jones HE. et al. 2004; Hiscox S. et al. 2005).

It's well know that the p53 pathway is inactivated in the majority of human cancers, most likely because the pro-apoptotic function of p53 is critical to the inhibition of tumor development and progression. Although it is clearly established the role of p53 as a nuclear transcription factor able to activate or repress a number of p53 transcriptional targets with the potential to promote or inhibit apoptosis, many evidences support a transcriptional-independent function of p53 in apoptosis. Indeed, an unexpected turn in the p53-mediated pathway to programmed cell death has emerged with accumulating data that p53 has a direct cytoplasmic role at mitochondria in activating the apoptotic machinery (Murphy ME. et al. 2004). Thus, a major question is to define the apoptotic function of mitochondrial p53. Increased evidences suggest that mitochondrial p53 localization is sufficient for initiating p53-dependent apoptosis (Marchenko ND. et al. 2000; Katsumoto T. et al. 1995). Furthermore, some studies reported that p53 may induce apoptosis by forming complexes with mitochondrial apoptotic

proteins such as Bcl-2/Bcl-xL (Mihara M. et al. 2003), Bad (Jiang P. et al. 2006) or Bid (Song G. et al. 2009), which are located in the outer membrane of mitochondria. We hypothesize that mechanistic insight into this process could be obtained from the identification of mitochondrial p53-interacting protein in SKBR-3 and T-47D cells that expressed a p53 mutation in the DBD (DNA binding domain). The novelty of the present study raises by the evidence that in response to the combined BRL and 9RA treatment in breast cancer cells we observed a PPARγ-dependent upregulation of Bid expression. Although it has been reported that Bid is transcriptionally regulated by p53 (Sax JK. et al. 2002), our results address an independent-p53 transcriptional regulation of Bid gene since we found increased Bid transcript levels also in SKBR-3 and T-47D breast cancer cells harboring p53 mutated. Having demonstrated that PPARγ activation increased both p53 and Bid expression we moved to study their enhanced association in different cellular compartments in response to BRL plus 9RA. Here we showed that p53 interacts with Bid in cytosol and exclusively with the truncated more active tBid in mitochondria, showing a slight increase upon BRL and 9RA treatment.

Bid is a member of the 'BH3 domain only'subgroup of Bcl-2 family members proposed to connect proximal death and survival signals to the core apoptotic pathway at the level of the classic family members which bear multiple BH domains.(Adams JM. et al. 1998; Gross A. et al. 1999). It has been reported that Bid is able to bind mitochondrial proteins and promote cell death, suggesting a model in which Bid served as a 'death ligand' which moved from the cytosol to the mitochondrial membrane to inactivate Bcl-2 or activate Bax and Bak and to result in cytochrome c release (Rieusset J. et al. 1999).

The release of cytochrome c from mitochondria has been shown to promote the oligomerization of a cytochrome c/Apaf-1/Caspase-9 complex that activates caspase-9 to result in the cleavage of downstream effector caspases (Rieusset J. et al. 1999).

We showed the involvement of Bak protein as a component of a p53/Bid protein-protein interaction in breast cancer cells hypothesizing that it contributes to form a large pore responsible for triggering apoptotic events.

Given the discovery that nanomolar concentrations of BRL and 9RA upregulate Bid expression in mitochondria, we sought to elucidate the role of Bid in mitochondrial function of breast cancer cells. Mitochondria, as central point of oxidative metabolism, are a major source of intracellular reactive oxygen species (ROS), which cause, sequentially, cellular injury to DNA, protein and lipid peroxidation, followed by loss of cell membrane integrity leading to cell death (Cohen RN. 2006). ROS, however, have also been implicated as second messengers in apoptotic processes (Ricote M. et al. 2007). Under normal physiological conditions, cellular ROS generation is controlled by antioxidant enzymes and other small-molecule antioxidants (van der Laan S. et al. 2008). We observed upon the combined treatment with PPARγ and RXRα ligands a significant reduction of GST enzymatic activity in mitochondrial extracts which was no longer noticeable after knocking down Bid. These results highlighting the crucial role played by Bid might provide a correlation between the mitochondrial dysfunction and the enhanced apoptotic response of different breast cancer cells to PPARγ and RXRα ligands.

In the last part of our study, we demonstrated, for the first time, that activation of PPARγ reverses leptin-mediated promotion of breast tumor growth either in *vivo* in MCF-7 xenografts implanted in female nude mice or in *vitro* in MCF-7 three-dimensional and monolayer cultured breast cancer cells. Elevated leptin levels strongly correlate with obesity, hyperinsulinemia, and insulin resistance, conditions found in most patients with diabetes mellitus (Zimmet P. et al. 1999). PPARγ ligands, thiazolidinediones, able to reduce hyperglycemia and hyperinsulinemia in insulin-resistant states, also down-regulate gene expression of pluripotent hormone leptin in vivo and in vitro (De Vos P. et al. 1996; Rieusset G. et al. 1999). Besides, previous observations have reported that PPARγ agonists inhibited leptin induced proliferation in hepatic stellate cells by suppression of MAPK activation (Lee JI. et al. 2007) and abolished leptin-directed migration of endothelial cells through Akt (Goetze S. et al. 2002). Thus, regulation and function of leptin and PPARγ are possibly interrelated and relevant in obese patients in whom metabolic changes are major contributors to the development of breast carcinoma. The present results show that the PPARγ ligand BRL prevents

the development of leptin-induced MCF-7 tumor xenografts in the presence of significantly lower plasma leptin levels and inhibits the increased cell-cell aggregation and proliferation observed on leptin exposure. The in vitro results were also reproduced in ERα-negative breast cancer cells BT20, addressing how the mechanism by which PPARγ activation affects breast tumor cell growth is not tightly related to estrogen dependency. Moreover BRL down-regulates the enhanced expression of ObRs induced by leptin and inhibits MAPK/Akt/STAT3 leptin downstream signaling pathways. These results are in agreement with data obtained in other cell models showing that PPARγ ligands suppress ObR mRNA and its promoter activity and block leptin signaling (Goetze S. et al. 2002; Lee JI. et al. 2007; Tang Y. et al. 2009). It emerges from recent studies that leptin and estrogen systems are involved in a functional cross talk. For example, leptin has been shown to directly transactivate ERα (Catalano S. et al. 2004) and positively modulate aromatase activity (Catalano S. et al. 2003). We demonstrated in MCF-7 cells that BRL, interfering with leptin signaling, could reverse the effects of leptin on estrogen signal specifically, counteracting ERα activation and its classic target genes in either in *vitro* or in *vivo* models.

Furthermore, the leptin-enhanced aromatase expression was completely abrogated by BRL treatment as we observed in xenografts and in monolayer cultures of MCF-7 cells, underlying the ability of this new class of oral antidiabetic drugs to inhibit local estrogen production, which represents an important factor of tumor microenvironment able to maintain tumor growth and progression.

Activated PPARγ is also known to inhibit the expression of Ob in adipose tissue (Callen CB. et al. 1996; Rieusset J. et al. 1999). Herein, we demonstrated in MCF-7 cells the ability of BRL to reverse the leptin-induced Ob mRNA expression and its transcriptional activity, showing how PPARγ negatively interferes in the short autocrine loop maintained by leptin on Ob gene in breast cancer cells. The human Ob promoter contains multiple transcription regulatory elements, including several CRE, Sp1, and NFkB sites and one GRE site (Gong DW. et al.1996).

Functional experiments using Ob promoter–deleted constructs and site-directed mutagenesis studies have shown that the up-regulatory effects induced by leptin on Ob promoter activity completely reversed by BRL occurred through the GRE

site. These latter results fit well with the evidence that leptin induced GR translocation and phosphorylation at S211, which was inhibited by MAPK and JAK/STAT inhibitors. It was reported that the S211 phosphorylated GR strongly correlates with GR transcriptional activation; indeed, inhibition of this phosphorylation is associated with decreased nuclear retention of GR and inhibited gene transcription (Chen W. et al. 2008).

The important role of GRE in regulating Ob promoter activity was also shown by electrophoretic mobility shift assays. We found in nuclear extracts from MCF-7 cells treated with leptin plus BRL a strong increase in the GRE-DNA binding that was immunodepleted by anti-GR and anti-PPARγ antibodies, suggesting the presence of the two proteins in the complex. The physiologic relevance of GRE in the Ob promoter in vivo is pointed out by ChIP analysis showing that the GR/PPARγ occupancy of the GRE-containing promoter region, induced by leptin plus BRL treatment, is concomitant with a decrease in RNA Pol II recruitment and a reduction in Ob transcriptional activity. It is known that members of the nuclear hormone receptor superfamily, including GR and PPARγ, once activated, can interact physically and modulate target gene transcription (Ialenti A. et al. 2005; Nie M. et al. 2005). We have shown a strong association of PPARγ with GR in the nuclear fraction of untreated MCF-7 cells that was further potentiated by leptin plus BRL treatments.

PPARγ and GR can regulate transcription by several distinct mechanisms, and their functions, as shown for other corticosteroid receptors, seem to depend not only on ligand binding, which is known to regulate receptor conformation, but also on the context of the gene and associated promoter factors that contribute to create a gene-specific topography, achieving specific profiles of gene expression (Hall JM. et al. 2001; Katzenellenbogen BS. et al. 2002). Our proposed model for PPARγ-mediated repression of the Ob gene involves its interaction with GR and recruitment of the corepressors NCoR and SMRT, which share the same molecular architecture, interact with many of the same transcription factors, and assemble into similar corepressor complexes (Ghisletti S. et al. 2009). NCoR and SMRT are recruited by PPARγ and GR to regulate the transcription of different genes (Gurnell M. et al. 2000; Wang Q. et al. 2004). Overexpression of NCoR and

SMRT represses PPARγ-mediated gene transcription in certain cell types (Krogsdam et al. 2002), and recently, increasing evidence suggests that these two corepressors modulate adipogenesis most likely via their ability to repress PPARγ action (Powell E. et al. 2007; Samarasinghe et al. 2009). The present results suggest that in MCF-7 cells on BRL and to a higher extent leptin plus BRL stimulation, NCoR and SMRT are recruited on the GRE site of the Ob promoter together with GR and PPARγ. In addition, activation of PPARγ also decreases ObRs, inhibits its transductional pathways, and negatively interferes with estrogen signaling through the down-regulation of aromatase gene expression and the inhibition of ERα transactivation.

Taken together the present data: 1) suggest the potential use of the combined therapy with low doses of both BRL and 9RA as therapeutic tool also for breast cancer patients who develop resistance to anti-estrogen therapy; 2) address Bid as a potential target in the novel therapeutical strategies for breast cancer treatments; 3) further support the use of PPARγ ligands since rather than ameliorate metabolic parameters may represent pharmacologic tools exploited in breast cancer treatment, particularly for obese women.

References

Adams JM, Cory S: The Bcl-2 protein family: arbiters of cell survival. Science 1998; 281:1322-1326.

Ahima RS, Flier JS: Leptin. Annu Rev Physiol 2006; 2:413–437

Ahima RS, Osei SY: Leptin signaling. Physiol Behav 2004; 81:223–241

Andrews NC and Faller DV: A rapid micropreparation technique for extraction of DNA-binding proteins from limiting numbers of mammalian cells. Nucleic Acids Res 1991; 9:2499

Arakawa K, Ishihara T, Aoto M, Inamasu M, Kitamura K, and Saito A: An antidiabetic thiazolidinedione induces eccentric cardiac hypertrophy by cardiac volume overload in rats. Clin Exp Pharmacol Physiol 2004; 31:8–13

Bischoff ED, Gottardis MM, Moon TE, Heyman RA, Lamph WW: Beyond tamoxifen: the retinoid X receptor selective ligand LGD1069 (TARGRETIN) causes complete regression of mammary carcinoma. Cancer Res 1998; 58:479–484

Bonofiglio D, Aquila S, Catalano S, Gabriele S, Belmonte M, Middea E, Qi H, Morelli C, Gentile M, Maggiolini M, Ando` S: Peroxisome proliferator-activated receptor-gamma activates p53 gene promoter binding to the nuclear factor-kappaB sequence in human MCF7 breast cancer cells. Mol Endocrinol 2006; 20:3083–3092

Bonofiglio D, Aquila S, Catalano S, Gabriele S, Belmonte M, Middea E, Qi H, Morelli C, Gentile M, Maggiolini M, Andò S: Peroxisome proliferatoractivated receptor-gamma activates p53 gene promoter binding to the nuclear factor-kappaB sequence in human MCF7 breast cancer cells. Mol Endocrinol 2006; 20:3083-92.

Bonofiglio D, Gabriele S, Aquila S, Catalano S, Gentile M, Middea E, Giordano F, Ando` S: Estrogen receptor alpha binds to peroxisome proliferator-activated receptor (PPAR) response element and negatively interferes with PPAR gamma signalling in breast cancer cells. Clin Cancer Res 2005; 11:6139–6147

Bonofiglio D, Gabriele S, Aquila S, Qi H, Belmonte M, Catalano S, Ando` S: Peroxisome proliferator-activated receptor gamma activates fas ligand gene promoter inducing apoptosis in human breast cancer cells. Breast Cancer Res Treat 2009; 113:423–434

Bonofiglio D, Qi H, Gabriele S, Catalano S, Aquila S, Belmonte M, Andò S: Peroxisome proliferator-activated receptor-gamma inhibits follicular and anaplastic thyroid carcinoma cells growth by upregulating p21Cip/WAF1 in a Sp1-dependent manner. Endocr Relat Cancer 2008; 15:545-557.

Catalano S, Marsico S, Giordano C, Mauro L, Rizza P, Panno ML, Andò S: Leptin enhances, via AP-1, expression of aromatase in the MCF-7 cell line. J Biol Chem 2003; 278:28668–28676

Catalano S, Mauro L, Marsico S, Giordano C, Rizza P, Rago V, Montanaro D, Maggiolini M, Panno ML, Andó S: Leptin induces, via ERK1/ERK2 signal, functional activation of estrogen receptor α in MCF-7 cells. J Biol Chem 2004; 279:19908–19915

Chen W, Dang T, Blind RD, Wang Z, Cavasotto CN, Hittelman AB, Rogatsky I, Logan SK, Garabedian MJ: Glucocorticoid receptor phosphorylation differentially affects target gene expression. Mol Endocrinol 2008; 22:1754–1766

Chung SH, Onoda N, Ishikawa T, Ogisawa K, Takenaka C, Yano Y. Peroxisome proliferatoractivated receptor gamma activition induce cell cycarrest via p53-independent pathway in human anaplastic thyroid cancer cells. Jap J Cancer Res 2002; 93:1358-1365

Chung SW, Kang BY, Kim SH, Pak YK, Cho D, Trinchieri G, Kim TS: Oxidized low density lipoprotein inhibits interleukin-12 production in lipopolysaccharide-activated mouse macrophages via direct interactions between peroxisome proliferator-activated receptor- and nuclear factorkB. J Biol Chem 2000; 275:32681–32687

Clarke AR, Purdie CA, Harrison DJ, Morris RG, Bird CC, Hooper ML, Wyllie AH: Thymocyte apoptosis induced by p53-dependent and independent pathways. Nature 1993; 362:849-852

Cohen RN: Nuclear receptor corepressors and PPARγ. Nucl Recept Signal 2006.

Cossarizza A, Baccarani-Contri M, Kalashnikova G, Franceschi C: A new method for the cytofluorimetric analysis of mitochondrial membrane potential using the J-aggregate forming lipophilic cation 5,5',6,6'-tetrachloro-1,1',3,3'tetraethylbenzimidazolylcarbo-cyanine iodide (JC-1). Biochem Biophys Res Commun 1993; 197:40–45

Couturier C, Brouillet A, Couriaud C, Koumanov K, Bereziat G, Andreani M: Interleukin 1beta induces type II-secreted phospholipase A2 gene in vascular

smooth muscle cells by a nuclear factor k B and peroxisome proliferator-activated receptor-mediated process. J Biol Chem 1999; 274:23085–23093

Crowe DL, Chandraratna RA: A retinoid X receptor (RXR)-selective retinoid reveals that RXR-alpha is potentially a therapeutic target in breast cancer cell lines, and that it potentiates antiproliferative and apoptotic responses to peroxisome proliferator-activated receptor ligands. Breast Cancer Res 2004; 6:R546–R555

De Vos P, Lefebvre AM, Miller SG, Guerre-Millo M, Wong K, Saladin R, Hamann LG, Staels B, Briggs MR, Auwerx J: Thiazolidinediones repress ob gene expression in rodents via activation of peroxisome proliferator-activated receptor γ. J Clin Invest 1996; 98:1004–1009

Demetri GD, Fletcher CDM, Mueller E, Sarraf P, Naujoks R, Campbell N, Spiegelman BM, Singer S: Induction of solid tumor differentiation by the peroxisome proliferator activated receptor ligand troglitazone in patients with liposarcoma. Proc Natl Acad Sci USA 1999; 96:3951–3956

Elstner E, Muller C, Koshizuka K, Williamson EA, Park D, Asou H, Shintaku P, Said JW, Heber D, Koeffler HP: Ligands for peroxisome proliferator-activated receptor and retinoic acid receptor inhibit growth and induce apoptosis of human breast cancer cells in vitro and in BNX mice. Proc Natl Acad Sci USA 1998; 95:8806–8811

Elstner E, Williamson EA, Zang C, Fritz J, Heber D, Fenner M, Possinger K, Koeffler HP: Novel therapeutic approach: ligands for PPAR and retinoid receptors induce apoptosis in bcl-2-positive human breast cancer cells. Breast Cancer Res Treat 2002; 74:155–165

Garofalo C, Surmacz E: Leptin and cancer. J Cell Physiol 2006; 207:12–22

Gee MF, Tsuchida R, Eichler-Jonsson C, Das B, Baruchel S, Malkin D: Vascular endothelial growth factor acts in an autocrine manner in rhabdomyosarcoma cell lines and can be inhibited with all-transretinoic acid. Oncogene 2005; 24:8025–8037

Ghisletti S, Huang W, Jepsen K, Benner C, Hardiman G, Rosenfeld MG, Glass CK: Cooperative NCoR/SMRT interactions establish a corepressor-based strategy for integration of inflammatory and anti-inflammatory signaling pathways. Genes Dev 2009; 23:681–693

Goetze S, Bungenstock A, Czupalla C, Eilers F, Stawowy P, Kintscher U, Spencer-Hänsch C, Graf K, Nürnberg B, Law RE, Fleck E, Gräfe M: Leptin

induces endothelial cell migration through Akt, which is inhibited by PPAR-ligands. Hypertension 2002, 40:748–754

Gong DW, Bi S, Pratley RE, Weintraub BD: Genomic structure and promoter analysis of the human obese gene. J Biol Chem 1996; 271:3971–3974

Grommes C, Landreth GE, Heneka MT: Antineoplastic effects of peroxisome proliferator-activated receptor gamma agonists. Lancet Oncol 2004; 5:419–429

Gross A, McDonnell JM, Korsmeyer SJ. BCL-2 family members and the mitochondria in apoptosis. Genes Dev 1999; 13:1899-911.

Gurnell M, Wentworth JM, Agostini M, Adams M, Collingwood TN, Provenzano C, Browne PO, Rajanayagam O, Burris TP, Schwabe JW, Lazar MA, Chatterjee VK: A dominant-negative peroxisome proliferatoractivated receptor (PPAR) mutant is a constitutive repressor and inhibits PPAR-mediated adipogenesis. J Biol Chem 2000; 275:5754–5759

Hall JM, Couse JF, Korach KS: The multifaceted mechanisms of estradiol and estrogen receptor signaling. J Biol Chem 2001; 276: 36869–36872

Heyman RA, Mangelsdorf DJ, Dyck JA, Stein RB, Eichele G, Evans RM, Thaller C: 9-cis retinoic acid is a high affinity ligand for the retinoid X receptor. Cell 1992; 68:397–406

Hiscox S, Morgan L, Green TP, Barrow D, Gee J, Nicholson RI: Elevated Src activity promotes cellular invasion and motility in tamoxifen resistant breast cancer cells. Breast Cancer Res Treat 2005; 7:1–12

Hong J, Samudio I, Liu S, Abdelrahim M, Safe S. Peroxisome proliferator-activited receptor γ-dependent activation of p21 in panc-28 pancreatic cancer cells involves Sp1 and Sp4 proteins. Endocrinology 2004; 145:5774-5785

Ialenti A, Grassia G, Di Meglio P, Maffia P, Di Rosa M, Ianaro A: Mechanism of the anti-inflammatory effect of thiazolidinediones: relationship with the glucocorticoid pathway. Mol Pharmacol 2005; 67:1620–1628

Ikawa H, Kameda H, Kamitani H, Baek SJ, Nixon JB, His LC, Eling TE: Effect of PPAR activators on cytokine stimulated cyclooxygenase-2 expression in human colorectal carcinoma cells. Exp Cell Res 2001; 267:73–80

Jones HE, Goddard L, Gee JMW, Hiscox S, Rubini M, Barrow D, Knowlden JM, Williams S. Wakeling AE, Nicholson RI: Insulin-like growth factor-I receptor signaling and acquired resistance to gefitinib (ZD1839, Iressa) in human breast and prostate cancer cells. Endocr Relat Cancer 2004; 11:793–814

Katsumoto T, Higaki K, Ohno K, Onodera K. Cell cycle dependent biosynthesis and localization of p53 protein in untransformed human cells. Biol Cell 1995; 84:167-173

Katzenellenbogen BS, Katzenellenbogen JA: Biomedicine: defining the "S" in SERMs. Science 2002; 295:2380–2381

Kitamura S, Miyazaki Y, Shinomura Y, Kondo S, Kanayama S, Matsuzawa Y: Peroxisome proliferator activated receptor induces growth arrest and differentiation markers of human colon cancer cells. Jpn J Cancer Res 1999; 90:75–80

Kliewer SA, Umesono K, Mangelsdorf DJ, Evans RM: Retinoid X receptor interacts with nuclear receptors in retinoic acid, thyroid hormone, and vitamin D3 signaling. Nature 1992, 355:446–449.

Knowlden JM, Hutcheson IR, Jones HE, Madden T, Gee JMW, Harper ME, Barrow D, Wakeling AE, Nicholson RI: Elevated levels of EGFR/ c-erbB2 heterodimers mediate an autocrine growth regulatory pathway in tamoxifen-resistant MCF-7 cells. Endocrinology 2003; 144:1032–1044

Korsmeyer SJ, Wei MC, Saito M, Weiler S, Oh KJ, Schlesinger PH: Pro-apoptotic cascade activates BID, which oligomerizes BAK or BAX into pores that result in the release of cytochrome c. Cell Death Differ 2000; 7:1166-1173

Krogsdam AM, Nielsen CA, Neve S, Holst D, Helledie T, Thomsen B, Bendixen C, Mandrup S, Kristiansen K: Nuclear receptor corepressor-dependent repression of peroxisome-proliferator-activated receptor delta-mediated transactivation. Biochem J 2002; 363:157–165

Lee JI, Paik YH, Lee KS, Lee JW, Kim YS, Jeong S, Kwon KS, Lee DH, Kim HG, Shin YW, Kim MA: A peroxisome-proliferator activated receptor-gamma ligand could regulate the expression of leptin receptor on human hepatic stellate cells. Histochem Cell Biol 2007, 127:495–502

Lefebvre P, Chinetti G, Fruchart JC & Staels B Sorting out the roles of PPARα in energy metabolism and vascular homeostasis. Journal of Clinical Investigation 2006; 116 571–580

Lehrke M & Lazar MA The many faces of PPARγ. Cell 2005; 123:993–999

Lemberger T, Desvergne B & Wahli W: Peroxisome proliferator-activated receptors: a nuclear receptor signaling pathway in lipid physiology. Annual Review of Cell and Developmental Biology 1996; 12:335–363

Lowe SW, Bodis S, McClatchey A, Remington L, Ruley HE, Fisher DE, Housman DE, Jacks T: p53 status and the efficacy of cancer therapy in vivo. Science 1994; 266:807-8 10.

Lowe SW, Schmitt EM, Smith SW, Osborne BA, Jacks T: p53 is required for radiation-induced apoptosis in mouse thymocytes. Nature 1993; 362:847-849.

Marchenko ND, Zaika A, Moll UM: Death signalinduced localization of p53 protein to mitochondria. A potential role in apoptotic signaling. J Biol Chem 2000; 275:16202-16212

Mauro L, Catalano S, Bossi G, Pellegrino M, Barone I, Morales S, Giordano C, Bartella V, Casaburi I, Andò S: Evidences that leptin up-regulates E-cadherin expression in breast cancer: effects on tumor growth and progression. Cancer Res 2007; 67:3412–3421

Mauro L, Surmacz E: IGF-I receptor, cell-cell adhesion, tumor development and progression. J Mol Histol 2004; 35:247–253

Mehta RG, Williamson E, Patel MK, Koeffler HP: A ligand of peroxisome proliferator-activated receptor gamma, retinoids, and prevention of preneoplastic mammary lesions. J Natl Cancer Inst 2000; 92:418–423

Mihara M, Erster S, Zaika A, Petrenko O, Chittenden T, Pancoska P. p53 has a direct apoptogenic role at the mitochondria. Mol Cell 2003; 11:577-590.

Mizuguchi Y, Wada A, Nakagawa K, Ito M, Okano T: Antitumoral activity of 13-demethyl or 13-substituted analogues of all-trans retinoic acid and 9-cis retinoic acid in the human myeloid leukemia cell line HL-60. Biol Pharm Bull 2006; 29:1803–1809

Mosmann T: Rapid colorimetric assay for cellular growth and survival: application to proliferation and cytotoxicity assays. J Immunol Methods 1983, 65:55–63

Mueller E, Sarraf P, Tontonoz P, Evans RM, Martin KJ, Zhang M, Fletcher C, Singer S, Spiegelman BM: Terminal differentiation of human breast cancer through PPAR. Mol Cell 1998; 1:465–470

Murphy ME, Leu JIJ, George DL: p53 moves to mitochondria. A turn on the path to apoptosis. Cell Cycle 2004; 3:836-839

Nie M, Corbett L, Knox AJ, Pang L: Differential regulation of chemokine expression by peroxisome proliferator-activated receptor γ agonists: interactions with glucocorticoids and 2-agonists. J Biol Chem 2005; 280:2550–2561

Pinaire JA, Reifel-Miller A: Therapeutic potential of retinoid x receptor modulators for the treatment of the metabolic syndrome. PPAR Res 2007; 2007:94156

Powell E, Kuhn P, Xu W: Nuclear receptor cofactors in PPARγ-mediated adipogenesis and adipocyte energy metabolism. PPAR Res 2007; 2007:53843

Qin C, Nguyen T, Stewart J, Samudio I, Burghardt R, Safe S: Estrogen up-regulation of p53 gene expression in MCF-7 breast cancer cells is mediated by calmodulin kinase IV-dependent activation of a nuclear factor kB/CCAAT-binding transcription factor-1 complex. Mol Endocrinol 2002; 16:1793–1809

Rangwala SM and Lazar MA: Peroxisome proliferator-activated receptor gamma in diabetes and metabolism. Trends Pharmacol Sci 2004; 25:331–336

Ricote M, Glass CK: PPARs and molecular mechanisms of transrepression. Biochim Biophys Acta 2007; 1771:926–935

Rieusset J, Auwerx J, Vidal H: Regulation of gene expression by activation of the peroxisome proliferator-activated receptor γ with rosiglitazone (BRL 49653) in human adipocytes. Biochem Biophys Res Commun 1999; 265:265–271

Roberts-Thomson SJ: Peroxisome proliferator activated receptors in tumorigenesis: targets of tumor promotion and treatment. Immunol Cell Biol 2000; 78:436–441

Ronacher K, Hadley K, Avenant C, Stubsrud E, Simons SS Jr, Louw A, Hapgood JP: Ligand-selective transactivation and transrepression via the glucocorticoid receptor: role of cofactor interaction. Mol Cell Endocrinol 2009; 299:219–231

Saez E, Rosenfeld J, Livolsi A, Olson P, Lombardo E, Nelson M, Banayo E, Cardiff RD, Izpisua-Belmonte JC, Evans RM: PPARgamma signaling exacerbates mammary gland tumor development. Genes Dev 2004; 18:528–540

Samarasinghe SP, Sutanto MM, Danos AM, Johnson DN, Brady MJ, Cohen RN: Altering PPARγ ligand selectivity impairs adipogenesis by thiazolidinediones but not hormonal inducers. Obesity (Silver Spring) 2009; 17:965–972

Sax JK, Fei P, Murphy ME, Bernhard E, Korsmeyer SJ, El-Deiry WS: BID regulation by p53 contributes to chemosensitivity. Nat Cell Biol 2002; 4:842-849

Schlezinger JJ, Jensen BA, Mann KK, Ryu HY, Sherr DH: Peroxisome proliferator-activated receptor γ-mediated NFkB activation and apoptosis in pre-B cells. J Immunol 2002; 169:6831–6841

Simeone AM, Tari AM: How retinoids regulate breast cancer cell proliferation and apoptosis. Cell Mol Life Sci 2004; 61:1475–1484

Smiley ST, Reers M, Mottola-Hartshorn C, Lin M, Chen A, Smith TW, Steele GD, Chen LB: Intracellular heterogeneity in mitochondrial membrane potentials revealed by a J-aggregate forming lipophilic cation JC-1. Proc Natl Acad Sci USA 1991; 88:3671–3675

Song G, Chen GG, Yun JP, Lai PB: Association of p53 with Bid induces cell death in response to etoposide treatment in hepatocellular carcinoma. Curr Cancer Drug Targets 2009; 9:871-880

Sporn MB, Suh N, Mangelsdorf DJ: Prospects for prevention and treatment of cancer with selective PPARgamma modulators (SPARMs). Trends Mol Med 2001; 7:395–400

Staels B: Fluid retention mediated by renal PPARgamma. Cell Metab 2005; 2:77–78

Suh N, Wang Y, Williams CR, Risingsong R, Gilmer T, Willson TM, Sporn MB: A new ligand for the peroxisome proliferator-activated receptor-gamma (PPAR-gamma). GW7845, inhibits rat mammary carcinogenesis. Cancer Res 1999; 59:5671–5673

Sun YX, Wright HT, Janciasukiene S: Alpha1-antichymotrypsin/Alzheimer's peptide Abeta (1–42) complex perturbs lipid metabolism and activates transcription factors PPARγ and NFkB in human neuroblastoma (Kelly) cells. J Neurosci Res 2002; 67:511–522

Sweeney G: Leptin signalling. Cell Signal 2002; 14:655–663

Tang Y, Zheng S, Chen A: Curcumin eliminates leptin's effects on hepatic stellate cell activation via interrupting leptin signaling. Endocrinology 2009; 150:3011–3020

Tontonoz P, Hu E, Spiegelman BM: Stimulation of adipogenesis in fibroblasts by PPAR gamma 2, a lipid-activated transcription factor. Cell 1994; 79:1147–1156

Tsubouchi Y, Sano H, Kawahito Y, Mukai S, Yamada R, Kohno M, Inoue K, Hla T, Kondo M: Inhibition of human lung cancer cell growth by the peroxisome proliferator activated receptor agonists through induction of apoptosis. Biochem Biophys Res Commun 2000; 270:400–405

van der Laan S, Meijer OC: Pharmacology of glucocorticoids: beyond receptors. Eur J Pharmacol 2008; 585:483–491

Vona-Davis L, Rose DP: Adipokines as endocrine, paracrine and autocrine factors in breast cancer risk and progression. Endocr Relat Cancer 2007; 14:189–206

Wan H, Hong WK, Lotan R: Increased retinoic acid responsiveness in lung carcinoma cells that are nonresponsive despite the presence of endogenous retinoic acid receptor (RAR) beta by expression of exogenous retinoid receptors retinoid X receptor alpha, RAR alpha, and RAR gamma. Cancer Res 2001; 61:556–564

Wang Q, Blackford JA Jr, Song LN, Huang Y, Cho S, Simons SS Jr: Equilibrium interactions of corepressors and coactivators with agonist and antagonist complexes of glucocorticoid receptors. Mol Endocrinol 2004; 18:1376–1395

Wang X, Southard RC, Kilgore MW: The increased expression of peroxisome proliferator-activated receptor-gamma1 in human breast cancer is mediated by selective promoter usage. Cancer Res 2004; 64:5592–5596

Wei MC, Lindsten T, Mootha VK, Weiler S, Gross A, Ashiya M.,tBID, a membrane-targeted death ligand, oligomerizes BAK to release cytochrome c. Genes Dev 2000; 14:2060-2071

Wei MC, Zong WX, Cheng EH, Lindsten T, Panoutsakopoulou V, Ross AJ, Proapoptotic BAX and BAK: A requisite gateway to mitochondrial dysfunction and death. Science 2001; 292:727-730

Wu K, DuPre´ E, Kim H, Tin-U CK, Bissonnette RP, Lamph WW, Brown PH: Receptor-selective retinoids inhibit the growth of normal and malignant breast cells by inducing G1 cell cycle blockade. Breast Cancer Res Treat 2006; 96:147–157

Yee LD, Williams N, Wen P, Young DC, Lester J, Johnson MV, Farrar WB, Walker MJ, Povoski SP, Suster S, Eng C: Pilot study of rosiglitazone therapy in women with breast cancer: effects of short-term therapy on tumor tissue and serum markers. Clin Cancer Res 2007; 13:246–252

Zhang XK, Hoffmann B, Tran PBV, Graupner G, Pfahl M: Retinoid X receptor is an auxiliary protein for thyroid hormone and retinoic acid receptors. Nature 1992, 355:441–445.

Zimmet P, Boyko EJ, Collier GR, de Courten M: Etiology of the metabolic syndrome: potential role of insulin resistance, leptin resistance, and other players. Ann N Y Acad Sci 1999; 892:25–44

The American Journal of Pathology, Vol. 175, No. 3, September 2009

DOI: 10.2353/ajpath.2009.081078

Tumorigenesis and Neoplastic Progression

Combined Low Doses of PPARγ and RXR Ligands Trigger an Intrinsic Apoptotic Pathway in Human Breast Cancer Cells

Daniela Bonofiglio,* Erika Cione,* Hongyan Qi,* Attilio Pingitore,* Mariarita Perri,* Stefania Catalano,* Donatella Vizza,* Maria Luisa Panno,† Giuseppe Genchi,* Suzanne A.W. Fuqua,‡ and Sebastiano Andò†§¶

From the Departments of Pharmaco-Biology, and Cellular Biology,† the Centro Sanitario,§ and the Faculty of Pharmacy Nutritional and Health Sciences,¶ University of Calabria, Arcavacata di Rende (Cosenza), Italy; and the Lester and Sue Smith Breast Center,‡ Department of Medicine, Baylor College of Medicine, Houston, Texas*

Ligand activation of peroxisome proliferator-activated receptor (PPAR)γ and retinoid X receptor (RXR) induces antitumor effects in cancer. We evaluated the ability of combined treatment with nanomolar levels of the PPARγ ligand rosiglitazone (BRL) and the RXR ligand 9-*cis*-retinoic acid (9RA) to promote antiproliferative effects in breast cancer cells. BRL and 9RA in combination strongly inhibit of cell viability in MCF-7, MCF-7TR1, SKBR-3, and T-47D breast cancer cells, whereas MCF-10 normal breast epithelial cells are unaffected. In MCF-7 cells, combined treatment with BRL and 9RA up-regulated mRNA and protein levels of both the tumor suppressor p53 and its effector $p21^{WAF1/Cip1}$. Functional experiments indicate that the nuclear factor-κB site in the p53 promoter is required for the transcriptional response to BRL plus 9RA. We observed that the intrinsic apoptotic pathway in MCF-7 cells displays an ordinated sequence of events, including disruption of mitochondrial membrane potential, release of cytochrome *c*, strong caspase 9 activation, and, finally, DNA fragmentation. An expression vector for p53 antisense abrogated the biological effect of both ligands, which implicates involvement of p53 in PPARγ/RXR-dependent activity in all of the human breast malignant cell lines tested. Taken together, our results suggest that multidrug regimens including a combination of PPARγ and RXR ligands may provide a therapeutic advantage in breast cancer treatment. ***(Am J Pathol 2009, 175:1270–1280; DOI: 10.2353/ajpath.2009.081078)***

Breast cancer is the leading cause of death among women in the world. The principal effective endocrine therapy for advanced treatment on this type of cancer is anti-estrogens, but therapeutic choices are limited for estrogen receptor (ER)α-negative tumors, which are often aggressive. The development of cancer cells that are resistant to chemotherapeutic agents is a major clinical obstacle to the successful treatment of breast cancer, providing a strong stimulus for exploring new approaches *in vitro*. Using ligands of nuclear hormone receptors to inhibit tumor growth and progression is a novel strategy for cancer therapy. An example of this is the treatment of acute promyelocytic leukemia using all-*trans* retinoic acid, the specific ligand for retinoic acid receptors.[1–3] A further paradigm for the use of retinoids in cancer therapy is for early lesions of head and neck cancer[4] and squamous cell carcinoma of the cervix.[5]

The retinoic acid receptor, retinoid X receptor (RXR), and peroxisome proliferator receptor (PPAR)γ, ligand-activated transcription factors belonging to the nuclear hormone receptor superfamily, are able to modulate gene networks involved in controlling growth and cellular differentiation.[6] Particularly, heterodimerization of PPARγ with RXR by their own ligands greatly enhances DNA binding to the direct-repeated consensus sequence AGGTCA, which leads to transcriptional activation.[7] Previous data show that PPARγ, poorly expressed in normal breast epithelial cells,[8] is present at higher levels in

Supported by AIRC, MURST, and Ex 60%.

Portions of this work were presented as an Abstract at Società Italiana di Patologia XXIX National Congress in Rende, Italy, on September 10–13, 2008.

Accepted for publication June 5, 2009.

Supplemental material for this article can be found on *http://ajp.amjpathol.org*.

Address reprint requests to Prof. Sebastiano Andò, Faculty of Pharmacy Nutritional and Health Sciences, University of Calabria, 87036 Arcavacata - Rende (Cosenza), Italy. E-mail: sebastiano.ando@unical.it.

breast cancer cells,[9] and its synthetic ligands, such as thiazolidinediones, induce growth arrest and differentiation in breast carcinoma cells *in vitro* and in animal models.[10–11] Recently, studies in human cultured breast cancer cells show the thiazolidinedione rosiglitazone (BRL), promotes antiproliferative effects and activates different molecular pathways leading to distinct apoptotic processes.[12–14]

Apoptosis, genetically controlled and programmed death leading to cellular self-elimination, can be initiated by two major routes: the intrinsic and extrinsic pathways. The intrinsic pathway is triggered in response to a variety of apoptotic stimuli that produce damage within the cell, including anticancer agents, oxidative damage, and UV irradiation, and is mediated through the mitochondria. The extrinsic pathway is activated by extracellular ligands able to induce oligomerization of death receptors, such as Fas, followed by the formation of the death-inducing signaling complex, after which the caspases cascade can be activated.

Previous data show that the combination of PPARγ ligand with either all-*trans* retinoic acid or 9-*cis*-retinoic acid (9RA) can induce apoptosis in some breast cancer cells.[15] Furthermore, Elstner et al demonstrated that the combination of these drugs at micromolar concentrations reduced tumor mass without any toxic effects in mice.[8] However, in humans PPARγ agonists at high doses exert many side effects including weight gain due to increased adiposity, edema, hemodilution, and plasma-volume expansion, which preclude their clinical application in patients with heart failure.[16–18] The undesirable effects of RXR-specific ligands on hypertriglyceridemia and suppression of the thyroid hormone axis have been also reported.[19] Thus, in the present study we have elucidated the molecular mechanism by which combined treatment with BRL and 9RA at nanomolar doses triggers apoptotic events in breast cancer cells, suggesting potential therapeutic uses for these compounds.

Materials and Methods

Reagents

BRL49653 (BRL) was from Alexis (San Diego, CA), the irreversible PPARγ-antagonist GW9662 (GW), and 9RA were purchased from Sigma (Milan, Italy).

Plasmids

The p53 promoter-luciferase plasmids, kindly provided by Dr. Stephen H. Safe (Texas A&M University, College Station, TX), were generated from the human p53 gene promoter as follows: p53-1 (containing the −1800 to + 12 region), p53-6 (containing the −106 to + 12 region), p53-13 (containing the −106 to −40 region), and p53-14 (containing the −106 to −49 region).[20] As an internal transfection control, we cotransfected the plasmid pRL-CMV (Promega Corp., Milan, Italy) that expresses Renilla luciferase enzymatically distinguishable from firefly luciferase by the strong cytomegalovirus enhancer promoter. The pGL3 vector containing three copies of a peroxisome proliferator response element sequence upstream of the minimal thymidine kinase promoter ligated to a luciferase reporter gene (3XPPRE-TK-pGL3) was a gift from Dr. R. Evans (The Salk Institute, San Diego, CA). The p53 antisense plasmid (AS/p53) was kindly provided from Dr. Moshe Oren (Weizmann Institute of Science, Rehovot, Israel).

Cell Cultures

Wild-type human breast cancer MCF-7 cells were grown in Dulbecco's modified Eagle's medium-F12 plus glutamax containing 5% newborn calf serum (Invitrogen, Milan, Italy) and 1 mg/ml penicillin-streptomycin. MCF-7 tamoxifen resistant (MCF-7TR1) breast cancer cells were generated in Dr. Fuqua's laboratory similar to that described by Herman[21] maintaining cells in modified Eagle's medium with 10% fetal bovine serum (Invitrogen), 6 ng/ml insulin, penicillin (100 units/ml), streptomycin (100 μg/ml), and adding 4-hydroxytamoxifen in tenfold increasing concentrations every weeks (from 10^{-9} to 10^{-6} final). Cells were thereafter routinely maintained with 1 μmol/L 4-hydroxytamoxifen. SKBR-3 breast cancer cells were grown in Dulbecco's modified Eagle's medium without red phenol, plus glutamax containing 10% fetal bovine serum and 1 mg/ml penicillin-streptomycin. T-47D breast cancer cells were grown in RPMI 1640 medium with glutamax containing 10% fetal bovine serum, 1 mmol/L sodium pyruvate, 10 mmol/L HEPES, 2.5g/L glucose, 0.2 U/ml insulin, and 1 mg/ml penicillin-streptomycin. MCF-10 normal breast epithelial cells were grown in Dulbecco's modified Eagle's medium-F12 plus glutamax containing 5% horse serum (Sigma), 1 mg/ml penicillin-streptomycin, 0.5 μg/ml hydrocortisone, and 10 μg/ml insulin.

Cell Viability Assay

Cell viability was determined with the 3-(4,5-dimethylthiazol-2-yl)-2,5-diphenyltetrazolium (MTT) assay.[22] Cells (2×10^5 cells/ml) were grown in 6 well plates and exposed to 100 nmol/L BRL, 50 nmol/L 9RA alone or in combination in serum free medium (SFM) and in 5% charcoal treated (CT)-fetal bovine serum; 100 μl of MTT (5 mg/ml) were added to each well, and the plates were incubated for 4 hours at 37°C. Then, 1 ml 0.04 N HCl in isopropanol was added to solubilize the cells. The absorbance was measured with the Ultrospec 2100 Pro-spectrophotometer (Amersham-Biosciences, Milan, Italy) at a test wavelength of 570 nm.

Immunoblotting

Cells were grown in 10-cm dishes to 70% to 80% confluence and exposed to treatments in SFM as indicated. Cells were then harvested in cold PBS and resuspended in lysis buffer containing 20 mmol/L HEPES (pH 8), 0.1 mmol/L EGTA, 5 mmol/L $MgCl_2$, 0.5 M/L NaCl, 20% glycerol, 1% Triton, and inhibitors (0.1 mmol/L sodium orthovanadate, 1% phenylmethylsulfonylfluoride, and 20

mg/ml aprotinin). Protein concentration was determined by Bio-Rad Protein Assay (Bio-Rad Laboratories, Hercules, CA). A 40 μg portion of protein lysates was used for Western blotting, resolved on a 10% SDS-polyacrylamide gel, transferred to a nitrocellulose membrane, and probed with an antibody directed against the p53, $p21^{WAF1/Cip1}$ (Santa Cruz Biotechnology, CA). As internal control, all membranes were subsequently stripped (0.2 M/L glycine, pH 2.6, for 30 minutes at room temperature) of the first antibody and reprobed with anti-glyceraldehyde-3-phosphate dehydrogenase antibody (Santa Cruz Biotechnology). The antigen–antibody complex was detected by incubation of the membranes for 1 hour at room temperature with peroxidase-coupled goat anti-mouse or anti-rabbit IgG and revealed using the enhanced chemiluminescence system (Amersham Pharmacia, Buckinghamshire UK). Blots were then exposed to film (Kodak film, Sigma). The intensity of bands representing relevant proteins was measured by Scion Image laser densitometry scanning program.

Reverse Transcription-PCR Assay

MCF-7 cells were grown in 10 cm dishes to 70% to 80% confluence and exposed to treatments in SFM as indicated. Total cellular RNA was extracted using TRIZOL reagent (Invitrogen) as suggested by the manufacturer. The purity and integrity were checked spectroscopically and by gel electrophoresis before carrying out the analytical procedures. Two micrograms of total RNA were reverse transcribed in a final volume of 20 μl using a RETROscript kit as suggested by the manufacturer (Promega). The cDNAs obtained were amplified by PCR using the following primers: 5′-GTGGAAGGAAATTTGCGTGT-3′ (p53 forward) and 5′-CCAGTGTGATGATGGTGAGG-3′ (p53 reverse), 5′-GCTTCATGCCAGCTACTTCC-3′ (p21 forward) and 5′-CTGTGCTCACTTCAGGGTCA-3′ (p21 reverse), 5′-CTCAACATCTCCCCCTTCTC-3′ (36B4 forward) and 5′-CAAATCCCATATCCTCGTCC-3′ (36B4 reverse) to yield, respectively, products of 190 bp with 18 cycles, 270 bp with 18 cycles, and 408 bp with 12 cycles. To check for the presence of DNA contamination, reverse transcription (RT)-PCR was performed on 2 μg of total RNA without Monoley murine leukemia virus reverse transcriptase (the negative control). The results obtained as optical density arbitrary values were transformed to percentage of the control taking the samples from untreated cells as 100%.

Transfection Assay

MCF-7 cells were transferred into 24-well plates with 500 μl of regular growth medium/well the day before transfection. The medium was replaced with SFM on the day of transfection, which was performed using Fugene 6 reagent as recommended by the manufacturer (Roche Diagnostics, Mannheim, Germany) with a mixture containing 0.5 μg of promoter-luc or reporter-luc plasmid and 5 ng of pRL-CMV. After transfection for 24 hours, treatments were added in SFM as indicated, and cells were incubated for an additional 24 hours. Firefly and Renilla luciferase activities were measured using the Dual Luciferase Kit (Promega). The firefly luciferase values of each sample were normalized by Renilla luciferase activity, and data were reported as relative light units.

MCF-7 cells plated into 10 cm dishes were transfected with 5 μg of AS/p53 using Fugene 6 reagent as recommended by the manufacturer (Roche Diagnostics). The activity of AS/p53 was verified using Western blot to detect changes in p53 protein levels. Empty vector was used to ensure that DNA concentrations were constant in each transfection.

Electrophoretic Mobility Shift Assay

Nuclear extracts from MCF-7 cells were prepared as previously described.[23] Briefly, MCF-7 cells plated into 10-cm dishes were grown to 70% to 80% confluence, shifted to SFM for 24 hours, and then treated with 100 nmol/L BRL, 50 nmol/L 9RA alone and in combination for 6 hours. Thereafter, cells were scraped into 1.5 ml of cold PBS, pelleted for 10 seconds, and resuspended in 400 μl cold buffer A (10 mmol/L HEPES-KOH [pH 7.9] at 4°C, 1.5 mmol/L $MgCl_2$, 10 mmol/L KCl, 0.5 mmol/L dithiothreitol, 0.2 mmol/L phenylmethylsulfonyl fluoride, and 1 mmol/L leupeptin) by flicking the tube. Cells were allowed to swell on ice for 10 minutes and were then vortexed for 10 seconds. Samples were then centrifuged for 10 seconds and the supernatant fraction was discarded. The pellet was resuspended in 50 μl of cold Buffer B (20 mmol/L HEPES-KOH [pH 7.9], 25% glycerol, 1.5 mmol/L $MgCl_2$, 420 mmol/L NaCl, 0.2 mmol/L EDTA, 0.5 mmol/L dithiothreitol, 0.2 mmol/L phenylmethylsulfonyl fluoride, and 1 mmol/L leupeptin) and incubated in ice for 20 minutes for high-salt extraction. Cellular debris was removed by centrifugation for 2 minutes at 4°C, and the supernatant fraction (containing DNA-binding proteins) was stored at −70°C. The probe was generated by annealing single-stranded oligonucleotides and labeled with [^{32}P]ATP (Amersham Pharmacia) and T4 polynucleotide kinase (Promega) and then purified using Sephadex G50 spin columns (Amersham Pharmacia). The DNA sequence of the nuclear factor (NF)κB located within p53 promoter as probe is 5′-AGTTGAGGGGACTTTCCCAGGC-3′ (Sigma Genosys, Cambridge, UK). The protein-binding reactions were performed in 20 μl of buffer [20 mmol/L HEPES (pH 8), 1 mmol/L EDTA, 50 mmol/L KCl, 10 mmol/L dithiothreitol, 10% glycerol, 1 mg/ml bovine serum albumin, 50 μg/ml polydeoxyinosinic deoxycytidylic acid] with 50,000 cpm of labeled probe, 20 μg of MCF7 nuclear protein, and 5 μg of polydeoxyinosinic deoxycytidylic acid. The mixtures were incubated at room temperature for 20 minutes in the presence or absence of unlabeled competitor oligonucleotides. For the experiments involving anti-PPARγ and anti-RXRα antibodies (Santa Cruz Biotechnology), the reaction mixture was incubated with these antibodies at 4°C for 30 minutes before addition of labeled probe. The entire reaction mixture was electrophoresed through a 6% polyacrylamide gel in 0.25× Tris borate-EDTA for 3 hours at 150 V. Gel was dried and subjected to autoradiography at −70°C.

Chromatin Immunoprecipitation Assay

MCF-7 cells were grown in 10 cm dishes to 50% to 60% confluence, shifted to SFM for 24 hours, and then treated for 1 hour as indicated. Thereafter, cells were washed twice with PBS and cross-linked with 1% formaldehyde at 37°C for 10 minutes. Next, cells were washed twice with PBS at 4°C, collected and resuspended in 200 μl of lysis buffer (1% SDS, 10 mmol/L EDTA, 50 mmol/L Tris-HCl, pH 8.1), and left on ice for 10 minutes. Then, cells were sonicated four times for 10 seconds at 30% of maximal power (Vibra Cell 500 W; Sonics and Materials, Inc., Newtown, CT) and collected by centrifugation at 4°C for 10 minutes at 14,000 rpm. The supernatants were diluted in 1.3 ml of immunoprecipitation buffer (0.01% SDS, 1.1% Triton X-100, 1.2 mmol/L EDTA, 16.7 mmol/L Tris-HCl [pH 8.1], 16.7 mmol/L NaCl) followed by immunoclearing with 60 μl of sonicated salmon sperm DNA/protein A agarose (DBA Srl, Milan, Italy) for 1 hour at 4°C. The precleared chromatin was immunoprecipitated with anti-PPARγ, anti-RXRα, or anti-RNA Pol II antibodies (Santa Cruz Biotechnology). At this point, 60 μl salmon sperm DNA/protein A agarose was added, and precipitation was further continued for 2 hours at 4°C. After pelleting, precipitates were washed sequentially for 5 minutes with the following buffers: Wash A [0.1% SDS, 1% Triton X-100, 2 mmol/L EDTA, 20 mmol/L Tris-HCl (pH 8.1), 150 mmol/L NaCl]; Wash B [0.1% SDS, 1% Triton X-100, 2 mmol/L EDTA, 20 mmol/L Tris-HCl (pH 8.1), 500 mmol/L NaCl]; and Wash C [0.25 M/L LiCl, 1% NP-40, 1% sodium deoxycholate, 1 mmol/L EDTA, 10 mmol/L Tris-HCl (pH 8.1)], and then twice with 10 mmol/L Tris, 1 mmol/L EDTA. The immunocomplexes were eluted with elution buffer (1% SDS, 0.1 M/L NaHCO3). The eluates were reverse cross-linked by heating at 65°C and digested with proteinase K (0.5 mg/ml) at 45°C for 1 hour. DNA was obtained by phenol-chloroform-isoamyl alcohol extraction. Two microliters of 10 mg/ml yeast tRNA (Sigma) were added to each sample, and DNA was precipitated with 95% ethanol for 24 hours at −20°C and then washed with 70% ethanol and resuspended in 20 μl of 10 mmol/L Tris, 1 mmol/L EDTA buffer. A 5 μl volume of each sample was used for PCR with primers flanking a sequence present in the p53 promoter: 5′-CTGAGAGCAAACGCAAAAG-3′ (forward) and 5′-CAGCCCGAACGCAAAGTGTC- 3′ (reverse) containing the κB site from −254 to −42 region. The PCR conditions for the p53 promoter fragments were 45 seconds at 94°C, 40 seconds at 57°C, and 90 seconds at 72°C. The amplification products obtained in 30 cycles were analyzed in a 2% agarose gel and visualized by ethidium bromide staining. The negative control was provided by PCR amplification without a DNA sample. The specificity of reactions was ensured using normal mouse and rabbit IgG (Santa Cruz Biotechnology).

JC-1 Mitochondrial Membrane Potential Detection Assay

The loss of mitochondrial membrane potential was monitored with the dye 5,5′,6,6′tetra-chloro-1,1′,3,3′-tetraethylbenzimidazolyl-carbocyanine iodide (JC-1) (Biotium, Hayward). In healthy cells, the dye stains the mitochondria bright red. The negative charge established by the intact mitochondrial membrane potential allows the lipophilic dye, bearing a delocalized positive charge, to enter the mitochondrial matrix where it aggregates and gives red fluorescence. In apoptotic cells, the mitochondrial membrane potential collapses, and the JC-1 cannot accumulate within the mitochondria, it remains in the cytoplasm in a green fluorescent monomeric form.[24] MCF-7 cells were grown in 10 cm dishes and treated with 100 nmol/L BRL and/or 50 nmol/L 9RA for 48 hours, then cells were washed in ice-cold PBS, and incubated with 10 mmol/L JC-1 at 37°C in a 5% CO_2 incubator for 20 minutes in darkness. Subsequently, cells were washed twice with PBS and analyzed by fluorescence microscopy. The red form has absorption/emission maxima of 585/590 nm. The green monomeric form has absorption/emission maxima of 510/527 nm. Both healthy and apoptotic cells can be visualized by fluorescence microscopy using a wide band-pass filter suitable for detection of fluorescein and rhodamine emission spectra.

Cytochrome C Detection

Cytochrome *C* was detected by western blotting in mitochondrial and cytoplasmatic fractions. Cells were harvested by centrifugation at 2500 rpm for 10 minutes at 4°C. The pellets were suspended in 36 μl RIPA buffer plus 10 μg/ml aprotinin, 50 mmol/L PMSF and 50 mmol/L sodium orthovanadate and then 4 μl of 0.1% digitonine were added. Cells were incubated for 15 minutes at 4°C and centrifuged at 12,000 rpm for 30 minutes at 4°C. The resulting mitochondrial pellet was resuspended in 3% Triton X-100, 20 mmol/L Na_2SO_4, 10 mmol/L PIPES, and 1 mmol/L EDTA (pH 7.2) and centrifuged at 12,000 rpm for 10 minutes at 4°C. Proteins of the mitochondrial and cytosolic fractions were determined by Bio-Rad Protein Assay (Bio-Rad Laboratories). Equal amounts of protein (40 μg) were resolved by 15% SDS-polyacrylamide gel electrophoresis, electrotransferred to nitrocellulose membranes, and probed with an antibody directed against the cytochrome *C* (Santa Cruz Biotechnology). Then, membranes were subjected to the same procedures described for immunoblotting.

Flow Cytometry Assay

MCF-7 cells (1×10^6 cells/well) were grown in 6 well plates and shifted to SFM for 24 hours before adding treatments for 48 hours. Thereafter, cells were trypsinized, centrifuged at 3000 rpm for 3 minutes, washed with PBS. Addition of 0.5 μl of fluorescein isothiocyanate-conjugated antibodies, anti-caspase 9 and anti-caspase 8 (Calbiochem, Milan, Italy), in all samples was performed and then incubated for 45 minutes in at 37°C. Cells were centrifuged at 3000 rpm for 5 minutes, the pellets were washed with 300 μl of wash buffer and centrifuged. The last passage was repeated twice, the supernatant removed, and cells dissolved in 300 μl of wash buffer.

Finally, cells were analyzed with the FACScan (Becton Dickinson and Co., Franklin Lakes, NJ).

DNA Fragmentation

DNA fragmentation was determined by gel electrophoresis. MCF-7 cells were grown in 10 cm dishes to 70% confluence and exposed to treatments. After 56 hours cells were collected and washed with PBS and pelleted at 1800 rpm for 5 minutes. The samples were resuspended in 0.5 ml of extraction buffer (50 mmol/L Tris-HCl, pH 8; 10 mmol/L EDTA, 0.5% SDS) for 20 minutes in rotation at 4°C. DNA was extracted three times with phenol-chloroform and one time with chloroform. The aqueous phase was used to precipitate nucleic acids with 0.1 volumes of 3M sodium acetate and 2.5 volumes cold ethanol overnight at −20°C. The DNA pellet was resuspended in 15 μl of H_2O treated with RNase A for 30 minutes at 37°C. The absorbance of the DNA solution at 260 and 280 nm was determined by spectrophotometry. The extracted DNA (40 μg/lane) was subjected to electrophoresis on 1.5% agarose gels. The gels were stained with ethidium bromide and then photographed.

Statistical Analysis

Statistical analysis was performed using analysis of variance followed by Newman-Keuls testing to determine differences in means. $P < 0.05$ was considered as statistically significant.

Results

Nanomolar Concentrations of the Combined BRL and 9RA Treatment Affect Cell Viability in Breast Cancer Cells

Previous studies demonstrated that micromolar doses of PPARγ ligand BRL and RXR ligand 9RA exert antiproliferative effects on breast cancer cells.[13,15,25–26] First, we tested the effects of increasing concentrations of both ligands on breast cancer cell proliferation at different times in the presence or absence of serum media (see Supplemental Figure 1 at *http://ajp.amjpathol.org*). Thus, to investigate whether low doses of combined agents are able to inhibit cell growth, we assessed the capability of 100 nmol/L BRL and 50 nmol/L 9RA to affect normal and malignant breast cell lines. We observed that treatment with BRL alone does not elicit any significant effect on cell viability in all breast cell lines tested, while 9RA alone reduces cell vitality only in T47-D cells (Figure 1A). In the presence of both ligands, cell viability is strongly reduced in all breast cancer cells: MCF-7, its variant MCF-7TR1, SKBR-3, and T-47D; while MCF-10 normal breast epithelial cells are completely unaffected (Figure 1A). In MCF-7 cells the effectiveness of both ligands in reducing tumor cell viability still persists in SFM, as well as in 5% CT-FBS (Figure 1B).

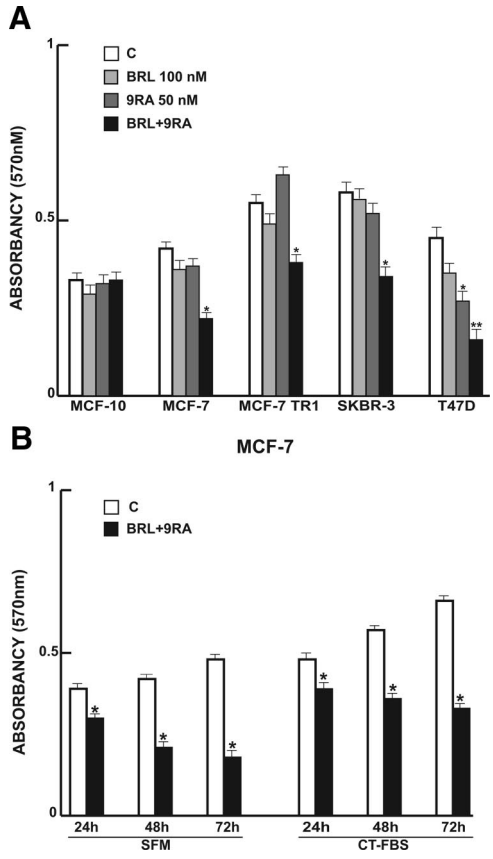

Figure 1. Cell vitality in breast cell lines. **A:** Breast cells were treated for 48 hours in SFM in the presence of 100 nmol/L BRL or/and 50 nmol/L. 9RA Cell vitality was measured by MTT assay. Data are presented as mean ± SD of three independent experiments done in triplicate. **B:** MCF-7 cells were treated for 24, 48, and 72 hours with 100 nmol/L BRL and 50 nmol/L 9RA in the presence of SFM and 5% CT-FBS. *$P < 0.05$ and **$P < 0.01$ treated versus untreated cells.

BRL and 9RA Up-Regulate p53 and p21$^{WAF1/Cip1}$ Expression in MCF-7 Cells

Our recent work demonstrated that micromolar doses of BRL activate PPARγ, which in turn triggers apoptotic events through an up-regulation of p53 expression.[12] On the basis of these results, we evaluated the ability of nanomolar doses of BRL and 9RA alone or in combination to modulate p53 expression along with its natural target gene p21$^{WAF1/Cip1}$ in MCF-7 cells. A significant increase in p53 and p21$^{WAF1/Cip1}$ content was observed by Western blot only on combined treatment after 24 and 36 hours (Figure 2A). Furthermore, we showed an up-regulation of p53 and p21$^{WAF1/Cip1}$ mRNA levels induced by BRL plus 9RA after 12 and 24 hours (Figure 2B).

Low Doses of PPARγ and RXR Ligands Transactivate p53 Gene Promoter

To investigate whether low doses of BRL and 9RA are able to transactivate the p53 promoter gene, we transiently transfected MCF-7 cells with a luciferase reporter construct (named p53-1) containing the upstream region of the p53 gene spanning from −1800 to + 12 (Figure

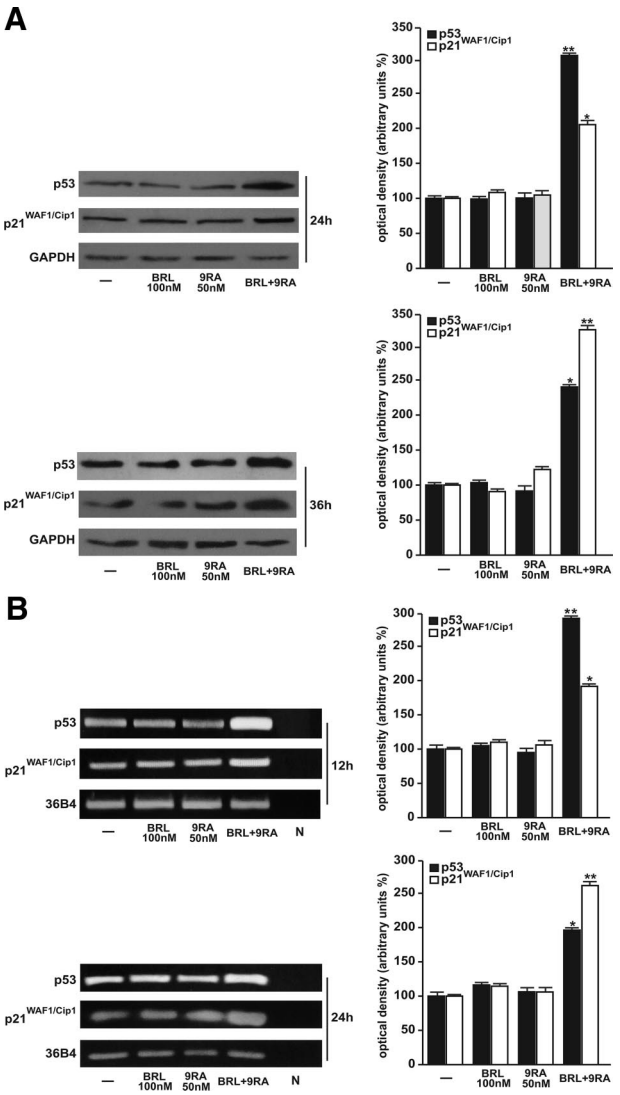

Figure 2. Upregulation of p53 and $p21^{WAF1/Cip1}$ expression induced by BRL plus 9RA in MCF-7 cells. **A:** Immunoblots of p53 and $p21^{WAF1/Cip1}$ from extracts of MCF-7 cell treated with 100 nmol/L BRL and 50 nmol/L 9RA alone or in combination for 24 and 36 hours. GAPDH was used as loading control. The side panels show the quantitative representation of data (mean ± SD) of three independent experiments after densitometry. **B:** p53 and $p21^{WAF1/Cip1}$ mRNA expression in MCF-7 cells treated as in A for 12 and 24 hours. The side panels show the quantitative representation of data (mean ± SD) of three independent experiments after densitometry and correction for 36B4 expression. $^{*}P < 0.05$ and $^{**}P < 0.01$ combined-treated versus untreated cells. N: RNA sample without the addition of reverse transcriptase (negative control).

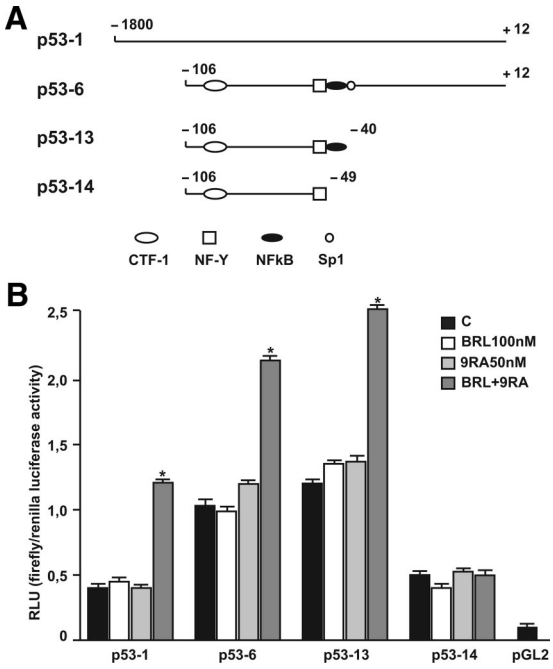

Figure 3. BRL and 9RA transactivate p53 promoter gene in MCF-7 cells. **A:** Schematic map of the p53 promoter fragments used in this study. **B:** MCF-7 cells were transiently transfected with p53 gene promoter-luc reporter constructs (p53-1, p53-6, p53-13, p53-14) and treated for 24 hours with 100 nmol/L BRL and 50 nmol/L 9RA alone or in combination. The luciferase activities were normalized to the Renilla luciferase as internal transfection control and data were reported as RLU values. Columns are mean ± SD of three independent experiments performed in triplicate. $^{*}P < 0.05$ combined-treated versus untreated cells. pGL2: basal activity measured in cells transfected with pGL2 basal vector; RLU, relative light units; CTF-1, CCAAT-binding transcription factor-1; NF-Y, nuclear factor-Y; NFκB, nuclear factor κB.

3A). Treatment for 24 hours with 100 nmol/L BRL or 50 nmol/L 9RA did not induce luciferase expression, whereas the presence of both ligands increased in the transactivation of p53-1 promoter (Figure 3B). To identify the region within the p53 promoter responsible for its transactivation, we used constructs with deletions to different binding sites such as CTF-1, nuclear factor-Y, NFκB, and GC sites (Figure 3A). In transfection experiments performed using the mutants p53-6 and p53-13 encoding the regions from −106 to + 12 and from −106 to −40, respectively, the responsiveness to BRL plus 9RA was still observed (Figure 3B). In contrast, a construct with a deletion in the NFκB domain (p53-14) encoding the sequence from −106 to −49, the transactivation of p53 by both ligands was absent (Figure 3B), suggesting that NFκB site is required for p53 transcriptional activity.

Heterodimer PPARγ/RXRα binds to NFκB Sequence in Electrophoretic Mobility Shift Assay and in Chromatin Immunoprecipitation Assay

To gain further insight into the involvement of NFκB site in the p53 transcriptional response to BRL plus 9RA, we performed electrophoretic mobility shift assay experiments using synthetic oligodeoxyribonucleotides corresponding to the NFκB sequence within p53 promoter. We observed the formation of a specific DNA binding complex in nuclear extracts from MCF-7 cells (Figure 4A, lane 1), where specificity is supported by the abrogation of the complex by 100-fold molar excess of unlabeled probe (Figure 4A, lane 2). BRL treatment induced a slight increase in the specific band (Figure 4A, lane 3), while no changes were observed on 9RA exposure (Figure 4A, lane 4). The combined treatment increased the DNA binding complex (Figure 4A, lane 5), which was immunodepleted and supershifted using anti-PPARγ (Figure 4A, lane 6) or anti-RXRα (Figure 4A, lane 7) antibodies. These data indicate that heterodimer PPARγ/RXRα binds to NFκB site located in the promoter of p53 *in vitro*.

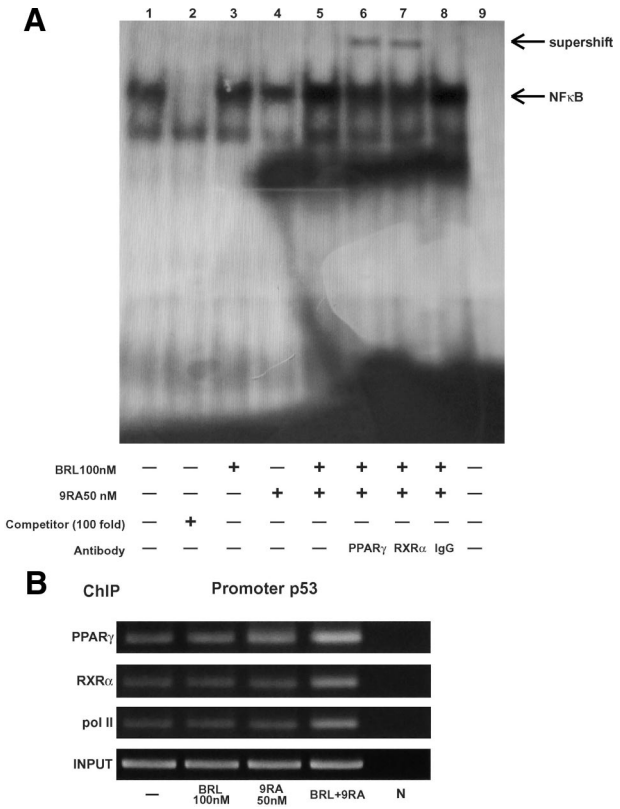

Figure 4. PPARγ/RXRα binds to NFκB sequence in electrophoretic mobility shift assay and in chromatin immunoprecipitation assay. **A:** Nuclear extracts from MCF-7 cells (lane 1) were incubated with a double-stranded NFκB consensus sequence probe labeled with [^{32}P] and subjected to electrophoresis in a 6% polyacrylamide gel. Competition experiments were done, adding as competitor a 100-fold molar excess of unlabeled probe (lane 2). Nuclear extracts from MCF-7 were treated with 100 nmol/L BRL (lane 3), 50 nmol/L 9RA (lane 4), and in combination (lane5). Anti-PPARγ (lane 6), anti-RXRα (lane 7), and IgG (lane 8) antibodies were incubated. Lane 9 contains probe alone. **B:** MCF-7 cells were treated for 1 hour with 100 nmol/L BRL and/or 50 nmol/L 9RA as indicated, and then cross-linked with formaldehyde and lysed. The soluble chromatin was immunoprecipitated with anti-PPARγ, anti-RXRα, and anti-RNA Pol II antibodies. The immunocomplexes were reverse cross-linked, and DNA was recovered by phenol/chloroform extraction and ethanol precipitation. The p53 promoter sequence containing NFκB was detected by PCR with specific primers. To control input DNA, p53 promoter was amplified from 30 μl of initial preparations of soluble chromatin (before immunoprecipitation). N: negative control provided by PCR amplification without DNA sample.

The interaction of both nuclear receptors with the p53 promoter was further elucidated by chromatin immunoprecipitation assays. Using anti-PPARγ and anti-RXRα antibodies, protein-chromatin complexes were immunoprecipitated from MCF-7 cells treated with 100 nmol/L BRL and 50 nmol/L 9RA. PCR was used to determine the recruitment of PPARγ and RXRα to the p53 region containing the NFκB site. The results indicated that either PPARγ or RXRα was constitutively bound to the p53 promoter in untreated cells and this recruitment was increased on BRL plus 9RA exposure (Figure 4B). Similarly, an augmented RNA-Pol II recruitment was obtained by immunoprecipitating cells with an anti-RNA-Pol II antibody, indicating that a positive regulation of p53 transcription activity was induced by combined treatment (Figure 4B).

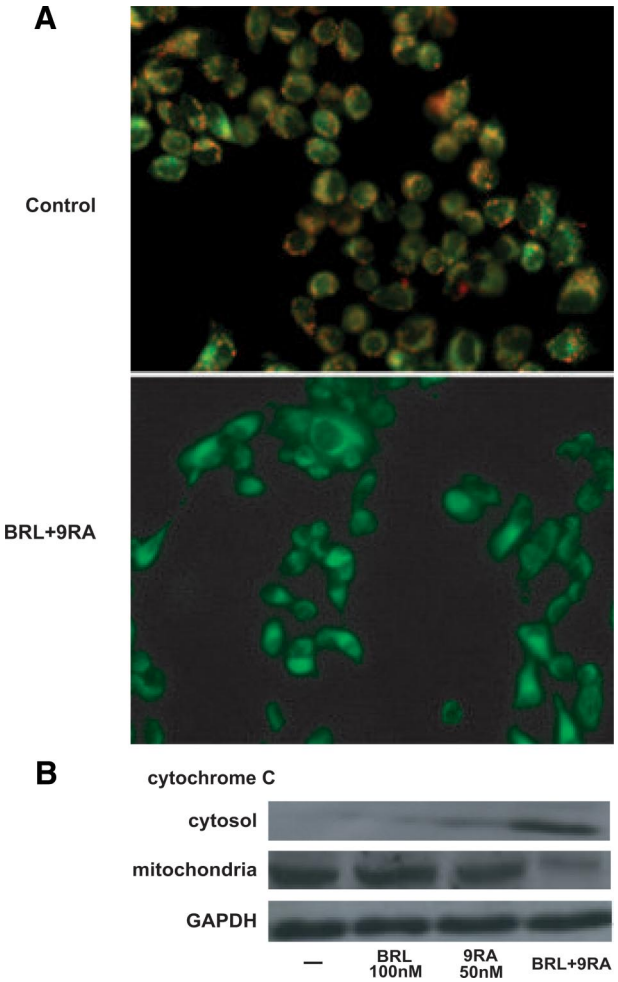

Figure 5. Mitochondrial membrane potential disruption and release of cytochrome *C* induced by BRL and 9RA in MCF-7 cells. **A:** MCF-7 cells were treated with 100 nmol/L BRL plus 50 nmol/L 9RA for 48 hours and then used fluorescent microscopy to analyze the results of JC-1 (5,5′,6,6′-tetrachloro-1,1′,3,3′- tetraethylbenzimidazolylcarbocyanine iodide) kit. In control non-apoptotic cells, the dye stains the mitochondria red. In treated apoptotic cells, JC-1 remains in the cytoplasm in a green fluorescent form. **B:** MCF-7 cells were treated for 48 hours with 100 nmol/L BRL and/or 50 nmol/L 9RA. GAPDH was used as loading control.

BRL and 9RA Induce Mitochondrial Membrane Potential Disruption and Release of Cytochrome C from Mitochondria into the Cytosol in MCF-7 Cells

The role of p53 signaling in the intrinsic apoptotic cascades involves a mitochondria-dependent process, which results in cytochrome *C* release and activation of caspase-9. Because disruption of mitochondrial integrity is one of the early events leading to apoptosis, we assessed whether BRL plus 9RA could affect the function of mitochondria by analyzing membrane potential with a mitochondria fluorescent dye JC-1.[24,27] In non-apoptotic cells (control) the intact mitochondrial membrane potential allows the accumulation of lipophilic dye in aggregated form in mitochondria, which display red fluorescence (Figure 5A). MCF-7 cells treated with 100 nmol/L BRL or 50 nmol/L 9RA exhibit red fluorescence indicating

Table 1. Activation of caspases in MCF-7 cells

	% of Activation	SD
Caspase 9		
Control	14.16	± 2.565
BRL 100 nmol/L	17.23	± 1.678
9RA 50 nmol/L	18.14	± 0.986
BRL + 9RA	33.88*	± 5.216
Caspase 8		
Control	9.20	± 1.430
BRL 100 nmol/L	8.12	± 1.583
9RA 50 nmol/L	7.90	± 0.886
BRL + 9RA	10.56	± 2.160

Cells were stimulated for 48 hours in presence of 100 nmol/L BRL and 50 nmol/L 9RA, alone or in combination. The activation of caspase 9 and caspase 8 was analyzed by flow cytometry. Data are presented as mean ± SD of triplicate experiments. *$P < 0.05$ combined-treated versus untreated cells.

intact mitochondrial membrane potential (data not shown). Cells treated with both ligands exhibit green fluorescence, indicating disrupted mitochondrial membrane potential, where JC-1 cannot accumulate within the mitochondria, but instead remains as a monomer in the cytoplasm (Figure 5A). Concomitantly, cytochrome *C* release from mitochondria into the cytosol, a critical step in the apoptotic cascade, was demonstrated after combined treatment (Figure 5B).

Caspase-9 Cleavage and DNA Fragmentation Induced by BRL Plus 9RA in MCF-7 Cells

BRL and 9RA at nanomolar concentration did not induce any effects on caspase-9 separately, but activation was observed in the presence of both compounds (Table 1). No effects were elicited by either the combined or the separate treatment on caspase-8 activation, a marker of extrinsic apoptotic pathway (Table 1). Since internucleosomal DNA degradation is considered a diagnostic hallmark of cells undergoing apoptosis, we studied DNA fragmentation under BRL plus 9RA treatment in MCF-7 cells, observing that the induced apoptosis was prevented by either the PPARγ-specific antagonist GW or by AS/p53, which is able to abolish p53 expression (Figure 6A).

To test the ability of low doses of both BRL and 9RA to induce transcriptional activity of PPARγ, we transiently transfected a peroxisome proliferator response element reporter gene in MCF-7 cells and observed an enhanced luciferase activity, which was reversed by GW treatment (see Supplemental Figure 2 at *http://ajp.amjpathol.org*). These data are in agreement with previous observations demonstrating that PPARγ/RXR heterodimerization enhances DNA binding and transcriptional activation.[28–29]

Finally, we examined in three additional human breast malignant cell lines: MCF-7 TR1, SKBR-3, and T-47D the capability of low doses of a PPARγ and an RXR ligand to trigger apoptosis. DNA fragmentation assay showed that only in the presence of combined treatment did cells undergo apoptosis in a p53-mediated manner (Figure 6B), implicating a general mechanism in breast carcinoma.

Discussion

The key finding of this study is that the combined treatment with low doses of a PPARγ and an RXR ligand can selectively affect breast cancer cells through cell growth inhibition and apoptosis.

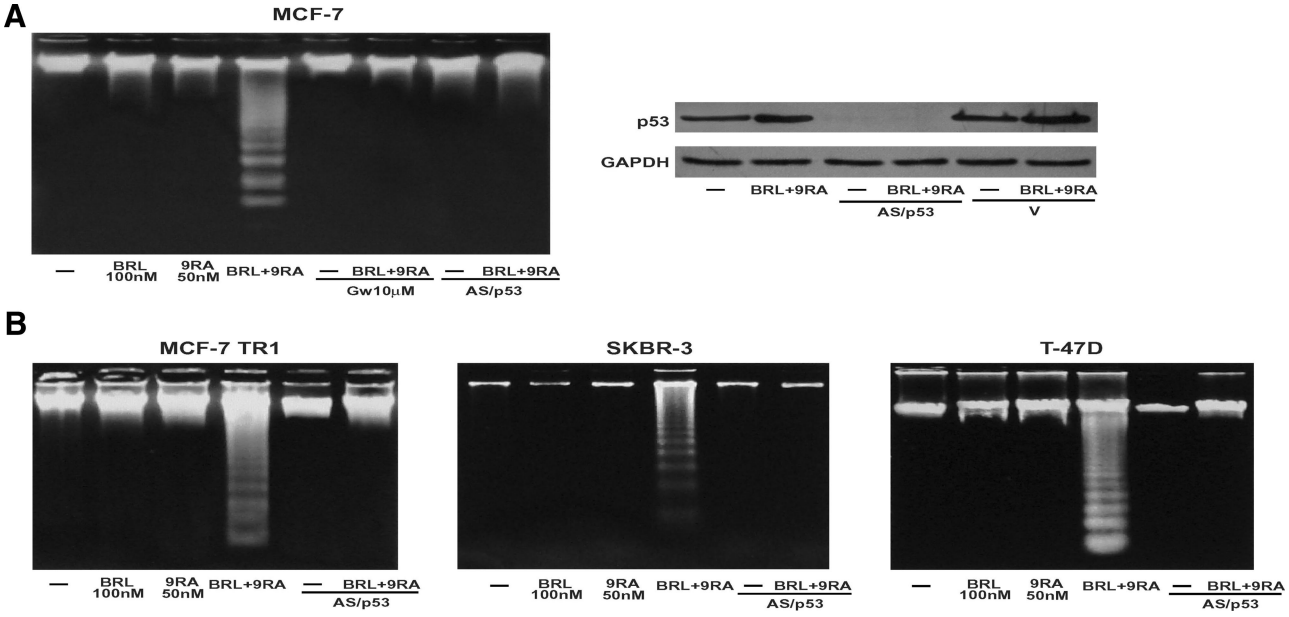

Figure 6. Combined treatment of BRL and 9RA trigger apoptosis in breast cancer cells. **A:** DNA laddering was performed in MCF-7 cells transfected and treated as indicated for 56 hours. One of three similar experiments is presented. The side panel shows the immunoblot of p53 from MCF-7 cells transfected with an expression plasmid encoding for p53 antisense (AS/p53) or empty vector (v) and treated with 100 nmol/L BRL plus 50 nmol/L 9RA for 56 hours. GAPDH was used as loading control. **B:** DNA laddering was performed in MCF-7 TR1, SKBR-3, and T47-D cells transfected with AS/p53 or empty vector (v) and treated as indicated. One of three similar experiments is presented.

The ability of PPARγ ligands to induce differentiation and apoptosis in a variety of cancer cell types, such as human lung,[30] colon,[31] and breast,[10] has been exploited in experimental cancer therapies.[32] PPARγ agonist administration in liposarcoma patients resulted in histological and biochemical differentiation markers *in vivo*.[33] However, a pilot study of short-term therapy with the PPARγ ligand rosiglitazone in early-stage breast cancer patients did not elicit significant effects on tumor cell proliferation, although the changes observed in PPARγ expression may be relevant to breast cancer progression.[34] On the other hand, the natural ligand for RXR, 9RA,[35] has been effective *in vitro* against many types of cancer, including breast tumor.[36–40] Recently, RXR-selective ligands were discovered to inhibit proliferation of all-*trans* retinoic acid–resistant breast cancer cells *in vitro* and caused regression of the disease in animal models.[41] The additive antitumoral effects of PPARγ and RXR agonists, both at elevated doses, have been shown in human breast cancer cells ([15,42] and references therein). However, high doses of both ligands have remarkable side effects in humans, such as weight gain and plasma volume expansion for PPARγ ligands,[16–18] and hypertriglyceridemia and suppression of the thyroid hormone axis for RXR ligands.[19]

In the present study, we demonstrated that nanomolar concentrations of BRL and 9RA in combination exert significant antiproliferative effects on breast cancer cells, whereas they do not induce noticeable influences on normal breast epithelial MCF10 cells. However, the induced overexpression of PPARγ in MCF10 cells makes these cells responsive to the low combined concentration of BRL and 9RA (data not shown). Although PPARγ is known to mediate differentiation in most tissues, its role in either tumor progression or suppression is not yet clearly elucidated. It has been demonstrated in animals studies that an overexpression of PPARγ increases the risk of breast cancer already in mice susceptible to the disease.[43] However, it remains still questionable if the enhanced PPARγ expression does correspond to an enhanced content of functional protein, which according to previous suggestion should be carefully controlled in a dose-response study.[44] For instance, the expression of PPARγ is under complex regulatory mechanisms, sustained by cell-specific distinct promoters mediating the changes in expression of PPARγ.[45]

Here we demonstrated for the first time the molecular mechanism underlying antitumoral effects induced by combined low doses of both ligands in MCF-7 cells, where an up-regulation of tumor suppressor gene p53 was concomitantly observed. Functional assays with deletion constructs of the p53 promoter showed that the NFκB site is required for the transcriptional response to BRL plus 9RA treatment. NFκB was shown to physically interact with PPARγ,[46] which in some circumstances binds to DNA cooperatively with NFκB.[47–49] It has been previously reported that micromolar doses of both PPARγ and RXR agonists synergize to generate an increased level of NFκB-DNA binding able to trigger apoptosis in Pre-B cells.[50] Our electrophoretic mobility shift assay and chromatin immunoprecipitation assay demonstrated that PPARγ/RXRα complex is present on p53 promoter in the absence of exogenous ligand. Only BRL and 9RA in combination increased the binding and the recruitment of either PPARγ or RXRα on the NFκB site located in the p53 promoter sequence. BRL plus 9RA at the doses tested also increased the recruitment of RNA-Pol II to p53 promoter gene illustrating a positive transcriptional regulation able to produce a consecutive series of events in the apoptotic pathway.

Changes in mitochondrial membrane permeability, an important step in the induction of cellular apoptosis, is concomitant with collapse of the electrochemical gradient across the mitochondrial membrane, through the formation of pores in the mitochondria leading to the release of cytochrome *C* into the cytoplasm, and subsequently with cleavage of procaspase-9. This cascade of events, featuring the mitochondria-mediated death pathway, was detected in BRL plus 9RA-treated MCF-7 cells. The activation of caspase 9, in the presence of no changes in the biological activity of caspase 8, support that in our experimental model only the intrinsic apoptotic pathway is the effector of the combined treatment with the two ligands.

The crucial role of p53 gene in mediating apoptosis is raised by the evidence that the effects on the apoptotic cascade were abrogated in the presence of AS/p53 in all breast cancer cell lines tested, including tamoxifen resistant breast cancer cells. In tamoxifen-resistant breast cancer cells, other authors have observed that epidermal growth factor receptor, insulin-like growth factor-1R, and c-Src signaling are constitutively activated and responsible for a more aggressive phenotype consistent with an increased motility and invasiveness.[51–53] Although more relevance of our findings should derive from *in vivo* studies, these results give emphasis to the potential use of the combined therapy with low doses of both BRL and 9RA as novel therapeutic tool particularly for breast cancer patients who develop resistance to anti-estrogen therapy.

References

1. Ryningen A, Stapnes C, Paulsen K, Lassalle P, Gjertsen BT, Bruserud O: In vivo biological effects of ATRA in the treatment of AML. Expert Opin Investig Drugs 2008, 17:1623–1633
2. Ravandi F, Estey E, Jones D, Faderl S, O'Brien S, Fiorentino J, Pierce S, Blamble D, Estrov Z, Wierda W, Ferrajoli A, Verstovsek S, Garcia-Manero G, Cortes J, Kantarjian H: Effective treatment of acute promyelocytic leukemia with all-trans-retinoic acid, arsenic trioxide, and gemtuzumab ozogamicin. J Clin Oncol 2009, 27:504–510
3. Montesinos P, Bergua JM, Vellenga E, Rayón C, Parody R, de la Serna J, León A, Esteve J, Milone G, Debén G, Rivas C, González M, Tormo M, Díaz-Mediavilla J, González JD, Negri S, Amutio E, Brunet S, Lowenberg B, Sanz MA: Differentiation syndrome in patients with acute promyelocytic leukemia treated with all-trans retinoic acid and anthracycline chemotherapy: characteristics, outcome, and prognostic factors. Blood 2009, 113:775–783
4. Sun SY, Yue P, Mao L, Dawson MI, Shroot B, Lamph WW, Heyman RA, Chandraratna RA, Shudo K, Hong WK, Lotan R: Identification of receptor-selective retinoids that are potent inhibitors of the growth of human head and neck squamous cell carcinoma cells. Clin Cancer Res 2000, 6:1563–1573
5. Abu J, Batuwangala M, Herbert K, Symonds P: Retinoic acid and retinoid receptors: potential chemopreventive and therapeutic role in cervical cancer. Lancet Oncol 2005, 6:712–720

6. Mangelsdorf DJ, Thummel C, Beato M, Herrlich P, Schütz G, Umesono K, Blumberg B, Kastner P, Mark M, Chambon P, Evans RM: The nuclear receptor superfamily: the second decade. Cell 1995, 83:835–839
7. Heyman RA, Mangelsdorf DJ, Dyck JA, Stein RB, Eichele G, Evans RM, Thaller C: 9-cis retinoic acid is a high affinity ligand for the retinoid X receptor. Cell 1992, 68:397–406
8. Elstner E, Müller C, Koshizuka K, Williamson EA, Park D, Asou H, Shintaku P, Said JW, Heber D, Koeffler HP: Ligands for peroxisome proliferator-activated receptor γ and retinoic acid receptor inhibit growth and induce apoptosis of human breast cancer cells *in vitro* and in BNX mice. Proc Natl Acad Sci USA 1998, 95:8806–8811
9. Tontonoz P, Hu E, Spiegelman BM: Stimulation of adipogenesis in fibroblasts by PPAR gamma 2, a lipid-activated transcription factor. Cell 1994, 79:1147–1156
10. Mueller E, Sarraf P, Tontonoz P, Evans RM, Martin KJ, Zhang M, Fletcher C, Singer S, Spiegelman BM: Terminal differentiation of human breast cancer through PPARγ. Mol Cell 1998, 1:465–470
11. Suh N, Wang Y, Williams CR, Risingsong R, Gilmer T, Willson TM, Sporn MB: A new ligand for the peroxisome proliferator-activated receptor-gamma (PPAR-gamma). GW7845, inhibits rat mammary carcinogenesis. Cancer Res 1999, 59:5671–5673
12. Bonofiglio D, Aquila S, Catalano S, Gabriele S, Belmonte M, Middea E, Qi H, Morelli C, Gentile M, Maggiolini M, Andò S: Peroxisome proliferator-activated receptor-gamma activates p53 gene promoter binding to the nuclear factor-kappaB sequence in human MCF7 breast cancer cells. Mol Endocrinol 2006, 20:3083–3092
13. Bonofiglio D, Gabriele S, Aquila S, Catalano S, Gentile M, Middea E, Giordano F, Andò S: Estrogen receptor alpha binds to peroxisome proliferator-activated receptor (PPAR) response element and negatively interferes with PPAR gamma signalling in breast cancer cells. Clin Cancer Res 2005, 11:6139–6147
14. Bonofiglio D, Gabriele S, Aquila S, Qi H, Belmonte M, Catalano S, Andò S: Peroxisome proliferator-activated receptor gamma activates fas ligand gene promoter inducing apoptosis in human breast cancer cells. Breast Cancer Res Treat 2009, 113:423–434
15. Elstner E, Williamson EA, Zang C, Fritz J, Heber D, Fenner M, Possinger K, Koeffler HP: Novel therapeutic approach: ligands for PPARγ and retinoid receptors induce apoptosis in bcl-2-positive human breast cancer cells. Breast Cancer Res Treat 2002, 74:155–165
16. Arakawa K, Ishihara T, Aoto M, Inamasu M, Kitamura K, and Saito A: An antidiabetic thiazolidinedione induces eccentric cardiac hypertrophy by cardiac volume overload in rats. Clin Exp Pharmacol Physiol 2004, 31:8–13
17. Rangwala SM and Lazar MA: Peroxisome proliferator-activated receptor gamma in diabetes and metabolism. Trends Pharmacol Sci 2004, 25:331–336
18. Staels B: Fluid retention mediated by renal PPARgamma. Cell Metab 2005, 2:77–78
19. Pinaire JA, Reifel-Miller A: Therapeutic potential of retinoid x receptor modulators for the treatment of the metabolic syndrome. PPAR Res 2007, 2007:94156
20. Qin C, Nguyen T, Stewart J, Samudio I, Burghardt R, Safe S: Estrogen up-regulation of p53 gene expression in MCF-7 breast cancer cells is mediated by calmodulin kinase IV-dependent activation of a nuclear factor κB/CCAAT-binding transcription factor-1 complex. Mol Endocrinol 2002, 16:1793–1809
21. Herman ME, Katzenellenbogen BS: Response-specific antiestrogen resistance in a newly characterized MCF-7 human breast cancer cell line resulting from long-term exposure to trans-hydroxytamoxifen. J Steroid Biochem Mol Biol 1996, 59:121–134
22. Mosmann T: Rapid colorimetric assay for cellular growth and survival: application to proliferation and cytotoxicity assays. J Immunol Methods 1983, 65:55–63
23. Andrews NC, Faller DV: A rapid micropreparation technique for extraction of DNA-binding proteins from limiting numbers of mammalian cells. Nucleic Acids Res 1991, 19:2499
24. Cossarizza A, Baccarani-Contri M, Kalashnikova G, Franceschi C: A new method for the cytofluorimetric analysis of mitochondrial membrane potential using the J-aggregate forming lipophilic cation 5,5′,6,6′-tetrachloro-1,1′,3,3′ tetraethylbenzimidazolylcarbo-cyanine iodide (JC-1). Biochem Biophys Res Commun 1993, 197:40–45
25. Mehta RG, Williamson E, Patel MK, Koeffler HP: A ligand of peroxisome proliferator-activated receptor gamma, retinoids, and prevention of preneoplastic mammary lesions. J Natl Cancer Inst 2000, 92:418–423
26. Crowe DL, Chandraratna RA: A retinoid X receptor (RXR)-selective retinoid reveals that RXR-alpha is potentially a therapeutic target in breast cancer cell lines, and that it potentiates antiproliferative and apoptotic responses to peroxisome proliferator-activated receptor ligands. Breast Cancer Res 2004, 6:R546–R555
27. Smiley ST, Reers M, Mottola-Hartshorn C, Lin M, Chen A, Smith TW, Steele GD, Chen LB: Intracellular heterogeneity in mitochondrial membrane potentials revealed by a J-aggregate forming lipophilic cation JC-1. Proc Natl Acad Sci USA 1991, 88:3671–3675
28. Kliewer SA, Umesono K, Mangelsdorf DJ, Evans RM: Retinoid X receptor interacts with nuclear receptors in retinoic acid, thyroid hormone, and vitamin D3 signaling. Nature 1992, 355:446–449
29. Zhang XK, Hoffmann B, Tran PBV, Graupner G, Pfahl M: Retinoid X receptor is an auxiliary protein for thyroid hormone and retinoic acid receptors. Nature 1992, 355:441–445
30. Tsubouchi Y, Sano H, Kawahito Y, Mukai S, Yamada R, Kohno M, Inoue K, Hla T, Kondo M: Inhibition of human lung cancer cell growth by the peroxisome proliferator activated receptor γ agonists through induction of apoptosis. Biochem Biophys Res Commun 2000, 270:400–405
31. Kitamura S, Miyazaki Y, Shinomura Y, Kondo S, Kanayama S, Matsuzawa Y: Peroxisome proliferator activated receptor γ induces growth arrest and differentiation markers of human colon cancer cells. Jpn J Cancer Res 1999, 90:75–80
32. Roberts-Thomson SJ: Peroxisome proliferator activated receptors in tumorigenesis: targets of tumor promotion and treatment. Immunol Cell Biol 2000, 78:436–441
33. Demetri GD, Fletcher CDM, Mueller E, Sarraf P, Naujoks R, Campbell N, Spiegelman BM, Singer S: Induction of solid tumor differentiation by the peroxisome proliferator activated receptor γ ligand troglitazone in patients with liposarcoma. Proc Natl Acad Sci USA 1999, 96:3951–3956
34. Yee LD, Williams N, Wen P, Young DC, Lester J, Johnson MV, Farrar WB, Walker MJ, Povoski SP, Suster S, Eng C: Pilot study of rosiglitazone therapy in women with breast cancer: effects of short-term therapy on tumor tissue and serum markers. Clin Cancer Res 2007, 13:246–252
35. Leblanc BP, Stunnenberg HG: 9-cis retinoic acid signaling: changing partners causes some excitement. Genes Dev 1995, 9:1811–1816
36. Gee MF, Tsuchida R, Eichler-Jonsson C, Das B, Baruchel S, Malkin D: Vascular endothelial growth factor acts in an autocrine manner in rhabdomyosarcoma cell lines and can be inhibited with all-trans-retinoic acid. Oncogene 2005, 24:8025–8037
37. Mizuguchi Y, Wada A, Nakagawa K, Ito M, Okano T: Antitumoral activity of 13-demethyl or 13-substituted analogues of all-trans retinoic acid and 9-cis retinoic acid in the human myeloid leukemia cell line HL-60. Biol Pharm Bull 2006, 29:1803–1809
38. Wan H, Hong WK, Lotan R: Increased retinoic acid responsiveness in lung carcinoma cells that are nonresponsive despite the presence of endogenous retinoic acid receptor (RAR) beta by expression of exogenous retinoid receptors retinoid X receptor alpha, RAR alpha, and RAR gamma. Cancer Res 2001, 61:556–564
39. Wu K, DuPré E, Kim H, Tin-U CK, Bissonnette RP, Lamph WW, Brown PH: Receptor-selective retinoids inhibit the growth of normal and malignant breast cells by inducing G1 cell cycle blockade. Breast Cancer Res Treat 2006, 96:147–157
40. Simeone AM, Tari AM: How retinoids regulate breast cancer cell proliferation and apoptosis. Cell Mol Life Sci 2004, 61:1475–1484
41. Bischoff ED, Gottardis MM, Moon TE, Heyman RA, Lamph WW: Beyond tamoxifen: the retinoid X receptor selective ligand LGD1069 (TARGRETIN) causes complete regression of mammary carcinoma. Cancer Res 1998, 58:479–484
42. Grommes C, Landreth GE, Heneka MT: Antineoplastic effects of peroxisome proliferator-activated receptor gamma agonists. Lancet Oncol 2004, 5:419–429
43. Saez E, Rosenfeld J, Livolsi A, Olson P, Lombardo E, Nelson M, Banayo E, Cardiff RD, Izpisua-Belmonte JC, Evans RM: PPARgamma signaling exacerbates mammary gland tumor development. Genes Dev 2004, 18:528–40
44. Sporn MB, Suh N, Mangelsdorf DJ: Prospects for prevention and treatment of cancer with selective PPARgamma modulators (SPARMs). Trends Mol Med 2001, 7:395–400
45. Wang X, Southard RC, Kilgore MW: The increased expression of

peroxisome proliferator-activated receptor-gamma1 in human breast cancer is mediated by selective promoter usage. Cancer Res 2004, 64:5592–5596
46. Chung SW, Kang BY, Kim SH, Pak YK, Cho D, Trinchieri G, Kim TS: Oxidized low density lipoprotein inhibits interleukin-12 production in lipopolysaccharide-activated mouse macrophages via direct interactions between peroxisome proliferator-activated receptor-γ and nuclear factor κB. J Biol Chem 2000, 275:32681–32687
47. Couturier C, Brouillet A, Couriaud C, Koumanov K, Bereziat G, Andreani M: Interleukin 1beta induces type II-secreted phospholipase A2 gene in vascular smooth muscle cells by a nuclear factor κB and peroxisome proliferator-activated receptor-mediated process. J Biol Chem 1999, 274:23085–23093
48. Sun YX, Wright HT, Janciasukiene S: Alpha1-antichymotrypsin/Alzheimer's peptide Abeta (1–42) complex perturbs lipid metabolism and activates transcription factors PPARγ and NFκB in human neuroblastoma (Kelly) cells. J Neurosci Res 2002, 67:511–522
49. Ikawa H, Kameda H, Kamitani H, Baek SJ, Nixon JB, His LC, Eling TE: Effect of PPAR activators on cytokine stimulated cyclooxygenase-2 expression in human colorectal carcinoma cells. Exp Cell Res 2001, 267:73–80
50. Schlezinger JJ, Jensen BA, Mann KK, Ryu HY, Sherr DH: Peroxisome proliferator-activated receptor γ-mediated NFkB activation and apoptosis in pre-B cells. J Immunol 2002, 169:6831–6841
51. Knowlden JM, Hutcheson IR, Jones HE, Madden T, Gee JMW, Harper ME, Barrow D, Wakeling AE, Nicholson RI: Elevated levels of EGFR/c-erbB2 heterodimers mediate an autocrine growth regulatory pathway in tamoxifen-resistant MCF-7 cells. Endocrinology 2003, 144:1032–1044
52. Jones HE, Goddard L, Gee JMW, Hiscox S, Rubini M, Barrow D, Knowlden JM, Williams S. Wakeling AE, Nicholson RI: Insulin-like growth factor-I receptor signaling and acquired resistance to gefitinib (ZD1839, Iressa) in human breast and prostate cancer cells. Endocr Relat Cancer 2004, 11:793–814
53. Hiscox S, Morgan L, Green TP, Barrow D, Gee J, Nicholson RI: Elevated Src activity promotes cellular invasion and motility in tamoxifen resistant breast cancer cells. Breast Cancer Res Treat 2005, 7:1–12

Cell Cycle 10:14, 1-11; July 15, 2011; © 2011 Landes Bioscience

Bid as a potential target of apoptotic effects exerted by low doses of PPARγ and RXR ligands in breast cancer cells

Daniela Bonofiglio,[1,†] Erika Cione,[1,†] Donatella Vizza,[1] Mariarita Perri,[1] Attilio Pingitore,[1] Hongyan Qi,[1] Stefania Catalano,[1] Daniela Rovito,[1] Giuseppe Genchi[1] and Sebastiano Andò[2-4,*]

[1]Department of Pharmaco-Biology; [2]Department of Cellular Biology; [3]Centro Sanitario; [4]Faculty of Pharmacy Nutritional and Health Sciences; University of Calabria; Cosenza, Italy

[†]These authors contributed equally to this work.

Key words: PPARγ, RXR, apoptosis, mitochondria, bid, breast cancer

The combined treatment with nanomolar doses of the PPARγ ligand Rosiglitazone (BRL) and the RXR ligand 9-cis-retinoic acid (9RA) induces a p53-dependent apoptosis in MCF7, SKBR3 and T47D human breast cancer cells. Since MCF7 cells express a wild type p53 protein, while SKBR3 and T47D cells harbor endogenous mutant p53, we elucidated the mechanism through which PPARγ and RXR ligands triggered apoptotic processes independently of p53 transcriptional activity. We showed an upregulation of Bid expression enhancing the association between Bid/p53 in both cytosol and mitochondria after the ligands treatment. Particularly, in the mitochondria the complex involves the truncated Bid that plays a key role in the apoptotic process induced by BRL and 9RA since the disruption of mitochondrial membrane potential, the induction of PARP cleavage and the percentage of TUNEL-positive cells were reversed after knocking down Bid. Moreover, PPARγ and RXR ligands were able to reduce mitochondrial GST activity which was no longer noticeable silencing Bid expression, suggesting the potential of Bid in the regulation of mitochondrial intracellular reactive oxygen species scavenger activity. Our data, providing new insight into the role of p53/Bid complex at the mitochondria in promoting breast cancer cell apoptosis upon low doses of PPARγ and RXR ligands, address Bid as a potential target in the novel therapeutical strategies for breast cancer.

Introduction

The p53 mutation is found in more than half of all human cancer patients. Cancers with loss of p53 function are often resistant to chemotherapeutic agents mainly because of the absence of p53-dependent apoptosis.[1-3] The p53-dependent apoptosis largely relies on the capability of p53 to act as a transcription factor, although recent reports show that the transcription-independent function of p53 plays a role in this process as well. For instance, apoptosis can still occur in the presence of inhibitors of protein synthesis, or when p53 mutants unable of acting as transcription factors are ectopically expressed. The mechanism through which p53 mediates apoptosis in various cancer cells includes the activation of two major execution programs downstream of the death signal: the caspase pathway and organelle dysfunction, of which mitochondrial dysfunction is best characterized.[4-9] Part of the transcription-independent mechanism may also involve a direct interaction between p53 and multiple targets in the mitochondria, such as the apoptotic member Bcl-x_L, leading to the release of both Bax and Bid from Bcl-x_L sequestration. Following a death signal, these pro-apoptotic members undergo a conformational change that enables them to target and integrate into membranes, especially the outer mitochondrial membrane leading to an increased permeabilization.[10,11] As noted Bid might serve as a 'death ligand' which translocates as truncated p15Bid (tBid) to mitochondria where it inserts into the outer membrane to activate other resident mitochondrial 'receptor' proteins to release cytochrome *c*. Alternatively, it is also conceivable that Bid would itself function as a downstream effector participating in an intramembranous pore which releases cytochrome *c*. To date, Bid is the one molecule absolutely required for the release of cytochrome *c* in loss-of-function approaches including immunodepletion and gene knockout.[12]

In a recent work, we demonstrated that combined treatment with nanomolar levels of the PPARγ ligand Rosiglitazone (BRL) and the RXR ligand 9-cis-retinoic acid (9RA) induce a p53-dependent intrinsic apoptosis in MCF7, SKBR3 and T47D breast cancer cells.[13] Of note, MCF7 cells express the wild type p53 protein able to induce growth arrest and apoptosis, mainly through the activation of a growing plethora of p53-responsive target genes,[14-16] while SKBR3 and T47D human breast carcinoma cell lines carry endogenous mutant p53His175 and p53Phe194, respectively, which affect p53 transcriptional activity.

*Correspondence to: Sebastiano Andò; Email: sebastiano.ando@unical.it
Submitted: 04/21/11; Accepted: 05/16/11
DOI:

In this report we extend our previous study on p53-mediated apoptosis induced by low doses of BRL and 9RA in MCF7, SKBR3 and T47D breast cancer cells to elucidate the mechanism through which PPARγ and RXR ligands can trigger apoptotic processes independently of p53 transcriptional activity. Our results showed that BRL and 9RA induce the intrinsic apoptotic pathway through an upregulation of Bid expression and a formation of p53/tBid/Bak multicomplex localized on mitochondria of breast carcinoma cells.

Results

p53 and p21 expression upon combined low doses of BRL plus 9RA in breast cancer cells. We aimed to examine the potential ability of nanomolar concentrations of BRL and 9RA to modulate p53 and its natural target gene $p21^{WAF1/Cip1}$. We revealed that only the combination of both ligands enhanced p53 expression in all breast cancer cells tested in terms of mRNA and protein content, while the increased expression of $p21^{WAF1/Cip1}$ was highlighted only in MCF7 cells (**Fig. 1A–E**), suggesting that p53 mutated form in the other two cell lines tested does not exhibit any transactivation properties. Moreover, as expected we did not observe in SKBR3 and T47D cells any modulation of the human wild-type $p21^{WAF1/Cip1}$ promoter luciferase activity upon nanomolar concentrations of BRL and 9RA alone or in combination (data not shown), even though PPARγ can mediate the upregulation of $p21^{WAF1/Cip1}$ independently of p53.[17-19]

BRL plus 9RA treatment improves the association between p53 and bid in breast cancer cells. p53 participates in apoptosis, even by acting directly on multiple mitochondrial targets.[20] Therefore, we evaluated the involvement of Bcl-2 proteins family in regulating apoptosis. After 48 h BRL plus 9RA treatment, we determined the protein levels of Bid, Bad, Bcl-x_L in both cytosolic and mitochondrial fractions of breast cancer cells. The separate treatment with low doses of either BRL or 9RA did not elicit any noticeable effect on Bid expression (**Sup. Fig. 1**), in contrast an upregulation of Bid protein content upon the combined treatment was observed in both cytosolic and mitochondrial extracts, while unchanged levels of Bad and Bcl-x_L were detected in all the fractions tested (**Fig. 2A**). The protein synthesis inhibitor cycloheximide (CX) prevented the enhancement of Bid expression, suggesting that Bid is ex novo synthesized (**Fig. 2B**). The transcriptional activity of Bid was confirmed by using qtPCR, which clearly showed a significant upregulation of Bid mRNA in all breast cancer cells (**Fig. 2C**). The enhancement of Bid transcript levels upon treatments was reversed after silencing PPARγ, addressing that the effect is PPARγ-mediated (**Fig. 2D and E**).

To examine whether wt and/or mutant p53 protein could associate with Bid in the cytoplasm and colocalize to the mitochondria, we performed co-immunoprecipitation experiments using cytosolic and either whole mitochondria or mitochondrial matrix extracts from breast cancer cells treated for 48 h with BRL plus 9RA. Equal amounts of protein extracts were immunoprecipitated with an anti-p53 antibody and then subjected to immunoblot with anti-Bid antibody. As seen in **Figure 3A**, in cytosolic immunoprecipitates we detected under physiological conditions the association between p53 and Bid that slightly increased upon BRL plus 9RA treatment, while in whole mitochondria we revealed that p53 was able to interact with the more active truncated Bid, tBid particularly in the presence of the combined treatment (**Fig. 3B**). In the matrix of mitochondria no association between the two proteins was observed, suggesting that this physical interaction occurs in mitochondrial membrane likely initiating this organelle dysfunction (**Fig. 3C**). Since it has been reported the interaction of tBid with other proapoptotic proteins resulting in a more global permeabilization of the outer mitochondrial membrane,[12] we also explored the involvement of Bak and Bax. We detected the presence of Bak (**Fig. 3A and B**), but not of Bax (data not shown) as component of this multiprotein complex. Stemming from our previous findings demonstrating that p53 binds to PPARγ in breast cancer cells,[21] we investigated in our cellular context a possible association of PPARγ to this protein complex together with its heterodimer RXRα. We observed the presence of both receptors in this complex in cytosol as well as in whole mitochondria, but not in mitochondrial matrix (**Fig. 3A–C**). The p53/Bid association still occured after knocking down PPARγ and RXRα as shown in **Supplemental Figure 2**. To better define the mitochondrial colocalization of p53 and Bid, we used a red-fluorescent dye that passively diffuses across the plasma membrane and accumulates in active mitochondria. In MCF7 cells the coexpression of both proteins gave rise to a merged image which appears further enhanced in cells treated with BRL plus 9RA (**Fig. 3D**).

Bid is involved in apoptotic events triggered by BRL plus 9RA treatment in breast cancer cells. In order to validate the key role of Bid in the apoptotic process we used different experimental approaches after silencing Bid expression. We analyzed mitochondrial membrane potential using a fluorescent dye JC-1 in all cell lines tested after BRL plus 9RA treatment. Cells transfected with control RNAi allowed the accumulation of lipophilic dye in aggregated form in mitochondria, displaying red fluorescence as shown in **Figure 4A**, demonstrating the integrity of the mitochondrial membrane potential. Cells treated with both ligands exhibited green fluorescence, indicating the disruption of mitochondrial integrity, because JC-1 cannot accumulate within the mitochondria, but instead remained as a monomer in the cytoplasm. After silencing Bid expression, red fluorescence was evident in treated cells (**Fig. 4A**), suggesting that the integrity of the mitochondrial membrane potential is maintained in MCF7, SKBR3 and T47D cells. This result well fits with a significant decrease of PARP cleavage in cells transfected with Bid RNAi and treated with ligands respect to treated cells transfected with control RNAi (**Fig. 4B**). Indeed in transfected cells with Bid-RNAi TUNEL assay showed after 72 h treatment a strong reduction of the percentage of apoptotic cells respect to treated cells trasfected with control RNAi (**Fig. 4C**). All these data indicate that Bid plays an important role in the death pathway induced by low doses of PPARγ and RXR ligands in breast cancer cells.

BRL plus 9RA reduce glutathione S-transferase antioxidative enzyme activity and induce lipid peroxidation in breast cancer cells. Since, an isoform of the antioxidant defense

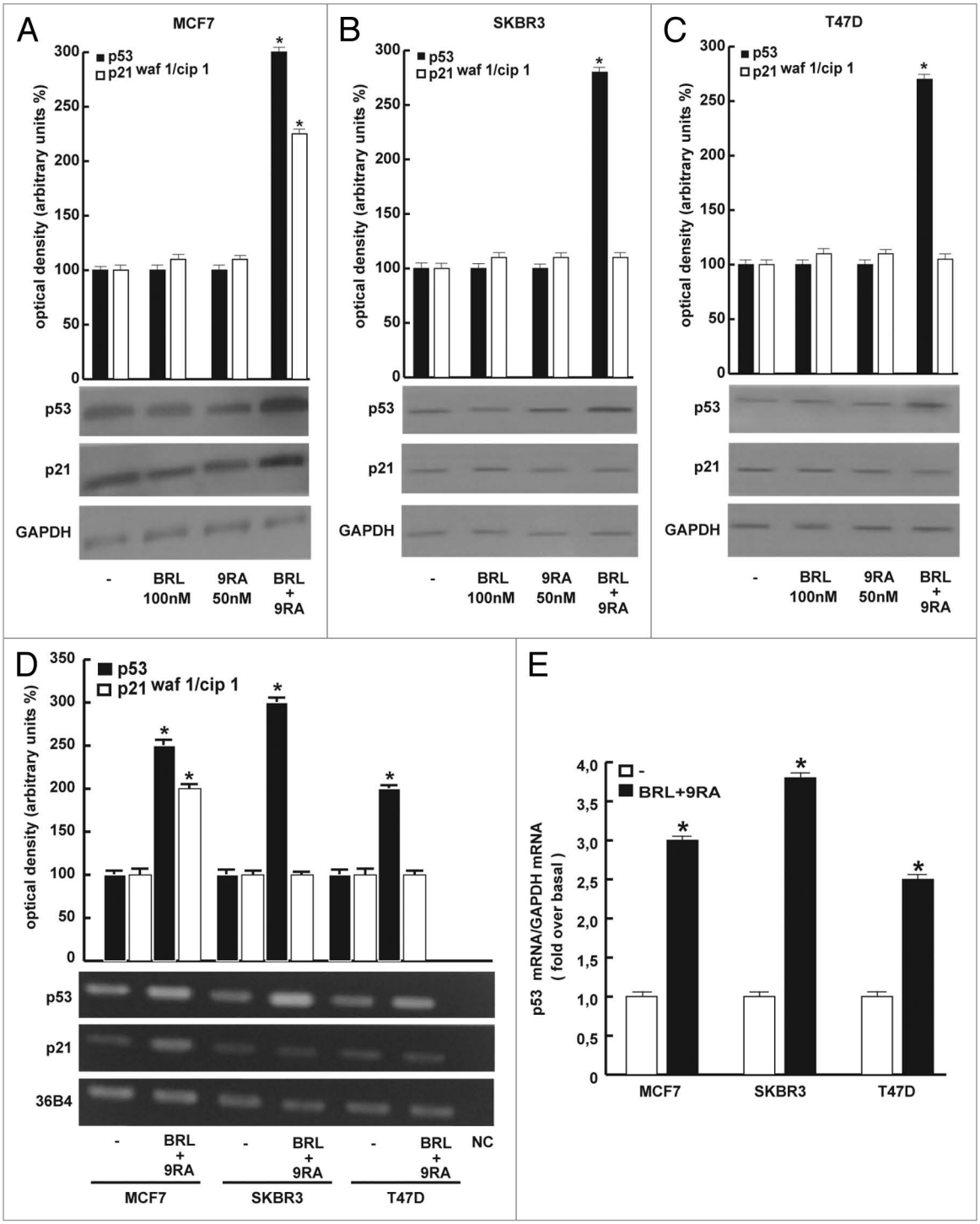

Figure 1. Combined low doses of BRL and 9RA upregulate p53 expression in MCF7, SKBR3 and T47D breast cancer cells. (A–C) Immunoblots of p53 and p21 from extracts of MCF7, SKBR3 and T47D cells untreated (-) or treated with 100 nM BRL and/or 50 nM 9RA for 24 hours. GAPDH was used as loading control. The histograms show the quantitative representation of data (mean ± SD) of three independent experiments in which band intensities were evaluated in terms of optical density arbitrary units and expressed as percentages of the control which was assumed to be 100%. (D) p53 and p21 mRNA expression in MCF7, SKBR3 and T47D cells untreated (-) or treated with 100 nM BRL plus 50 nM 9RA for 12 hours. The histograms show the quantitative representation of data (mean ± SD) of three independent experiments after densitometry and correction for 36B4 expression and expressed as percentages of the control which was assumed to be 100%. (E) Quantitative real-time PCR analysis of p53 mRNA expression in MCF7, SKBR3 and T47D cells treated as in (D). The histograms show the quantitative representation of data (mean ± SD) of three independent experiments after correction for GAPDH expression. NC: RNA samples without the addition of reverse transcriptase (negative control). *$p < 0.05$ combined-treated vs. untreated cells.

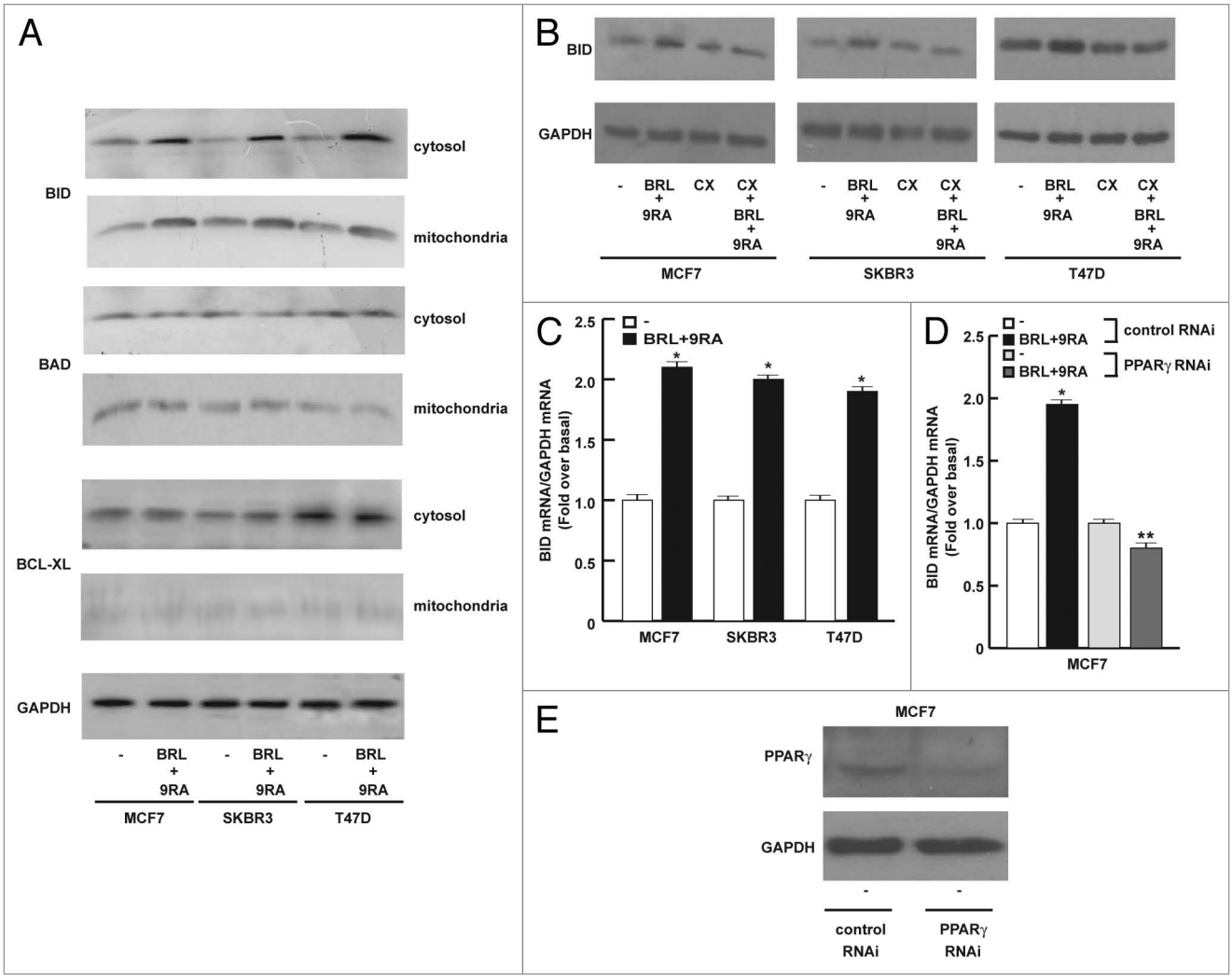

Figure 2. Upregulation of BID expression by BRL and 9RA in breast cancer cells. (A) Cytosolic and mitochondrial expression of BID, BAD and BCL-X_L proteins in MCF7, SKBR3 and T47D breast cancer cells untreated (-) or treated for 48 hours with 100 nM BRL plus 50 nM 9RA. GAPDH was used as loading control. One of three similar experiments is presented. (B) Immunoblots of BID from total extracts of MCF7, SKBR3 and T47D cells treated as in (A) and/or with 50 μM protein synthesis inhibitor cycloheximide (CX). GAPDH was used as loading control. One of three similar experiments is presented. (C) Quantitative real-time PCR analysis of BID mRNA expression in MCF7, SKBR3 and T47D cells treated for 24 hours as indicated. (D) Quantitative real-time PCR analysis of BID mRNA expression in MCF7 cells transfected with control RNAi or with PPARγ RNAi and treated for 24 hours as indicated. The histograms show the quantitative representation of data (mean ± SD) of three independent experiments after correction for GAPDH expression. (E) Immunoblots of PPARγ from extracts of MCF7 cells transfected with control RNAi or with PPARγ RNAi. GAPDH was used as loading control. *$p < 0.05$ combined-treated vs. untreated cells. **$p < 0.05$ combined-treated cells transfected with PPARγ RNAi vs. combined-treated cells transfected with control RNAi.

glutathione S-transferase (GST) is located at mitochondrial membranes, we measured its enzimatic activity in mitochondrial extracts of MCF7, SKBR3 and T47D cells after BRL plus 9RA treatment. Interestingly, GST activity was reduced respect to untreated cells, while in the presence of Bid RNAi this effect was no longer noticeable (**Fig. 5A**), addressing that BRL plus 9RA treatment negatively regulate mitochondrial scavenger activity via Bid. Moreover, we estimated the presence of malondialdehyde (MDA), a common end products of lipid peroxidation, as index of oxidative stress induced by both ligands. As shown in **Figure 5B**, the lipid peroxidation was considerably increased by the treatment in both total cellular and mitochondrial extracts of all breast cancer cells.

Discussion

In the present study we provided the first evidence that low doses of PPARγ and RXR ligands through PPARγ increasing Bid expression and its association with p53 in mitochondria induces apoptosis in different breast carcinoma cells.

The p53 pathway is inactivated in the majority of human cancers, most likely because the pro-apoptotic function of p53 is critical to the inhibition of tumor development and progression. Although it is clearly established the role of p53 as a nuclear transcription factor able to activate or repress a number of p53 transcriptional targets with the potential to promote or inhibit apoptosis, many evidences support a transcriptional-independent

Figure 3A–C (For D, see following page). Physical association between p53 and BID in breast cancer cells. MCF7, SKBR3 and T47D cells were untreated (-) or treated for 48 hours with BRL plus 9RA. Cytosolic (A), whole mitochondrial (B) and mitochondrial matrix (C) extracts were immunoprecipitated with an antiserum against p53 (IP:p53) and then the immunocomplexes were resolved in SDS-PAGE. The membrane was probed with anti-BID, anti-BAK, anti-PPARγ and anti-RXRα antibodies. To verify equal loading, the membrane was probed with an antibody against p53. One of three similar experiments is presented. MCF7 lysates were used as positive control.

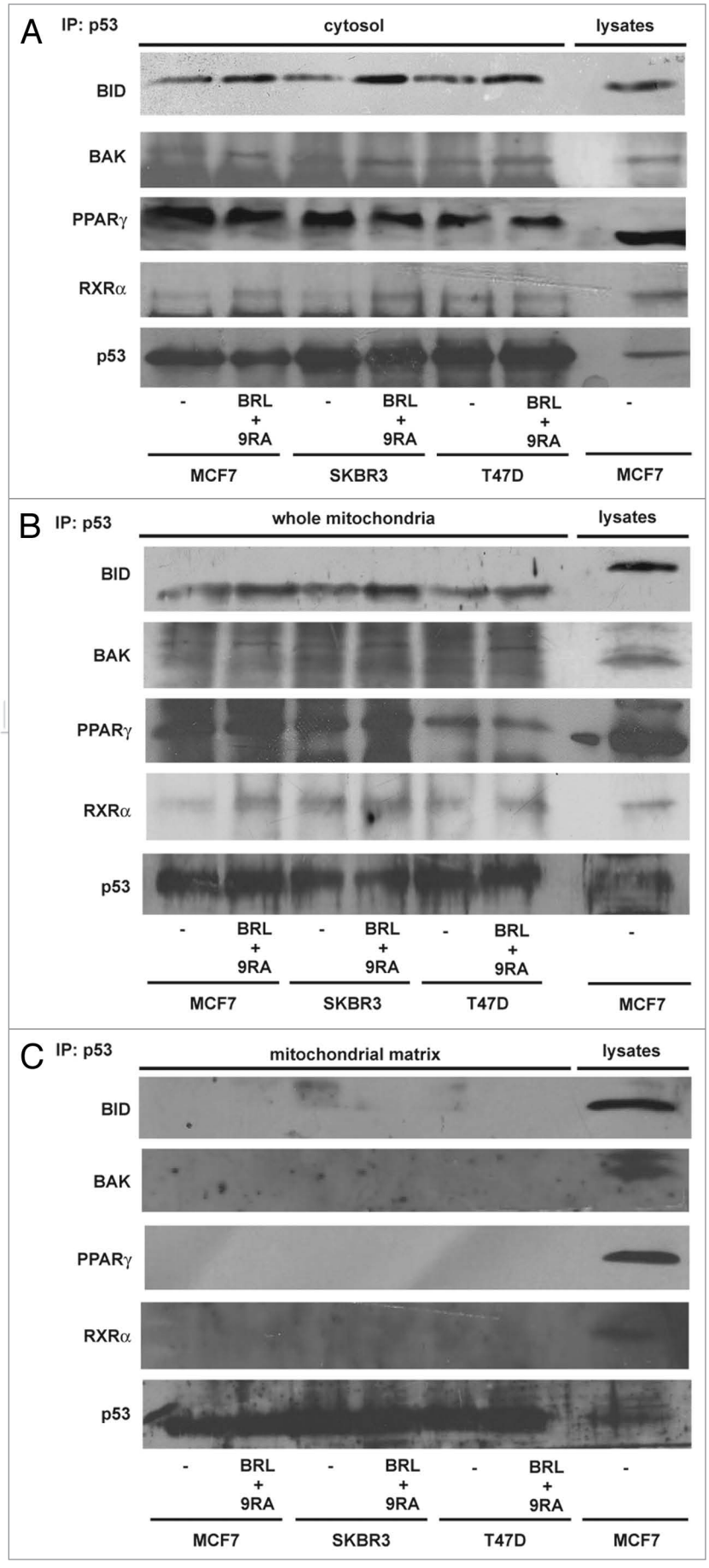

function of p53 in apoptosis. Indeed, an unexpected turn in the p53-mediated pathway to programmed cell death has emerged with accumulating data that p53 has a direct cytoplasmic role at mitochondria in activating the apoptotic machinery.[20] Thus, a major question is to define the apoptotic function of mitochondrial p53. Increased evidences suggest that mitochondrial p53 localization is sufficient for initiating p53-dependent apoptosis.[22,23] Furthermore, some studies reported that p53 may induce apoptosis by forming complexes with mitochondrial apoptotic proteins such as Bcl-2/Bcl-x_L,[24] Bad[25] or Bid,[26] which are located in the outer membrane of mitochondria. We hypothesize that mechanistic insight into this process could be obtained from the identification of mitochondrial p53-interacting protein.

The novelty of the present study raises by the evidence that in response to the combined BRL and 9RA treatment in breast cancer cells we observed a PPARγ-dependent upregulation of Bid expression. Although it has been reported that Bid is transcriptionally regulated by p53,[27] our results address an independent-p53 transcriptional regulation of Bid gene since we found increased Bid transcript levels also in SKBR3 and T47D breast cancer cells harboring p53 mutated. Having demonstrated that PPARγ activation increased both p53 and Bid expression we moved to study their enhanced association in different cellular compartments in response to BRL plus 9RA. Here we showed that p53 interacts with Bid in cytosol and exclusively with the truncated more active tBid in mitochondria, showing a slight increase upon BRL and 9RA treatment.

Bid is a member of the 'BH3 domain only' subgroup of Bcl-2 family members proposed to connect proximal death and survival signals to the core apoptotic pathway at the level of the classic family members which bear multiple BH domains.[28,29] It has been reported that Bid is able to bind mitochondrial proteins and promote cell death, suggesting a model in which Bid served as a 'death ligand' which moved from the cytosol to

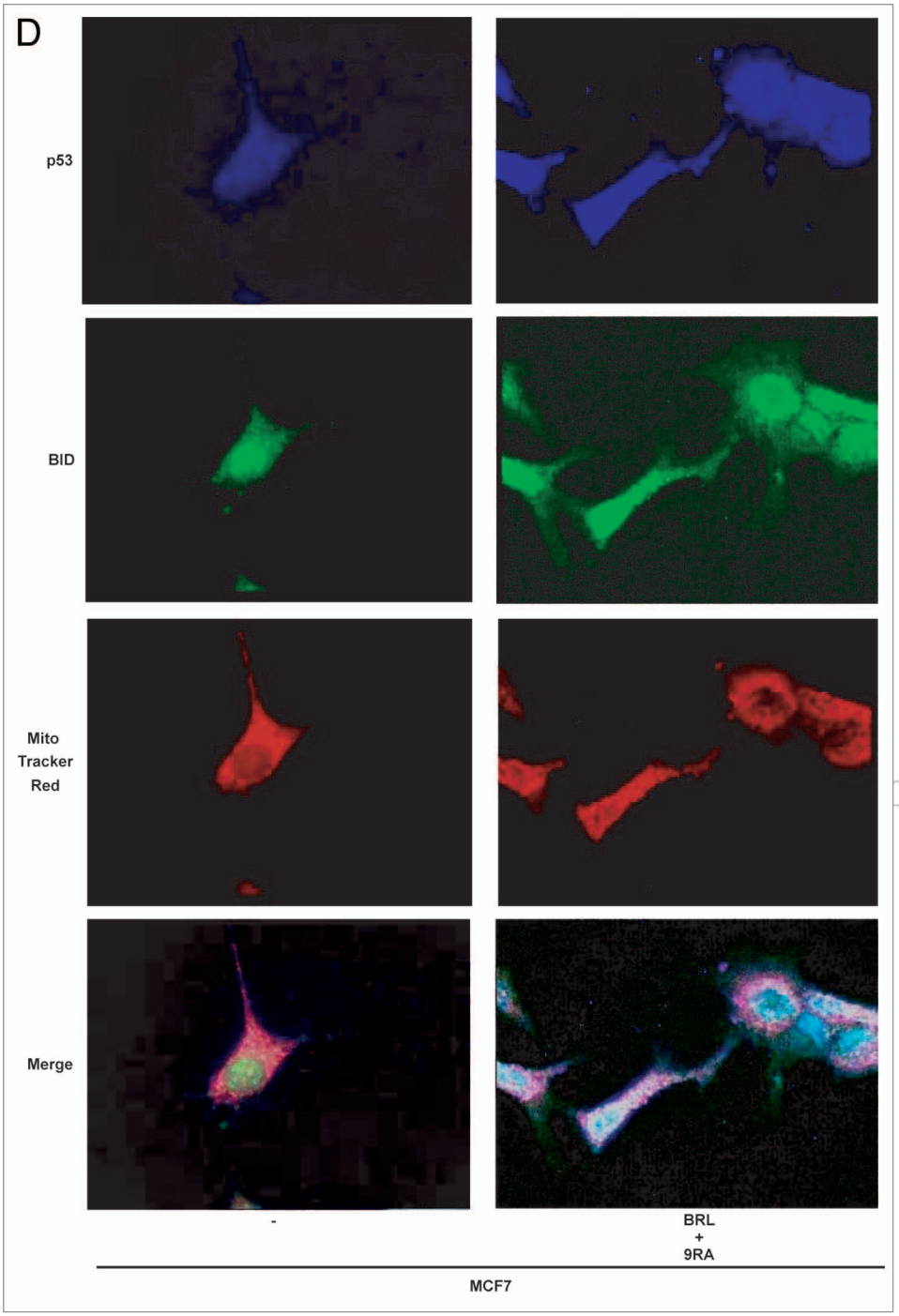

Figure 3D (For A–C, see previous page). Physical association between p53 and BID in breast cancer cells. (D) MCF7 cells untreated (-) or treated with BRL plus 9RA for 48 hours were incubated in MitoTracker Red dye. Cells were immunostained with p53 and BID and then examined by fluorescent microscopy. Blue, p53; green, BID; red, MitoTracker; merge of blue, green and red as expression of co-localization in mitochondria.

the mitochondrial membrane to inactivate Bcl-2 or activate Bax and Bak and to result in cytochrome *c* release.[12] The release of cytochrome *c* from mitochondria has been shown to promote the oligomerization of a cytochrome *c*/Apaf-1/Caspase-9 complex that activates caspase-9 to result in the cleavage of downstream effector caspases.[12] We showed the involvement of Bak protein as a component of a p53/Bid protein-protein interaction in breast cancer cells hypothesizing that it contributes to form a large pore responsible for triggering apoptotic events.

Given the discovery that nanomolar concentrations of BRL and 9RA upregulate Bid expression in mitochondria, we sought to elucidate the role of Bid in mitochondrial function of breast cancer cells.

Mitochondria, as central point of oxidative metabolism, are a major source of intracellular reactive oxygen species (ROS), which cause, sequentially, cellular injury to DNA, protein and lipid peroxidation, followed by loss of cell membrane integrity leading to cell death.[30] ROS, however, have also been implicated as second messengers in apoptotic processes.[31] Under normal physiological conditions, cellular ROS generation is controlled by antioxidant enzymes and other small-molecule antioxidants.[32] We observed upon the combined treatment with PPARγ and RXR ligands a significant reduction of GST enzymatic activity in mitochondrial extracts which was no longer noticeable after knocking down Bid. These results highlighting the crucial role played by Bid might provide a correlation between the mitochondrial dysfunction and the enhanced apoptotic response of different breast cancer cells to PPARγ and RXR ligands.

The data described above providing new insight into the role of p53/

Figure 4 (See opposite page). Knocking down BID abrogates apoptotic events in breast cancer cells. (A) MCF7, SKBR3 and T47D cells were transfected with control RNAi or with BID RNAi and treated for 48 hours as indicated. The results of JC-1 kit were examined by fluorescent microscopy. (B) Immunoblots of PARP and BID from total extracts of MCF7, SKBR3 and T47D cells transfected and treated as in (A). GAPDH was used as loading control. One of three similar experiments is presented. (C) Cells were transfected as in (A) and treated for 72 hours as indicated. The histograms show the quantitative representation of data (mean ± SD) of three independent experiments performed in triplicates. *p < 0.05 combined-treated vs. untreated cells.

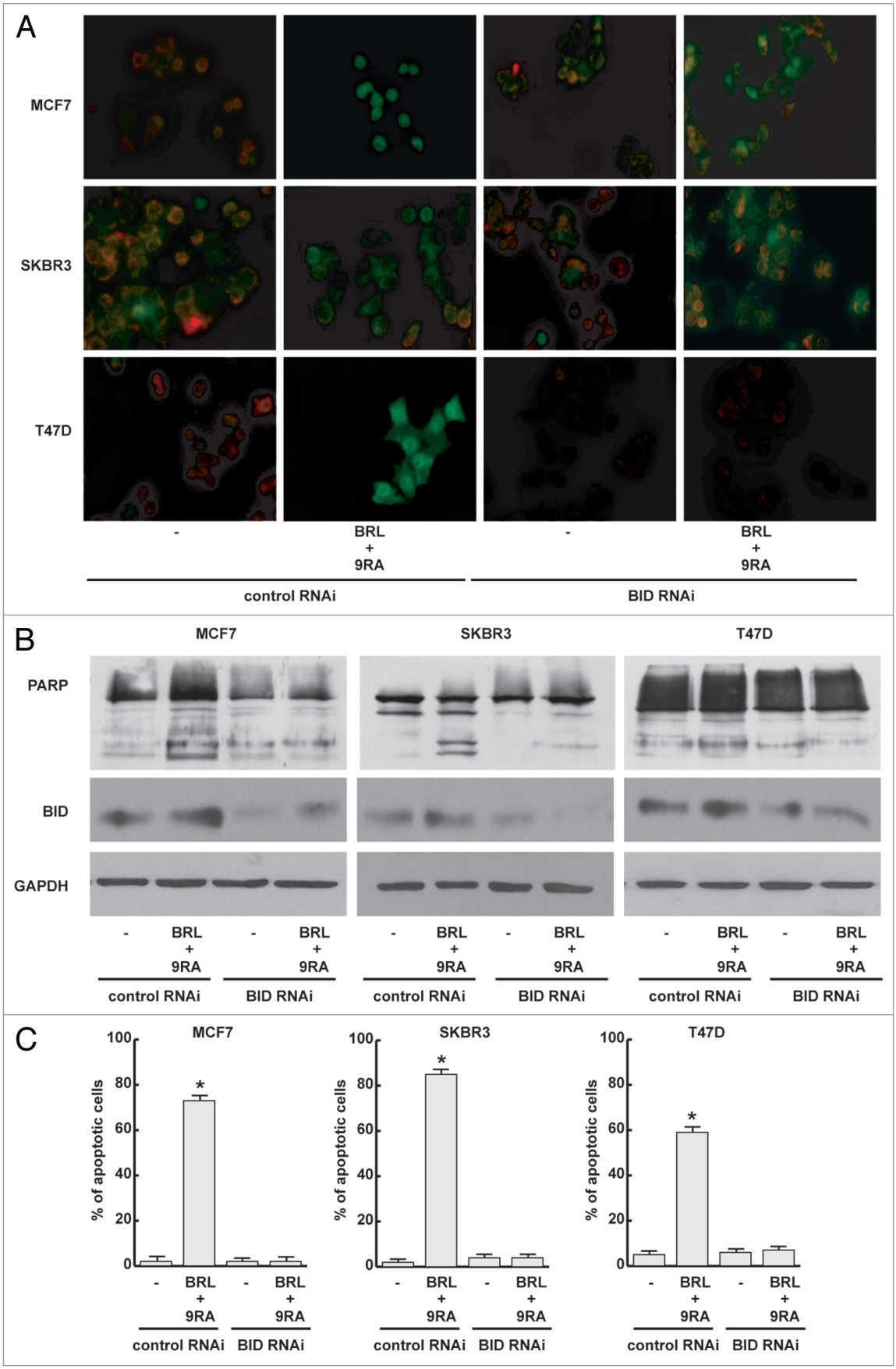

Figure 4. For figure legend, see page 6.

Bid complex at the mitochondria in promoting breast cancer cell apoptosis upon low doses of PPARγ and RXR ligands, address Bid as a potential target in the novel therapeutical strategies for breast cancer treatments.

Materials and Methods

Reagents. BRL 49,653 (BRL) was purchased from Alexis (San Diego, CA USA) and solubilised in DMSO. 9-cis retinoic acid (9RA) was obtained from Sigma-Aldrich (Milan, Italia). 9RA was prepared just before use (Sigma-Aldrich) and diluted into medium at the indicated concentration. All experiments involving 9RA were performed under yellow light, and the tubes and culture plates containing 9RA were covered with aluminium foils. Cycloheximide (CX) was obtained from Sigma-Aldrich.

Plasmids. The human wild-type $p21^{WAF1/Cip1}$ promoter-luciferase (luc) reporter was a kind gift from Dr. T. Sakai (Kyoto Prefectural University of Medicine, Kyoto, Japan). As an internal transfection control we co-transfected the plasmid pRL-CMV (Promega Corp., Milan, Italy), which expresses Renilla luciferase enzymatically distinguishable from firefly luciferase by the strong cytomegalovirus enhancer/promoter.

Cells. Wild-type human breast cancer MCF7 cells were grown in DMEM-F12 plus glutamax containing 5% new-born calf serum (Invitrogen, Milan, Italy) and 1 mg/ml penicillin-streptomycin (P/S). SKBR3 breast cancer cells were grown in RPMI 1640 without red phenol, plus glutamax containing 10% fetal bovine serum (FBS) and 1 mg/ml P/S. T47D breast cancer cells were grown in RPMI 1640 with glutamax and red phenol containing 10% FBS, 1 mM sodium pyruvate, 10 mM HEPES, 2.5 g/L glucose, 0.2 U/ml insulin and 1 mg/ml P/S.

Immunoblotting. Cells were grown in 6 cm dishes to 70–80% confluence and exposed to treatments in 1% charcoal treated (CT)-FBS as indicated. Cells were harvested in cold phosphate-buffered saline (PBS) and resuspended in total ripa buffer containing 1% NP40, 0.5% Na-deoxycholate, 0.1% SDS and inhibitors (0.1 mM sodium orthovanadate, 1% phenylmethylsulfonylfluoride or PMSF, 20 mg/ml aprotinin). Protein concentration was determined by Bio-Rad Protein Assay (Bio-Rad Laboratories, Hercules, CA USA). A 40 μg portion of total lysates was used for western blotting (WB), resolved on a 11% SDS-polyacrylamide gel, transferred to a nitrocellulose membrane and probed with an antibody directed against the p53 (cat#sc-126), $p21^{WAF1/Cip1}$ (cat#sc-756), PARP (cat#sc-7150), Bid (cat#sc-11423), anti-PPARγ (cat#sc-7196) and anti-RXRα (cat#sc-774) antibodies (Santa Cruz Biotechnology, CA USA). As internal control, all membranes were subsequently stripped (0.2 M glycine, pH 2.6, for 30 min at room temperature) of the first antibody and reprobed with anti-GAPDH antibody (cat#sc-25778, Santa Cruz Biotechnology). The antigen-antibody complex was detected by incubation of the membranes for 1 h at room temperature with peroxidase-coupled goat anti-mouse or anti-rabbit IgG and revealed using the enhanced chemiluminescence system (Amersham Pharmacia, Buckinghamshire UK). Blots were then exposed to film (Kodak film, Sigma). The intensity of bands representing relevant proteins was measured by Scion Image laser densitometry scanning program.

To obtain cytosolic and total mitochondrial fraction of proteins, cells were grown in 10 cm dishes to 70–80% confluence and exposed to treatments as for 48 h. Cells were harvested by centrifugation at 2,500 rpm for 10 min at 4°C. The pellets were suspended in 250 μl of RIPA buffer plus 10 μg/ml aprotinin, 50 mM PMSF and 50 mM sodium orthovanadate and then 0.1% digitonine (final concentration) was added. Cells were incubated for 15 min at 4°C and centrifuged at 3,000 rpm for 10 min at 4°C, supernatants were collected and further centrifuged at 14,000 rpm for 10 min at 4°C. The supernatant, containing cytosolic fraction of proteins, was collected, while the resulting mitochondrial pellet was resuspended in 3% Triton X-100, 20 mM Na_2SO_4, 10 mM PIPES and 1 mM EDTA, pH 7.2, incubated for 15 min at 4°C and centrifuged at 12,000 rpm for 10 min at 4°C. Alternatively, to provide matrix mitochondrial fraction of proteins, mitochondrial pellet was further solubilised in 6% of digitonine in RIPA buffer, for 10 min at 4°C then centrifuged at 14,000 rpm, 4°C, 10 min. The pellets (mitoplasts) were then lysed osmotically and centrifuged at 14,000 rpm 4°C 10 min to discard the membrane residues and recover the soluble matrix content. Proteins of the mitochondrial and cytosolic fractions were determined by Bio-Rad Protein Assay (Bio-Rad Laboratories). Equal amounts of cytosolic and mitochondrial proteins (40 μg) were resolved by 11% SDS-PAGE, electrotransferred to nitrocellulose membranes and probed with antibodies directed against Bid, Bad (cat#sc-8044) and BCL-X_L (cat#sc-7195) (Santa Cruz Biotechnology). As the internal loading, all membranes were stripped and reprobed with anti GAPDH (Santa Cruz Biotechnology) antibody.

Immunoprecipitation. 300 μg of mitochondrial and cytosolic proteins were incubated overnight with the anti-p53 (cat#sc-126) or anti-Bid (cat#sc-135847) antibodies (Santa Cruz Biotechnology) and 500 μL of HNTG (immunoprecipitation) buffer [50 mmol/L HEPES (pH 7.4), 50 mmol/L NaCl, 0.1% Triton X-100, 10% glycerol, 1 mmol/L phenylmethylsulfonyl fluoride, 10 μg/mL leupeptin, 10 μg/mL aprotinin, 2 μg/mL pepstatin]. Immunocomplexes were recovered by incubation with protein A/G-agarose. The immunoprecipitates were centrifuged, washed twice with HNTG buffer and then used for western blotting (WB). Membranes were probed with anti-p53 (cat#sc-6243), anti-Bid (cat#sc-11423), anti-Bak (cat#sc-832), anti-Bax (cat#sc-7480), anti-PPARγ (cat#sc-7196) and anti-RXRα (cat#sc-774) antibodies (Santa Cruz Biotechnology).

RT-PCR/real-time PCR. MCF7, SKBR3 and T47D cells were grown in 10 cm dishes to 70–80% confluence, and exposed to treatments in 1% CT-FBS as indicated. Total cellular RNA was extracted using TRIZOL reagent (Invitrogen) as suggested by the manufacturer. The RNA sample was treated with DNase I (Ambion, Austin, TX), and purity and integrity of the RNA was confirmed both spectroscopically and electrophoretically. RNA was then reversed transcribed with High Capacity cDNA Reverse Transcription Kit (Applied Biosystems, Applera Italia, Monza, Milano, Italy). The evaluation of p53, $p21^{WAF1/Cip1}$ and the internal control gene 36B4 was performed by RT-PCR method

using the following primers: 5'-CCA GTG TGA TGA TGG TGA GG-3' (p53 forward) and 5-GCT TCA TGC CAG CTA CTT CC-3 (p53 reverse), 5'-CTG TGC TCA CTT CAG GGT CA-3' (p21 forward) and 5'-CTC AAC ATC TCC CCC TTC-3' (p21 reverse), 5'-CTC AAC ATC TCC CCC TTC TC-3' (36B4 forward) and 5'-CAA ATC CCA TAT CCT CGT CC-3' (36B4 reverse) to yield, respectively, products of 190 bp with 18 cycles, 270 bp with 18 cycles and 408 bp with 18 cycles. The results obtained as optical density arbitrary values were transformed to percentage of the control (percent control) taking the samples from untreated cells as 100%.

Analysis of p53 and Bid gene expression was performed using Real-time reverse transcription PCR. cDNA was diluted 1:3 in nuclease-free water and 5 μl were analyzed in triplicates by real-time PCR in an iCycler iQ Detection System (Bio-Rad, USA) using SYBR Green Universal PCR Master Mix with 0.1 mmol/l of each primer in a total volume of 30 μl reaction mixture following the manufacturer's recommendations. Each sample was normalized on its GAPDH mRNA content. Relative gene expression levels were normalized to the basal, untreated sample chosen as calibrator. Final results are expressed as folds of difference in gene expression relative to GAPDH mRNA and calibrator, calculated following the ΔCt method, as follows:

Relative expression (folds) = $2^{-(\Delta Ctsample - \Delta Ctcalibrator)}$

where ΔCt values of the sample and calibrator were determined by subtracting the average Ct value of the GAPDH mRNA reference gene from the average Ct value of the analyzed gene. For p53, Bid and GAPDH the primers were: 5'-GCT GCT CAG ATA GCG ATG GTC-3' (p53 forward) and 5-CTC CCA GGA CAG GCA CAA ACA-3 (p53 reverse), 5'-CCA TGG ACT GTG AGG TCA AC-3' (Bid forward) and 5'-CTT TGG AGG AAG CCA AAC AC-3' (Bid reverse), 5'-CCC ACT CCT CCA CCT TTG AC-3' (GAPDH forward), 5'-TGT TGC TGT AGC CAA ATT CGT-3' (GAPDH reverse). Negative controls contained water instead of first strand cDNA.

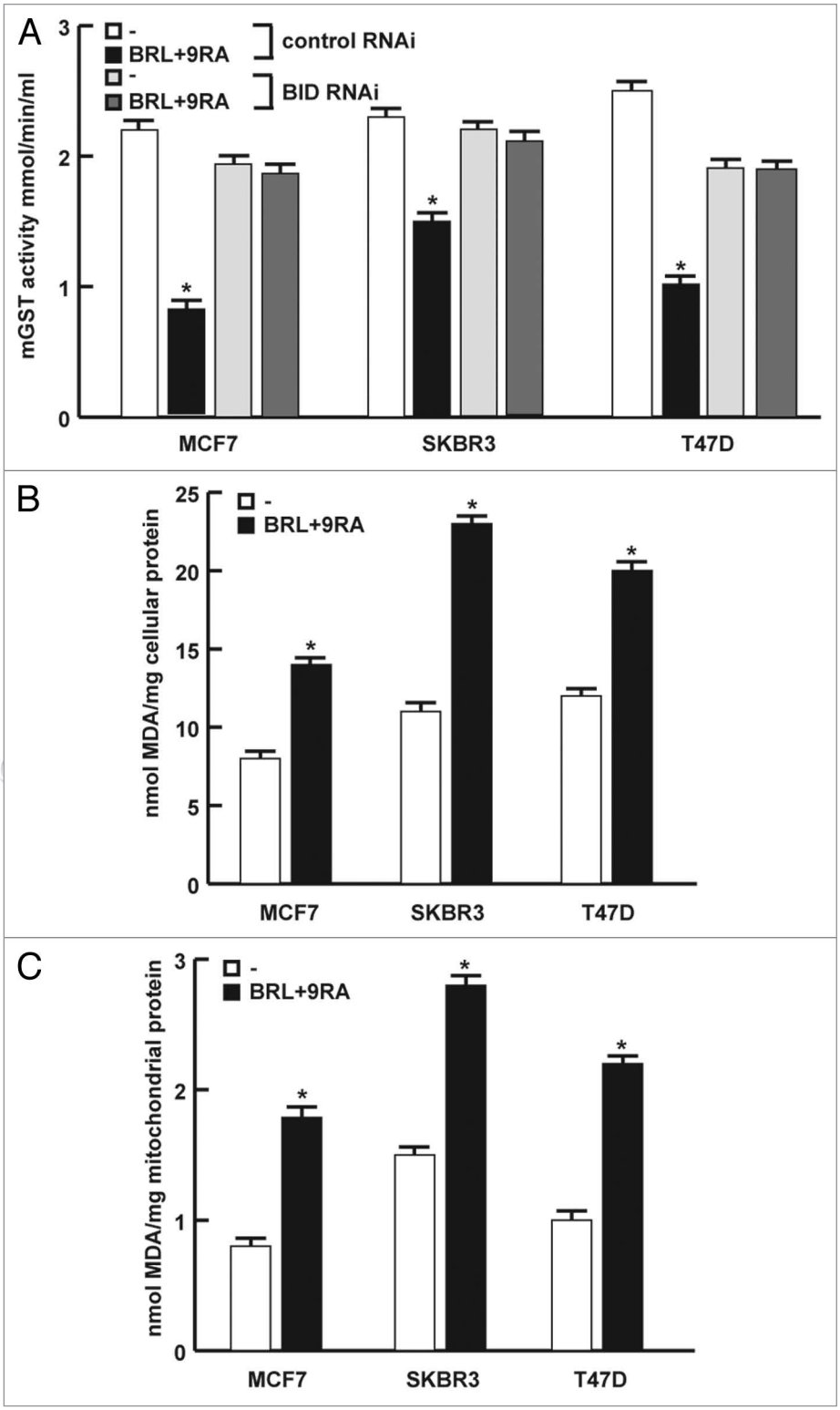

Figure 5. BRL and 9RA reduce glutathione S-transferase (GST) antioxidative enzyme activity and induce lipid peroxidation in breast cancer cells. (A) Glutathione S-transferase activity from mitochondrial extracts (mGST) of MCF7, SKBR3 and T47D cells transfected with control RNAi or with BID RNAi and treated for 24 hours as indicated. (B) Lipid peroxidation from total and (C) mitochondrial cell extracts of all breast cancer cells treated for 48 h as indicated. *$p < 0.05$ combined-treated vs. untreated cells. MDA: Malondialdehyde.

Transient transfection assay. SKBR3 and T47D cells were transferred into 24 well plates with 500 μl of regular growth medium/well the day before transfection. The medium was replaced with 1% CT-FBS on the day of transfection, which was performed using Fugene 6 reagent as recommended by the manufacturer (Roche Diagnostics, Mannheim, Germany) with a mixture containing 0.5 μg of p21 promoter-luc plasmid and 10 ng of pRL-CMV. After transfection for 24 h, treatments were added in 1% CT-FBS, and cells were incubated for an additional 24 h. Firefly and Renilla luciferase activities were measured using the Dual Luciferase Kit (Promega).

RNA interference (RNAi). Cells were plated in 10 cm dishes with regular growth medium the day before transfection to 60–70% confluence. On the second day the medium was changed with 1% CT-FBS without P/S and cells were transfected with stealth RNAi targeted human Bid mRNA sequence -5'-UGC GGU UGC CAU CAG UCU GCA GCU C-3' (Invitrogen), with a stealth RNAi targeted human PPARγ mRNA sequence 5'-AGA AUA AUA AGG UGG AGA UGC AGG C-3' (Invitrogen), a stealth RNAi targeted human RXRα mRNA sequence 5'-UCG UCC UCU UUA ACC CUG ACU CCA A-3' or with a stealth RNAi-negative control (Invitrogen) to a final concentration of 100 nM using Lipofectamine 2000 (Invitrogen) as recommended by the manufacturer. After 5 h the transfection medium was changed with complete 1% CT-FBS with P/S in order to avoid Lipofectamine 2000 toxicity, cells were exposed to combined treatment and subjected to different experiments.

Immunofluorescence. MCF7 cells were plated in 6 cm dishes in complete growth medium. On the second day, the medium was changed with 1% CT-FBS and cells were treated with BRL plus 9RA for 48 h. p53 and Bid staining was carried out using anti-p53 and anti-Bid primary antibodies followed by Alexa-fluo 350 (blue) and Alexa-fluo 488 (green) (Invitrogen) as secondary antibodies, respectively. Mitochondria were stained with MitoTracker mitochondrion selective probe (cat#MP07510, Invitrogen) according to manufacturer's instructions. The images were acquired using fluorescent microscopy (Leica AF6000).

JC-1 mitochondrial membrane potential detection assay. Alteration of mitochondrial membrane potential was detected using the dye 5,5',6,6'-tetra-chloro-1,1',3,3'-tetraethylbenzimidazolyl-carbocyanine iodide (JC-1) as recommended by manufacturing instruction (Biotium, Hayward, USA). MCF7, SKBR3 and T47D cells were grown in 10 cm dishes, transfected with control RNAi or Bid RNAi and then treated with BRL and 9RA for 56 h in 1% CT-FBS. Subsequently cells were washed in ice-cold PBS, and incubated with 10 mM JC-1 at 37°C in a 5% CO_2 incubator for 20 min in darkness. Subsequently, cells were extensively washed with PBS and analyzed by fluorescence microscopy. The red form has absorption/emission maxima of 585/590 nm. The green monomeric form has absorption/emission maxima of 510/527 nm.

TUNEL assay. Apoptosis was determined by enzymatic labelling of DNA strand breaks using terminal deoxynucleotidyl transferase-mediated deoxyuridine triphosphate nick end-labeling (TUNEL). TUNEL labelling was conducted using APO-BrdU™ TUNEL Assay Kit (Invitrogen) and performed according to the manufacturer's instructions. Briefly, cells were trypsinized after treatments and resuspended in 0.5 ml of PBS. After fixation with 1% paraformaldehyde for 15 min on ice, cells were incubated on ice-cold 70% ethanol overnight. After washing twice with washing buffer for 5 min, the labelling reaction was performed using terminal deoxynucleotidyl transferase end-labeling cocktail for each sample and incubated for 1 h at 37°C. After rinsing, cells were incubated with antibody staining solution prepared with Alexa Fluor 488 dye-labeled anti-BrdU for 30 min at room temperature. Subsequently 0.5 mL of propidium iodide/RNase A buffer were added for each sample. Cells were incubated 30 min at room temperature, protected from light, analyzed and photographed by using a fluorescent microscope.

GST antioxidant enzyme activity and lipid peroxidation. To measure mitochondrial glutathione S-transferase (GST) activity the mitochondrial suspension was used. Enzyme activity was detected according to the method provided by the manufacturer (Sigma Aldrich). To evaluate lipid peroxidation cells were sonicated in PBS and the crude homogenate was used. The level of lipid peroxidation in control as well as treated cell samples was assayed through the formation of thiobarbituric acid reactive species (TBARS) during an acid-heating reaction as previously described in reference 33. Briefly, the samples were mixed with 1 ml of 10% trichloroacetic acid (TCA) and 1 ml of 0.67% thiobarbituric acid (TBA), then heated in a boiling water bath for 15 min. TBARS were determined by the absorbance at 535 nm and were expressed as malondialdehyde equivalents (MDA) (nmol/mg protein) respect to cellular and mitochondrial.

Statistical analyses. Each datum point represents the mean ± SD of three different experiments. Statistical analysis was performed using ANOVA followed by Newman-Keuls testing to determine differences in means. $p < 0.05$ was considered as statistically significant.

Acknowledgments

We thank Dr. Maureen A. Kane for English revision.

Financial Support

This work was supported by AIRC, Foundation Lilli Funaro, MURST and Ex 60%.

Note

Supplemental materials can be found at:
www.landesbioscience.com/journals/cc/article/15917

References

1. Clarke AR, Purdie CA, Harrison DJ, Morris RG, Bird CC, Hooper ML, et al. Thymocyte apoptosis induced by p53-dependent and independent pathways. Nature 1993; 362:849-52.
2. Lowe SW, Schmitt EM, Smith SW, Osborne BA, Jacks T. p53 is required for radiation-induced apoptosis in mouse thymocytes. Nature 1993; 362:847-9.
3. Lowe SW, Bodis S, McClatchey A, Remington L, Ruley HE, Fisher DE, et al. p53 status and the efficacy of cancer therapy in vivo. Science 1994; 266:807-10.
4. El-Deiry WS. Insights into cancer therapeutic design based on p53 and TRAIL receptor signaling. Cell Death Differ 2001; 8:1066-75.
5. Caelles C, Helmberg A, Karin M. p53-dependent apoptosis in the absence of transcriptional activation of p53-target genes. Nature 1994; 370:220-3.
6. Haupt Y, Rowan S, Shaulian E, Vousden KH, Oren M. Induction of apoptosis in HeLa cells by trans-activation-deficient p53. Genes Dev 1995; 9:2170-83.
7. Ding HF, Lin YL, McGill G, Juo P, Zhu H, Blenis J, et al. Essential role for caspase-8 in transcription-independent apoptosis triggered by p53. J Biol Chem 2000; 275:38905-11.
8. Chipuk JE, Maurer U, Green DR, Schuler M. Pharmacologic activation of p53 elicits Bax-dependent apoptosis in the absence of transcription. Cancer Cell 2003; 4:371-81.
9. Chipuk JE, Kuwana T, Bouchier-Hayes L, Droin NM, Newmeyer DD, Schuler M, et al. Direct activation of Bax by p53 mediates mitochondrial membrane permeabilization and apoptosis. Science 2004; 303:1010-4.
10. Wei MC, Zong WX, Cheng EH, Lindsten T, Panoutsakopoulou V, Ross AJ, et al. Proapoptotic BAX and BAK: A requisite gateway to mitochondrial dysfunction and death. Science 2001; 292:727-30.
11. Wei MC, Lindsten T, Mootha VK, Weiler S, Gross A, Ashiya M, et al. tBID, a membrane-targeted death ligand, oligomerizes BAK to release cytochrome *c*. Genes Dev 2000; 14:2060-71.
12. Korsmeyer SJ, Wei MC, Saito M, Weiler S, Oh KJ, Schlesinger PH. Pro-apoptotic cascade activates BID, which oligomerizes BAK or BAX into pores that result in the release of cytochrome *c*. Cell Death Differ 2000; 7:1166-73.
13. Bonofiglio D, Cione E, Qi H, Pingitore A, Perri M, Catalano S, et al. Combined low doses of PPARgamma and RXR ligands trigger an intrinsic apoptotic pathway in human breast cancer cells. Am J Pathol 2009; 175:1270-80.
14. Levine AJ. p53, the cellular gatekeeper for growth and division. Cell 1997; 88:323-31.
15. Hansen R, Oren M. p53; from inductive signal to cellular effect. Curr Opin Genet Dev 1997; 7:46-51.
16. Oren M. Regulation of the p53 tumor suppressor protein. J Biol Chem 1999; 274:36031-4.
17. Chung SH, Onoda N, Ishikawa T, Ogisawa K, Takenaka C, Yano Y, et al. Peroxisome proliferator-activated receptor gamma activition induce cell cycle arrest via p53-independent pathway in human anaplastic thyroid cancer cells. Jap J Cancer Res 2002; 93:1358-65.
18. Hong J, Samudio I, Liu S, Abdelrahim M, Safe S. Peroxisome proliferator-activited receptor γ-dependent activation of p21 in panc-28 pancreatic cancer cells involves Sp1 and Sp4 proteins. Endocrinology 2004; 145:5774-85.
19. Bonofiglio D, Qi H, Gabriele S, Catalano S, Aquila S, Belmonte M, et al. Peroxisome proliferator-activated receptor-gamma inhibits follicular and anaplastic thyroid carcinoma cells growth by upregulating $p21^{Cip/WAF1}$ in a Sp1-dependent manner. Endocr Relat Cancer 2008; 15:545-57.
20. Murphy ME, Leu JIJ, George DL. p53 moves to mitochondria. A turn on the path to apoptosis. Cell Cycle 2004; 3:836-9.
21. Bonofiglio D, Aquila S, Catalano S, Gabriele S, Belmonte M, Middea E, et al. Peroxisome proliferator-activated receptor-gamma activates p53 gene promoter binding to the nuclear factor-kappaB sequence in human MCF7 breast cancer cells. Mol Endocrinol 2006; 20:3083-92.
22. Marchenko ND, Zaika A, Moll UM. Death signal-induced localization of p53 protein to mitochondria. A potential role in apoptotic signaling. J Biol Chem 2000; 275:16202-12.
23. Katsumoto T, Higaki K, Ohno K, Onodera K. Cell cycle dependent biosynthesis and localization of p53 protein in untransformed human cells. Biol Cell 1995; 84:167-73.
24. Mihara M, Erster S, Zaika A, Petrenko O, Chittenden T, Pancoska P, et al. p53 has a direct apoptogenic role at the mitochondria. Mol Cell 2003; 11:577-90.
25. Jiang P, Du WJ, Heese K, Wu M. The Bad Guy Cooperates with Good Cop p53: Bad is transcriptionally upregulated by p53 and forms a Bad/p53 complex at the mitochondria to induce apoptosis. Mol Cell Biol 2006; 26:9071-82.
26. Song G, Chen GG, Yun JP, Lai PB. Association of p53 with Bid induces cell death in response to etoposide treatment in hepatocellular carcinoma. Curr Cancer Drug Targets 2009; 9:871-80.
27. Sax JK, Fei P, Murphy ME, Bernhard E, Korsmeyer SJ, El-Deiry WS. BID regulation by p53 contributes to chemosensitivity. Nat Cell Biol 2002; 4:842-9.
28. Adams JM, Cory S. The Bcl-2 protein family: arbiters of cell survival. Science 1998; 281:1322-6.
29. Gross A, McDonnell JM, Korsmeyer SJ. BCL-2 family members and the mitochondria in apoptosis. Genes Dev 1999; 13:1899-911.
30. Pelicano H, Carney D, Huang P. ROS stress in cancer cells and therapeutic implications. Drug Resistance Updates 2004; 7:97-110.
31. Simon HU, Haj-Yehia A, Levi-Schaffer F. Role of reactive oxygen species (ROS) in apoptosis induction. Apoptosis 2000; 5:415-8.
32. Fruehauf JP, Meyskens FL Jr. Reactive oxygen species: A breath of life or death? Clin Cancer Res 2007; 13:789-94.
33. Ohkawa H, Ohishi N, Yagi K. Assay for lipid peroxides in animal tissues by thiobarbituric acid reaction. Anal Biochem 1979; 95:351-8.

The American Journal of Pathology, Vol. 179, No. 2, August 2011

DOI: 10.1016/j.ajpath.2011.04.026

Tumorigenesis and Neoplastic Progression

In Vivo and *in Vitro* Evidence That PPARγ Ligands Are Antagonists of Leptin Signaling in Breast Cancer

Stefania Catalano,* Loredana Mauro,† Daniela Bonofiglio,* Michele Pellegrino,† Hongyan Qi,* Pietro Rizza,† Donatella Vizza,* Gianluca Bossi,‡ and Sebastiano Andò†

From the Departments of Pharmaco-Biology, and Cell-Biology,† University of Calabria, Arcavacata; and the Regina Elena Cancer Institute,‡ Rome, Italy*

Obesity is a major risk factor for the development and progression of breast cancer. Leptin, a cytokine mainly produced by adipocytes, plays a crucial role in mammary carcinogenesis and is elevated in hyperinsulinemia and insulin resistance. The antidiabetic thiazolidinediones inhibit leptin gene expression through ligand activation of the peroxisome proliferator-activated receptor-γ (PPARγ) and exert antiproliferative and apoptotic effects on breast carcinoma. In this study, we investigated the ability of PPARγ ligands to counteract leptin stimulatory effects on breast cancer growth in either *in vivo* or *in vitro* models. The results show that activation of PPARγ prevented the development of leptin-induced MCF-7 tumor xenografts and inhibited the increased cell-cell aggregation and proliferation observed on leptin exposure. PPARγ ligands abrogated the leptin-induced up-regulation of leptin gene expression and its receptors in breast cancer. PPARγ-mediated repression of leptin gene involved the recruitment of nuclear receptor corepressor protein and silencing mediator of retinoid and thyroid hormone receptors corepressors on the glucocorticoid responsive element site in the leptin gene expression regulatory region in the presence of glucocorticoid receptor and PPARγ. In addition, PPARγ ligands inhibited leptin signaling mediated by MAPK/STAT3/Akt phosphorylation and counteracted leptin stimulatory effect on estrogen signaling. These findings suggest that PPARγ ligands may have potential therapeutic benefits in the treatment of breast cancer. ***(Am J Pathol 2011, 179:1030–1040; DOI: 10.1016/j.ajpath.2011.04.026)***

Several epidemiologic findings have established that obesity is a risk factor for human breast cancer.[1] Indeed, increased body weight has been associated with shorter disease-free and overall survival in patients with breast cancer.[2]

Leptin, a peptide hormone mainly secreted by adipocytes, is a pleiotropic molecule that regulates food intake, hematopoiesis, inflammation, immunity, cell differentiation, and proliferation.[3] More recently, leptin has been found to be involved in neoplastic processes, particularly in mammary tumorigenesis.[4,5] Specifically, *in vitro* and *in vivo* studies have shown that leptin stimulates tumor growth, cell survival, and transformation[4,6,7] and amplifies estrogen signaling, contributing to hormone-dependent breast cancer growth and progression.[6,8]

Peroxisome proliferator-activated receptor-γ (PPARγ) is a member of the nuclear receptor family of ligand-dependent transcription factors, which is best known for its differentiating effects on adipocytes and insulin-mediated metabolic functions.[9] Activators of PPARγ include thiazolidinediones, a new class of antidiabetic drugs, such as rosiglitazone (BRL), that rather than reducing hyperglycemia and hyperinsulinemia in insulin-resistant states[10] inhibit leptin expression and its signal transduction in different cell and animal models.[11–14] PPARγ is also involved in cell-cycle control, inflammation, atherosclerosis, apoptosis, and carcinogenesis.[15] The controversial role of PPARγ ligands in carcinogenesis has been reported, although the precise mechanisms responsible for differential effects (ie, proapoptotic versus proliferative) remain incompletely clarified. Some studies have demonstrated that activation of PPARγ increases tumor cell growth.[16–18] However, most published studies imply the inhibitory effects of PPARγ ligands on the tumor growth of several carcinomas, including breast cancer.[19,20] In the past few years, we have investigated different molecular mechanisms through which PPARγ

Supported by Associazione Italiana Ricerca Cancro grants IG 1482, IG 8804, and MFAG 6180, ex 60% Ministero Istruzione Università Ricerca.

Accepted for publication April 22, 2011.

S.C., L.M., and D.B. contributed equally to this work.

Supplemental material for this article can be found at *http://ajp.amjpathol.org* or at doi: 10.1016/j.ajpath.2011.04.026.

Address reprint requests to Sebastiano Andò, Ph.D., Department Cell-Biology, University of Calabria, Arcavacata (CS) 87036, Italy. E-mail: sebastiano.ando@unical.it.

may induce antiproliferative effects, cell-cycle arrest, and apoptosis in human MCF-7 breast cancer cells.[21–23]

In this study, we evaluated the ability of PPARγ ligands to counteract leptin stimulatory effects on breast cancer growth in either *in vivo* or *in vitro* models. These results have shown that PPARγ ligands reverse the enhanced expression of leptin gene (*Lep*; formerly *Ob*) and its receptor (*Lepr*; formerly *ObR*), inhibiting the downstream signaling pathways induced by leptin. Transcriptional repression of *Ob* gene by PPARγ seems to be consequent to the recruitment of nuclear receptor corepressor protein (NCoR) and silencing mediator of retinoid and thyroid hormone receptors (SMRT) corepressors involving the participation of glucocorticoid receptor (GR).

Materials and Methods

Plasmids

The pHEGO plasmid, encoding the full length of estrogen receptor α (ERα) cDNA, and the reporter plasmid XETL, a construct containing an estrogen-responsive element, were gifts from Dr. Didier Picard (University of Geneva, Geneva, Switzerland). The plasmids containing the full-length human leptin promoter or its deletions were gifts from Dr. Marc Reitman (NIH, Bethesda, MD).

Site-Directed Mutagenesis

The leptin promoter plasmid-bearing glucocorticoid responsive element–mutated site (p1775 GRE mut) was created by site-directed mutagenesis using a QuikChange kit (Stratagene, La Jolla, CA) and as template the human leptin promoter p1775. The mutagenic primers were 5′-CCAGGCTGTAGTGCAATG*GTCTtgcCTTGGC*TCACTGCAACC-3′ and 5′-GGTTGCAGTGAG*CCAAGgcaAGAC*CATTGCACTACAGCCTGG-3′. Mutations are shown as italic and lower case letters. The constructed reporter vector was confirmed by DNA sequencing.

Cell Cultures

MCF-7, BT-20, and CHO cells were obtained from the American Type Culture Collection (Manassas, VA), were maintained in Dulbecco's modified Eagle's medium/Ham's F-12 containing 5% fetal bovine serum (Sigma, Milan, Italy), and were cultured in serum-free medium for at least 24 hours before treatments. All the media were supplemented with 1% L-glutamine and 1% penicillin/streptomycin (Sigma).

In Vivo *Experiments*

Female 45-day-old athymic nude mice (*nu/nu Swiss*; Charles River Laboratories, Milan, Italy) were maintained in a sterile environment. At day 0, estradiol pellets (1.7 mg per pellet, 90-day release; Innovative Research of America, Sarasota, FL) were subcutaneously implanted into the intrascapular region of the mice. The next day, MCF-7 cells (5.0×10^6 cells per mouse) were inoculated subcutaneously in 0.1 mL of Matrigel (BD Biosciences, Bedford, MA). Leptin treatment was performed as previously described.[7] When the tumors reached ~0.2 cm^3 (ie, in 4 weeks), the animals received rosiglitazone (10 mg/kg/day) in drinking tap water (Avandia, GlaxoSmith Kline, Middlesex, UK) for 8 weeks. MCF-7 xenograft tumor growth was monitored twice a week by caliper measurements, and tumor volumes (in cubic centimeters) were estimated by the following formula: $TV = a \times (b^2)/2$, where *a* and *b* are tumor length and width, respectively, in centimeters. At week 12, blood samples were collected from the mice, and the animals were sacrificed following standard protocols; the tumors were dissected from the neighboring connective tissue, frozen in nitrogen, and stored at −80°C for further analyses. After blood centrifugation, plasma was collected and kept at −80°C for analyses. Plasma leptin concentration was measured using a commercially available mouse and rat leptin enzyme-linked immunosorbent assay kit (BioVendor, Heidelberg, Germany). All the procedures involving animals and their care were conducted in accordance with the institutional guidelines and regulations at the Laboratory of Molecular Oncogenesis, Regina Elena Cancer Institute, Rome, Italy.

Histologic Analysis

Tumors, livers, lungs, spleens, and kidneys were fixed in 4% formalin, sectioned at 5 μm, and stained with hematoxylin and eosin Y (Bio-Optica, Milan, Italy). The epithelial nature of the tumors was verified by immunostaining with mouse monoclonal antibody directed against human cytokeratin 18 (Santa Cruz Biotechnology, Milan, Italy), and nuclei were counterstained with hematoxylin. For negative controls, nonimmune serum replaced the primary antibody.

Three-Dimensional Spheroid Culture and Cell Growth Assays

For three-dimensional cultures, MCF-7 and BT-20 cells plated on 2% agar–coated plates were treated with 1000 ng/mL of leptin (Invitrogen, Carlsbad, CA) and/or 10 μmol/L BRL (Alexis, San Diego, CA) and 10 μmol/L 15-deoxy-Δ12,14-prostaglandin J2 (PGJ2) (Sigma). After 48 hours, three-dimensional cultures were photographed using a phase-contrast microscope (Olympus, Milan, Italy). The extent of aggregation and cell numbers were evaluated as reported.[7]

[^{3}H]Thymidine Incorporation Assays

MCF-7 and BT-20 cells were treated with leptin (1000 ng/mL) and/or BRL (10 μmol/L) and PGJ2 (10 μmol/L) for 48 hours and were pretreated for 2 hours with GW9662 (10 μmol/L; Sigma) or transfected with RNA interference (RNAi) for PPARγ where necessary. The assay was performed as previously reported.[6]

RT-PCR Assays

Total RNA was extracted using TRIzol reagent (Invitrogen). Reverse transcription was performed using a RETROscript kit (Ambion, Austin, TX). The cDNAs were amplified by PCR using the following primers: long isoform of ObR (ObRL): 5′-CGAGAAACGTTTCAGCATCT-3′ and 5′-CAAAAGCACACCACTCTCTC-3′; short isoform of ObR (ObRS): 5′-GAAGGAGTCGGAAAACCAAAG-3′ and 5′-CCACCATATGTTAACTCTCAG-3′; Ob: 5′-AGAGCCTTTGGATGACCAGAACAAGGTTCCCT-3′ and 5′-TTACGAGAGAACTAACTGGAGAGCGACCTTT-3′; cathepsin D: 5′-AACAACAGGGTGGGCTTC-3′ and 5′-ATGCACGAAACAGATCTGTGCT-3′; pS2 5′-TTCTATCCTAATACCATCGACG-3′ and 5′-TTTGAGTAGTCAAAGTCAGAGC-3′; cyclin D1: 5′-TCTAAGATGAAGGAGACCATC-3′ and 5′-GCGGTAGTAGGACAGGAAGTTGTT-3′; P450arom: 5′-CAAGGTTATTTTGATGCATGG-3′ and 5′-TTCTAAGGTTTGCGCATGA-3′; and 36B4: 5′-CTCAACATCTCCCCCTTCTC-3′ and 5′-CAAATCCCATATCCTCGT-3′.

The PCR was performed for 30 cycles for cathepsin D and cyclin D1; for 35 cycles for ObRL, ObRS, Ob, and P450arom; and for 15 cycles to amplify pS2 and 36B4 in the presence of 1 μL of first-strand cDNA, 1 μmol/L each primer, 0.5 mmol/L dNTP, and TaqDNA polymerase (2 U per tube) (Promega Corp, Madison, WI) in a final volume of 25 μL.

Western Blot Analysis and Immunoprecipitation Assays

The phosphorylated forms of MAPK, STAT3, Akt, and GR S211 were identified by Western blot analysis in 50 μg of whole lysate. The immunoblots were stripped and reprobed to determine total levels of MAPK, STAT3, Akt (Cell Signaling Technology, Milan, Italy), and GR (Santa Cruz Biotechnology). Immunoprecipitation was performed in 300 μg of nuclear extracts in the presence of appropriate antibodies (Santa Cruz Biotechnology). Proteins were resolved on 8% to 10% SDS-polyacrylamide gels, transferred to a nitrocellulose membrane, and probed with specific antibodies (Novus Biologicals, Milan, Italy). The antigen-antibody complex was detected by incubation of the membrane at room temperature with a peroxidase-coupled goat anti-mouse or anti-rabbit IgG and revealed using the ECL system (Amersham, Buckinghamshire, UK).

Transfection Assays

MCF-7 cells were transfected using the FuGENE 6 reagent (Roche Diagnostics, Mannheim, Germany) with the mixture containing 0.5 μg of luciferase-reporter plasmid and 5 ng of pRL-CMV. CHO cells were transfected with XETL (0.5 μg per well) in the presence of HEGO (0.2 μg per well). After 24 hours of transfection, treatments were added and cells were incubated for 24 hours. The firefly luciferase values of each sample were normalized by Renilla luciferase activity, and the data are reported in relative light units.

Electrophoretic Mobility Shift Assays

Nuclear extracts were prepared from MCF-7 cells as previously described.[24] The probe was generated by annealing single-stranded oligonucleotides labeled with [γ^{32}P]ATP and tyrosine polynucleotide kinase and then purified using Sephadex G-50 spin columns (Sigma). The DNA sequences used as probe or as cold competitors were as follows: GRE: 5′-ATGGTCTGATCTTGGCTCAC-3′ and 5′-GTGAGCCAAGATCAGACCAT-3′; CRE: 5′-CACCGACGTCATTTGCAGTTCC-3′ and 5′-CACCGACAGCTTTTGCAGTTCC-3′; and Sp1: 5′GAAAAACTCCGCCCTGGTAAAT-3′ and 5′-ATTTACCAGGCGCGGAGTTTTTC-3′. The protein-binding reactions were performed as reported.[7] The specificity of the binding was tested by adding to the mixture the reaction-specific antibodies anti-GR and anti-PPARγ. The entire reaction mixture was electrophoresed through a 6% polyacrylamide gel in 0.25x Tris-borate-EDTA for 3 hours at 150 V.

Chromatin Immunoprecipitation and Re–Chromatin Immunoprecipitation Assays

MCF-7 cells were cross-linked with 1% formaldehyde and sonicated. Supernatants were immunocleared with salmon sperm DNA/protein A agarose for 1 hour at 4°C. The precleared chromatin was immunoprecipitated with specific anti-GR (E-20), PPARγ (H-100), or anti-polymerase II (RNA-PolI H-224) antibodies (Santa Cruz Biotechnology) and were reimmunoprecipitated with anti-PPARγ, anti-NCoR (NB120-2781), or anti-SMRT (NB300-732) antibodies (Novus Biologicals).

Normal mouse serum IgG was used as negative control. Pellets were washed as reported, eluted with elution buffer (1% SDS, 0.1 mol/L $NaHCO_3$), and digested with proteinase K.[25] DNA was obtained by phenol/chloroform/isoamyl alcohol extractions and were precipitated with ethanol; 5 μL of each sample and input were used for real-time PCR with the primers flanking GRE sequence present in the leptin promoter region: 5′-GCCCAGGCTGTAGTGCAAT-3′ and 5′-TAGCCAGGTGTGGTGG-3′. PCR reactions were performed as reported.[26]

Immunocytochemical Staining

Cells were fixed in 4% paraformaldehyde, and hydrogen peroxide was used to inhibit endogenous peroxidase activity. Cells were incubated with 10% normal horse serum to block nonspecific binding sites. Immunocytochemical staining was performed using specific primary antibodies (Santa Cruz Biotechnology). A biotinylated universal antibody made in horse was applied as secondary antibody (Vector Laboratories, Burlingame, CA). Amplification of avidin-biotin–horseradish peroxidase complex was performed, and 3,3′-diaminobenzidine tetrachloride dihydrate was used as a detection system. In

control experiments (negative control), cells were processed, replacing the primary antibody with nonimmune rabbit IgG (Vector Laboratories).

RNAi

MCF-7 cells were transfected with 25-bp RNA duplex of validated RNAi-targeted human PPARγ mRNA sequence 5′-AGAAUAAUAAGGUGGAGAUGCAGGC-3′ or with a stealth RNAi-negative control low GC (Invitrogen) to a final concentration of 100 nmol/L using Lipofectamine 2000 (Invitrogen), as recommended by the manufacturer. After 5 hours, the transfection medium was changed with serum-free medium to avoid Lipofectamine 2000 toxicity, and then cells were exposed to treatments.

Statistical Analysis

Each data point represents the mean ± SE of at least three different experiments. Statistical analysis was performed using analysis of variance followed by Newman-Keuls testing to determine differences in means. Statistical comparisons for *in vivo* studies were made using the Wilcoxon-Mann-Whitney test. $P < 0.05$ was considered statistically significant.

Results

PPARγ Ligands Reverse Leptin-Induced Tumor Cell Growth in Vivo *and* in Vitro

First we explored the ability of BRL to inhibit leptin-induced breast tumor growth *in vivo*. To this aim, female nude mice, bearing into the intrascapular region of MCF-7 cell tumor xenografts, were treated with leptin and/or BRL. This administration was well tolerated because no change in body weight (see Supplemental Table S1 at *http://ajp.amjpathol.org*) or in food and water consumption was observed together with no evidence of reduced motor function. In addition, no significant difference in the mean weights or histologic features of the major organs (liver, lung, spleen, and kidney) after sacrifice was observed between vehicle-treated mice and those that received treatment, indicating a lack of toxic effects at the dose given.

Histologic examination of MCF-7 xenografts revealed that tumors were primarily composed of tumor epithelial cells (see Supplemental Figure S1 at *http://ajp.amjpathol.org*). Our results showed that leptin treatment induced tumor growth in mice, as we previously demonstrated,[7] whereas a significant reduction in tumor volume was observed in the animal group receiving leptin plus BRL (Figure 1A). At week 12, tumor sizes were markedly smaller in

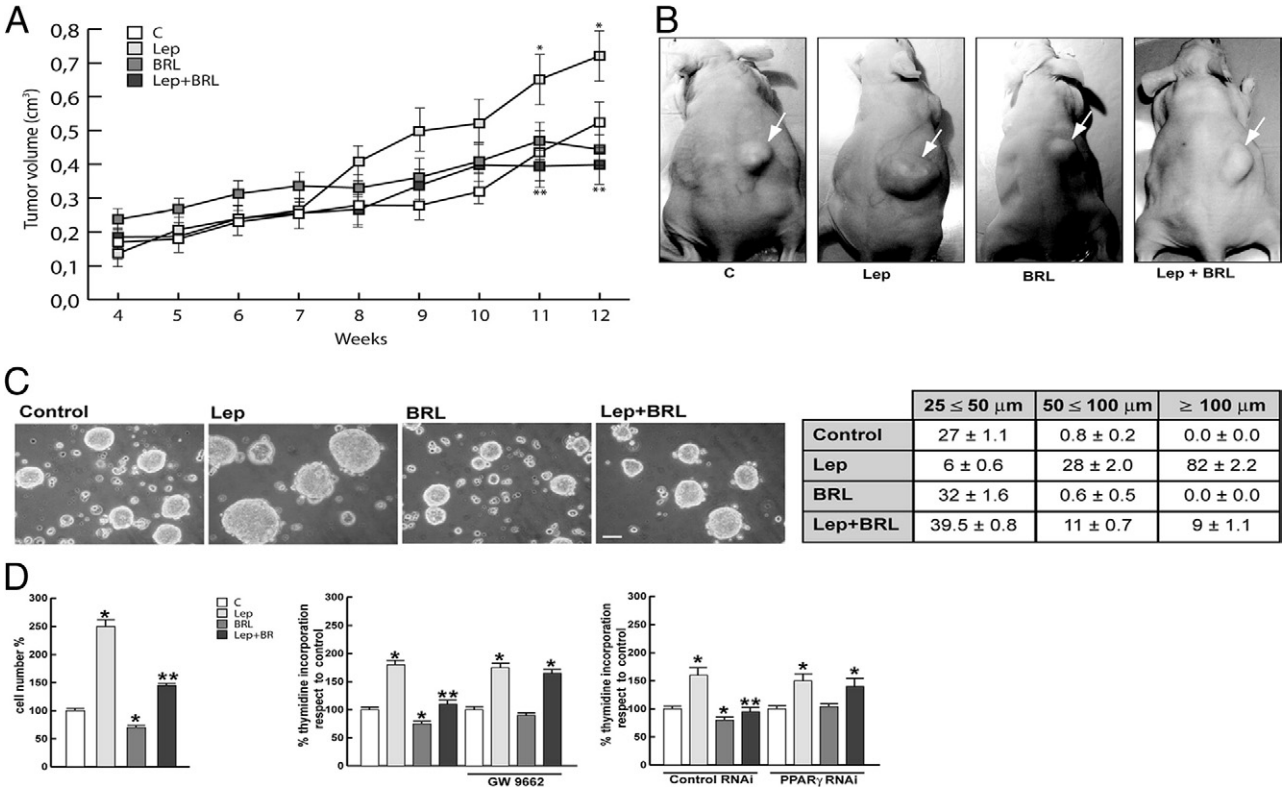

	25 ≤ 50 μm	50 ≤ 100 μm	≥ 100 μm
Control	27 ± 1.1	0.8 ± 0.2	0.0 ± 0.0
Lep	6 ± 0.6	28 ± 2.0	82 ± 2.2
BRL	32 ± 1.6	0.6 ± 0.5	0.0 ± 0.0
Lep+BRL	39.5 ± 0.8	11 ± 0.7	9 ± 1.1

Figure 1. BRL reverses leptin-induced tumor cell growth. **A:** Tumor volume from MCF-7 xenografts implanted with estradiol pellets in female nude mice at weeks 4 and 12. The animals were treated with 230 μg/kg/day leptin (Lep) ($n = 8$), 10 mg/kg/day BRL ($n = 8$), Lep and BRL ($n = 8$), or vehicle as control ($n = 8$). *$P < 0.05$, leptin-treated group versus control group; **$P < 0.05$, leptin plus BRL–treated group versus leptin-treated group. **B:** Representative images of experimental tumors at week 12 (**arrows**). **C:** MCF-7 three-dimensional cultures were untreated or treated as indicated for 48 hours (**top**). Scale bar = 50 μm. The extent of aggregation was scored by measuring the spheroid diameters. The values represent the sum of spheroids in 10 optical fields under ×10 magnification (**bottom**). **D:** Cell numbers obtained from three-dimensional spheroids and proliferation determined by [^{3}H]thymidine incorporation in MCF-7 cells transfected and treated as indicated for 48 hours. The results are mean ± SE of three experiments. *$P < 0.05$ versus untreated cells; **$P < 0.05$ versus leptin.

animals treated with leptin plus BRL than with leptin alone (Figure 1B). Mean ± SE plasma leptin levels measured at week 12 were significantly higher in leptin-treated mice (2.05 ± 0.087 ng/mL, $P < 0.01$) than in vehicle-treated mice (1.50 ± 0.05 ng/mL); in contrast, in BRL- (1.13 ± 0.06 ng/mL, $P < 0.01$) and BRL + leptin– (1.36 ± 0.078 ng/mL, $P < 0.01$) treated mice, leptin concentrations were decreased compared with those in the control and leptin groups.

We then performed three-dimensional MCF-7 cell cultures, which closely mimic some *in vivo* biologic features of tumors.[27] We showed that BRL treatment (10 μmol/L) inhibited the enhanced cell-cell adhesion induced by leptin (1000 ng/mL) exposure as evidenced by the extent of aggregation scored by measuring the spheroid diameters (Figure 1C). In three-dimensional cultures, BRL decreased cell growth compared with untreated cells and reversed the enhanced leptin cell numbers. Moreover, the effects of leptin and/or BRL on cell proliferation were assessed by [^{3}H]-thymidine DNA incorporation assay. Leptin stimulated the growth of MCF-7 cells; this effect was completely inhibited by BRL treatment (Figure 1D). Similar results were also obtained using the natural PPARγ ligand PGJ2 (see Supplemental Figure S2 at *http://ajp.amjpathol.org*). The inhibitory effects exerted by PPARγ ligands were no longer noticeable in the presence of the specific PPARγ antagonist GW9662 as well as PPARγ RNAi, demonstrating direct involvement of this nuclear receptor in antagonizing leptin-induced tumor growth (Figure 1D).

In ERα-negative breast cancer cells BT-20, BRL also reversed leptin-induced cell aggregation and cell proliferation (see Supplemental Figure S3 at *http://ajp.amjpathol.org*), suggesting that BRL effects are estrogen independent.

BRL Represses Activation of Leptin Signal Transduction Pathways in MCF-7 Cells

Leptin exerts its biologic function through binding to its receptors, which mediate a downstream signal by activating multiple signaling pathways.[28,29] We examined the effects of BRL on ObRs and its transduction pathways. Stimulation of MCF-7 cells with leptin resulted in an increase in ObRL and ObRS, which was reversed by treatment with BRL (Figure 2A). Similar results were also obtained in MCF-7 xenografts (Figure 2B). In addition, as expected, leptin significantly induced phosphorylation of MAPK/STAT3/Akt in *in vivo* and *in vitro* models, whereas treatment with BRL completely abrogated the leptin activation of these signaling pathways (Figure 2, C and D). All these data suggest that the inhibitory action of BRL on leptin-induced tumor growth, cell adhesion, and proliferation involves, at least in part, the ability of PPARγ ligand to modulate ObR expression and antagonize its signaling pathways.

Modulation of Ob Expression and Its Transcriptional Activity by BRL

To assess whether BRL can also affect Ob, we performed RT-PCR in MCF-7 cells. We showed in *in vitro* and *in vivo*

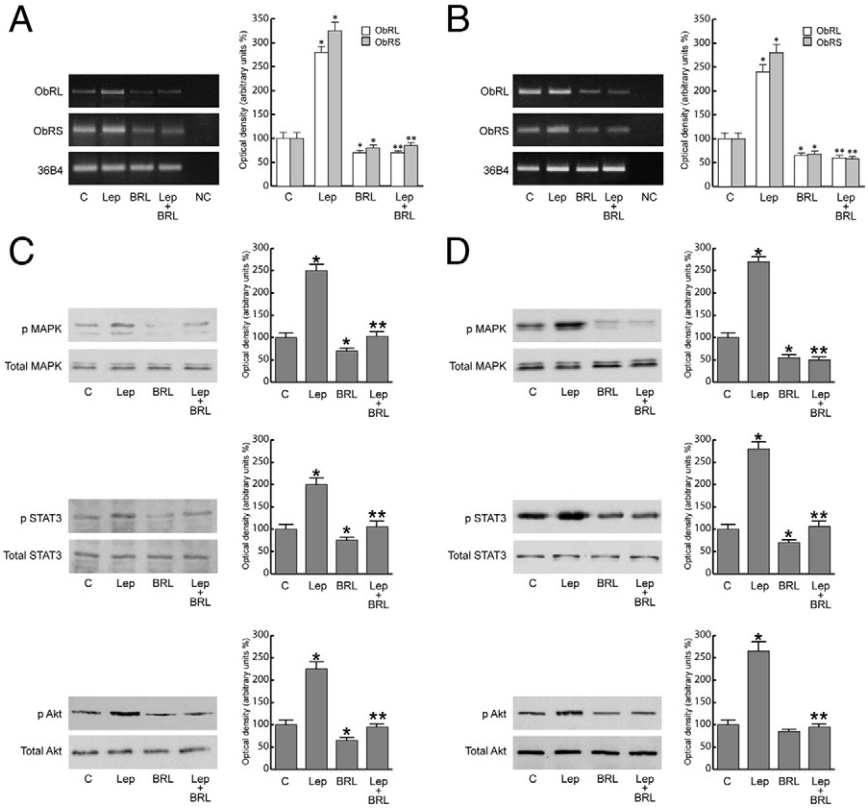

Figure 2. BRL represses leptin (Lep) signaling in MCF-7 cells and xenografts. RT-PCR of ObRL and ObRS mRNA from MCF-7 cells stimulated for 48 hours (**A**) and from xenografts (**B**). 36B4 mRNA levels were determined as control. NC indicates RNA sample without the addition of reverse transcriptase (negative control). Representative Western blot analysis on protein extracts from MCF-7 cells stimulated for 15 minutes (**C**) and xenografts excised from control and treated mice (**D**) showing MAPK/STAT3/Akt activation. The immunoblots were stripped and reprobed with total MAPK/STAT3/Akt as loading control. The results are mean ± SE of three separate experiments in which the band intensities were evaluated in terms of optical density arbitrary units and expressed as the percentage of the control assumed to be 100%. $^*P < 0.05$ versus untreated cells; $^{**}P < 0.05$ versus leptin.

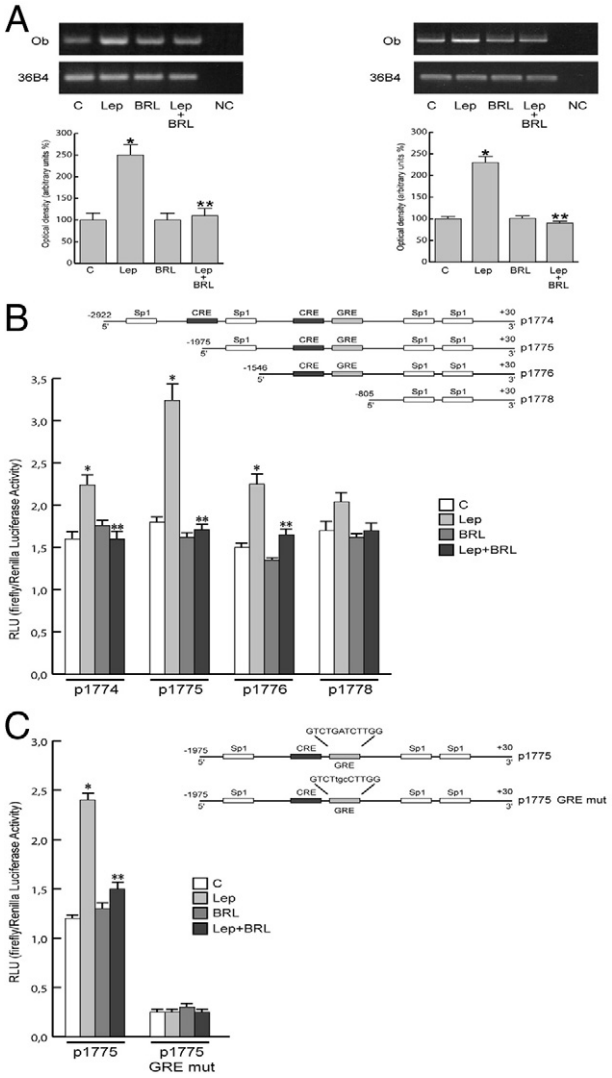

Figure 3. BRL negatively regulates leptin (Lep)-induced Ob expression and its transcriptional activity. **A:** RT-PCR of Ob was performed in MCF-7 cells stimulated for 48 hours (**left panel**) and in xenografts (**right panel**). 36B4 mRNA levels were determined as control. NC, negative control. MCF-7 cells were transiently transfected with luciferase plasmids containing the human leptin promoter (p1774) or its deletions (p1775, p1776, and p1778) (**B**) or p1775 mutated in the GRE site (p1775 GRE mut) (**C**). Schematic maps of the human leptin promoter constructs are included. Cells were untreated or treated with leptin (1000 ng/mL) and/or 10 μmol/L BRL for 24 hours. RLU indicates relative light units. The results are mean ± SE of three separate experiments. $^{*}P < 0.05$ versus untreated cells; $^{**}P < 0.05$ versus leptin.

models that leptin increased Ob mRNA, whereas BRL reversed this effect (Figure 3A). This latter result led us to ascertain whether PPARγ activation can modulate leptin transcriptional activity. To this aim, we transiently transfected MCF-7 cells with a plasmid containing leptin regulatory sequences p1774 (−2922/+30) and found that leptin induced luciferase activity, which was inhibited by treatment with BRL (Figure 3B). The Ob promoter contains multiple transcription factor binding motifs, including CRE and Sp1 sites and one GRE site (Figure 3B). To determine which *cis*-acting elements in the Ob promoter can mediate the previously mentioned effects, Ob promoter–deleted constructs −1975/+30 (p1775), −1546/+30 (p1776), and −805/+30 (p1778) were tested. In transfection experiments performed using p1775 and p1776 constructs, the responsiveness to leptin was still observed, and BRL still inhibited the increase induced by leptin. In contrast, in the presence of the construct p1778, no up-regulatory effects were noticeable on leptin exposure (Figure 3B). Thus, we performed site-directed mutagenesis assays to evaluate which site was responsible for leptin-induced Ob promoter activation. We found that only the mutation of the GRE site was involved in mediating the stimulatory effect of leptin (Figure 3C), addressing that the up-regulatory effect of leptin requires the GRE motif. To explore whether leptin affects the activity of GR, we tested its nuclear translocation and phosphorylation at S211. Leptin induced GR nuclear localization with a concomitant increase in S211 phosphorylated GR levels, which were significantly reduced by pretreatment with the MAPK inhibitor PD98059 and the JAK/STAT inhibitor AG490. In contrast, the PI3K inhibitor LY294002 did not affect GR phosphorylation status (Figure 4).

PPARγ Reverses Leptin-Induced Effects on Ob Promoter at the GRE Site through Corepressor Recruitment

To provide insight into the molecular mechanism by which the GRE motif modulates Ob promoter activity, we performed electrophoretic mobility shift assay experi-

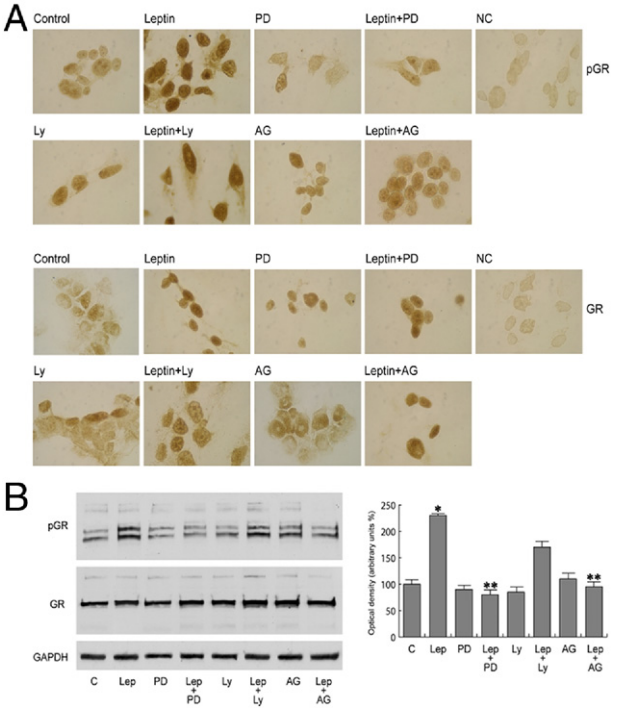

Figure 4. Leptin (Lep) induces nuclear translocation of GR and its phosphorylation (pGR). MCF-7 cells were untreated or treated with 1000 ng/mL of leptin for 15 minutes or pretreated with 10 μmol/L PD98059 (PD), AG490 (AG), or LY294002 (LY). **A:** Immunostaining of pGR and GR. No immunodetection was observed replacing the antibodies with horse serum [negative control (NC)]. **B:** Representative Western blotting for pGR on S211 and GR. Glyceraldehyde-3-phosphate dehydrogenase (GAPDH) was used as loading control. The results are mean ± SE of three separate experiments for pGR in which the band intensities were evaluated in terms of optical density arbitrary units and expressed as the percentage of the control assumed to be 100%. $^{*}P < 0.05$ versus untreated cells; $^{**}P < 0.05$ versus leptin.

ments using as a probe the GRE sequence present in the Ob regulatory region. We observed the formation of a complex in nuclear extracts from MCF-7 cells (Figure 5A, lane 1), which was abrogated by 100-fold molar excess of unlabeled probe (Figure 5A, lane 2), demonstrating the specificity of the DNA binding complex. This inhibition was no longer observed using a mutated oligodeoxyribonucleotide as competitor (Figure 5A, lane 3). Leptin and BRL induced a slight increase in the specific band (Figure 5A, lanes 4 and 5), whereas an enhanced DNA binding complex was observed on combined treatments (Figure 5A, lane 6). The inclusion of anti-GR and anti-PPARγ antibodies in the reactions attenuated the specific bands, suggesting the presence of both proteins in the complex (Figure 5A, lanes 7 and 8). Note that the leptin-induced increase in the DNA binding complex was no longer noticeable when a synthetic oligodeoxyribonucleotide corresponding to the CRE or Sp1 motif was used as probe (data not shown).

The interaction of GR and PPARγ receptors with the Ob promoter was further elucidated by chromatin immunoprecipitation (ChIP) assays. Using anti-GR or anti-PPARγ antibodies, protein-chromatin complexes were immunoprecipitated from MCF-7 cells treated for 1 hour with leptin and/or BRL. Real-time PCR was used to determine the recruitment of GR and PPARγ to the Ob region containing the GRE site. The results indicate that GR was constitutively bound to the Ob promoter in untreated cells and that this recruitment was increased on leptin or BRL exposure and to a higher extent after combined treatments. Immunoprecipitation with anti-PPARγ antibody showed enhanced recruitment of this nuclear receptor to the Ob promoter in the presence of BRL and BRL plus leptin treatments. Similar results were also obtained by GR/PPARγ Re-ChIP assay. We revealed after leptin treatment an enhanced association of RNA Pol II that was drastically reduced by leptin plus BRL exposure (Figure 5B).

To assess whether the decrease in Ob promoter transcriptional activity might be caused by the cooperative interaction between GR/PPARγ and negative transcriptional regulators, we investigated the involvement of NCoR and SMRT, which interact with and function as negative coregulators of GR and PPARγ.[30–33] A coimmunoprecipitation assay was performed on nuclear protein fractions from MCF-7 cells treated with leptin and/or BRL. The formation of GR and PPARγ complex was clearly detected in all the conditions tested. Moreover, GR/NCoR and GR/SMRT complexes were slightly revealed in untreated cells, but this association was enhanced by combined treatments. No interaction of the orphan nuclear receptor DAX-1, a corepressor for GR,[34] was observed under the same experimental conditions (Figure 5D). Similar results were obtained in MCF-7 cells immmunoprecipitated with anti-PPARγ antibody (Figure 5D).

Re-ChIP assays demonstrated increased NCoR and SMRT occupancy of the GRE-containing region of the Ob promoter after BRL exposure and particularly on combined treatments (Figure 5C). In the presence of a MAPK inhibitor able to interfere with GR phosphorylation, the

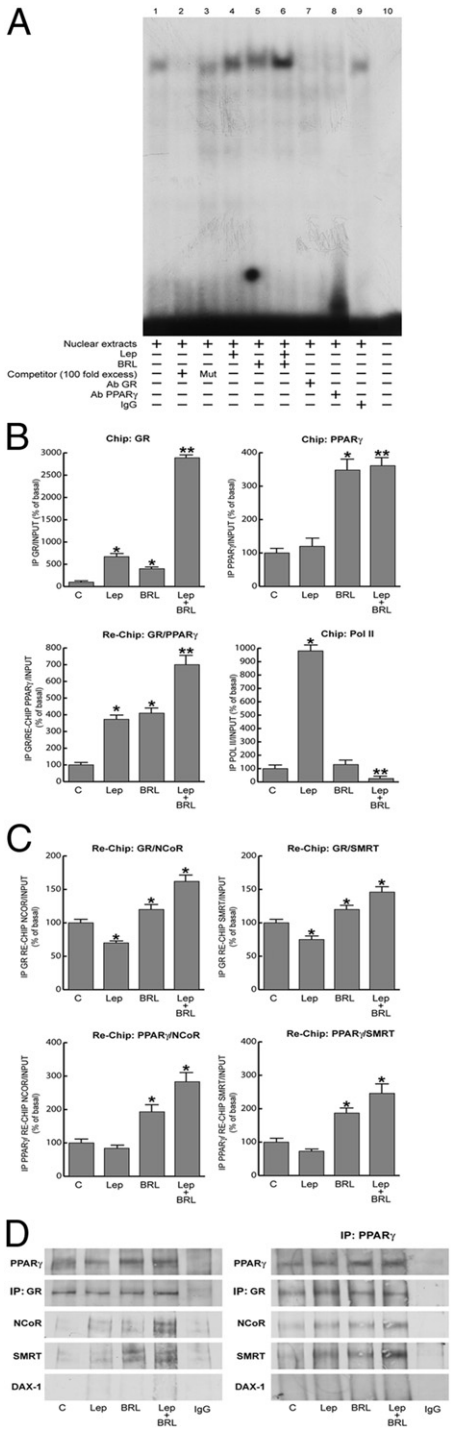

Figure 5. PPARγ binds and recruits corepressors to the GRE site in the Ob promoter. **A:** Nuclear extracts from MCF-7 cells were incubated with GRE probe (**lane 1**). A 100-fold molar excess of unlabeled (**lane 2**) and mutated (Mut) (**lane 3**) probe was added. MCF-7 nuclear extracts treated with 1000 ng/mL of leptin and/or 10 μmol/L BRL for 6 hours (**lanes 4, 5,** and **6**). Anti-GR (**lane 7**), anti-PPARγ (**lane 8**) antibodies (Abs) or IgG (**lane 9**) were added to the mixture. **Lane 10** shows probe alone. **B:** ChIP with the anti-GR, anti-PPARγ, and anti-Pol II antibodies. ChIP with the anti-GR antibody was re-ChIP with anti-PPARγ antibody. **C:** ChIP with the anti-GR or anti-PPARγ antibodies was re-ChIP with either anti-NCoR or anti-SMRT antibodies. The leptin (Lep) promoter sequence including the GRE site was detected by real-time-PCR with specific primers (see *Materials and Methods*). The results are mean ± SE of three separate experiments expressed as the percentage of control. $^{*}P < 0.05$ versus untreated cells; $^{**}P < 0.05$ versus leptin. **D:** MCF-7 cells were treated with 1000 ng/mL of leptin and/or 10 μmol/L BRL for 48 hours. Immunoprecipitation was performed using anti-GR (**left panel**) or anti-PPARγ (**right panel**) antibodies and then blotted with anti-PPARγ, GR, NCoR, SMRT, or DAX-1 antibodies.

recruitment of corepressors to the Ob promoter was markedly reduced (data not shown).

BRL Abrogates Leptin-Activated Estrogen Signaling in MCF-7 Cells

We previously demonstrated that leptin can transactivate ERα and enhance aromatase gene expression in breast cancer cells.[6,8] Thus, because PPARγ ligands interfere with leptin signaling, we investigated the ability of BRL to reverse the leptin effects on estrogen signaling.

In MCF-7 cells transiently transfected with XETL construct, we observed that BRL significantly inhibited ERE-dependent transactivation induced by leptin (Figure 6A), and this effect was reversed by pretreatment with GW9662 (data not shown). Similar results were reproduced in ER-negative CHO cells in which ERα was ectopically expressed (Figure 6A).

These data correlated well with the ability of BRL to abrogate in *in vivo* and *in vitro* models the up-regulatory effects of leptin on mRNA expression levels of the classic estrogen genes cathepsin, pS2, and cyclin D1 (Figure 6B). Besides, in MCF-7 cell cultures and in xenografts, BRL reversed the increase in aromatase expression induced by leptin (Figure 6C). These results indicate that treatment with BRL counteracting leptin action on estrogen signaling may contribute to reduce breast cancer cell growth and progression.

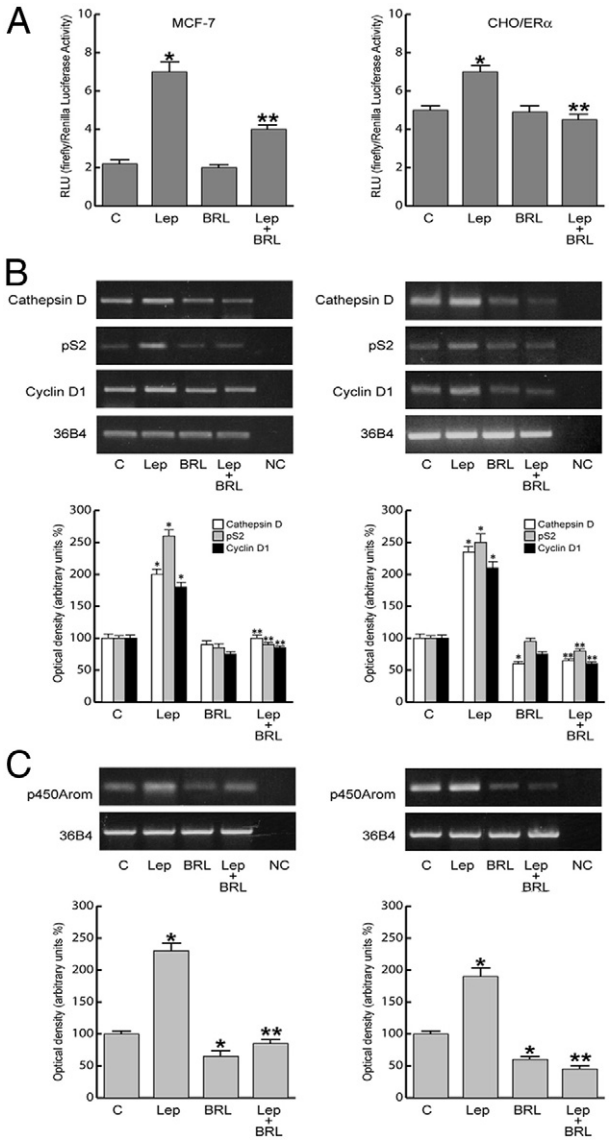

Figure 6. BRL antagonizes estrogen signaling induced by leptin (Lep). **A:** MCF-7 cells were transfected with XETL plasmid. CHO cells were cotransfected with XETL and HEGO plasmids (CHO/ERα). RLU, relative light unit. The results are mean ± SE of three independent experiments performed in triplicate. $^{*}P < 0.05$ versus untreated cells; $^{**}P < 0.05$ versus leptin. Cathepsin D, pS2, and cyclin D1 (**B**) and aromatase (**C**) mRNA expression in MCF-7 cells treated for 48 hours as indicated (**left panel**) and in xenografts (**right panel**). 36B4 mRNA levels were determined as control. NC indicates negative control. The results are mean ± SE of three separate experiments in which the band intensities were evaluated in terms of optical density arbitrary units and expressed as the percentage of the control assumed to be 100%. $^{*}P < 0.05$ versus untreated cells; $^{**}P < 0.05$ versus leptin.

Discussion

For the first time, we demonstrate that activation of PPARγ reverses leptin-mediated promotion of breast tumor growth either *in vivo* in MCF-7 xenografts implanted in female nude mice or *in vitro* in MCF-7 three-dimensional and monolayer cultured breast cancer cells.

Elevated leptin levels strongly correlate with obesity, hyperinsulinemia, and insulin resistance, conditions found in most patients with diabetes mellitus.[35] PPARγ ligands, thiazolidinediones, able to reduce hyperglycemia and hyperinsulinemia in insulin-resistant states, also down-regulate gene expression of pluripotent hormone leptin *in vivo* and *in vitro*.[11,12] Besides, previous observations have reported that PPARγ agonists inhibited leptin-induced proliferation in hepatic stellate cells by suppression of MAPK activation[14] and abolished leptin-directed migration of endothelial cells through Akt.[13] Thus, regulation and function of leptin and PPARγ are possibly interrelated and relevant in obese patients in whom metabolic changes are major contributors to the development of breast carcinoma.

The present results show that the PPARγ ligand BRL prevents the development of leptin-induced MCF-7 tumor xenografts in the presence of significantly lower plasma leptin levels and inhibits the increased cell-cell aggregation and proliferation observed on leptin exposure. The *in vitro* results were also reproduced in ERα-negative breast cancer cells BT20, addressing how the mechanism by which PPARγ activation affects breast tumor cell growth is not tightly related to estrogen dependency. Moreover BRL down-regulates the enhanced expression of ObRs induced by leptin and inhibits MAPK/Akt/STAT3 leptin downstream signaling pathways. These results are in agreement with data obtained in other cell models showing that PPARγ ligands suppress ObR mRNA and its promoter activity and block leptin signaling.[13,14,36]

It emerges from recent studies that leptin and estrogen systems are involved in a functional cross talk. For example, leptin has been shown to directly transactivate ERα[8] and positively modulate aromatase activity.[6]

We demonstrated in MCF-7 cells that BRL, interfering with leptin signaling, could reverse the effects of leptin on estrogen signal specifically, counteracting ERα activation and its classic target genes in either *in vitro* or *in vivo* models.

Furthermore, the leptin-enhanced aromatase expression was completely abrogated by BRL treatment as we observed in xenografts and in monolayer cultures of MCF-7 cells, underlying the ability of this new class of oral antidiabetic drugs to inhibit local estrogen production, which represents an important factor of tumor microenvironment able to maintain tumor growth and progression.

Activated PPARγ is also known to inhibit the expression of Ob in adipose tissue.[12,37] Herein, we demonstrated in MCF-7 cells the ability of BRL to reverse the leptin-induced Ob mRNA expression and its transcriptional activity, showing how PPARγ negatively interferes in the short autocrine loop maintained by leptin on *Ob* gene in breast cancer cells. The human Ob promoter contains multiple transcription regulatory elements, including several CRE, Sp1, and NFkB sites and one GRE site.[38] Functional experiments using Ob promoter–deleted constructs and site-directed mutagenesis studies have shown that the up-regulatory effects induced by leptin on Ob promoter activity completely reversed by BRL occurred through the GRE site. These latter results fit well with the evidence that leptin induced GR translocation and phosphorylation at S211, which was inhibited by MAPK and JAK/STAT inhibitors. It was reported that the S211 phosphorylated GR strongly correlates with GR transcriptional activation; indeed, inhibition of this phosphorylation is associated with decreased nuclear retention of GR and inhibited gene transcription.[39]

The important role of GRE in regulating Ob promoter activity was also shown by electrophoretic mobility shift assays. We found in nuclear extracts from MCF-7 cells treated with leptin plus BRL a strong increase in the GRE-DNA binding that was immunodepleted by anti-GR and anti-PPARγ antibodies, suggesting the presence of the two proteins in the complex.

The physiologic relevance of GRE in the Ob promoter *in vivo* is pointed out by ChIP analysis showing that the GR/PPARγ occupancy of the GRE-containing promoter region, induced by leptin plus BRL treatment, is concomitant with a decrease in RNA Pol II recruitment and a reduction in Ob transcriptional activity.

It is known that members of the nuclear hormone receptor superfamily, including GR and PPARγ, once activated, can interact physically and modulate target gene transcription.[40,41] We have shown a strong association of PPARγ with GR in the nuclear fraction of untreated MCF-7 cells that was further potentiated by leptin plus BRL treatments.

PPARγ and GR can regulate transcription by several distinct mechanisms, and their functions, as shown for other corticosteroid receptors, seem to depend not only on ligand binding, which is known to regulate receptor conformation, but also on the context of the gene and associated promoter factors that contribute to create a gene-specific topography, achieving specific profiles of gene expression.[42,43] Our proposed model for PPARγ-mediated repression of the *Ob* gene involves its interaction with GR and recruitment of the corepressors NCoR and SMRT, which share the same molecular architecture, interact with many of the same transcription factors, and assemble into similar corepressor complexes.[44] NCoR and SMRT are recruited by PPARγ and GR to regulate the transcription of different genes.[45,46] Overexpression of NCoR and SMRT represses PPARγ-mediated gene transcription in certain cell types,[47] and recently, increasing evidence suggests that these two corepressors modulate adipogenesis most likely via their ability to repress PPARγ action.[48,49] The present results suggest that in MCF-7 cells on BRL and to a higher extent leptin plus BRL stimulation, NCoR and SMRT are recruited on the GRE site of the Ob promoter together with GR and PPARγ.

A hypothetical model of the possible mechanism through which PPARγ activation may modulate leptin expression and function in reducing breast cancer growth is shown in Figure 7. Leptin, through JAK/STAT/MAPK activation, may phosphorylate GR and induce its transactivation, resulting in an increase in leptin promoter activity. This up-regulatory effect on Ob is counteracted by PPARγ through the recruitment of corepressors NCoR and SMRT on the GRE site of the Ob regulatory region in the presence of GR and PPARγ.

Moreover, activation of PPARγ also decreases ObRs, inhibits its transductional pathways, and negatively interferes with estrogen signaling through the down-regulation of aromatase gene expression and the inhibition of ERα transactivation.

In conclusion, these data suggest that PPARγ ligands rather than ameliorate metabolic parameters may represent pharmacologic tools to be exploited in the novel therapeutic adjuvant strategies for breast cancer treatment.

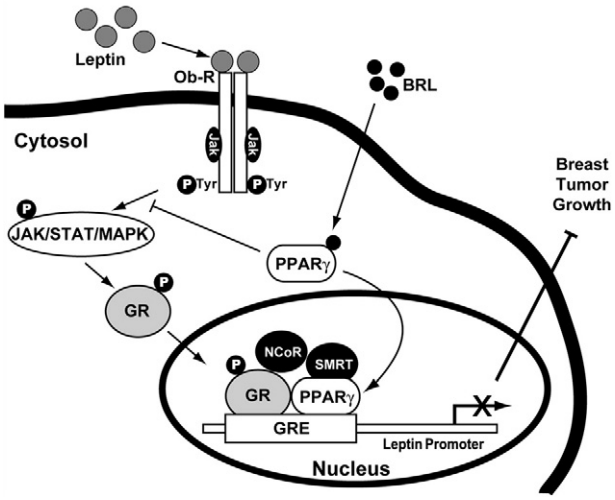

Figure 7. Molecular mechanism through which PPARγ counteracts leptin expression and function in breast cancer. Leptin, through JAK/STAT/MAPK activation, increases GR phosphorylation (pGR) and its nuclear translocation. pGR transactivates leptin promoter by binding to GRE motif. In the presence of BRL, PPARγ binds to GRE and, through the formation of GR/PPARγ complex, allows the recruitment of NCoR and SMRT corepressors, thus inhibiting Ob transcription and reducing breast tumor growth.

Acknowledgments

We thank Dr. Vittoria Rago for her support in immunostaining assays and Dr. Pasquale Cicirelli for his technical assistance.

References

1. Calle EE, Kaaks R: Overweight, obesity and cancer: epidemiological evidence and proposed mechanisms. Nat Rev Cancer 2004, 4:579–591
2. Chlebowski RT, Aiello E, McTiernan A: Weight loss in breast cancer patient management. J Clin Oncol 2002, 20:1128–1143
3. Ahima RS, Flier JS: Leptin. Annu Rev Physiol 20006, 2:413–437
4. Garofalo C, Surmacz E: Leptin and cancer. J Cell Physiol 2006, 207:12–22
5. Vona-Davis L, Rose DP: Adipokines as endocrine, paracrine and autocrine factors in breast cancer risk and progression. Endocr Relat Cancer 2007, 14:189–206
6. Catalano S, Marsico S, Giordano C, Mauro L, Rizza P, Panno ML, Andò S: Leptin enhances, via AP-1, expression of aromatase in the MCF-7 cell line. J Biol Chem 2003, 278:28668–28676
7. Mauro L, Catalano S, Bossi G, Pellegrino M, Barone I, Morales S, Giordano C, Bartella V, Casaburi I, Andò S: Evidences that leptin up-regulates E-cadherin expression in breast cancer: effects on tumor growth and progression. Cancer Res 2007, 67:3412–3421
8. Catalano S, Mauro L, Marsico S, Giordano C, Rizza P, Rago V, Montanaro D, Maggiolini M, Panno ML, Andó S: Leptin induces, via ERK1/ERK2 signal, functional activation of estrogen receptor α in MCF-7 cells. J Biol Chem 2004, 279:19908–19915
9. Desvergne B, Wahli W: Peroxisome proliferator-activated receptors: nuclear control of metabolism. Endocr Rev 1999, 20:649–688
10. Quinn CE, Hamilton PK, Lockhart CJ, McVeigh GE: Thiazolidinediones: effects on insulin resistance and the cardiovascular system. Br J Pharmacol 2008, 153:636–645
11. De Vos P, Lefebvre AM, Miller SG, Guerre-Millo M, Wong K, Saladin R, Hamann LG, Staels B, Briggs MR, Auwerx J: Thiazolidinediones repress ob gene expression in rodents via activation of peroxisome proliferator-activated receptor γ. J Clin Invest 1996, 98:1004–1009
12. Rieusset J, Auwerx J, Vidal H: Regulation of gene expression by activation of the peroxisome proliferator-activated receptor γ with rosiglitazone (BRL 49653) in human adipocytes. Biochem Biophys Res Commun 1999, 265:265–271
13. Goetze S, Bungenstock A, Czupalla C, Eilers F, Stawowy P, Kintscher U, Spencer-Hänsch C, Graf K, Nürnberg B, Law RE, Fleck E, Gräfe M: Leptin induces endothelial cell migration through Akt, which is inhibited by PPARγ-ligands. Hypertension 2002, 40:748–754
14. Lee JI, Paik YH, Lee KS, Lee JW, Kim YS, Jeong S, Kwon KS, Lee DH, Kim HG, Shin YW, Kim MA: A peroxisome-proliferator activated receptor-γ ligand could regulate the expression of leptin receptor on human hepatic stellate cells. Histochem Cell Biol 2007, 127:495–502
15. Rocchi S, Auwerx J: Peroxisome proliferator-activated receptor-γ: a versatile metabolic regulator. Ann Med 1999, 31:342–351
16. Lefebvre AM, Chen I, Desreumaux P, Najib J, Fruchart JC, Geboes K, Briggs M, Heyman R, Auwerx J: Activation of the peroxisome proliferators-activated receptor γ promotes the development of colon tumors in C57BL/6J-APC^{Min}/+ mice. Nat Med 1998, 4:1053–1057
17. Saez E, Tontonoz P, Nelson MC, Alvarez JG, Ming UT, Baird SM, Thomazy VA, Evans RM: Activators of the nuclear receptors PPARγ enhance colon polyp formation. Nat Med 1998, 4:1058–1061
18. Chinery R, Coffey RJ, Graves-Deal R, Kirkland SC, Sanchez SC, Zackert WE, Oates JA, Morrow JD: Prostaglandin J2 and 15-deoxy-Δ 12,14-prostaglandin J2 induce proliferation of cyclooxygenase-depleted colorectal cancer cells. Cancer Res 1999, 59:2739–2746
19. Elstner E, Müller C, Koshizuka K, Williamson EA, Park D, Asou H, Shintaku P, Said JW, Heber D, Koeffler HP: Ligands for peroxisome proliferator-activated receptorγ and retinoic acid receptor inhibit growth and induce apoptosis of human breast cancer cells in vitro and in BNX mice. Proc Natl Acad Sci U S A 1998, 95:8806–8811
20. Grommes C, Landreth GE, Heneka MT: Antineoplastic effects of peroxisome proliferator-activated receptor γ agonists. Lancet Oncol 2004, 5:419–429
21. Bonofiglio D, Gabriele S, Aquila S, Catalano S, Gentile M, Middea E, Giordano F, Andò S: Estrogen receptor α binds to peroxisome proliferator-activated receptor (PPAR) response element and negatively interferes with PPAR γ signalling in breast cancer cells. Clin Cancer Res 2005, 11:6139–6147
22. Bonofiglio D, Aquila S, Catalano S, Gabriele S, Belmonte M, Middea E, Qi H, Morelli C, Gentile M, Maggiolini M, Andò S: Peroxisome proliferator-activated receptor γ activates p53 gene promoter binding to the nuclear factor-κB sequence in human MCF7 breast cancer cells. Mol Endocrinol 2006, 20:3083–3092
23. Bonofiglio D, Gabriele S, Aquila S, Qi H, Belmonte M, Catalano S, Andò S: Peroxisome proliferator-activated receptor γ activates fas ligand gene promoter inducing apoptosis in human breast cancer cells. Breast Cancer Res Treat 2009, 113:423–434
24. Andrews NC, Faller DV: A rapid micropreparation technique for extraction of DNA-binding proteins from limiting numbers of mammalian cells. Nucleic Acids Res 1991, 19:2499
25. Morelli C, Garofalo C, Sisci D, del Rincon S, Cascio S, Tu X, Vecchione A, Sauter ER, Miller WH Jr, Surmacz E: Nuclear insulin receptor substrate 1 interacts with estrogen receptor α at ERE promoters. Oncogene 2004, 23:7517–7526
26. Sirianni R, Chimento A, Malivindi R, Mazzitelli I, Andò S, Pezzi V: Insulin-like growth factor-I, regulating aromatase expression through steroidogenic factor 1, supports estrogen-dependent tumor Leydig cell proliferation. Cancer Res 2007, 67:8368–8377
27. Mauro L, Surmacz E: IGF-I receptor, cell-cell adhesion, tumor development and progression. J Mol Histol 2004, 35:247–253
28. Sweeney G: Leptin signalling. Cell Signal 2002, 14:655–663
29. Ahima RS, Osei SY: Leptin signaling. Physiol Behav 2004, 81:223–241
30. Cohen RN: Nuclear receptor corepressors and PPARγ. Nucl Recept Signal 2006, 4:e003
31. Ricote M, Glass CK: PPARs and molecular mechanisms of transrepression. Biochim Biophys Acta 2007, 1771:926–935
32. van der Laan S, Meijer OC: Pharmacology of glucocorticoids: beyond receptors. Eur J Pharmacol 2008, 585:483–491
33. Ronacher K, Hadley K, Avenant C, Stubsrud E, Simons SS Jr, Louw A, Hapgood JP: Ligand-selective transactivation and transrepression via the glucocorticoid receptor: role of cofactor interaction. Mol Cell Endocrinol 2009, 299:219–231
34. Zhou J, Oakley RH, Cidlowski JA: DAX-1 (dosage-sensitive sex reversal-adrenal hypoplasia congenita critical region on the X-chromosome, gene 1) selectively inhibits transactivation but not transrepression mediated by the glucocorticoid receptor in a LXXLL-dependent manner. Mol Endocrinol 2008, 22:1521–1534
35. Zimmet P, Boyko EJ, Collier GR, de Courten M: Etiology of the metabolic syndrome: potential role of insulin resistance, leptin resistance, and other players. Ann N Y Acad Sci 1999, 892:25–44
36. Tang Y, Zheng S, Chen A: Curcumin eliminates leptin's effects on hepatic stellate cell activation via interrupting leptin signaling. Endocrinology 2009, 150:3011–3020
37. Kallen CB, Lazar MA: Antidiabetic thiazolidinediones inhibit leptin (ob) gene expression in 3T3-L1 adipocytes. Proc Natl Acad Sci U S A 1996, 93:5793–5796
38. Gong DW, Bi S, Pratley RE, Weintraub BD: Genomic structure and promoter analysis of the human obese gene. J Biol Chem 1996, 271:3971–3974
39. Chen W, Dang T, Blind RD, Wang Z, Cavasotto CN, Hittelman AB, Rogatsky I, Logan SK, Garabedian MJ: : Glucocorticoid receptor phosphorylation differentially affects target gene expression. Mol Endocrinol 2008, 22:1754–1766
40. Ialenti A, Grassia G, Di Meglio P, Maffia P, Di Rosa M, Ianaro A: Mechanism of the anti-inflammatory effect of thiazolidinediones: relationship with the glucocorticoid pathway. Mol Pharmacol 2005, 67:1620–1628
41. Nie M, Corbett L, Knox AJ, Pang L: Differential regulation of chemokine expression by peroxisome proliferator-activated receptor γ agonists: interactions with glucocorticoids and β2-agonists. J Biol Chem 2005, 280:2550–2561
42. Hall JM, Couse JF, Korach KS: The multifaceted mechanisms of estradiol and estrogen receptor signaling. J Biol Chem 2001, 276: 36869–36872
43. Katzenellenbogen BS, Katzenellenbogen JA: Biomedicine: defining the "S" in SERMs. Science 2002, 295:2380–2381
44. Ghisletti S, Huang W, Jepsen K, Benner C, Hardiman G, Rosenfeld MG, Glass CK: Cooperative NCoR/SMRT interactions establish a

corepressor-based strategy for integration of inflammatory and anti-inflammatory signaling pathways. Genes Dev 2009, 23:681–693
45. Gurnell M, Wentworth JM, Agostini M, Adams M, Collingwood TN, Provenzano C, Browne PO, Rajanayagam O, Burris TP, Schwabe JW, Lazar MA, Chatterjee VK: A dominant-negative peroxisome proliferator-activated receptor γ (PPARγ) mutant is a constitutive repressor and inhibits PPARγ-mediated adipogenesis. J Biol Chem 2000, 275:5754–5759
46. Wang Q, Blackford JA Jr, Song LN, Huang Y, Cho S, Simons SS Jr: Equilibrium interactions of corepressors and coactivators with agonist and antagonist complexes of glucocorticoid receptors. Mol Endocrinol 2004, 18:1376–1395
47. Krogsdam AM, Nielsen CA, Neve S, Holst D, Helledie T, Thomsen B, Bendixen C, Mandrup S, Kristiansen K: Nuclear receptor corepressor-dependent repression of peroxisome-proliferator-activated receptor delta-mediated transactivation. Biochem J 2002, 363:157–165
48. Powell E, Kuhn P, Xu W: Nuclear receptor cofactors in PPARγ-mediated adipogenesis and adipocyte energy metabolism. PPAR Res 2007, 2007:53843
49. Samarasinghe SP, Sutanto MM, Danos AM, Johnson DN, Brady MJ, Cohen RN: Altering PPARγ ligand selectivity impairs adipogenesis by thiazolidinediones but not hormonal inducers. Obesity (Silver Spring) 2009, 17:965–972

Oncogene (2011) 1–12

www.nature.com/onc

ORIGINAL ARTICLE

Farnesoid X receptor inhibits tamoxifen-resistant MCF-7 breast cancer cell growth through downregulation of HER2 expression

C Giordano[1,5], S Catalano[1,2,5], S Panza[2], D Vizza[2], I Barone[1,3], D Bonofiglio[1,2], L Gelsomino[2], P Rizza[3], SAW Fuqua[4] and S Andò[1,3]

[1]*Centro Sanitario, University of Calabria, Arcavacata di Rende, Italy;* [2]*Department of Pharmaco-Biology, University of Calabria, Arcavacata di Rende, Italy;* [3]*Department of Cellular Biology, University of Calabria, Arcavacata di Rende, Italy and* [4]*Lester and Sue Smith Breast Center and Department of Molecular and Cellular Biology, Baylor College of Medicine, One Baylor Plaza, Houston, TX, USA*

Tamoxifen (Tam) treatment is a first-line endocrine therapy for estrogen receptor-α-positive breast cancer patients. Unfortunately, resistance frequently occurs and is often related with overexpression of the membrane tyrosine kinase receptor HER2. This is the rationale behind combined treatments with endocrine therapy and novel inhibitors that reduce HER2 expression and signaling and thus inhibit Tam-resistant breast cancer cell growth. In this study, we show that activation of farnesoid X receptor (FXR), by the primary bile acid chenodeoxycholic acid (CDCA) or the synthetic agonist GW4064, inhibited growth of Tam-resistant breast cancer cells (termed MCF-7 TR1), which was used as an *in vitro* model of acquired Tam resistance. Our results demonstrate that CDCA treatment significantly reduced both anchorage-dependent and anchorage-independent epidermal growth factor (EGF)-induced growth in MCF-7 TR1 cells. Furthermore, results from western blot analysis and real-time reverse transcription–PCR revealed that CDCA treatment reduced HER2 expression and inhibited EGF-mediated HER2 and p42/44 mitogen-activated protein kinase (MAPK) phosphorylation in these Tam-resistant breast cancer cells. Transient transfection experiments, using a vector containing the human HER2 promoter region, showed that CDCA treatment downregulated basal HER2 promoter activity. This occurred through an inhibition of nuclear factor-κB transcription factor binding to its specific responsive element located in the HER2 promoter region as revealed by mutagenesis studies, electrophoretic mobility shift assay and chromatin immunoprecipitation analysis. Collectively, these data suggest that FXR ligand-dependent activity, blocking HER2/MAPK signaling, may overcome anti-estrogen resistance in human breast cancer cells and could represent a new therapeutic tool to treat breast cancer patients that develop resistance.

Correspondence: Professor S Andò, Department of Cell Biology and Faculty of Pharmacy, Nutritional and Health Sciences, University of Calabria, Via P. Bucci, Arcavacata di Rende (CS) 87036, Italy.
E-mail: sebastiano.ando@unical.it
[5]These authors contributed equally to this work.
Received 15 November 2010; revised 8 March 2011; accepted 15 March 2011

Oncogene advance online publication, 18 April 2011; doi:10.1038/onc.2011.124

Keywords: FXR; breast cancer; tamoxifen resistance; HER2; NF-κB

Introduction

Administration of the selective estrogen receptor (ER) modulator tamoxifen (Tam), to block ERα activity, is still a first-line endocrine therapy for the management of all stages of ERα-positive breast cancer (Fisher *et al.*, 1998; Gradishar, 2004). Unfortunately, not all patients who have ERα-positive tumors respond to Tam (*de novo* resistance), and a large number of patients who do respond will eventually develop disease progression or recurrence while on therapy (acquired resistance), limiting the efficacy of the treatment.

Multiple mechanisms are responsible for the development of endocrine resistance. Among these are the loss of ERα expression or function (Encarnacion *et al.*, 1993), alterations in the balance of regulatory cofactors, increased oncogenic kinase signaling (Blume-Jensen and Hunter, 2001), and altered expression of growth factor signaling pathways (Arpino *et al.*, 2004; Schiff *et al.*, 2004; Sabnis *et al.*, 2005; Staka *et al.*, 2005). For instance, several preclinical and clinical studies suggest that both *de novo* and acquired resistance to Tam in breast cancers can be associated with elevated levels of the membrane tyrosine kinase HER2 (c-ErbB2, Her2/neu) (Chung *et al.*, 2002; Meng *et al.*, 2004; Shou *et al.*, 2004; Gutierrez *et al.*, 2005).

The *HER2* gene codes for a 185 kDa receptor, a member of the epidermal growth factor receptor (EGFR) family of transmembrane tyrosine kinases, which also includes HER3 and HER4, mainly involved in signal transduction pathways that regulate cell growth and differentiation. This receptor has no ligand of its own, but is activated by hetero-oligomerization with other ligand-activated receptors (Yarden, 2001). The *HER2* gene is amplified and/or overexpressed in 20–25% of ERα-positive breast cancers (Slamon *et al.*, 1989), and

clinical observations indicate that tumors with high levels of HER2 have poor outcome when treated with Tam (Osborne *et al*., 2003; Kirkegaard *et al*., 2007).

The mechanisms by which HER2 overexpression mediates Tam resistance result from an intimate cross-talk between ERα and growth factor receptors kinase cascades, such as Ras/mitogen-activated protein kinase (MAPK) signaling, that in turn can promote growth and progression in breast cancer cells, negating the inhibitory effects of Tam on nuclear ERα activity (Arpino *et al*., 2008). HER2 overexpression is not attributed solely to amplification of the *HER2* gene copy number, but can also occur from a single-copy gene due to deregulation events at the transcriptional level (Hurst, 2001).

Thus, an analysis of new mechanisms controlling HER2/neu receptor gene expression could be important to enhance strategies to reverse Tam resistance in breast cancer patients.

Farnesoid X receptor (FXR), a member of the nuclear receptor superfamily of ligand-dependent transcription factors, is mainly expressed in the liver and the gastrointestinal tract, where it regulates expression of genes involved in bile acids, cholesterol and triglyceride metabolism (Forman *et al*., 1995; Makishima *et al*., 1999; Parks *et al*., 1999). Recently, this receptor was also detected in different non-enterohepatic compartments, including breast cancer tissue and breast cancer cell lines (Bishop-Bailey, 2004; Swales *et al*., 2006; Journe *et al*., 2008; Catalano *et al*., 2010). For instance, FXR activation inhibits breast cancer cell proliferation and negatively regulates aromatase activity reducing local estrogen production (Swales *et al*., 2006), whereas other authors have reported that FXR activation stimulates MCF-7 cell proliferation but only in steroid-free medium (Journe *et al*., 2008). However, the functions of FXR in breast cancer tissue are still not completely understood, and there are no data regarding its role in the endocrine-resistant breast cancer phenotype. Thus, we have investigated whether activated FXR may modulate the growth of human MCF-7 Tam-resistant breast cancer cells, a model that was developed to mimic *in vitro* the occurrence of acquired Tam resistance.

Here, we demonstrate that a specific FXR ligand chenodeoxycholic acid (CDCA) or its synthetic agonist GW4064 inhibited Tam-resistant breast cancer cell proliferation and EGF-induced growth, by reducing expression of the HER2 receptor. This occurs through an FXR-mediated inhibition of nuclear factor (NF)-κB binding on the human HER2 promoter region.

Results

FXR expression in Tam-resistant breast cancer cells

Acquired resistance to Tam has been associated with elevated levels of the membrane tyrosine kinase HER2 (Knowlden *et al*., 2003; Nicholson *et al*., 2004; Gutierrez *et al*., 2005). In agreement with these reports, we found a marked increase in the levels of total HER2 protein content in Tam-resistant MCF-7 TR1 compared with MCF-7 cells, whereas no differences were seen in the expression of EGFR and ERα (Figure 1a). We therefore evaluated anchorage-independent growth of MCF-7 and MCF-7 TR1 cells after treatment with herceptin, a humanized monoclonal antibody directed against the extracellular domain of HER2, in the presence or not of EGF. Herceptin had no effect on MCF-7 growth, whereas significantly inhibited anchorage-independent growth of MCF-7 TR1 cells in basal conditions as well as upon EGF treatment (Figure 1b). These data confirm that the HER2 overexpression found in the MCF-7 TR1 cells renders them more sensitive to the inhibitory effect of this selective HER2-targeted agent.

Next, we evaluated the expression of FXR in MCF-7 and MCF-7 TR1 cells. Our results revealed the presence of FXR mRNA (Figure 1c, upper panel) and protein (Figure 1c, lower panel) in both MCF-7 and MCF-7 TR1 cells. To assess the ability of FXR to be transactivated by CDCA, we transiently transfected cells with an FXR-responsive reporter gene (*FXRE-IR1*) followed by treatment with increasing doses of CDCA. The specificity of the system was tested by co-transfecting the cells with a dominant negative FXR (FXR-DN) plasmid. As shown in Figure 1d, CDCA treatment induced a dose-dependent FXR activation in both cell lines and expression of the FXR-DN completely abrogated the CDCA-induced transactivation.

FXR activation inhibits Tam-resistant breast cancer cell growth

We examined, by MTT growth assays, the effects of increasing doses of CDCA and GW4064. Treatment with both ligands reduced cell proliferation in a dose-dependent manner in MCF-7 and MCF-7 TR1 cells, whereas had no effects on normal breast epithelial cells MCF-10A (Figures 2a and b). Similar results in growth inhibition were also obtained in another Tam-resistant breast cancer cell line termed MCF-7 TR2 (Supplementary Figures 2a and b). It is worth noting that the inhibitory effects exerted by FXR ligands on cell proliferation were significant at lower dose in MCF-7 TR1 cells compared with MCF-7 cells, as evidenced by half-maximal inhibitory concentration (IC_{50}) values (Table 1). The antiproliferative effects exerted by CDCA were completely reversed in the presence of a FXR-DN plasmid, supporting the specific involvement of the FXR (Figure 2c).

Next, we tested the effects of CDCA in the presence of Tam on cell growth (Figure 2d). As expected, with anti-estrogen treatment, cell viability was significantly reduced in MCF-7 cells, whereas MCF-7 TR1 cells growth was unaffected, confirming the Tam-resistant phenotype. Interestingly, combined treatment with CDCA and Tam reduced growth of MCF-7 TR1 cells compared with treatment with Tam alone, but showed no additive effects in MCF-7 cells (Figure 2d). The ability of CDCA and Tam to inhibit Tam-resistant growth was also confirmed using anchorage-independent growth assays (Figure 2e). These results suggest that FXR activation can interfere with the cellular

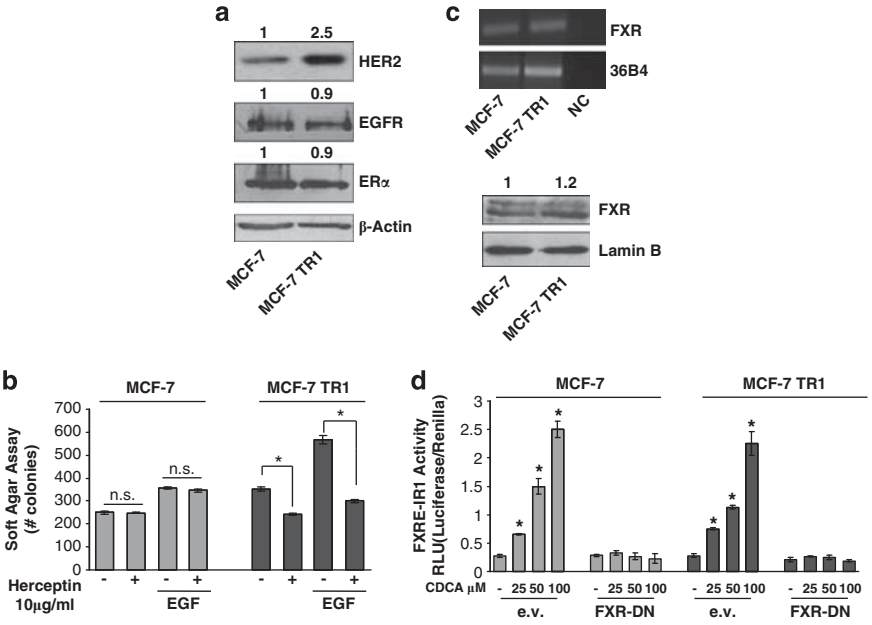

Figure 1 FXR expression and activation in MCF-7 and MCF-7 TR1 cells. (**a**) Western blot analysis of HER2, EGFR, ERα in total protein extracts from MCF-7 and MCF-7 TR1 cells; β-Actin was used as loading control. (**b**) Soft-agar growth assay in MCF-7 and MCF-7 TR1 cells plated in 0.35% agarose and treated with EGF 100 ng/ml in the presence or absence of herceptin (10 μg/ml). After 14 days of growth, colonies >50 μm diameter were counted. n.s., nonsignificant; $*P<0.05$ compared with vehicle or EGF. (**c**) Total RNA was extracted from MCF-7 and MCF-7 TR1 cells, reverse transcribed and cDNA was subjected to PCR using primers specific for FXR or 36B4 (upper panel). NC: negative control, RNA sample without the addition of reverse transcriptase. Nuclear proteins were extracted from MCF-7 and MCF-7 TR1 and then western blotting analysis was performed using anti-FXR antibody. Lamin B was used as loading control (lower panel). (**d**) MCF-7 and MCF-7 TR1 cells were transiently transfected with a FXR-responsive reporter gene (*FXRE-IR1*), with either empty vector (e.v.) or FXR-DN expression plasmid. After transfection, cells were treated for 24 h with vehicle (−) or increasing doses of CDCA (25–50–100 μM) and then luciferase activity was measured. Results represent the mean ± s.d. of three different experiments each performed in triplicate. $*P<0.05$ compared with vehicle. Numbers on top of the blots represent the average fold change versus control of MCF-7 cells normalized for β-Actin or Lamin B.

mechanisms by which MCF-7 TR1 cells escape antihormonal treatments.

CDCA reduces HER2 expression and signaling in MCF-7 TR1 cells

To understand the mechanisms associated with CDCA-mediated inhibition of Tam-resistant growth in breast cancer cells, we evaluated the possible role of FXR ligands in modulating HER2 expression. As shown in Figure 3a, treatment with CDCA downregulated HER2 protein expression in both cell lines, but with higher reduction seen in MCF-7 TR1 cells. Similar results were also observed after treatment with GW4064 (data not shown). A reduction in HER2 levels was also found upon CDCA treatment in MCF-7 TR2 cells (Supplementary Figure 2c). No differences were found in EGFR expression upon CDCA treatment (Supplementary Figure 3), confirming that activated FXR specifically target HER2 expression in breast cancer cells. In the presence of an FXR-DN the HER2 downregulation was completely abrogated, confirming FXR involvement in CDCA-induced effects on HER2 (Figure 3b). Next, we questioned whether these HER2-decreased levels could modify the responsiveness of breast cancer cells after growth factor stimulation. Thus, we investigated the effects of short-term stimulation with EGF, in the presence of CDCA treatment, on phosphorylation levels of HER2 and MAPK, the main downstream effectors of the growth factor signaling. EGF treatment increased phosphorylation of both HER2 and MAPK, even though in higher extent in MCF-7 TR1 cells. However, pretreatment with CDCA reduced EGF-induced phosphorylation of HER2 in both cell lines and drastically prevented MAPK activation in MCF-7 TR1 cells (Figure 3c). In addition, data obtained from MTT (Figure 3d upper panel) as well as soft-agar (Figure 3d lower panel) growth assays revealed that CDCA treatment inhibited EGF-induced growth by 70% in anchorage-dependent and 50% in anchorage-independent assays in MCF-7 TR1 cells. CDCA was less effective in MCF-7 cells. These results well correlated with the downregulatory effect of CDCA on EGF-induced cyclin D1 expression, particularly in MCF-7 TR1 cells (Figure 3e).

Activated FXR inhibits the binding of NF-kB to HER2 promoter region

To explore whether HER2 downregulation relies on transcriptional mechanisms, we evaluated, using real-time reverse transcription (RT)–PCR, HER2 mRNA levels after treatment with CDCA for different times. Exposure to CDCA exhibited a time-dependent reduction in HER2 mRNA levels in both MCF-7 and MCF-7 TR1 cells (Figure 4a). Also, transcriptional activity of a

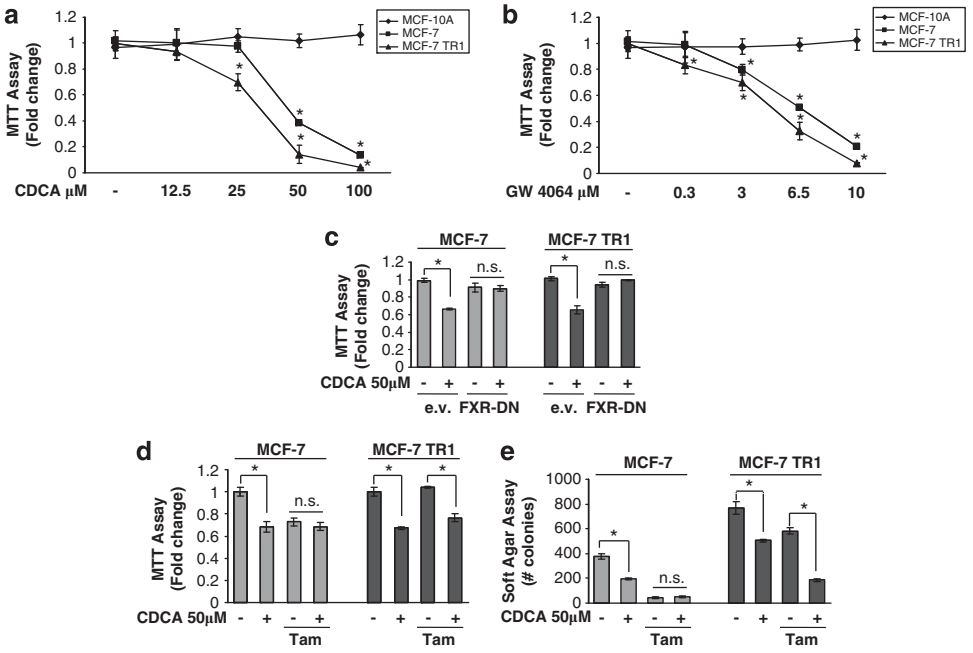

Figure 2 FXR ligands effects on breast cancer cells proliferation. MTT growth assays in MCF-10A, MCF-7 and MCF-7 TR1 cells treated with vehicle (−) or increasing doses of CDCA (12.5–25–50–100 μM) (**a**) or GW4064 (0.3–3–6.5–10 μM) (**b**) for 7 days. Cell proliferation is expressed as fold change ± s.d. relative to vehicle-treated cells and is representative of three different experiments each performed in triplicate. (**c**) MCF-7 and MCF-7 TR1 cells, transiently transfected with either empty vector (e.v.) or FXR-DN vector plasmids, were treated with vehicle (−) or CDCA 50 μM for 4 days before testing cell viability using MTT assay. Results are expressed as fold change ± s.d. relative to vehicle-treated cells and are representative of three different experiments each performed in triplicate. (**d**) MTT growth assay in MCF-7 and MCF-7 TR1 cells treated with vehicle (−) or CDCA 50 μM in the presence or not of Tam 1 μM for 4 days. Results are expressed as fold change ± s.d. relative to vehicle-treated cells and are representative of three different experiments each performed in triplicate. (**e**) Soft-agar growth assay in MCF-7 and MCF-7 TR1 cells plated in 0.35% agarose and treated as indicated above. After 14 days of growth, colonies >50 μm diameter were counted. n.s. (nonsignificant); $*P<0.05$ compared with vehicle or Tam.

Table 1 IC_{50} of CDCA and GW4064 for MCF-7 and MCF-7 TR1 cells on anchorage-dependent growth

Cell lines	*IC_{50} (μmol/l) CDCA*	*95% confidence interval*	P	*IC_{50} (μmol/l) GW4064*	*95% confidence interval*	P
MCF-7	46	42.2–50.1		6.04	5.44–6.70	
MCF-7 TR1	31	28.6–33.9	0.0001	4.47	3.6–5.49	0.008

Abbreviations: CDCA, chenodeoxycholic acid; IC_{50}, half-maximal inhibitory concentration.

reporter plasmid containing the human HER2 promoter region (pNeuLite) was significantly reduced with CDCA treatment in both cell lines (Figures 4c and d).

The human HER2 promoter contains multiple consensus sites for several transcription factors, including Sp1, as well as activator protein (AP)-1 and NF-κB, the well known effectors of FXR transrepression (He *et al*., 2006; Vavassori *et al*., 2009) (Figure 4b). To identify the region within the HER2 promoter responsible for CDCA inhibitory effects, HER2 promoter-deleted construct (−232 pNeuLite) activity was tested (Figure 4b). We observed that the responsiveness to CDCA was still maintained, suggesting that the region from −232 to +1 containing the NF-κB motif might be involved in transrepression mechanisms exerted by activated FXR (Figures 4c and d). Thus, we performed site-directed mutagenesis on the NF-κB domain (NF-κB Mut) within the HER2 promoter (Figure 4b). Mutation of this domain abrogated CDCA effects (Figures 4c and d). These latter results demonstrate that the integrity of NF-κB-binding site is necessary for FXR modulation of HER2 promoter activity in breast cancer cells.

The specific role of the NF-κB motif in the transcriptional regulation of HER2 by CDCA was investigated using electrophoretic mobility shift assays. We observed the formation of a complex in nuclear extracts from MCF-7 and MCF-7 TR1 cells using synthetic oligodeoxyribonucleotides corresponding to the NF-κB motif (Figure 5a, lanes 1 and 5), which was abrogated by incubation with 100-fold molar excess of unlabeled probe (Figure 5a, lanes 2 and 6), demonstrating the specificity of the DNA-binding complex. This inhibition was no longer observed when mutated oligodeoxyribonucleotide was used as competitor (Figure 5a, lanes 3 and 7). Interestingly, treatment with CDCA strongly decreased the DNA-binding protein complex compared with

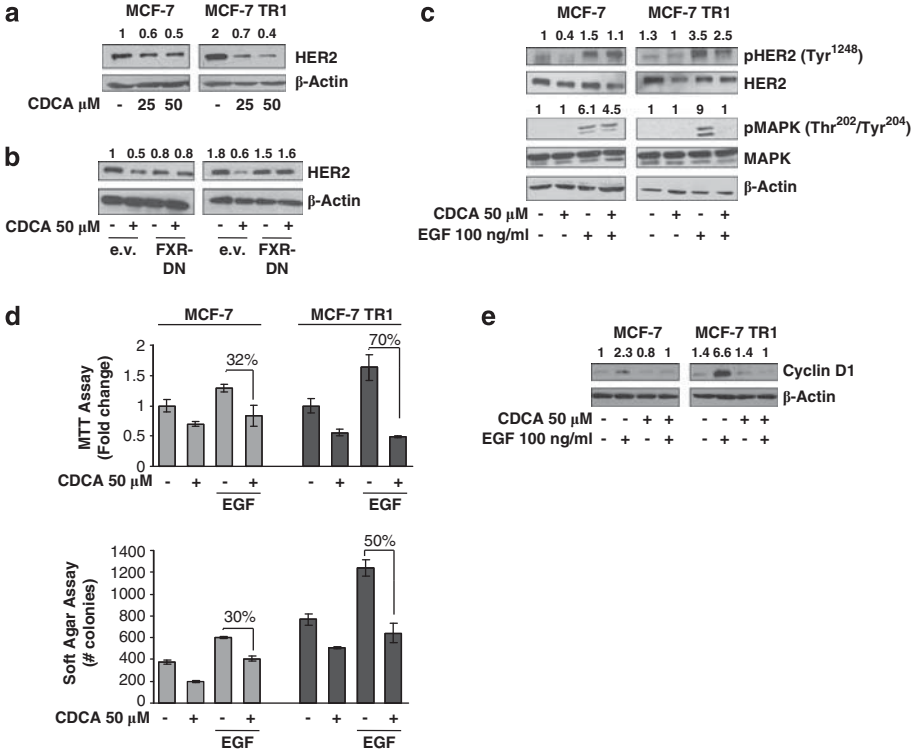

Figure 3 Effects of CDCA on HER2 expression and its transduction pathways in MCF-7 and MCF-7 TR1 cells. (**a**) MCF-7 and MCF-7 TR1 cells were treated for 24 h with vehicle (−) or CDCA 25 and 50 μM before lysis. Equal amounts of total cellular extract were analyzed for HER2 levels by western blotting. β-Actin was used as loading control. (**b**) Cells were transiently transfected with either empty vector (e.v.) or FXR-DN plasmids and then treated with vehicle (−) or CDCA 50 μM for 24 h and HER2 levels were evaluated by western blotting. β-Actin was used as loading control. (**c**) Immunoblot analysis showing phosphorylated HER2 (pHER2 Tyr[1248]) and MAPK (pMAPK Thr[202]/Tyr[204]), total HER2, total MAPK in MCF-7 and MCF-7 TR1 cells pretreated for 24 h with CDCA 50 μM and then treated for 10 min with EGF 100 ng/ml. β-Actin was used as loading control. (**d**) MTT growth assay (upper panel) and soft-agar assay (lower panel) in cells treated with CDCA 50 μM with or without EGF 100 ng/ml for 4 days and 14 days, respectively. The MTT assay results are expressed as fold change ± s.d. relative to vehicle-treated cells and are representative of three different experiments each performed in triplicate. The soft-agar assay values are represented as a mean of colonies number >50 μm diameter counted at the end of assay. Percentages of inhibition induced by CDCA versus EGF treatment alone are shown. (**e**) Cells were treated for 24 h with vehicle (−) or EGF 100 ng/ml in the presence or not of CDCA 50 μM before lysis and then cellular extracts were analyzed for cyclin D1 levels by western blot analysis. β-Actin was used as loading control. Numbers on top of the blots represent the average fold change versus control of MCF-7 cells normalized for β-Actin.

control samples (Figure 5a, lanes 4 and 8). The inclusion of an anti-NF-κB antibody in the reaction immunodepleted the specific band, confirming the presence of NF-κB in the complex (Figure 5b, lanes 3 and 9). Nonspecific IgG did not affect NF-κB complex formation (Figure 5b, lanes 4 and 10). Recombinant NF-κB protein revealed a complex migrating at the same level as that of nuclear extracts from cells (Figure 5a, lane 9; Figure 5b, lanes 5 and 11). Of note, the CDCA-induced reduction in the DNA-binding complex was no longer observed utilizing as probe synthetic oligodeoxyribonucleotides corresponding to the AP-1 and Sp1 motifs (Supplementary Figures 1a and b). To better define the role of FXR in the inhibition of NF-κB binding on HER2 promoter, a competition assay using recombinant NF-κB protein and increasing amounts of *in vitro*-translated FXR protein (1, 3 and 5 μl) was carried out. A dose-dependent reduction in the NF-κB complex was seen (Figure 5c, lanes 1–4), suggesting that physical interaction between these two transcription factors may inhibit the binding of NF-κB to human HER2 promoter region. To further test this possibility, we performed coimmunoprecipitation studies using nuclear protein fractions from MCF-7 and MCF-7TR1 cells treated with CDCA. As shown in Figure 6a, the formation of an FXR and NF-κB complex was detected in untreated cells, and this association was enhanced with FXR ligand treatment.

Moreover, to confirm the involvement of NF-κB in CDCA-mediated HER2-downregulation at the promoter level, ChIP assays were performed. Using specific antibodies against NF-κB and RNA-polymerase II, protein–chromatin complexes were immunoprecipitated from cells cultured with or without CDCA for 1 h. The resulting precipitated DNA was then quantified using real-time PCR with primers spanning the NF-κB-binding element in the HER2 promoter region. NF-κB recruitment was significantly decreased upon CDCA treatment in both cell lines (Figure 6b). This result was well correlated with a lower association of RNA-polymerase II to the HER2 regulatory region (Figure 6c).

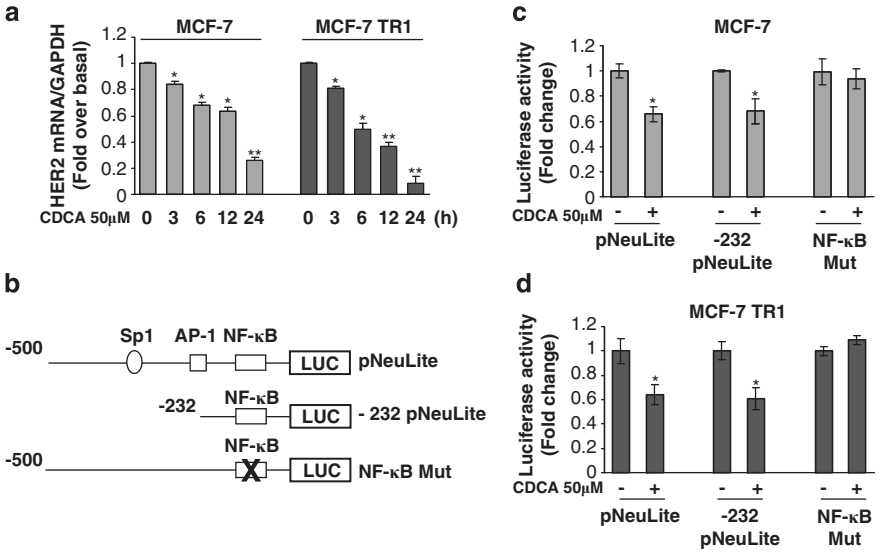

Figure 4 Effects of CDCA on human HER2 promoter activity. (**a**) mRNA HER2 content, evaluated by real-time RT–PCR, after treatment with vehicle or CDCA 50 μM, as indicated. Each sample was normalized to its GAPDH mRNA content. $*P<0.05$ and $**P<0.001$ compared with vehicle. (**b**) Schematic map of the human HER2/neu promoter region constructs used in this study. All of the promoter constructs contain the same 3′ boundary. The 5′ boundaries of the promoter fragments varied from −500 (pNeuLite) to −232 (−232 pNeuLite). A mutated NF-κB-binding site is present in NF-κB mut construct. HER2 transcriptional activity in MCF-7 (**c**) and MCF-7 TR1 (**d**) cells transfected with promoter constructs are shown. After transfection, cells were treated in the presence of vehicle (−) or CDCA 50 μM for 6 h. The values represent the means ± s.d. of three different experiments each performed in triplicate. $*P<0.05$ compared with vehicle.

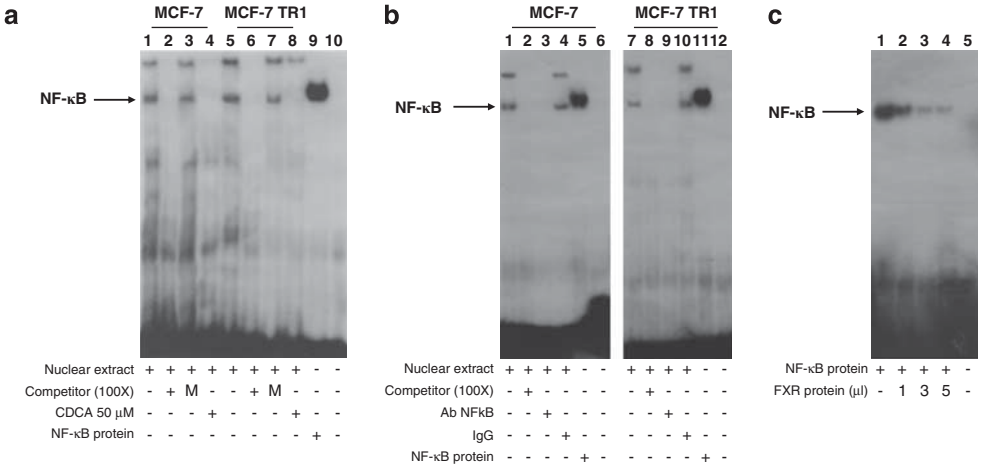

Figure 5 Electrophoretic mobility shift assay of the NF-κB-binding site in the HER2 promoter region. (**a**) Nuclear extracts from MCF-7 and MCF-7 TR1 cells were incubated with a double-stranded NF-κB specific sequence probe labeled with [γ^{32}P]ATP and subjected to electrophoresis in a 6% polyacrylamide gel (lanes 1 and 5). Competition experiments were performed adding as competitor a 100-fold molar excess of unlabeled probe (lanes 2 and 6) or a 100-fold molar excess of unlabeled oligonucleotide containing a mutated NF-κB RE (lanes 3 and 7). Lanes 4 and 8, nuclear extracts from CDCA (50 μM) -treated MCF-7 and MCF-7 TR1 cells, respectively, incubated with probe. Lane 9, NF-κB protein. Lane 10, probe alone. (**b**) Nuclear extracts from MCF-7 and MCF-7 TR1 cells were incubated with a double-stranded NF-κB specific sequence probe labeled with [γ^{32}P]ATP (lanes 1 and 7) or with a 100-fold molar excess of unlabeled probe (lanes 2 and 8). Nuclear extracts incubated with anti-NF-κB (lanes 3 and 9) or IgG (lanes 4 and 10). Lanes 5 and 11, NF-κB protein. Lanes 6 and 12, probe alone. (**c**) Lane 1, NF-κB protein. Lanes 2, 3 and 4, NF-κB protein incubated with increasing doses (1, 3 and 5 μl) of transcribed and translated *in vitro* FXR protein. Lane 5, probe alone.

To further confirm the transcriptional repression mediated by activated FXR, we also evaluated the histone deacetylase 3 association on the NF-κB-responsive sequence within the HER2 promoter. CDCA stimulation enhanced the recruitment of histone deacetylase 3 to this NF-κB promoter site (Figure 6d).

HER2 downregulation underlies the ability of FRX ligands to inhibit breast cancer cell growth

We evaluated the effects of CDCA on cell growth in the ERα-negative and HER2-overexpressing breast cancer cells SKBR3. Treatment with CDCA inhibited SKBR3 anchorage-dependent growth in a dose-dependent

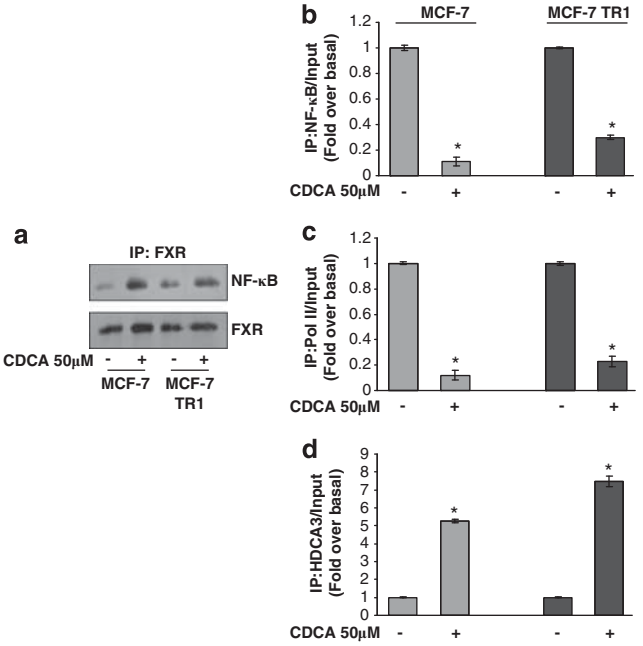

Figure 6 FXR inhibits NF-κB recruitment to HER2 promoter. (**a**) MCF-7 and MCF-7 TR1 cells were treated with vehicle (−) or CDCA 50 μM for 1 h before lysis. FXR protein was immunoprecipitated using an anti-FXR polyclonal antibody (IP:FXR) and resolved in SDS–polyacrylamide gel electrophoresis. Immunoblotting was performed using an anti-NF-κB (p65 subunit) monoclonal antibody and anti-FXR antibody. MCF-7 and MCF-7 TR1 cells were treated in the presence of vehicle (−) or CDCA 50 μM for 1 h, then crosslinked with formaldehyde, and lysed. The precleared chromatin was immunoprecipitated with anti-NF-κB (**b**), anti-RNA polymerase II (**c**) and anti-HDCA3 (**d**) antibodies. A 5 μl volume of each sample and input was analyzed by real-time PCR using specific primers to amplify HER2 promoter sequence, including the NF-κB site. Similar results were obtained in multiple independent experiments. $*P<0.01$ compared with vehicle.

manner (Figure 7a) and reduced colony growth in anchorage-independent assay (Figure 7b). Indeed, we found, after 48 h of treatment with CDCA, a marked decrease in both HER2 protein and mRNA levels (Figures 7c and d). In these cells, HER2 promoter activity was similarly reduced with CDCA treatment (Figure 7e).

Finally, we explored the ability of FXR ligands to inhibit proliferation using as additional model Tam-resistant derivative cell line engineered to stably overexpress HER2 (MCF-7/HER2-18). As expected, Tam-resistant growth in these cells was not affected by both CDCA and GW4064 treatments (Figure 7f). Altogether, these results well evidence how FXR-mediated downregulation of HER2 at transcriptional level is fully responsible for inhibiting breast cancer cell proliferation.

Discussion

In this study, we show for the first time that the activated FXR downregulates HER2 expression in ERα-positive breast cancer cells resistant to Tam. This occurs through the inhibition of NF-κB binding to its responsive element located in the human HER2 promoter region and results in a significant reduction of Tam-resistant growth.

The HER2/neu transmembrane kinase receptor is a signaling amplifier of the HER family network, as activation of membrane tyrosine receptors (EGFR, HER3 and HER4) by their respective ligands determines the formation of homodimeric and heterodimeric kinase complexes into which this receptor is recruited as a preferred partner (Yarden, 2001). Multiple lines of evidences suggest a role of HER2 in the pathogenesis of breast carcinoma (Allred *et al*., 1992; Glockner *et al*., 2001), and clinical data suggest that breast tumors expressing elevated levels of HER2 show a more aggressive phenotype and worse outcome when treated with Tam (Arpino *et al*., 2004; De Laurentiis *et al*., 2005). Thus, inhibitory agents targeting HER2, such as the monoclonal antibody trastuzumab (herceptin), have been explored to improve hormonal treatment or delay emergence of endocrine resistance in estrogen-dependent breast tumors (Johnston, 2009). However, even though an increased response rate is obtained when trastuzumab is used in combination with chemotherapeutic agents (Seidman *et al*., 2001; Slamon *et al*., 2001), patients can still develop resistance (Slamon *et al*., 2001). These observations highlight the importance of discovering new therapeutic tools interfering with HER2-driven signaling to overcome therapy resistance.

We have demonstrated that treatment of breast cancer cells resistant to Tam with the FXR natural ligand CDCA resulted in a reduction of HER2 protein expression. Similar results were also obtained in the ERα-negative and HER2-overexpressing SKBR3 breast cancer cells, suggesting that it may represent a general mechanism not related to cell specificity. Moreover, it assumes more relevance in Tam-resistant breast cancer cells, which are strongly dependent on HER2 activity for their growth. The complete abrogation of FXR-mediated HER2 downregulation with expression of an FXR-DN vector, along with the effects exerted by the synthetic FXR agonist GW4064, clearly demonstrated that activated FXR is involved in the regulation of HER2 expression. Furthermore, quantitative RT–PCR analysis demonstrated that HER2 mRNA levels were significantly decreased in both MCF-7 and MCF-7 TR1 cells treated with CDCA, suggesting that the FXR-induced HER2 downregulation arises via transcriptional mechanisms. Therefore, we focused on the molecular mechanisms by which FXR mediates repression of *HER2* gene expression and on the biological consequences of FXR activation on anti-estrogen-resistant growth of breast cancer cells.

FXR acts mainly by regulating the expression of target genes by binding either as a monomer or heterodimer with the retinoid X receptor to FXR response elements (Laffitte *et al*., 2000; Ananthanarayanan *et al*., 2001; Claudel *et al*., 2002; Kalaany and Mangelsdorf, 2006). Human HER2 promoter did not display any FXR response elements, thus it is reasonable to hypothesize that FXR-induced downregulation of HER2 promoter activity may occur through its interaction with other transcriptional factors. For instance, it

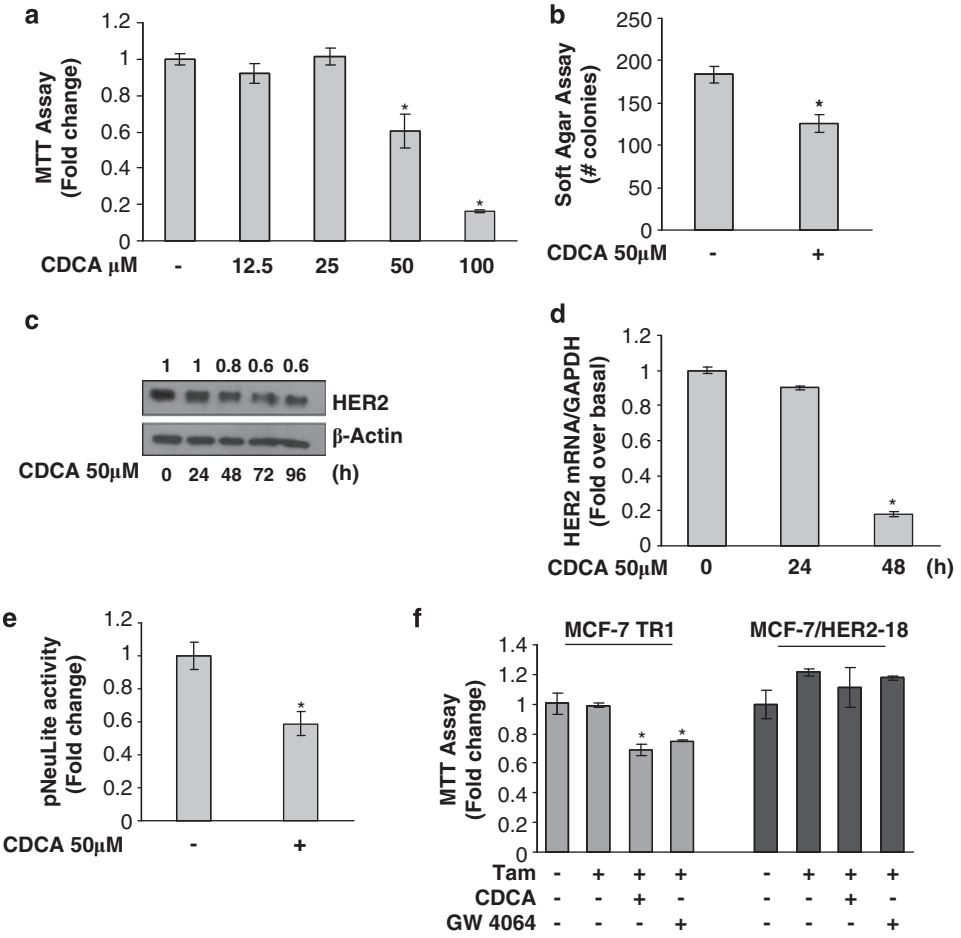

Figure 7 Effects of FXR ligand on SKBR3 breast cancer cells. (**a**) MTT proliferation assay of SKBR3 cells treated with vehicle (−) or increasing doses of CDCA (12,5–25–50–100 μM) for 7 days. Results are expressed as fold change ± s.d. relative to vehicle-treated cells and are representative of three different experiments each performed in triplicate. (**b**) Soft-agar growth assay in SKBR3 cells plated in 0.35% agarose and treated with vehicle (−) or CDCA 50 μM. After 14 days of growth, colonies >50 μm diameter were counted. (**c**) SKBR3 cells were treated with CDCA 50 μM as indicated before lysis. Equal amounts of total cellular extract were analyzed for HER2 levels by western blotting. β-Actin was used as loading control. Numbers on top of the blots represent the average fold change relative to control normalized for β-Actin. (**d**) mRNA HER2 content, evaluated by real-time RT–PCR, after treatment with CDCA 50 μM as indicated. Each sample was normalized to its GAPDH mRNA content. (**e**) SKBR3 cells were transiently transfected with pNeuLite construct. After transfection, cells were treated in the presence of vehicle (−) or CDCA 50 μM for 24 h and the promoter activity was evaluated. The values represent the means ± s.d. of three different experiments each performed in triplicate. $*P<0.05$ compared with vehicle. (**f**) MTT growth assay in MCF-7 TR1 and MCF-7/HER2-18 cells treated with vehicle (−), CDCA 50 μM and GW4064 3 μM in the presence or not of Tam 1 μM for 4 days. Results are expressed as fold change ± s.d. relative to vehicle-treated cells and are representative of three different experiments each performed in triplicate. $*P<0.05$ compared with Tam alone.

has been described the transrepression mechanisms for FXR-mediated inhibition of endothelin-1 expression in vascular endothelial cells (He *et al*., 2006). In addition, it has also been demonstrated that FXR negatively regulates IL-1β expression by stabilizing the nuclear corepressor NCoR on the NF-κB sequence within the IL-1β promoter (Vavassori *et al*., 2009). Several recognition elements are present within the HER2 proximal promoter (Ishii *et al*., 1987; Hurst, 2001) and among these functional motifs we have identified both AP-1 and NF-κB response elements as potential targets of FXR. We have demonstrated by functional studies and site-specific mutagenesis analysis that the integrity of the NF-κB sequence is a prerequisite for the downregulatory effects of the FXR ligand on HER2 promoter activity. These results were supported by electrophoretic mobility shift assays, which revealed a marked decrease in a specific DNA-binding complex in nuclear extracts from MCF-7 and MCF-7 TR1 cells treated with CDCA. *In vitro* competition studies showed that FXR protein was able to inhibit the binding of NF-κB to its consensus site on the HER2 promoter. Furthermore, we observed a reduced recruitment of both NF-κB and RNA polymerase II in CDCA-treated cells, concomitant with an enhanced recruitment of histone deacetylase 3 supporting a negative transcriptional role for FXR in modulating HER2 expression.

The physiological relevance of these effects is pointed out by proliferation studies showing that FXR activation reduced breast cancer cell growth, but did not affect

the proliferation of the non-tumorogenic breast epithelial MCF-10A cell line. MCF-7 TR1 cells exhibited lower IC_{50} values for both ligands compared with parental MCF-7 cells, suggesting a higher sensitivity of the Tam-resistant cells to the effects of FXR ligands. This suggestion is also well supported by the results obtained from growth assays, showing that combined treatment with CDCA and Tam significantly reduced Tam-resistant growth in MCF-7 TR1 cells, compared with Tam alone, but had no additive effects in MCF-7 parental cells. Moreover, FXR ligands failed to inhibit Tam-resistant growth in MCF-7/HER2-18 cells, in which HER2 expression is not driven by its own gene promoter activity. These latter results provided evidences that the downregulation of HER2 expression at transcriptional level underlies the ability of activated FXR to inhibit Tam-resistant growth in breast cancer cells.

Previous *in vitro* studies showed that enhanced EGFR/HER2 expression together with activation of downstream signaling pathways such as p42/44 MAPK are involved in acquired Tam resistance (Knowlden *et al*., 2003; Nicholson *et al*., 2004). Our studies showed that CDCA treatment significantly reduced the ability of EGF to activate its signal transduction cascade in MCF-7 TR1 cells, inhibiting both HER2 and MAPK phosphorylation. In addition, FXR activation was associated with a marked inhibition in EGF-induced growth, concomitant with a reduction in cyclin D1 expression in Tam-resistant breast cancer cells. All together these data demonstrate, as represented in Figure 8, that activated FXR, by preventing the binding of NF-κB to its response element located in the HER2 promoter sequence, abrogates HER2 expression and signaling, resulting in an inhibition of Tam-resistant growth in breast cancer cells.

Deciphering the molecular mechanisms responsible for the development of hormonal resistance is essential for establishing the most appropriate hormone agent according to tumor characteristics and for defining the optimal sequence of endocrine therapies. Moreover, this knowledge is critical for development of new therapeutic approaches able to either overcome or prevent endocrine resistance in breast cancer patients. Over the last years, significant survival benefits for breast cancer were derived from the use of combined treatment of endocrine therapies with new targeted therapies in endocrine responsive breast cancer (Johnston, 2009). In this scenario, the sequencing or the combination of Tam with FXR ligands may represent an important research issue to explore as an alternative therapeutic strategy to treat breast cancer patients whose tumors exploit HER2 signaling to escape Tam treatment.

Materials and methods

Reagents and antibodies

The following components were obtained from the given respective companies, with their addresses in brackets. DMEM, L-glutamine, penicillin, streptomycin, fetal bovine serum, MTT, 4-hydroxytamoxifen, CDCA and EGF from Sigma (Milan, Italy). TRIzol by Invitrogen (Carlsbad, CA, USA). FuGENE 6 by Roche (Indianapolis, IN, USA). TaqDNA polymerase, RETROscript kit, Dual Luciferase kit, TNT master mix and NF-κB protein from Promega (Madison, WI, USA). SYBR Green Universal PCR Master Mix by Biorad (Hercules, CA, USA). Antibodies against FXR, β-actin, Cyclin D1, p65, ERα, EGFR and Lamin B by Santa Cruz

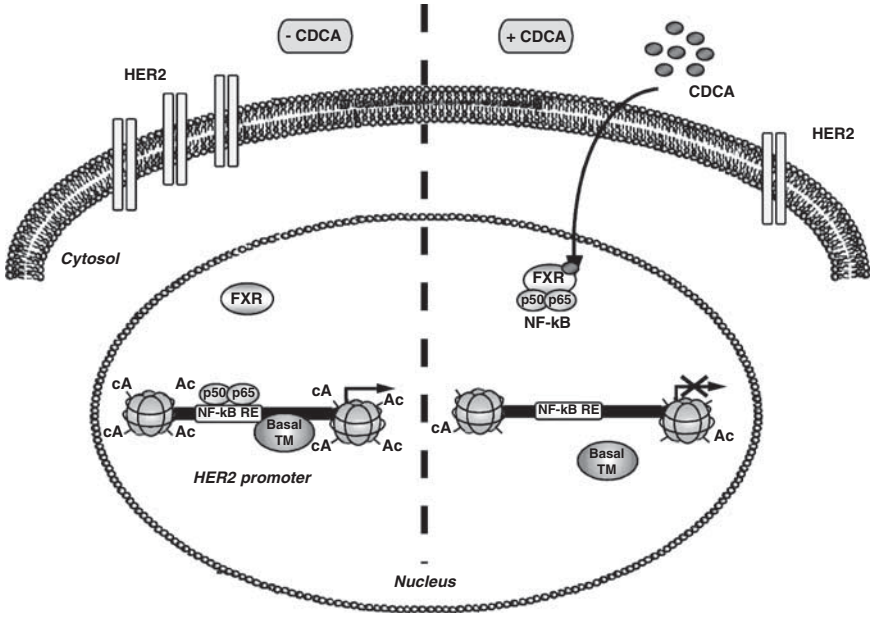

Figure 8 Proposed working model of the FXR-mediated regulation of HER2 expression in Tam-resistant breast cancer cells. In the absence of CDCA, HER2 expression is regulated by several serum factors, including NF-κB, acting through a regulatory region in HER2 promoter and enabling gene transcription. Upon CDCA treatment, FXR binds NF-κB, inhibiting its recruitment on the response element located in the proximal HER2 promoter, causing displacement of RNA polymerase II with consequent repression of HER2 expression.

Biotechnology (Santa Cruz, CA, USA). MAPK, phosphorylated p42/44 MAPK (Thr^{202}/Tyr^{204}), phosphorylated HER2 (Tyr^{1248}) from Cell Signaling Technology (Beverly, MA, USA). HER2 from NeoMarker (Fremont, CA, USA). ECL system and Sephadex G-50 spin columns from Amersham Biosciences (Buckinghamshire, UK). [γ^{32}P]ATP from PerkinElmer (Wellesley, MA, USA). Herceptin from Genentech (San Francisco, CA, USA).

Plasmids
The plasmid pNeuLite containing human HER2/neu promoter region was kindly provided by Dr Mien-Chie Hung (University of Texas, M.D. Anderson Cancer Center, Houston, TX, USA) (Xing *et al*., 2000). The FXR-responsive reporter gene (*FXRE-IR1*) and FXR-DN expression plasmids were provided from Dr T.A. Kocarek (Institute of Environmental Health Sciences, Wayne State University, USA) (Kocarek *et al*., 2002).

The −232 pNeuLite construct was generated by PCR using as template the pNeuLite plasmid with the following primers: forward 5′-GATAAGTGTGAGAACGGCTGCAGGC-3′ and reverse 5′-GGGCAGATCTGGTTTTCCGGTCCCAAT GGA-3′. The amplified DNA fragment was digested with *Bgl*II and *Kpn*I and ligated into pGL2-basic vector. Deletion was confirmed by DNA sequencing.

Site-directed mutagenesis
The pNeuLite promoter plasmid-bearing NF-κB-responsive element-mutated site (NF-κB mut) was created by site-directed mutagenesis using Quick Change kit (Stratagene, La Jolla, CA, USA), according to manufacturer's method. We used as template the pNeuLite plasmid and the following primers (mutations are shown as lowercase letters): 5′-AGAGAGGG AGAAAGTGAAGCTaatcGTTGCCGACTCCCAGACTTC G-3′ and 5′-CGAAGTCTGGGAGTCGGCAACgattAGC TTCACTTTCTCCCTCTCT-3′. Mutation was confirmed by DNA sequencing.

Cell culture
MCF-7 cells were cultured in DMEM containing 10% fetal bovine serum. MCF-7 TR1 and MCF-7 TR2 cells were generated in the laboratory of Dr Fuqua as previously described (Barone *et al*., 2011) and maintained with 10^{-6} M (MCF-7 TR1) and 10^{-7} M (MCF-7 TR2) of 4-hydroxytamoxifen. SKBR3 cells were cultured in phenol red-free RPMI medium containing 10% fetal bovine serum. MCF-10A normal breast epithelial cells were grown in DMEM–F12 medium containing 5% horse serum. MCF-7/HER2-18 were kindly provided by Dr Schiff (Baylor College of Medicine, Houston, TX, USA) and maintained as described (Shou *et al*., 2004). Before each experiment, cells were grown in phenol red-free medium, containing 5% charcoal-stripped fetal bovine serum for 2 days and treated as described.

Cell proliferation assays
Cell proliferation was assessed using MTT and soft-agar anchorage-independent growth assays as described (Barone *et al*., 2009; Giordano *et al*., 2010). The IC_{50} values were calculated using GraphPad Prism 4 (GraphPad Software Inc., San Diego, CA) as described (Herynk *et al*., 2006).

Immunoprecipitation and immunoblot analysis
Cells were treated as indicated before lysis for total protein extraction (Catalano *et al*., 2010). Nuclear extracts were prepared as described (Morelli *et al*., 2004). For coimmunoprecipitation experiments, we used 1 mg of nuclear protein extract and 2 μg of FXR antibody, followed by protein A/G precipitation. Equal amounts of cell extracts and coimmunoprecipitated protein were subjected to SDS–polyacrylamide gel electrophoresis, as described (Catalano *et al*., 2010).

RT–PCR and Real-time RT–PCR assays
FXR gene expression was evaluated by the RT–PCR method using a RETROscript kit. The cDNAs obtained were amplified using the following primers: forward 5′-CGAGCCTGAAG AGTGGTACTGTC-3′ and reverse 5′-CATTCAGCCAACA TTCCCATCTC-3′ (FXR); forward 5′-CTCAACATCTCCC CCTTCTC-3′ and reverse 5′-CAAATCCCATATCCTCGT-3′ (36B4).

The PCR was performed for 35 cycles for hFXR (94 °C 1 min, 65 °C 1 min, 72 °C 1 min) and 18 cycles for 36B4 (94 °C for 1 min, 58 °C for 1 min and 72 °C for 1 min), as described (Catalano *et al*., 2010).

HER2 gene expression was evaluated by real-time RT–PCR. Total RNA was reverse transcribed with the RETROscript kit; 5 μl of diluted (1:3) cDNA was analyzed in triplicates by real-time PCR in an iCycler iQ Detection System (Bio-Rad) using SYBR Green Universal PCR Master Mix, following the manufacturer's recommendations. Each sample was normalized on its GAPDH mRNA content. Primers used for the amplification were: forward 5′-CACCTACAACACAGACAC GTTTGA-3′ and reverse 5′-GCAGACGAGGGTGCAGGA T-3′ (HER2); forward 5′-CCCACTCCTCCACCTTTGAC-3′ and reverse 5′-TGTTGCTGTAGCCAAATTCGTT-3′ (GAPDH). The relative gene expression levels were calculated as described (Sirianni *et al*., 2007).

Transient transfection assays
MCF-7 and MCF-7 TR1 cells were transiently transfected using the FuGENE 6 reagent with FXR reporter gene (*FXRE-IR1*) in the presence or absence of FXR-DN plasmid. In a set of experiments, MCF-7, MCF-7 TR1 and SKBR3 cells were transfected with different HER2 promoter constructs. Luciferase activity was assayed as described (Catalano *et al*., 2010).

Electrophoretic mobility shift assays
Nuclear extracts from cells, treated or not for 3 h with CDCA, were prepared as described (Andrews and Faller, 1991). The DNA sequences used as probe or as cold competitors are the following (nucleotide motifs of interest are underlined and mutations are shown as lowercase letters): NF-κB, 5′-AA GTGAAGCTGGGAGTTGCCGACTCCCAGA-3′; mutated NF-κB, 5′-AAGTGAAGCTaatcGTTGCCGACTCCCAGA-3′; AP-1, 5′-AGGGGGCAGAGTCAC CAGCCTCTG-3′; mutated AP-1, 5′-AGGGGGCAtcaTCACCAGCCTCTG-3′; Sp1 5′-ATCCCGGACTCCGGGGGAGGGGGC-3′; mutated Sp1, 5′-ATCCCGGACCTCattG GGAGGGGGC-3′. *In vitro*-transcribed and -translated FXR protein was synthesized using the T7 polymerase in the rabbit reticulocyte lysate system. Probe generation and the protein-binding reactions were carried out as described (Catalano *et al*., 2010). For experiments involving anti-NF-κB (p65) antibody, the reaction mixture was incubated with this antibody at 4 °C for 12 h before addition of labeled probe.

Chromatin immunoprecipitation assays
Cells were treated with CDCA or left untreated for 1 h and then DNA/protein complexes were extracted as described (Catalano *et al*., 2010). The precleared chromatin was immunoprecipitated with anti-NF-κB (p65), anti-histone

deacetylase 3 or anti-polymerase II antibodies. A normal mouse serum IgG was used as negative control. A 5 µl volume of each sample and input DNA was used for real-time PCR using the primers flanking NF-κB sequence in the human HER2 promoter region: 5′-TGAGAACGGCTGCAGGCA AC-3′ and 5′-CCCACCAACTGCATTCCAA-3′. Real-time PCR was performed as described above. Final results were calculated using the ΔΔCt method, using input Ct values instead of the GAPDH mRNA. The basal sample was used as calibrator.

Statistical analyses

Each datum point represents the mean ± s.d. of three different experiments. Data were analyzed by Student's *t*-test using the GraphPad Prism 4 software program. $P<0.05$ was considered as statistically significant.

Conflict of interest

The authors declare no conflict of interest.

Acknowledgements

This work was supported by AIRC grants, MIUR Ex 60% 2009, PRIN 2009 and Lilli Funaro Foundation. NIH/NCI R01 CA72038 and RP101251 from the Cancer Prevention and Research Institute of Texas (SAWF). We thank Dr Mien-Chie Hung for providing the pNeuLite plasmid and Dr T.A. Kocarek for providing the FXR-responsive reporter gene and FXR-DN expression plasmids. We also thank Dr Rachel Schiff for providing the MCF-7/HER2-18 cells.

References

Allred DC, Clark GM, Molina R, Tandon AK, Schnitt SJ, Gilchrist KW *et al*. (1992). Overexpression of HER-2/neu and its relationship with other prognostic factors change during the progression of *in situ* to invasive breast cancer. *Hum Pathol* **23**: 974–979.

Ananthanarayanan M, Balasubramanian N, Makishima M, Mangelsdorf DJ, Suchy FJ. (2001). Human bile salt export pump promoter is transactivated by the farnesoid X receptor/bile acid receptor. *J Biol Chem* **276**: 28857–28865.

Andrews NC, Faller DV. (1991). A rapid micropreparation technique for extraction of DNA-binding proteins from limiting numbers of mammalian cells. *Nucleic Acids Res* **19**: 2499.

Arpino G, Green SJ, Allred DC, Lew D, Martino S, Osborne CK *et al*. (2004). HER-2 amplification, HER-1 expression, and tamoxifen response in estrogen receptor-positive metastatic breast cancer: a southwest oncology group study. *Clin Cancer Res* **10**: 5670–5676.

Arpino G, Wiechmann L, Osborne CK, Schiff R. (2008). Crosstalk between the estrogen receptor and the HER tyrosine kinase receptor family: molecular mechanism and clinical implications for endocrine therapy resistance. *Endocr Rev* **29**: 217–233.

Barone I, Brusco L, Gu G, Selever J, Beyer A, Covington KR *et al*. (2011). Loss of Rho GDI α and resistance to tamoxifen via effects on estrogen receptor α. *Journal Natl Cancer Inst* (in press).

Barone I, Cui Y, Herynk MH, Corona-Rodriguez A, Giordano C, Selever J *et al*. (2009). Expression of the K303R estrogen receptor-alpha breast cancer mutation induces resistance to an aromatase inhibitor via addiction to the PI3K/Akt kinase pathway. *Cancer Res* **69**: 4724–4732.

Bishop-Bailey D. (2004). FXR as a novel therapeutic target for vascular disease. *Drug News Perspect* **17**: 499–504.

Blume-Jensen P, Hunter T. (2001). Oncogenic kinase signalling. *Nature* **411**: 355–365.

Catalano S, Malivindi R, Giordano C, Gu G, Panza S, Bonofiglio D *et al*. (2010). Farnesoid X receptor, through the binding with steroidogenic factor 1-responsive element, inhibits aromatase expression in tumor Leydig cells. *J Biol Chem* **285**: 5581–5593.

Chung YL, Sheu ML, Yang SC, Lin CH, Yen SH. (2002). Resistance to tamoxifen-induced apoptosis is associated with direct interaction between Her2/neu and cell membrane estrogen receptor in breast cancer. *Int J Cancer* **97**: 306–312.

Claudel T, Sturm E, Duez H, Torra IP, Sirvent A, Kosykh V *et al*. (2002). Bile acid-activated nuclear receptor FXR suppresses apolipoprotein A-I transcription via a negative FXR response element. *J Clin Invest* **109**: 961–971.

De Laurentiis M, Arpino G, Massarelli E, Ruggiero A, Carlomagno C, Ciardiello F *et al*. (2005). A meta-analysis on the interaction between HER-2 expression and response to endocrine treatment in advanced breast cancer. *Clin Cancer Res* **11**: 4741–4748.

Encarnacion CA, Ciocca DR, McGuire WL, Clark GM, Fuqua SA, Osborne CK. (1993). Measurement of steroid hormone receptors in breast cancer patients on tamoxifen. *Breast Cancer Res Treat* **26**: 237–246.

Fisher B, Costantino JP, Wickerham DL, Redmond CK, Kavanah M, Cronin WM *et al*. (1998). Tamoxifen for prevention of breast cancer: report of the National Surgical Adjuvant Breast and Bowel Project P-1 Study. *J Natl Cancer Inst* **90**: 1371–1388.

Forman BM, Goode E, Chen J, Oro AE, Bradley DJ, Perlmann T *et al*. (1995). Identification of a nuclear receptor that is activated by farnesol metabolites. *Cell* **81**: 687–693.

Giordano C, Cui Y, Barone I, Andò S, Mancini MA, Berno V *et al*. (2010). Growth factor-induced resistance to tamoxifen is associated with a mutation of estrogen receptor alpha and its phosphorylation at serine 305. *Breast Cancer Res Treat* **119**: 71–85.

Glockner S, Lehmann U, Wilke N, Kleeberger W, Langer F, Kreipe H. (2001). Amplification of growth regulatory genes in intraductal breast cancer is associated with higher nuclear grade but not with the progression to invasiveness. *Lab Invest* **81**: 565–571.

Gradishar WJ. (2004). Tamoxifen—what next? *Oncologist* **9**: 378–384.

Gutierrez MC, Detre S, Johnston S, Mohsin SK, Shou J, Allred DC *et al*. (2005). Molecular changes in tamoxifen-resistant breast cancer: relationship between estrogen receptor, HER-2, and p38 mitogen-activated protein kinase. *J Clin Oncol* **23**: 2469–2476.

He F, Li J, Mu Y, Kuruba R, Ma Z, Wilson A *et al*. (2006). Downregulation of endothelin-1 by farnesoid X receptor in vascular endothelial cells. *Circ Res* **98**: 192–199.

Herynk MH, Beyer AR, Cui Y, Weiss H, Anderson E, Green TP *et al*. (2006). Cooperative action of tamoxifen and c-Src inhibition in preventing the growth of estrogen receptor-positive human breast cancer cells. *Mol Cancer Ther* **5**: 3023–3031.

Hurst HC. (2001). Update on HER-2 as a target for cancer therapy: the ERBB2 promoter and its exploitation for cancer treatment. *Breast Cancer Res* **3**: 395–398.

Ishii S, Imamoto F, Yamanashi Y, Toyoshima K, Yamamoto T. (1987). Characterization of the promoter region of the human c-erbB-2 protooncogene. *Proc Natl Acad Sci USA* **84**: 4374–4378.

Johnston SR. (2009). Enhancing the efficacy of hormonal agents with selected targeted agents. *Clin Breast Cancer* **9**(Suppl 1): S28–S36.

Journe F, Laurent G, Chaboteaux C, Nonclercq D, Durbecq V, Larsimont D *et al*. (2008). Farnesol, a mevalonate pathway intermediate, stimulates MCF-7 breast cancer cell growth through farnesoid-X-receptor-mediated estrogen receptor activation. *Breast Cancer Res Treat* **107**: 49–61.

Kalaany NY, Mangelsdorf DJ. (2006). LXRS and FXR: the yin and yang of cholesterol and fat metabolism. *Annu Rev Physiol* **68**: 159–191.

Kirkegaard T, McGlynn LM, Campbell FM, Muller S, Tovey SM, Dunne B *et al*. (2007). Amplified in breast cancer 1 in human epidermal growth factor receptor—positive tumors of tamoxifen-treated breast cancer patients. *Clin Cancer Res* **13**: 1405–1411.

Knowlden JM, Hutcheson IR, Jones HE, Madden T, Gee JM, Harper ME *et al*. (2003). Elevated levels of epidermal growth factor receptor/c-erbB2 heterodimers mediate an autocrine growth regulatory pathway in tamoxifen-resistant MCF-7 cells. *Endocrinology* **144**: 1032–1044.

Kocarek TA, Shenoy SD, Mercer-Haines NA, Runge-Morris M. (2002). Use of dominant negative nuclear receptors to study xenobiotic-inducible gene expression in primary cultured hepatocytes. *J Pharmacol Toxicol Methods* **47**: 177–187.

Laffitte BA, Kast HR, Nguyen CM, Zavacki AM, Moore DD, Edwards PA. (2000). Identification of the DNA binding specificity and potential target genes for the farnesoid X-activated receptor. *J Biol Chem* **275**: 10638–10647.

Makishima M, Okamoto AY, Repa JJ, Tu H, Learned RM, Luk A *et al*. (1999). Identification of a nuclear receptor for bile acids. *Science* **284**: 1362–1365.

Meng S, Tripathy D, Shete S, Ashfaq R, Haley B, Perkins S *et al*. (2004). HER-2 gene amplification can be acquired as breast cancer progresses. *Proc Natl Acad Sci USA* **101**: 9393–9398.

Morelli C, Garofalo C, Sisci D, del Rincon S, Cascio S, Tu X *et al*. (2004). Nuclear insulin receptor substrate 1 interacts with estrogen receptor alpha at ERE promoters. *Oncogene* **23**: 7517–7526.

Nicholson RI, Staka C, Boyns F, Hutcheson IR, Gee JM. (2004). Growth factor-driven mechanisms associated with resistance to estrogen deprivation in breast cancer: new opportunities for therapy. *Endocr Relat Cancer* **11**: 623–641.

Osborne CK, Bardou V, Hopp TA, Chamness GC, Hilsenbeck SG, Fuqua SA *et al*. (2003). Role of the estrogen receptor coactivator AIB1 (SRC-3) and HER-2/neu in tamoxifen resistance in breast cancer. *J Natl Cancer Inst* **95**: 353–361.

Parks DJ, Blanchard SG, Bledsoe RK, Chandra G, Consler TG, Kliewer SA *et al*. (1999). Bile acids: natural ligands for an orphan nuclear receptor. *Science* **284**: 1365–1368.

Sabnis GJ, Jelovac D, Long B, Brodie A. (2005). The role of growth factor receptor pathways in human breast cancer cells adapted to long-term estrogen deprivation. *Cancer Res* **65**: 3903–3910.

Schiff R, Massarweh SA, Shou J, Bharwani L, Mohsin SK, Osborne CK. (2004). Cross-talk between estrogen receptor and growth factor pathways as a molecular target for overcoming endocrine resistance. *Clin Cancer Res* **10**: 331S–336S.

Seidman AD, Fornier MN, Esteva FJ, Tan L, Kaptain S, Bach A *et al*. (2001). Weekly trastuzumab and paclitaxel therapy for metastatic breast cancer with analysis of efficacy by HER2 immunophenotype and gene amplification. *J Clin Oncol* **19**: 2587–2595.

Shou J, Massarweh S, Osborne CK, Wakeling AE, Ali S, Weiss H *et al*. (2004). Mechanisms of tamoxifen resistance: increased estrogen receptor-HER2/neu cross-talk in ER/HER2-positive breast cancer. *J Natl Cancer Inst* **96**: 926–935.

Sirianni R, Chimento A, Malivindi R, Mazzitelli I, Ando S, Pezzi V. (2007). Insulin-like growth factor-I, regulating aromatase expression through steroidogenic factor 1, supports estrogen-dependent tumor Leydig cell proliferation. *Cancer Res* **67**: 8368–8377.

Slamon DJ, Godolphin W, Jones LA, Holt JA, Wong SG, Keith DE *et al*. (1989). Studies of the HER-2/neu proto-oncogene in human breast and ovarian cancer. *Science* **244**: 707–712.

Slamon DJ, Leyland-Jones B, Shak S, Fuchs H, Paton V, Bajamonde A *et al*. (2001). Use of chemotherapy plus a monoclonal antibody against HER2 for metastatic breast cancer that overexpresses HER2. *N Engl J Med* **344**: 783–792.

Staka CM, Nicholson RI, Gee JM. (2005). Acquired resistance to oestrogen deprivation: role for growth factor signalling kinases/oestrogen receptor cross-talk revealed in new MCF-7X model. *Endocr Relat Cancer* **12**(Suppl 1): S85–S97.

Swales KE, Korbonits M, Carpenter R, Walsh DT, Warner TD, Bishop-Bailey D. (2006). The farnesoid X receptor is expressed in breast cancer and regulates apoptosis and aromatase expression. *Cancer Res* **66**: 10120–10126.

Vavassori P, Mencarelli A, Renga B, Distrutti E, Fiorucci S. (2009). The bile acid receptor FXR is a modulator of intestinal innate immunity. *J Immunol* **183**: 6251–6261.

Xing X, Wang SC, Xia W, Zou Y, Shao R, Kwong KY *et al*. (2000). The ets protein PEA3 suppresses HER-2/neu overexpression and inhibits tumorigenesis. *Nat Med* **6**: 189–195.

Yarden Y. (2001). Biology of HER2 and its importance in breast cancer. *Oncology* **61**(Suppl 2): 1–13.

Supplementary Information accompanies the paper on the Oncogene website (http://www.nature.com/onc)